



HAL
open science

New compacts systems for biogas upgrading

Pedro Carvalho Villarim

► **To cite this version:**

Pedro Carvalho Villarim. New compacts systems for biogas upgrading. Analytical chemistry. Université du Littoral Côte d'Opale, 2023. English. NNT : 2023DUNK0697 . tel-04578100

HAL Id: tel-04578100

<https://theses.hal.science/tel-04578100>

Submitted on 16 May 2024

HAL is a multi-disciplinary open access archive for the deposit and dissemination of scientific research documents, whether they are published or not. The documents may come from teaching and research institutions in France or abroad, or from public or private research centers.

L'archive ouverte pluridisciplinaire **HAL**, est destinée au dépôt et à la diffusion de documents scientifiques de niveau recherche, publiés ou non, émanant des établissements d'enseignement et de recherche français ou étrangers, des laboratoires publics ou privés.



Doctoral Thesis

Major: Chemistry
Specialty: Theoretical, physical, analytical chemistry

Presented at *l'Ecole Doctorale en Sciences Technologie et Santé (ED 585)*

From Université du Littoral Côte d'Opale

by
Pedro Villarim

to obtain the degree of Doctor of the Université du Littoral Côte d'Opale

New compacts systems for biogas upgrading

Defended on December 15, 2023, after approval by the rapporteurs, before the jury:

Pr Alessandro Triolo, ISM-CNR Italian
Pr Christophe Coquelet, IMT Mines Albi
Dr Leila Moura, Queen's University Belfast
Dr Patrycia Makos Chelstowska, École polytechnique de Gdańsk
Pr Abdenacer Idrissi, Université de Lille
Pr Annabelle Couvert, ENSCR de Rennes
Pr Sophie Fourmentin, ULCO
Pr Jaouad Zemmouri, Terrao

Reviewer
Reviewer
Examiner
Examiner
Examiner
President
Director
Co-director



*“If the path to what you want seems too easy,
then you are on the wrong path”*

Acknowledgments

First of all, I would like to thank all the support of my parents and my brother in Brazil, Silvio, Maria e Silvio Jr. They have always supported me and encouraged me to go further in my studies and gave me all the support I needed. Since the beginning of my studies, I have virtual family meetings, so this is the way when I feel most in Brazil. On this occasion, they always ask me how my research is going, so since then they have been following my little steps. I would also like to thank the entire Villarim family for always supporting me.

I would like to express my deepest gratitude to my thesis directors, Sophie Fourmentin and Jaouad Zemmouri, I appreciate all the support and conversation I had with both of them. I am grateful for all their help and confidence that they placed in me to be part of it. Also, I wanted to thank Fabrice Cazier for all the support I needed during my PhD. It was a huge privilege to work with them.

All my thanks also go to Leila Moura for being my examiner and for the collaboration during which I had the privilege of working with her for a month, as well as Mark and Sam. You have an amazing group.

I also thank my reviewers, Alessandro Triolo and Christophe Coquelet, and my examiners Patrycja Makoś, Abdenacer Idrissi and Annabelle Couvert for being a part of the jury for my thesis.

I would like to thank from the bottom of my heart all my friends in France, who have become my second family. I really appreciate the relaxing time during the weekends, and all the trips we have done together. Those moments and meeting all of you make me feel fortunate to be living abroad. Special thanks to Tiago, Icaro, Vinícius, Monacer, Priscila and Marcos.

I'm also grateful for the knowledge I've shared and the good times I've had with my friends at ULCO, which were Tarek, Lamia, Marc, Sarah, Mira, Mireille, Muriel, Micho, Mariebelle, Abir, Gautier, Chengmin and Hadhami. Our discussions really motivated me during my thesis.

I could not forget to mention Amandine who has lived a good part of this journey with me. Her unconditional support were essentials for me to finish my studies.

Finally, my decision to start a PhD in a country where I have never lived and barely spoke the language was not easy. But fortunately, everyone around me encouraged me to go for it. Especially my family, with their motivation was my inspiration every day.

Table of Contents

List of Table	1
List of Figures	3
List of Abbreviations	6
Introduction	1
References	4
Chapter 1 – STATE OF THE ART	7
I. Biogas origin and definition	7
II. Biogas production	8
II.1. Biogas Production by Anaerobic Digestion (AD)	9
II.2. Landfill	11
II.3. Pyro-gasification	13
III. Global, Europe and France situation of biogas production	13
IV. Biogas valorization	16
V. Biogas composition	18
V.1. CO₂ and CH₄	20
V.2. Volatile organic compounds (VOCs)	21
VI. Biogas upgrading to biomethane (technologies)	24
VI.1. Physicochemical Methods	25
VI.2. Physical Absorption	26
VI.2.1. Water scrubbing.....	27
VI.2.2. Organic solvent scrubbing.....	28
VI.3. Chemical scrubbing	30
VI.4. Membrane separation	32
VI.5. Cryogenic separation	34
VI.6. Pressure swing adsorption (PSA)	35
VI.7. Biological methods	37
VI.7.1. Chemoautotrophic biogas upgrading.....	37
VI.7.2. Photosynthetic biogas upgrading.....	38
VI.7.3. Microbial electrochemical technologies (METs)	39
VII. Economic and technological challenges of biogas upgrading	40
VIII. Deep Eutectic Solvents (DES)	42
VIII.1. DES characterization	46
VIII.1.1. Viscosity	47
VIII.1.2. Density	48
VIII.1.3. Polarity	49
VIII.1.4. Surface tension.....	50
VIII.2. DESs preparation	50

VIII.3. DESs application	50
VIII.3.1. Extraction	51
VIII.3.2. Solubilization	52
VIII.3.3. Absorption	53
VIII.3.3.1. Carbon dioxide (CO ₂)	53
VIII.3.3.2. Volatile organic compounds (VOCs)	54
VIII.3.3.3. Biogas upgrading	55
IX. Research overview	56
IX.1. Choice of biogas impurities	56
IX.2. Choice of DESs and conventional solvents	57
1. Aim of the study	61
X. References	63
Chapter 2- Preparation and physicochemical characterization of the DESs and conventional solvents	80
I. Preparation of the studied DES.....	80
II. Characterization of the DESs and conventional solvents	81
II.1. Water content %	81
II.2. Melting point	82
II.3. Viscosity.....	83
II.4. Density.....	87
II.5. Infrared spectroscopy (FT-IR).....	89
III. References	93
Chapter 3 - Deep eutectic solvents and conventional solvents as absorbents for the removal of biogas impurities in static and dynamic processes.....	96
I. Determination the vapor-liquid partition coefficients (K) of VOCs.....	96
I.1. Static headspace-gas chromatography (SH-GC)	97
I.2. K-value of VOC in water using phase ratio variation method (PRV)	97
I.3 K-value of VOC in solvents using the vapor phase calibration method (VPC).....	100
I.4. Results and discussion.....	101
I.4.1. Effect of equilibrium time.....	101
I.4.2. Determination of K-values of VOC at 30 °C	102
I.4.3. Effect of temperature.....	107
I.4.4. Effect of initial VOC concentration	111
I.4.5. Effect of water on VOC absorption.....	112
I.4.6. Toluene absorption in industrial solvents and water/solvent mixtures.....	114
I.4.7. Effect of VOC mixtures	117
I.4.8. Regeneration of the absorbent	120
I.4.8.1. DES regeneration.....	120
I.4.8.2. Regeneration of the industrial solvents and water/solvent mixtures.....	123
II. Determination of CO₂ sorption capacity	124

II.1. Overview of the method	124
II.2. Results of gas sorption	125
III. Dynamic absorption from laboratory to industrial scale	127
III.1. Methodology and experimental set-up	127
III.2. VOC absorption results.....	128
III.2.1. Individuals VOCs absorption.....	128
III.2.2. Effect of toluene initial concentration.....	131
III.2.3. Toluene absorption in available industrial solvents and water/solvent mixtures.....	133
III.2.4. Effect of VOC mixtures	134
III.3. Carbon dioxide and raw biogas absorption.....	136
III.3.1. Experimental methods and devices	136
III.3.2. CO ₂ absorption results.....	138
III.3.3. Biogas absorption	139
III.4. Dynamic method regeneration.....	141
III.5. Industrial scale dynamic absorption	141
IV. Absorption mechanism revealed by Conductor-like Screening Model for Real Solvents (COSMO-RS).....	144
IV.1. Analysis of σ -profiles.....	145
IV.2. Gibbs free energy of solvation	146
V. References	147
Conclusion and perspectives	151
List of publications and communication	154
Abstract.....	155
Résumé	156

List of Table

Table 1. Typical range of biogas and biomethane compositions.	19
Table 2. Sources and production processes of VOCs present in biogas.	23
Table 3. Comparison of different physicochemical biogas upgrading technologies.	25
Table 4. Comparison of water and organic solvent scrubbing.	26
Table 5. Physicochemical properties of DES used for VOCs absorption.	48
Table 6. Structures and characteristics of selected VOCs.	58
Table 7. Selected DES component structures.	59
Table 8. Selected conventional solvent's structure.	60
Table 9. Composition of the studied DES and their water content (%).	80
Table 10. Melting temperatures and molecular weight (MW) of fatty acid-based DESs, individual materials and conventional solvents used in this work.	82
Table 11. Experimental DESs and conventional solvents values of the dynamic viscosity as a function of temperature for the studied absorbent.	84
Table 12. Fitted parameters of Vogel–Fulcher–Tammann (VFT) model given by Equation (1) for the studied absorbents.	85
Table 13. Experimental densities of the studied absorbents as function of temperature.	88
Table 14. Parameters, A_0 and A_1 , of Equation (2) describing temperature dependence of density of the studied absorbents.	88
Table 15. Experimental conditions used in gas chromatography for measurements of VOCs individually.	99
Table 16. Partition coefficients (K) of VOCs at 30 °C in the different DES.	103
Table 17. Comparison of partition coefficient (K) for VOC in various solvents.	107
Table 18. Comparison of enthalpies ($\text{kJ}\cdot\text{mol}^{-1}$), entropies ($\text{J}\cdot\text{mol}^{-1}\cdot\text{K}^{-1}$), and Gibbs free energies ($\text{kJ}\cdot\text{mol}^{-1}$) of toluene absorption in different absorbents.	109
Table 19. Enthalpies ($\text{kJ}\cdot\text{mol}^{-1}$), entropies ($\text{J}\cdot\text{mol}^{-1}\cdot\text{K}^{-1}$), and Gibbs free energies ($\text{kJ}\cdot\text{mol}^{-1}$) of limonene absorption in different absorbents.	109
Table 20. Enthalpies ($\text{kJ}\cdot\text{mol}^{-1}$), entropies ($\text{J}\cdot\text{mol}^{-1}\cdot\text{K}^{-1}$), and Gibbs free energies ($\text{kJ}\cdot\text{mol}^{-1}$) of siloxane D4 absorption in different absorbents.	110

Table 21. Partition coefficients values (K) of toluene in water, solvents and water/solvent mixtures at 30 °C, and $K_{\text{water}}/K_{\text{absorbent}}$ ratio.	115
Table 22. Comparison of partition coefficient (K) for toluene in various solvents.	116
Table 23. Experimental conditions used in gas chromatography for measurements of VOCs mixture.	118
Table 24. K values of VOCs individually or in VOC mixtures in water (30°C).	118
Table 25. Absorption capacity of CO ₂ (50%) in different absorbents at 30 °C.	139
Table 26. Absorption capacity of CO ₂ (26%) CH ₄ (28%) in different absorbents at 30 °C.	139

List of Figures

Figure 1. Simplified schematic of an anaerobic digester process.....	9
Figure 2. Schematic of the AD process.	11
Figure 3. Typical sanitary landfill with underground protectors, leachate and gas collection systems, 2006 Brooks Cole-Thomson.....	12
Figure 4. Number of biomethane plants per country.....	16
Figure 5. Water scrubbing systems [84,118].	28
Figure 6. Selexol™ system (UOP Selexo (TM) Technology for Acid Gas Removal 2009 [84].	30
Figure 7. Chemical absorption scrubbing system [128].....	31
Figure 8. Principle of membrane separation [84].	33
Figure 9. Cryogenic separation system [118].	34
Figure 10. Pressure swing adsorption (PSA) [118].	36
Figure 11. Liquid-solid phase diagram of a binary mixture.	43
Figure 12. Deep eutectic solvents classification.	45
Figure 13. Distribution of publications on DES in the various domains (Scopus-consulted July 2023).	51
Figure 14. Methodology used in our study to evaluate DESs and conventional solvents as absorbents for biogas upgrading.....	62
Figure 15. Experimental viscosity of the studied DESs (a and b) and conventional solvents (c) as a function of temperature.	86
Figure 16. Experimental density of the studied DESs and conventional solvents as a function of temperature.	89
Figure 17. FT-IR of the prepared a) DES mixtures and their individual components: C ₁₀ :C ₁₂ , C ₁₂ and C ₁₀ . b) VOCs alone and VOCs mixture c) DES mixture, VOCs alone absorbed by DES and VOCs mixture absorbed by DES C ₁₀ :C ₁₂	90
Figure 18. Vial used for headspace analysis with different phases.	97
Figure 19. Several vials containing different amounts of water with the same amount of VOC [5].	98
Figure 20. Several vials containing same amounts of water with the different amount of VOC.....	100

Figure 21. Representation of the measurement of vapor–liquid partition coefficients (K) using static-headspace-gas chromatography (SH-GC).....	101
Figure 22. Areas of toluene in C ₉ :C ₁₂ and PC at 30 °C for different equilibrium times.	102
Figure 23. Partition coefficient (K) of a, b) toluene, c, d) limonene and e, f) siloxane D4 in the studied solvents at different temperatures.	108
Figure 24. Effect of initial toluene concentration on the absorption capacities of C ₉ :C ₁₂ at 30 °C.	111
Figure 25. Partition coefficient (K) of a, b) toluene, c, d) limonene and e, f) siloxane D4 in propylene carbonate (blue), propylene glycol (orange) and C ₉ :C ₁₂ DES (green) with different amount of water (10, 30 and 50 wt%) at 30 °C	113
Figure 26. K values of a) toluene in water, Rameb:Lev and ChCl:Lev in function of water and b) limonene and siloxane D4 in Rameb:Lev at 30 °C.	114
Figure 27. Absorption capacity of toluene (295 ppm) at 30 °C in the studied solvents and water/solvent mixtures.	117
Figure 28. Partition coefficient (K) of a, b) TLSD2 mixture in C ₁₀ :C ₁₂ , CO, BA, RL, PC, PG, PG16 and RPG at 30 °C.....	119
Figure 29. Absorption capacities of C ₉ :C ₁₂ for toluene during five consecutive cycles.	121
Figure 30. DES regeneration methods a) bubbling nitrogen + heating b) thermal desorption and c) bubbling nitrogen.	122
Figure 31. Three different types of regeneration capacity for absorption C ₁₀ :C ₁₂ for toluene during a period of twelve consecutive cycles.....	123
Figure 32. Absorption capacity of a) CO ₂ (99%) in C ₈ :C ₁₂ , C ₉ :C ₁₂ , C ₁₀ :C ₁₂ and RL, b) CH ₄ (99%) in C ₈ :C ₁₂ , C ₉ :C ₁₂ , C ₁₀ :C ₁₂ , and c) CO ₂ (50%) and CH ₄ (50%) in C ₈ :C ₁₂ at 35 °C.....	126
Figure 33. Dynamic absorption set-up used. For VOC absorption with syringe dispenser and N ₂ . In case of CO ₂ absorption, the syringe is replaced by a CO ₂ cylinder. For biogas absorption the N ₂ and syringe are replaced by a cylinder of biogas.	128
Figure 34. Absorption capacity (mg/g) of individuals VOCs, a) toluene, b) and c) siloxane D4 in water, PG16, RL, CO and C ₁₀ :C ₁₂ at 30 °C.....	130
Figure 35. Absorption capacity for different initial concentrations of toluene in C ₁₀ :C ₁₂ with different flow rates at 30 °C.	132
Figure 36. Absorption capacity of toluene in the water/solvent mixtures at 25 °C.	133
Figure 37. Toluene concentration in the outlet gas at 25 °C.	134

Figure 38. Absorption capacity of TLS mixture in water, PG16, RL, CO and C ₁₀ :C ₁₂ at 30 °C.	135
Figure 39. Absorption rate of an initial CO ₂ (50%) in TEPA:C ₈ :C ₁₂ :water _{20%} , C ₁₀ :C ₁₂ , C ₈ :C ₁₂ , PG, RL and water at 30 °C.	138
Figure 40. Absorption rate of biogas with initial concentration of CO ₂ (26%) and CH ₄ (28%) in C ₁₀ :C ₁₂ and RL at 30 °C.	140
Figure 41. Industrial-scale experiments with Terao® exchanger.....	142
Figure 42. Absorption capacity of toluene in the solvents and water/solvent mixtures at 20 °C.	143
Figure 43. Concentration of toluene in the outlet gas in water/BA mixtures at 20 °C.....	144
Figure 44. σ -Profiles of toluene, water, BA, AA and PG.	145
Figure 45. The free energy of solvation (ΔG_{sol}) of toluene in different solvents at 30 °C (a); the influence of temperature on the ΔG_{sol} of toluene in different pure solvents (b).	146
Figure 46. Absorption efficiency of VOCs in DESs and conventional solvents.....	151

List of Abbreviations

AA	Acetic acid
BA	Benzyl alcohol
C ₁₀	Decanoic acid
C ₁₂	Dodecanoic acid
C ₈	Octanoic acid
C ₉	Nonanoic acid
CH ₄	Methane
ChCl	Choline chloride
CO	Cooking oil
CO ₂	Carbon dioxide
COSMOS-RS	Conductor-like screening model for real solvents
DESs	Deep eutectic solvents
EBA	European biogas association
FT-IR	Infrared Spectroscopy
G	Glycerol
HBA	Hydrogen bond acceptor
HBD	Hydrogen bond donor
HS-GC	Head-space gas chromatography
K	Partition coefficient
L	Limonene
LA	Lactic acid
Lev	Levulinic acid
Mg/g	Milligram per gram
Mol/kg	Mol per kilogram
PC	Propylene carbonate
PG	Propylene glycol
PG16	Propylene Glycol (16% water content)
RAMEB	Randomly methylated β -cyclodextrin
RL	Rameb levulinic acid
RPG	Rameb propylene glycol
T	Toluene
TEPA	Tetraethylenepentamine
TLS	Toluene, limonene and siloxane D4
TLSD ₂	Toluene, limonene, siloxane D4 and decane
VOCs	Volatile organic compounds

Introduction

The way the world produces and uses energy is changing dramatically in the 21st century. Driving this change is a growing understanding of the environmental, economic and social benefits of switching to renewable energy sources. By moving away from the traditional reliance on finite fossil fuels, a more sustainable and environmentally conscious energy future is being explored. For nearly a century, fossil fuels such as coal, oil, and natural gas have been the world's primary source of energy [1,2]. However, their combustion releases greenhouse gases into the environment, including carbon dioxide and methane. These gases trap heat and contribute to global warming, causing climate change, extreme weather and rising sea levels. The environmental imperative of renewable energy stems from its ability to reduce greenhouse gas emissions, mitigate climate change, and preserve the planet's fragile ecosystems. The transition to renewable energy encourages innovation and economic expansion [3,4]. It motivates spending on manufacturing, R&D and building renewable energy infrastructure. Renewable energy is becoming more efficient and cost competitive as technology advances. Solar panels, wind turbines, energy storage devices and biogas have improved dramatically in terms of performance and cost effectiveness. With these improvements, renewable energy is becoming a viable and scalable alternative to traditional fossil fuel-based energy sources [5–7].

Biogas is a promising green and cost-effective energy source that aims at the valorization of waste materials from various industries. Therefore, the development of biogas plants for energy production is strongly encouraged [8,9]. Biogas could be produced from methanization of biomass and organic waste, anaerobic digestion of sewage sludge, commercial composting, landfills, anaerobic co-digestion of animal manure with energy plants, etc. [10]. Thus, a variety of feedstocks can be combined with different digestion techniques, resulting in biogas with different compositions. Besides the main compounds CH₄ (35-75%) and CO₂ (25-60%), biogas also contains many impurities, including gaseous inorganic compounds, nitrogen (N₂), oxygen (O₂), hydrogen sulfide (H₂S), ammonia (NH₃), carbon monoxide (CO), water vapor (H₂O), and numerous volatile organic compounds (VOCs) [11]. These VOCs include linear and aromatic hydrocarbons, terpenes, and siloxanes. Many of these compounds actively participate in ozone formation reactions and can have many

environmental, health and technological side effects. The upgrading of biogas to biomethane requires the removal of contaminants in the raw biogas to improve the quality, reducing the level of impurities to achieve a CH₄ content of about 90 to 99%, becoming a fully purified gas [12,13]. The applications of biogas are the same as natural gas, although it is a 100% renewable and non-fossil energy source. Many technologies have been tested and applied to remove impurities from biogas, such as water scrubbing, physical and chemical scrubbing, membrane separation, pressure swing adsorption, biological methods, etc. [14–17].

Physical absorption is considered to be an appropriate method that meets green technology and engineering standards [18,19]. Absorbents play an important role in removing impurities from biogas. Therefore, the development of novel absorbents with high absorption capacity and high recyclability is mandatory. The suitable absorbent should also have low viscosity, relatively low toxicity, low vapor pressure, high boiling point, high absorption capacity, and low cost [20,21]. Water, which combines all of these properties, is typically used in biogas purification processes, mostly for CO₂ capture [22,23]. However, since the majority of VOCs are hydrophobic, water is not the most suitable solvent for these compounds. Therefore, alternative green solvents are being sought to replace the currently used organic solvents. The first well-studied alternative solvents are ionic liquids (ILs), which are salts in the liquid state [24,25].

Recently, a new generation of green solvents, namely deep eutectic solvents (DESs), have also been successfully used as absorbents for VOCs [26–30]. DESs are a mixture of two or three chemical compounds that have a lower melting point than each of their pure components [31–33]. The typical DES components are hydrogen bond acceptors (HBAs), such as quaternary ammonium salts, combined with hydrogen bond donors (HBDs), such as amides, amines, alcohols, and carboxylic acids, in various molar ratios. DESs have similar physical and chemical properties to ILs and have some advantages such as easier preparation, lower cost, non-toxicity, non-reactivity, recyclability, non-corrosiveness, etc. The properties of DES are important factors in their applications. Physical solvents such as glycerol, propylene glycol, and propylene carbonate, which are considered environmentally friendly and green solvents, have also been studied for VOC or gas absorption [34–40].

In this context, the aim of the thesis was to evaluate DESs and conventional green solvents as VOC/CO₂ absorbers for biogas upgrading with a focus on biogas valorization. The manuscript is divided into four chapters: The first chapter consists of a state of the art of biogas upgrading to biomethane and its treatment methods will be presented in the first part. A second part is focused on the definition of eutectic solvents and an overview of the physicochemical properties of the most widely used DESs in the literature. The different applications of these solvents will also be presented. The strategy followed in our study to evaluate DESs and conventional solvents as VOC/CO₂ absorbers will also be presented.

The characterization of the studied DES and conventional solvents is presented in the second chapter. We measured the water content %, viscosities, densities as a function of temperature, and infrared spectra of DESs and its pure components, as well in presence of absorbed VOCs.

The third chapter evaluates the absorption capacity of DESs for different pure VOCs and their mixtures, by determining their partition coefficient between the gas phase and the absorbent, at different temperatures, concentrations and effects of water. The absorption capacity of CO₂/CH₄ in DES was also evaluated. To simulate an industrial absorption column, the absorption capacity was studied in dynamic bubbling method. This setup allowed us to test different conditions: Individual VOCs and their mixture, VOC concentration and CO₂/CH₄ absorption. This brought us closer to the reality of an industrial effluent. Finally, we determined the absorption capacities of absorbents using an exchanger developed by our industrial partner (Terrao®).

References

- [1] P. Pochwatka, S. Rozakis, A. Kowalczyk-Juśko, W. Czekata, W. Qiao, H.J. Nägele, D. Janczak, J. Mazurkiewicz, A. Mazur, J. Dach, The energetic and economic analysis of demand-driven biogas plant investment possibility in dairy farm, *Energy*. 283 (2023) 129165. <https://doi.org/10.1016/j.energy.2023.129165>.
- [2] O.O. Yolcan, World energy outlook and state of renewable energy: 10-Year evaluation, *Innovation and Green Development*. 2 (2023) 100070. <https://doi.org/10.1016/j.igd.2023.100070>.
- [3] M. Pouresmaeli, M. Ataei, A. Nouri Qarahasanlou, A. Barabadi, Integration of renewable energy and sustainable development with strategic planning in the mining industry, *Results in Engineering*. (2023) 101412. <https://doi.org/10.1016/j.rineng.2023.101412>.
- [4] C. Tansel Tugcu, A.N. Menegaki, The impact of renewable energy generation on energy security: Evidence from the G7 countries, *Gondwana Research*. 125 (2024) 253–265. <https://doi.org/10.1016/j.gr.2023.08.018>.
- [5] Y. Rao, K. Chibwe, D. Mantilla-Calderon, F. Ling, Z. He, Meta-analysis of biogas upgrading to renewable natural gas through biological CO₂ conversion, *J Clean Prod*. 426 (2023) 139128. <https://doi.org/10.1016/j.jclepro.2023.139128>.
- [6] P.F. Zito, A. Brunetti, G. Barbieri, Renewable biomethane production from biogas upgrading via membrane separation: Experimental analysis and multistep configuration design, *Renew Energy*. 200 (2022) 777–787. <https://doi.org/10.1016/j.renene.2022.09.124>.
- [7] A. Cabello, T. Mendiara, M. Teresa Izquierdo, F. García-Labiano, A. Abad, Energy use of biogas through chemical looping technologies with low-cost oxygen carriers, *Fuel*. 344 (2023) 128123. <https://doi.org/10.1016/j.fuel.2023.128123>.
- [8] T. Zhu, J. Curtis, M. Clancy, Promoting agricultural biogas and biomethane production: Lessons from cross-country studies, *Renewable and Sustainable Energy Reviews*. 114 (2019) 109332. <https://doi.org/10.1016/j.rser.2019.109332>.
- [9] A.K.P. Meyer, E.A. Ehimen, J.B. Holm-Nielsen, Future European biogas: Animal manure, straw and grass potentials for a sustainable European biogas production, *Biomass Bioenergy*. 111 (2018) 154–164. <https://doi.org/10.1016/j.biombioe.2017.05.013>.
- [10] D. Liu, B. Li, J. Wu, Y. Liu, Sorbents for hydrogen sulfide capture from biogas at low temperature: a review, *Environ Chem Lett*. 18 (2020) 113–128. <https://doi.org/10.1007/s10311-019-00925-6>.
- [11] I. Bragança, F. Sánchez-Soberón, G.F. Pantuzza, A. Alves, N. Ratola, Impurities in biogas: Analytical strategies, occurrence, effects and removal technologies, *Biomass Bioenergy*. 143 (2020) 105878. <https://doi.org/10.1016/j.biombioe.2020.105878>.
- [12] R. Noorain, T. Kindaichi, N. Ozaki, Y. Aoi, A. Ohashi, Biogas purification performance of new water scrubber packed with sponge carriers, *J Clean Prod*. 214 (2019) 103–111. <https://doi.org/10.1016/j.jclepro.2018.12.209>.
- [13] M.E. López, E.R. Rene, M.C. Veiga, C. Kennes, Biogas Technologies and Cleaning Techniques, in: *Environmental Chemistry for a Sustainable World*, Springer Netherlands, 2012: pp. 347–377. https://doi.org/10.1007/978-94-007-2439-6_9.

- [14] Adnan, Ong, Nomanbhay, Chew, Show, Technologies for Biogas Upgrading to Biomethane: A Review, *Bioengineering*. 6 (2019) 92. <https://doi.org/10.3390/bioengineering6040092>.
- [15] M. Struk, I. Kushkevych, M. Vítězová, Biogas upgrading methods: recent advancements and emerging technologies, *Rev Environ Sci Biotechnol*. 19 (2020) 651–671. <https://doi.org/10.1007/s11157-020-09539-9>.
- [16] J. Niesner, D. Jecha, P. Stehlík, Biogas upgrading technologies: State of art review in european region, in: *Chem Eng Trans, Italian Association of Chemical Engineering - AIDIC*, 2013: pp. 517–522. <https://doi.org/10.3303/CET1335086>.
- [17] K. Starr, X. Gabarrell, G. Villalba, L. Talens, L. Lombardi, Life cycle assessment of biogas upgrading technologies, *Waste Management*. 32 (2012) 991–999. <https://doi.org/10.1016/j.wasman.2011.12.016>.
- [18] Q. Sun, H. Li, J. Yan, L. Liu, Z. Yu, X. Yu, Selection of appropriate biogas upgrading technology—a review of biogas cleaning, upgrading and utilisation, *Renewable and Sustainable Energy Reviews*. 51 (2015) 521–532. <https://doi.org/10.1016/j.rser.2015.06.029>.
- [19] I. Angelidaki, L. Xie, G. Luo, Y. Zhang, H. Oechsner, A. Lemmer, R. Munoz, P.G. Kougias, Biogas Upgrading: Current and Emerging Technologies, in: *Biofuels: Alternative Feedstocks and Conversion Processes for the Production of Liquid and Gaseous Biofuels*, Elsevier, 2019: pp. 817–843. <https://doi.org/10.1016/B978-0-12-816856-1.00033-6>.
- [20] M. Ellacuriaga, J. García-Cascallana, X. Gómez, Biogas Production from Organic Wastes: Integrating Concepts of Circular Economy, *Fuels*. 2 (2021) 144–167. <https://doi.org/10.3390/fuels2020009>.
- [21] E. Ryckebosch, M. Drouillon, H. Vervaeren, Techniques for transformation of biogas to biomethane, *Biomass Bioenergy*. 35 (2011) 1633–1645. <https://doi.org/10.1016/j.biombioe.2011.02.033>.
- [22] E. Privalova, S. Rasi, P. Mäki-Arvela, K. Eränen, J. Rintala, D.Y. Murzin, J.-P. Mikkola, CO₂ capture from biogas: absorbent selection, *RSC Adv*. 3 (2013) 2979. <https://doi.org/10.1039/c2ra23013e>.
- [23] J.-G. Lu, X. Li, Y.-X. Zhao, H.-L. Ma, L.-F. Wang, X.-Y. Wang, Y.-F. Yu, T.-Y. Shen, H. Xu, Y.-T. Zhang, CO₂ capture by ionic liquid membrane absorption for reduction of emissions of greenhouse gas, *Environ Chem Lett*. 17 (2019) 1031–1038. <https://doi.org/10.1007/s10311-018-00822-4>.
- [24] W. Wang, X. Ma, S. Grimes, H. Cai, M. Zhang, Study on the absorbability, regeneration characteristics and thermal stability of ionic liquids for VOCs removal, *Chemical Engineering Journal*. 328 (2017) 353–359. <https://doi.org/10.1016/j.cej.2017.06.178>.
- [25] A.-S. Rodriguez Castillo, P.-F. Biard, S. Guihéneuf, L. Paquin, A. Amrane, A. Couvert, Assessment of VOC absorption in hydrophobic ionic liquids: Measurement of partition and diffusion coefficients and simulation of a packed column, *Chemical Engineering Journal*. 360 (2019) 1416–1426. <https://doi.org/10.1016/j.cej.2018.10.146>.
- [26] C.-C. Chen, Y.-H. Huang, J.-Y. Fang, Hydrophobic deep eutectic solvents as green absorbents for hydrophilic VOC elimination, *J Hazard Mater*. 424 (2022) 127366. <https://doi.org/10.1016/j.jhazmat.2021.127366>.
- [27] P. Makoś-Chełstowska, E. Słupek, J. Gębicki, Deep eutectic solvent-based green absorbents for the effective removal of volatile organochlorine compounds from

- biogas, *Green Chemistry*. 23 (2021) 4814–4827. <https://doi.org/10.1039/D1GC01735G>.
- [28] S. Fourmentin, D. Landy, L. Moura, S. Tilloy, H. Bricout, Ferreira M., Process for Purifying a Gaseous Effluent, WO 2018/091379 A1, 2018.
- [29] L. Moura, T. Moufawad, M. Ferreira, H. Bricout, S. Tilloy, E. Monflier, M.F. Costa Gomes, D. Landy, S. Fourmentin, Deep eutectic solvents as green absorbents of volatile organic pollutants, *Environ Chem Lett*. 15 (2017) 747–753. <https://doi.org/10.1007/s10311-017-0654-y>.
- [30] P. Villarim, E. Genty, J. Zemmouri, S. Fourmentin, Deep eutectic solvents and conventional solvents as VOC absorbents for biogas upgrading: A comparative study, *Chemical Engineering Journal*. 446 (2022). <https://doi.org/10.1016/j.cej.2022.136875>.
- [31] A.P. Abbott, G. Capper, D.L. Davies, R.K. Rasheed, V. Tambyrajah, Novel solvent properties of choline chloride/urea mixtures., *Chemical Communications*. (2003) 70–71. <https://doi.org/10.1039/b210714g>.
- [32] T. El Achkar, H. Greige-Gerges, S. Fourmentin, Basics and properties of deep eutectic solvents: a review, *Environ Chem Lett*. 19 (2021) 3397–3408. <https://doi.org/10.1007/s10311-021-01225-8>.
- [33] Q. Zhang, K. De Oliveira Vigier, S. Royer, F. Jérôme, Deep eutectic solvents: syntheses, properties and applications, *Chem Soc Rev*. 41 (2012) 7108. <https://doi.org/10.1039/c2cs35178a>.
- [34] C. Florindo, F. Lima, B.D. Ribeiro, I.M. Marrucho, Deep eutectic solvents: overcoming 21st century challenges, *Curr Opin Green Sustain Chem*. 18 (2019) 31–36. <https://doi.org/10.1016/j.cogsc.2018.12.003>.
- [35] H. Nie, H. Jiang, D. Chong, Q. Wu, C. Xu, H. Zhou, Comparison of Water Scrubbing and Propylene Carbonate Absorption for Biogas Upgrading Process, *Energy & Fuels*. 27 (2013) 3239–3245. <https://doi.org/10.1021/ef400233w>.
- [36] C. Ma, C. Liu, X. Lu, X. Ji, Techno-economic analysis and performance comparison of aqueous deep eutectic solvent and other physical absorbents for biogas upgrading, *Appl Energy*. 225 (2018) 437–447. <https://doi.org/10.1016/j.apenergy.2018.04.112>.
- [37] F. Lima, J. Gouvenaux, L.C. Branco, A.J.D. Silvestre, I.M. Marrucho, Towards a sulfur clean fuel: Deep extraction of thiophene and dibenzothiophene using polyethylene glycol-based deep eutectic solvents, *Fuel*. 234 (2018) 414–421. <https://doi.org/10.1016/j.fuel.2018.07.043>.
- [38] C. Florindo, L. Romero, I. Rintoul, L.C. Branco, I.M. Marrucho, From Phase Change Materials to Green Solvents: Hydrophobic Low Viscous Fatty Acid-Based Deep Eutectic Solvents, *ACS Sustain Chem Eng*. 6 (2018) 3888–3895. <https://doi.org/10.1021/acssuschemeng.7b04235>.
- [39] S. Panda, S. Fourmentin, Cyclodextrin-based supramolecular low melting mixtures: efficient absorbents for volatile organic compounds abatement, *Environmental Science and Pollution Research*. 29 (2022) 264–270. <https://doi.org/10.1007/s11356-021-16279-y>.
- [40] E. Słupek, P. Makoś-Chełstowska, J. Gębicki, Removal of siloxanes from model biogas by means of deep eutectic solvents in absorption process, *Materials*. 14 (2021) 1–20. <https://doi.org/10.3390/ma14020241>.

Chapter 1 – STATE OF THE ART

I. Biogas origin and definition

Biogas is a renewable energy source produced by the anaerobic digestion of organic materials such as agricultural waste, animal manure, sewage sludge, and food waste. It has been used for countless years, with roots in ancient cultures. The first use of biogas to heat bath water was discovered in Assyria in the 10th century. However, the first scientific studies on the combustible power of biogas were not carried out until the 18th century [1–3]. In 1884, Ulysse Gayon, a student of Louis Pasteur, concluded that the gas released from fermentation could be used as a source of energy for heating and lighting. The discovery and understanding of the process of anaerobic digestion in the 19th century led to advances in biogas technology. Sir Humphry Davy, an English chemist, discovered methane as the major component of biogas in 1808. Later, in the mid-1800s, an Indian civil engineer named Sir John Bennet Lawes created the first anaerobic digester, often known as a "septic tank," for sewage treatment. Biogas gained prominence as an alternative energy source in the early twentieth century, when high oil prices motivated the research for alternative energy sources [3–5]. The first biogas plant was developed in the United Kingdom in 1901, and similar plants were later erected in other regions of Europe. Biogas technology advanced further in the 1930s with the creation of the Kassel gas engine, which enabled the use of biogas as a fuel for internal combustion engines. In recent decades, due to the outbreak of the oil crisis, countries were forced to restructure their energy chain, especially considering the availability of non-renewable resources and the environmental impact of energy production processes [3,5–7]. The future energy matrices should reflect actions that reduce the burning of oil, natural gas, coal, and fuels of non-renewable origin. Great efforts and actions by governments are needed to minimize the concentration of greenhouse gases (GHG) emitted into the atmosphere. For instance, the Paris agreement determines a global strategy in order to limit the global warming to well below 2°C. Such negotiation is the main and most up-to-date international agreement against man-made climate change [8].

In this context, the renewable energies have gained representativity in the energy landscape thus, favoring the development, dissemination, and application of energy worldwide, providing a viable alternative to the current situation of scarcity of resources [9–12]. Rising

oil prices and environmental concerns have rekindled interest in alternative energy sources such as biogas. Governments and scholars began investigating biogas's potential as a sustainable energy source [13–15]. Biogas technology has changed over time, and many types of anaerobic digesters have been developed to improve the efficiency and scalability of biogas production. Biogas is a promising green and cost-effective energy sources, which aims at the valorization of waste materials from various industries. The development of biogas plants for energy production is therefore greatly encouraged [16].

Biogas is a flammable and colorless gas mixture produced by microbial communities, specifically methanogenic bacteria, during the anaerobic digestion of wet organic materials. Methanization is a naturally occurring biological mechanism in piles of decomposing organic matter, anaerobic sediments, or waterlogged soils [17,18]. In biogas manufacturing plants (anaerobic digester tanks), where the organic feedstocks are ideally from anthropogenic organic waste: agricultural waste, manure, food processing and food waste, municipal and domestic organic and green waste, sewage sludge, the methanization mechanism is now replicated on a large scale. Anaerobic digestion of organic matter produced digestate while also biogas, which is an advantageous byproduct. This is the undigested organic matter and (dead) microorganisms found in the solid-liquid fraction that is left over after digestion. It makes up approximately 90 percent of the volume of organic matter that was first injected into the digester [19,20]. The digests are being employed as alternatives to artificial fertilizers in the agricultural sector because they are high in nutrients (nitrogen, phosphorus, potassium, etc.). The degradable portion of the trash can be anaerobically digested by specific bacteria in landfills (landfill gas), where the compaction of the waste ensures that there is no oxygen present [17,21–25].

II. Biogas production

Biogas production is the process of producing an alternative source of energy, by the anaerobic digestion of organic waste. It consists of using the natural breakdown of biomass by microorganisms in the absence of oxygen, such as agricultural waste, animal manure, sewage sludge, and food waste [19,26–29]. The gathering and preparation of organic resources is the first step in the production of biogas. These materials are normally held in an anaerobic digester (AD), which is a closed container in which the anaerobic digestion process occurs. Continuous stirred-tank reactors, plug-flow digesters, covered lagoons, and fixed-

dome digesters are all forms of digesters, each one offering a specific set of advantages and applications [30,31]. In order to collect organic materials and turn them into biogas, either large-scale wastewater treatment facilities or small-scale household digesters may be implemented. The environment's conditions and the technology being used are related. Environmental factors like humidity and temperature promote the production of biogas. The leftovers from farming and domestic activities are converted into biogas, which is then used to produce electricity and heat [32,33]. There are several methods of producing biogas, each suited to different kinds of organic waste and varying scales of production. Here are some of the commonly used methods:

- Anaerobic digester (methanization)
- Landfill gas extraction
- Pyro-gasification

II.1. Biogas Production by Anaerobic Digestion (AD)

AD is a biological process that uses microorganisms to breakdown organic materials in the absence of oxygen, resulting in biogas production. Methanization, also known as methanogenesis, is a critical phase in anaerobic digestion in which specific bacteria transform organic breakdown intermediate products into CH_4 , CO_2 and other compounds [34,35]. Anaerobic digesters are home to complex microbial communities that collaborate to complete the various stages of organic waste breakdown as shown in figure 1.

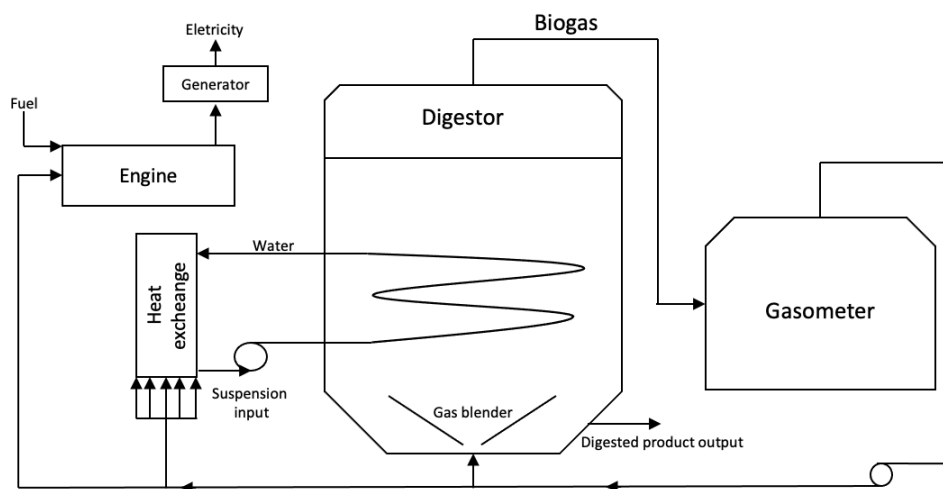


Figure 1. Simplified schematic of an anaerobic digester process.

Methanogenic microorganisms are essential to the methanization process. These microorganisms are classified into two groups: acetoclastic methanogens and hydrogenotrophic methanogens. Acetoclastic methanogens make methane directly from acetate, a byproduct of organic breakdown, while hydrogenotrophic methanogens produce methane from hydrogen and carbon dioxide. Each stage of the methanization process is supported by a certain microbial community. The main 4 stages include (1) hydrolysis, (2) fermentation or acidogenesis, (3) acetogenesis, and (4) methanogenesis (Figure 2) [36,37].

- Hydrolysis as the first stage of AD, hydrolyzed macromolecules of proteins, lipids and carbohydrates are broken down (or depolymerized) into smaller molecules such as amino acids (AA), monosaccharides (sugars) and long-chain fatty acids (LCFA). This is a slow stage, usually 2 or 3 days, in which the bacteria involved are not very sensitive to the pH or the redox potential of the medium.
- In the second stage, acidogenesis, the hydrolysis products are taken up and converted to volatile fatty acids (VFAs) such as propionate, butyrate, valerate and others, in addition to the formation of hydrogen.
- In the third step in acetogenesis, the VFAs are oxidized to acetate, hydrogen, and carbon dioxide. Acetogenesis is carried out through the action of two types of bacteria, acetogenic obligate hydrogen producing bacteria, which stimulate the anaerobic oxidation of VFA to acetate, and acetogenic hydrogen using bacteria, which produce acetate, as well as propionate and butyrate from hydrogen and carbon dioxide, thus helping to keep the partial pressure of hydrogen low in the process.
- Finally, in the last fourth stage methanogenesis, two classes of archaea produce methane. Hydrogen-trophic archaea use hydrogen as substrate and acetolactic archaea, which are predominant, use acetate as substrate. The efficiency and rate of biogas production can be influenced by various factors, such as temperature, pH, the composition of the organic matter, and the presence of inhibitory substances. The biogas production process is typically monitored and controlled to ensure optimal conditions for biogas production and to prevent the growth of harmful microorganisms. The process of methanization, where specialized bacteria transform intermediate chemicals into methane, the main component of biogas, is an essential stage in the anaerobic digestion process.

Anaerobic digesters can operate at their best and produce biogas with minimal waste by having a thorough understanding of the methanization process and the elements that influence it. Anaerobic digestion applications for waste management and sustainable energy production are being expanded, the methanization process is being further improved, and biogas outputs are being increased [38–40].

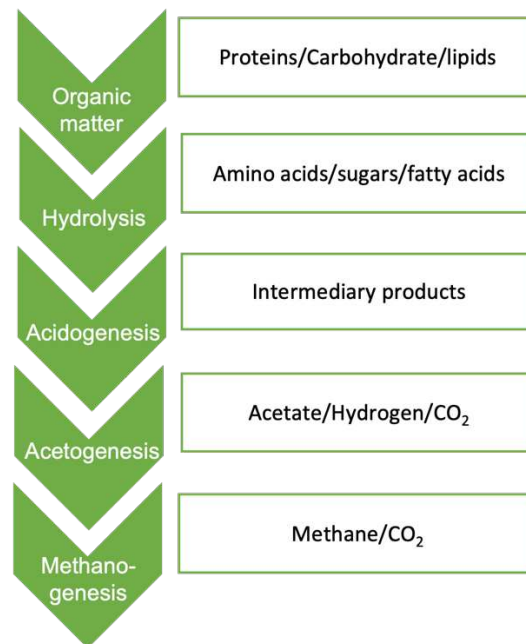


Figure 2. Schematic of the AD process.

II.2. Landfill

Another important source of biogas production is landfill gas (Figure 3). Landfill gas (LFG) is a mixture of gases that are produced when organic waste, such as food scraps, yard trash, and other biodegradable materials, decomposes in a landfill [41,42]. In essence, landfills are sizable locations for disposing of solid trash where waste is placed and covered with soil or other materials for faster up decomposition and reduce environmental damage. As organic waste decomposes in an anaerobic (oxygen-free) environment, it produces biogas, primarily methane, through the spontaneous methanization of the organic (fermentable) fraction of solid wastes buried and compacted in sanitary landfills. Gas collecting systems are installed to gather and utilize the biogas produced in landfills. In order to extract gas, these systems typically comprise wells or pipes strategically positioned within the landfill. Therefore, sanitary landfills produce more gas than non-sanitary landfills because leachate and rainwater

are collected at the bottom, and it can be re-injected into the cells to keep the waste hydrated and further stimulate gas production [24,43,44]. Other factors influencing gas production include the pH, the kind and age of the wastes, and the temperature in the waste cells (the higher the temperature, the more favorable for the microbiota, and the more gas produced). The gas is then collected and delivered to a treatment facility, where it is purified to eliminate contaminants and enhance its methane content. During the landfill's lifetime, the rate and content of landfill gas vary. In general, considerable gas production begins 1 to 3 years following the waste burial, peaks after 5-7 years, and continues at appreciable levels for up to 20 years. Limited gas amounts may continue to be produced for up to 50 years. The efficiency and composition of landfill gas might vary based on variables such as waste age and composition, landfill management procedures, and environmental conditions. To achieve optimal gas recovery and minimize environmental consequences, landfill gas collection systems must be monitored and maintained on a regular basis. Due to the vast amounts of waste generated and degraded in landfills, landfill gas is considered a significant renewable energy source. The capture and use of landfill gas not only provides a sustainable energy choice, but also helps with waste management and environmental preservation by lowering methane emissions, minimizing odor issues, and facilitating the controlled breakdown of organic waste [25,45].

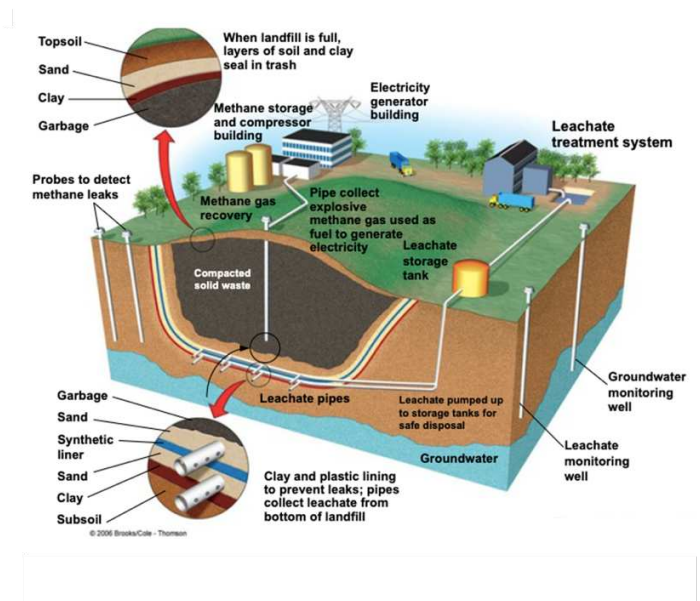


Figure 3. Typical sanitary landfill with underground protectors, leachate and gas collection systems, 2006 Brooks Cole-Thomson.

II.3. Pyro-gasification

Pyro-gasification is a thermal conversion process that converts biomass into syngas, a useful gas combination. It refers to exposing biomass to high temperatures in a controlled setting, usually without or with a limited oxygen supply. Pyro-gasification is an effective and sustainable technique of utilizing biomass, producing syngas that may be utilized for a variety of energy and chemical applications [46,47]. Pyro-gasification involves a biomass preparation step, which begins with the processing of biomass feedstock. Biomass can consist of a wide range of organic resources, including wood chips, agricultural leftovers, energy crops, and dedicated energy crops. Typically, the biomass is dried to minimize moisture content and thus improve the effectiveness of the pyro-gasification process.

The pyrolysis stage is where the biomass heads after it is fully prepared. Pyrolysis is the heat breakdown of biomass without oxygen or with little oxygen present. High temperatures are applied to the biomass in a reactor, typically between 600°C and 1200°C. The complex organic constituents of biomass decompose into volatile vapors, coal tars and solid coal at extremely high temperatures [48–50].

In the gasification stage, the pyrolysis-produced volatile gases receive additional processing to create syngas. Reforming, steam gasification, and partial oxidation are a few of the reactions that occur during gasification. These processes turn the solid coal and volatile gases into syngas. Carbon monoxide CO, H₂, CH₄, CO₂, and trace amounts of other gases represent the majority of the syngas. Through the processes of pyrolysis and gasification, the thermal conversion process known as pyro-gasification converts biomass into syngas. It provides an effective and sustainable way of using biomass, allowing for the formation of syngas that may be used for energy production [51–53].

III. Global, Europe and France situation of biogas production

The global biogas production industry is growing rapidly, driven by increasing demand for renewable energy, the need to reduce greenhouse gas emissions, and the desire to improve waste management practices. In 2021, the global biogas market was valued at around \$11 billion and is expected to grow at a compound annual growth rate (CAGR) of over 8% through to 2026. Between 2000 and 2017, the production of biogas on a global scale more than tripled

(from 78 to 364 TWh). Europe, China, and the United States of America are the top three producers of biogas and biomethane globally [54–56]. The United States has established biogas industries in North America, but the market is still relatively limited in comparison to Europe and Asia, because landfill biogas accounts for 90% of biogas produced in the United States. However, there is growing interest in the development of biogas projects in the region, driven by the need to reduce greenhouse gas emissions and improve waste management practice. In Asia, China is emerging as a major player in the biogas market, driven by government support for renewable energy and efforts to reduce air pollution. Small-scale anaerobic digesters for households have received support, however, and can produce up to 70% of the country's installed biogas capacity. India is also making significant investments in biogas production, with the government aiming to increase the share of biogas in the country's energy mix to 10% by 2022 [1,57,58]. Additionally, Brazil has 127 biogas plants that use sewage sludge, landfill trash, industrial and agricultural waste to produce 584 billion Nm³ of biogas per year, which helped to produce 3835 GWh of energy in 2015 [59]. The global biogas production industry is expected to continue to grow in the coming years, as more countries adopt renewable energy targets and seek to reduce their environmental impact. The increasing availability of feedstocks, such as food waste and agricultural waste, and advances in technology are also expected to drive growth in the industry. Europe is the largest biogas production market in the world, with a long history of investment in the sector and a well-established infrastructure [60,61]. Due to the fact that anaerobic digesters produce most of their biogas from energy crops and organic waste. For instance, 1023 biomethane plants have been deployed in Europe, and about 20000 units in operation, which is total number of biogas and biomethane plants. France, Italy, and Denmark are the countries with the largest increase on the number of biomethane plants. No less than 91 new units began operation in France in 2020 and 123 plants started operation between January and October 2021. According to EBA estimates, 87% of currently active biomethane plants in Europe are connected to the gas grid (Figure 4). Germany is the leading biogas producer in Europe and has been at the forefront of the industry for many years. The country has a large number of biogas plants and a supportive policy environment, including incentives for renewable energy production. In addition, Germany has a well-developed infrastructure for the collection and treatment of organic waste, making it an ideal environment for biogas production. The UK is another major player in the European biogas market, with an increasing number of projects

being developed in the country, particularly in the agricultural and waste sectors. The UK government has set a target of generating 12% of its energy from renewable sources by 2020, which is driving investment in biogas production [62–65].

Other countries in Europe that have a significant biogas production industry include Italy, Sweden, France and the Netherlands. These countries have established policies to support the development of the biogas industry, including incentives for renewable energy production, feed-in tariffs and subsidies for research and development. Broadly, Europe is expected to continue leading the global biogas market in the coming years, driven by strong policy support for renewable energy, availability of feedstock, and growing demand for clean energy. According to the latest estimations of the European Biogas Association, biogas production will increase up to 20 billion Nm³ by 2020 and will represent a significant share of Europe's natural gas consumption. The region is also expected to benefit from advances in technology and increasing efficiency of biogas production processes.

France has a growing biogas industry, driven by the country's commitment to reducing greenhouse gas emissions and increasing the use of renewable energy. By the year 2020, there were 1075 biogas plants operating in France, of which 20% (214 plants) valorize biogas through combined heat and power generation and the remaining 80% (861 plants) convert biogas into biomethane for grid injection. Also, France has the most biomethane facilities, and in 2020, French biomethane accounted for 0.5% of French natural gas consumption. The French government has set a target of producing 6.5 TWh of energy from biogas by 2023 and has introduced a number of policy measures to support the development of the biogas industry. The most biogas production is based on the treatment of agricultural waste and sewage sludge, although there is also significant potential for the use of food waste and other organic waste streams [64,66–68]. The country has a well-developed waste management infrastructure, making it an ideal environment for the development of biogas projects. In terms of biogas use, France has a relatively small number of biogas-to-energy projects, but this is expected to change in the coming years as more biogas plants are developed. The French government has instituted a number of incentives for renewable energy production, including feed-in tariffs, research and development subsidies and tax credits, which are helping to stimulate investment in the biogas industry. In addition, according to the foregoing

tensions in the supply of Russian gas, France and the European Union are betting on biogas. Biogas could provide 7-10% of consumption in France by 2030, or half the gas imported from Moscow (Moussu, n.d.), April 2022, “Europe rediscovers biogas in search for energy independence” (www.euractiv.com/authors/nelly-moussu/). Overall, the biogas industry in France is expected to grow rapidly in the coming years, boosted by the country's commitment to reduce greenhouse gas emissions and increase the use of renewable energy. Increasing feedstock availability and technological advances are also expected to drive industry growth [55–57,61].



Figure 4. Number of biomethane plants per country.

(Source : <https://www.sia-partners.com/en/news-and-publications/from-our-experts/6th-european-biomethane-benchmark>).

IV. Biogas valorization

Biogas is a renewable energy source created by anaerobic digestion of organic waste, whereas biomethane is a purified and upgraded form of biogas. Biogas and biomethane both have various advantages, including lower greenhouse gas emissions, waste management, and energy independence. Biogas and biomethane can be efficiently valorized in various industries by tapping their potential, leading to a more sustainable and resilient energy system. Biogas may be used to create both heat and electricity in combined heat and power (CHP) systems [69–71]. This is especially valuable for on-site energy production in companies, agriculture, and wastewater treatment plants.

The electricity generated may be utilized to power equipment and lights, while waste heat can be collected and used for heating or other industrial operations, increasing total energy efficiency. Biogas can also be used directly for cooking and heating in places without access to clean cooking fuels or stable energy sources. Biogas-based cooking solutions, such as biogas stoves or biogas burners, offer a clean and sustainable choice for households and communities, increasing indoor air quality while decreasing dependency on traditional biomass fuels. Also, there are several industrial uses for biogas, including as a fuel for dryers, boilers, and other thermal operations [72–74]. Biogas can be used as an alternative to fossil fuels in industries including food processing, manufacturing, and chemical production, resulting in lower emissions and a less detrimental effect on the environment. Addressing renewable energy production in agricultural applications, thus being able to supply electricity for agricultural operations, irrigation systems and farm equipment, reducing dependence on grid electricity and fossil fuels. Furthermore, the digest produced during anaerobic digestion can be used as a nutrient-rich crop fertilizer, closing the nutrient loop and advancing sustainable agricultural methods [75–77].

Biogas can be further upgraded to remove impurities such as carbon dioxide and other trace gases, yielding pure biomethane, which is a higher quality fuel with higher energy content and lower carbon emissions. Biomethane can be used as a direct substitute for natural gas, and it may be injected into the gas grid. However, biomethane can be also further compressed as natural gas (CNG) or liquefied biogas (LBG), which can be utilized as a transportation fuel. By lowering greenhouse gas and air pollution emissions, improving air quality, and decreasing climate change, biogas-based transportation fuels provide considerable environmental advantages. Biomethane must meet certain quality standards, such as those set by the European Union, in order to be used for various applications [22,78]. The specific use of biogas valorization depends on its quality and availability, as well as local conditions and regulations. A complete strategy to optimize the advantages of this renewable energy source is provided by biogas valorization. Biogas helps to sustainable development, energy security, waste management, and environmental protection by utilizing a variety of applications across numerous industries. The utilization and potential of biogas valorization will be further improved by ongoing research, technological breakthroughs, and supportive legislation in the transition to a cleaner and more sustainable energy future [71,72,79].

V. Biogas composition

Biogas is a mixture of gases that are produced through the methanization of biomass and organic waste, from the anaerobic digestion of sewage sludge, commercial composting, landfills, anaerobic co-digestion of animal manure with energy plants, etc. The exact composition and concentration of biogas depends on the feedstock used, that can be combined with different digestion techniques. Biogas usually contains CH_4 (35-75%) and CO_2 (25-60%) as main components and many impurities, including gaseous inorganic compounds, nitrogen (N_2), oxygen (O_2), hydrogen sulfide (H_2S), ammonia (NH_3), carbon monoxide (CO), water vapor (H_2O) as well as numerous volatile organic compounds (VOCs) such as linear and aromatic hydrocarbons, halogenated compounds, terpenes, and siloxanes (Table 1) [78,80–82]. Many of these compounds, aggressively contribute to ozone formation reactions and can have many environmental, health problems and cause serious damage to equipment using biogas as fuel. Water vapor is one of those compounds that can condense on the surface of the equipment and consequently promote the corrosion of the metal parts. In addition, the high moisture content of the biogas can reduce the calorific value of the biogas [83,84]. The sulfur content of biogas is the main cause of corrosion in the pipes, in the recovery equipment and in the heat exchangers on the flue gas. Some bacteria (bacteroids or others) can also produce NH_3 , that can accelerate and amplify combustion, causing thermal stresses that can lead to the melting of pistons and heating of injectors. During the combustion of biogas, it is totally transformed into NO_x , which is a dangerous pollutant for the environment. However, oxygenated and halogenated compounds are generally produced by incomplete degradation of plastic or petroleum products causing problems of corrosion of metal surfaces by the formation of acid gas. Finally, aromatic, aliphatic compounds, terpenes and siloxanes are produced mainly by volatilization. These molecules are abundant in the presence of household products, pesticides, and products of plant origin [85,86].

Table 1. Typical range of biogas and biomethane compositions.

Compounds	Landfills	Anaerobic digestion	Biomethane
CH ₄ (vol %)	35–65	53–70	90-99
CO ₂ (vol %)	15-50	30-50	0.06
H ₂ S ppm	0-100	0-10	1-3
VOCs (mg.m ⁻³)	0-4500	0.5-1545	0 < 5
H ₂ O (vol %)	0-5	5-10	0
NH ₃ (vol %)	0-5	0-100	0
N ₂ (vol %)	5-40	0-3	0

Ref. [22,61,87]

Most of the secondary compounds are formed at different levels of methanization. In general, an initial concentration of secondary compounds is formed during the aerobic phase. It is caused by the evaporation of volatile compounds such as aerosols. A second concentration of compounds is observed during anaerobic methanogenesis. Those compounds are due to the production of by-products and intermediates of the anaerobic degradation. The concentration of these secondary products changes according to the nature of the initial substrate, the process conditions (temperature, pH, humidity, etc.) [84,88,89].

In summary, landfill biogas consists primarily of methane and carbon dioxide. It may also contain secondary compounds such as sulfur compounds, nitrogen compounds, heavy or light hydrocarbons. The differences in terms of composition are due to the nature of the waste used, the microorganisms carrying out the methanization and the conditions of the process [14,25].

The presence of these impurities reduces the usability of biogas, making it suitable only for low energy efficiency applications, such as heating and power generation, thus limiting the development of the anaerobic digestion industry. The methane content of biogas can exceed 90% when impurities are removed by upgrading technologies. The upgraded biogas can be used to power homes, factories and vehicles, or injected directly into a natural gas pipeline network. Furthermore, carbon dioxide capture helps meet government policy targets to reduce carbon emissions and achieve carbon neutrality. Consequently, biogas upgrading technology is now attracting worldwide attention [23,83,89].

V.1. CO₂ and CH₄

Carbon dioxide (CO₂) and methane (CH₄) are the two main compounds of biogas, each with unique properties and implications for their uses. The CO₂ is produced as a natural sub-product of the anaerobic digestion process, while methane is the desirable compound due to a high energy value. During anaerobic digestion, microorganisms break down organic matter in the absence of oxygen, thus producing biogas. CO₂ is generated as a result of microbial metabolism and the decomposition of carbon-rich organic compounds. The concentration of CO₂ in biogas can vary depending on several factors, including the type of feedstock, process conditions and the efficiency of the anaerobic digestion system. It is a colorless and odorless gas that is also present in the atmosphere. Higher concentrations of CO₂ in biogas reduce their energy content and calorific value, thus reducing their efficiency for certain applications[81,82,88].

Meanwhile, CH₄ is the main and most important compound responsible for the energy potential and versatile applications of biogas. It is a flammable, odorless gas with a much higher calorific value than CO₂. It is produced by specific groups of micro-organisms known as methanogens during the anaerobic digestion process. Methanogens are responsible for converting various organic compounds, such as carbohydrates, fats and proteins, through a series of biochemical reactions to produce methane. The concentration of methane in biogas is a critical factor in determining the energy potential and usability of biogas. Methane has a variety of applications, including electricity generation, heat production and use as a vehicle fuel. Nevertheless, the presence of methane in biogas also causes problems, mainly due to the fact that it is a potent greenhouse gas with a much higher global warming potential than CO₂ [67,90,91].

It is critical to understand the composition and properties of CO₂ and CH₄ in biogas in order to properly use and manage this renewable energy source. The presence of CO₂ influences the energy content and calorific value of biogas. CO₂ acts as a diluent, lowering the methane ratio and, as a result, the energy potential of biogas. High CO₂ concentrations also have a lower calorific value, limiting the efficiency of biogas use for applications such as electricity generation, heating, and transportation.

To fully utilize the energy value of biogas, methane content must be optimized, and CO₂ levels must be reduced. Strategies for increasing CH₄ concentrations and decreasing CO₂ concentrations in biogas are critical for optimizing their energy potential and environmental impact [92]. Once released into the atmosphere, both CO₂ and CH₄ causes environmental problems. While CO₂ is a greenhouse gas that contributes to long-term global warming and climate change, CH₄ has a much higher global warming potential. CH₄ is a strong greenhouse gas, and its emissions have a more immediate impact on climate change. It is critical to effectively manage CH₄ emissions from biogas systems in order to reduce the environmental impact and maximize the climate benefits of using biogas as a renewable energy source.

Operational process also can be used to optimize the CH₄ concentration in biogas. These include improving biogas performance by optimizing digester conditions, controlling feedstock composition, increasing microbial activity, and improving digester conditions. Furthermore, biogas uses can be improved through the procedure of combined heat and power (CHP) systems, increasing biomethane production. There are a variety of technologies available to remove or reduce the concentration of CO₂ in biogas. Water scrubbing, chemical absorption, membrane separation, cryogenic upgrading, pressure swing adsorption, and solid adsorbers are examples of these. These technologies remove CO₂ selectively, resulting in biogas with higher methane content and improved energy quality [84,86,89].

Finally, understanding the effects of CO₂ and CH₄ in biogas is critical for efficient biogas uses and environmental management. Biogas can be linked as a sustainable energy source by implementing appropriate CO₂ removal and CH₄ upgrading strategies, allowing the full potential of this renewable energy source to be achieved while minimizing the environmental footprint. This aims to provide information on the properties, management and potential applications of CO₂ and CH₄ in biogas, thus promoting the biogas industry and sustainable energy transition [93].

V.2. Volatile organic compounds (VOCs)

VOCs are organic molecules with high vapor pressure and low water solubility that can be easily released into the atmosphere from a variety of sources, including natural processes and human activities. Industrial processes, such as oil refining, chemical synthesis, flavor and paint

factories, transport, domestic activities are considered to be the largest sources of anthropogenic VOC emissions [94,95]. However, biogas contains not only CH₄ and CO₂, but also a variety of VOCs. Although biogas primarily is for use as a clean energy resource, the presence of VOCs can have consequences for biogas use, safety and environmental impact. Following this, understanding the nature and characteristics of VOCs in biogas is crucial for the effective management and optimization of this renewable energy source [96].

The precise composition of biogas varies depending on the feedstock and methanization process conditions, influencing the types and concentrations of VOCs present. Organic materials with varying chemical compositions, such as agricultural waste, food waste, and wastewater sludge, can contain a wide range of VOCs. Pesticides, herbicides, and other chemical residues in the feedstock can increase the VOC content of biogas [97–99]. In addition to these majority compounds, some minority compounds may also be produced. In fact, different types of secondary compounds are usually identified in landfill biogas. These can be classified into families of compounds according to their chemical structure and functional group [100–102].

Certain VOCs present in biogas can pose safety risks due to their flammability and potential toxicity. They are hazardous to human health and the environment, and when biogas is not properly treated or combusted, they can contribute to air pollution and ground-level ozone formation. Several VOCs can also reduce the combustion efficiency and stability of biogas in a variety of applications, including electricity generation and heating. Furthermore, the corrosive nature of some VOCs can cause problems with the equipment and infrastructure used in biogas uses. A variety of methods can be used to control and minimize VOC emissions, including improving industrial processes, using alternative materials and upgrades technologies. Regular inspection and analysis of VOCs present in biogas can provide useful information on VOC concentrations, composition, and potential hazards. Gas chromatography and other analytical techniques can be used to detect and determine the VOCs present in biogas [97,99,103,104].

VOCs are found in the final biogas in trace amounts (< 1%). They usually can come from biodegradation of organic matter, reactions between majority or minority products and volatilization of compounds. They may vary by feedstock composition. VOCs can be classified according to several criteria, and three categories can be identified:

- Chemical structure: the VOCs can be classified according to their chemical structure as aliphatic hydrocarbons, aromatic hydrocarbons, halogenated, oxygenated, terpenes, siloxanes compounds and nitrogen-containing compounds. Each category has distinct chemical properties and reactivity.
- Volatility: VOCs can be classified by their volatility. They are divided into two groups: low volatility compounds (LVOCs) and high volatility compounds (HVOCs). LVOCs have lower vapor pressures and tend to have a longer atmospheric lifetime, while HVOCs have higher vapor pressures and can evaporate quickly in the atmosphere.
- Source or origin: VOCs can be found by natural sources, such as biogenic VOCs emitted by plants and trees, as well as anthropogenic sources, such as industrial emissions, biogas production, vehicle exhaust and household products.

In order to avoid future problems with impurities in biogas, some upgrade technologies, such as physical and chemical absorption, adsorption, condensation, thermal or catalytic oxidation and advanced oxidation processes, can remove or decrease the concentrations of impurities in biogas [23,105].

Table 2. Sources and production processes of VOCs present in biogas.

VOCs	Group	Definition	Source
BTEX Benzene Toluene Ethylbenzene Xylene	Aromatic hydrocarbon	Hydrocarbons that include one or more benzene rings.	Solvents and petroleum products, plastic, cardboard and food additives
Limonene Pinene <i>p</i> -Cymene α -carene β -Carene	Terpene	Hydrocarbons containing 10-carbons with an isoprene unit	Decomposition of citrus fruit, wood, needles, plants waste, medicines and detergents.
Octamethyltri-siloxane (L3), Decamethyltetra-siloxane (L4),	Siloxanes	Cyclic compounds containing Si-O bonds	Household products such as shampoo and deodorant.

Hexamethylcyclotri- siloxane (D3), Octamethylcyclotetra- siloxane (D4)			
Pentane Pentene 1-Butene Nonane Decane Dodecane Undecane	Alkanes (Aliphatics)	Hydrocarbon chains, saturated, unsaturated, linear or branched	Oils, solvents, pesticides and detergents.
Dichloromethane 1,2-Dichlorobenzene 1,4 Dichlorobenzene	Halogens	Fluorine, chlorine or bromine compounds	Solvents, plastics, deodorants.

Ref. [78,97,99,102].

VI. Biogas upgrading to biomethane (technologies)

As biogas is the result of the breakdown of organic materials, biogas is not 100% pure, therefore, in order to fully maximize the energy potential of biogas, it can be upgraded to biomethane, a purified form of biogas with a higher methane content. Biogas upgrading technologies have a crucial contribution to be able to upgrade biogas to biomethane, thus, removing impurities such as CO₂, H₂S, VOCs and moisture, which increases the CH₄ concentration in the gas to up 95%. in order to use it for various applications, including electricity and gas grid injection, transport fuel and heat production [106,107].

Many technologies have been tested and applied to remove impurities from biogas, such as the most common ones currently used: water purification, physical and chemical purification, membrane separation, pressure balance adsorption, biological methods. The choice of upgrade method depends on the specific requirements and characteristic of the biogas, including the composition, flow rate and pressure. Table 3 shows the advantages and disadvantages of the different methods used for biogas upgrading. The biogas purification for biomethane production is based on leading technologies in the field of gas separation. This section gives an insight into the different biogas upgrading technologies, their operating principles and their applications in biomethane production [85,86,108–110]

Table 3. Comparison of different physicochemical biogas upgrading technologies.

Method	Mechanism	Material Condition	Advantage	Disadvantage	Efficiency
Pressure swing adsorption	According to the different affinity between gas molecules and adsorption materials, biogas components are separated	Zeolite; activated carbon; polymer, etc	Low-cost Simple operation; High methane content; No chemical demand	Pretreatment required; Risk of contamination	CH ₄ content 96–98%; CH ₄ loss ~4%; recovery >96%
Water scrubbing	Based on the solubility diversity of different gases in water under high pressure, CO ₂ and H ₂ S are removed	Water; 6–10 bars	No chemicals Renewable water	High voltage o High energy consumption o Risk of contamination	CH ₄ content 95–98%; CH ₄ loss 0.5–5%; recovery >97%
Organic solvents absorption	According to the solubility diversity of different gases in organic solvents, gas impurities are removed	Propylene glycol, propylene carbonate, DESs	Simple operation Low methane loss	Need for organic solvents; High temperature	CH ₄ content 93–98%; CH ₄ loss 1–4%; recovery >99%
Membrane separation	Separate biogas components in layers according to the selectivity and permeability of the membrane	Inorganic membrane; polymeric membrane; mixed matrix membrane	No chemicals Low energy consumption Simple operation; Environment friendly	High cost Easily damaged Low selectivity Pretreatment required	CH ₄ content 90–99%; CH ₄ loss <2%; recovery 96–98%
Cryogenic separation	Based on the principle that gas condenses or sublimates at low temperature or high pressure	80 bars; –170°C	High recovery; Environment friendly	High cost; High energy consumption Under development	CH ₄ content ~99%; CH ₄ loss <2%; recovery >99%

Ref. [80,111,112].

VI.1. Physicochemical Methods

Physicochemical methods are crucial in the biogas valorization and purification, allowing the removal of impurities, the increase of methane content and the production of high quality biomethane. The latest and most popular ones are based on the physicochemical removal of CO₂. These physicochemical methods include physical absorption (water scrubbing, organic solvent scrubbing), chemical absorption, adsorption, cryogenic separation, pressure swing adsorption (PSA), membrane technology and chemical hydrogenation process. Several of these are currently available commercially. These methods involve the use of physical and

chemical processes to upgrade the biogas, thus making it suitable for multiple energy applications. In general, methane recovery from physicochemical processes can be up to >96% [106,108,109,113].

VI.2. Physical Absorption

Physical absorption techniques, both water scrubbing and organic solvent scrubbing, utilize the fact that CO₂ and CH₄ have different solubilities in different solvents (Table 4). Thus, by selecting a solvent that has a high solubility for CO₂ but does not absorb CH₄, the two gases can be separated. These methods often use absorbent substances to remove specific impurities from the biogas stream, such as CO₂, H₂S, and trace VOCs. Absorption of VOCs from gases by dissolving them in liquid solvents has been considered an attractive method due to its low price, recyclability, simplicity, and safety. Typical absorption processes with an aqueous solution (acidic, basic, or oxidizing) have been widely employed to remove soluble pollutants from gaseous effluents by creating contact between contaminated gases and liquid solvents. While hydrophilic VOCs can be easily removed by water absorption, hydrophobic VOCs have low water solubility as the lower mass transfer properties of its gas phase to the aqueous phase make removal efficiencies very limited [89,114].

Table 4. Comparison of water and organic solvent scrubbing.

Characteristic	Water scrubbing	Organic solvent scrubbing
Absorbent	Water	Organic solvents (e.g. glycols)
Impurity Removal	Primarily water-soluble gases, especially CO ₂	Wide range of impurities including CO ₂ , H ₂ S, and trace contaminants
Application Scale	Small to medium-scale systems	Small to large-scale systems
Selectivity	Less selective, primarily removes CO ₂	High selectivity, can target specific impurities
Solvent Regeneration	Not required, water can be reused	Required, solvents need regeneration
Considerations	Contact time, mass transfer rates, managing absorbed impurities and wastewater	Solvent selection, optimization of operational parameters, solvent regeneration techniques, proper management of solvents and waste streams

Cost and Complexity	Relatively simple and cost-effective	Moderate complexity, may require additional equipment
Environmental Considerations	Minimal environmental impact	Proper management of solvents and waste streams required
Efficiency	Limited removal of non-water-soluble gases	Effective removal of both water-soluble and non-water-soluble gases

VI.2.1. Water scrubbing

The crucial requirement for absorption is the choice of a suitable solvent. In order to be suitable for gas solubility, a solvent must also have the following properties to be efficient and economical: availability, cost stability, volatility and non-hazardousness. Water is a selective absorbent in this scenario due to low sensitivity to biogas pollutants. A common physical absorption method used to purify biogas is water scrubbing, also known as wet scrubbing or water purification. It currently accounts for 41% of the global biogas recovery market. At approximately 25°C, CH₄ is 26 times less soluble than CO₂. Moreover, these molecules are separated through the various bonding forces between the non-polar CH₄ and the more polar CO₂ or H₂S. In general, H₂S and CO₂ can be eliminated jointly because H₂S is more soluble in water than CO₂.

However, it is desirable to separate the H₂S before the CO₂ due to a number of benefits, namely, the fact that removal of the dissolved H₂S reduces operational issues like motor corrosion and odor annoyance issues [75,85,88].

In order to achieve effective gas-liquid mass transfer, water scrubbing is performed in a column packed with unstructured packing material in a countercurrent with water pressures coming from the top and compressed gas pressures of 6–10 bar from the bottom as shown in Figure 5. Depending on the proportion of non-condensable gases, such as N₂ and O₂, which cannot be separated from CH₄, water scrubbing can yield a CH₄ purity of 80%–99%. Currently, there are two techniques for reusing water, The first method, which is called single pass scrubbing, is used if the water comes from wastewater treatment plants. The second technique, known as "regenerative scrubbing", allows the water to be decompressed (often by removing air) in a desorption column at atmospheric pressure, which removes CO₂ and H₂S [115].

The fact that no chemicals are used at any point during the procedure is certainly an advantage. The process of purifying water is, however, also linked to some operational issues, such as clogging of the purifiers owing to the growth of microorganisms while they are in use and the disposal of the wastewater. Additionally, bubbling can happen when the absorber's flow rate is improperly controlled and when there are contaminants in the water [110,116,117].

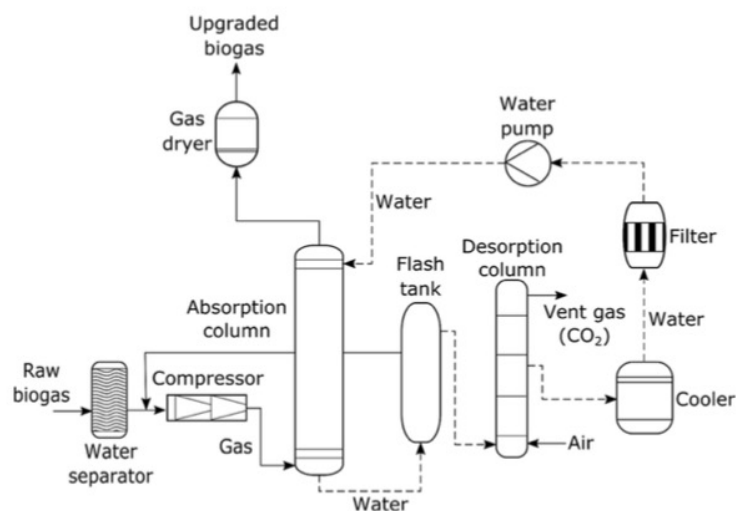


Figure 5. Water scrubbing systems [84,118].

VI.2.2. Organic solvent scrubbing

This technique is very similar to water scrubbing. The only difference is that the water is replaced by conventional organic solvents, such as methanol or glycols, as absorbents to selectively remove impurities, the most used nowadays. These organic solvents have an advantage over water due to the significantly greater solubility of CO₂ and their anticorrosive properties. The schematic for organic solvent scrubbing is shown in Figure 6. The commercial products are available under the trade names Selexol™ and Genosorb® and show considerably higher solubility of CO₂ and NH₃ compared to water. The use of organic solvents, compared to water scrubbing, requires a gas condition step, which the raw biogas is compressed and cooled (7-8 bar, 20 °C) in the first step of the process (Figure 6), after which it is injected into the bottom of the absorption column. The organic solvent is additionally cooled before being introduced to the column because Henry's constant is influenced by temperature. The desorption column is heated to 80 °C and the pressure is decreased to 1

bar in order to regenerate the organic solvent. By this method, in the the upgraded biogas, final methane concentration can range from 96 to 98.5%, and a fully optimized plant can produce less than 2% CH₄ losses [84,88,119].

Physical absorption is considered a proper method that conforms to green technology and engineering standards, which can be useful in industries in order to be economical, reusable and environmentally friendly. Absorbents perform a crucial function by removing impurities from the biogas. Therefore, the development of novel absorbents with high absorption capacity and high recyclability is mandatory [109,119]. The appropriate absorbent should also have low viscosity, relatively low toxicity, low vapor pressure, high boiling point, high absorption capacity, and low cost. Water, meeting all these characteristics, is typically used in biogas purification processes, mainly for CO₂ capture. However, as a majority of VOCs are hydrophobic, water is not the most appropriate solvent for these compounds. Several heavy organic solvents have been used to treat hydrophobic VOCs, including aqueous mixed solvents, silicone oils, and vegetable oils. Unfortunately, these absorbents have disadvantages, including inadequate absorption capacity, high cost, energy-intensive requirements for regeneration, solvent degradation, and equipment corrosion. However, substitute green solvents such as deep eutectic solvents (DES), ionic liquids (ILs) are being investigated to replace the currently used organic solvents, which also successfully used as absorbents for biogas impurities [120–123]. In addition, these absorbents are usually regenerated by heat distillation, leading to concerns about secondary pollution from both pollutants and absorbents.

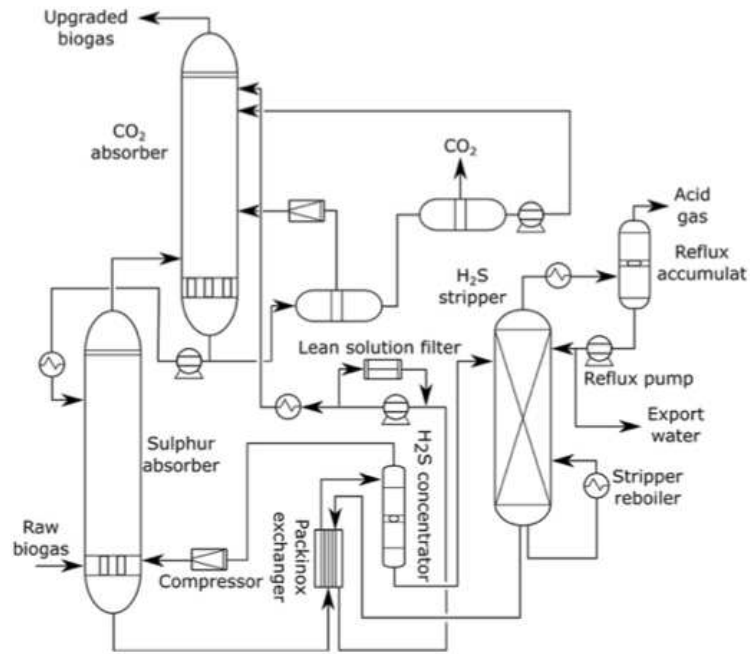


Figure 6. Selexol™ system (UOP Selexo (TM) Technology for Acid Gas Removal 2009 [84].

VI.3. Chemical scrubbing

The chemical reaction between the absorbent and the carbon dioxide molecules provides the basis for the removal of carbon dioxide from raw biogas by the chemical absorption process. At low CO₂ concentrations, chemical solvents typically outperform physical solvents. Amines are often used as chemical solvents to absorb CO₂ since they react only with CO₂ and cause no CH₄ losses. Aqueous amine solutions, such as diethanolamine (DEA), monoethanolamine (MEA), or methyldiethanolamine (MDEA), are the organic substances that are utilized the most frequently. In order to streamline the process set-up, the system consists of a packed bed (random or structural) connected to a desorption unit equipped with a reboiler (Figure 7) [106,124,125]. The high pH of the amine solutions supports the operation of the packed bed and considerably lowers the risk of biomass growth. Exothermic chemical reactions cause the CO₂ to get dissolved in the solvent.

As a result of the highly selective chemical reaction between the solvent and CO₂ in the liquid phase, very little CH₄ is absorbed, leading to a high CH₄ recovery of >99.95%. The resultant amine solution, which is high in CO₂ and H₂S, is then sent to a stripping process for regeneration [109,126]. The desorption system operates at a pressure of 1.5 to 3 bar and is

equipped with a boiler that gives off heat, reaching a temperature of 120 to 160 °C. The heat is used to release the chemical bonds that were created during the absorption phase and to produce a flow of steam that serves as a removal fluid. In this process, steam is produced by reversing the absorption action, which lowers the partial pressure of CO₂ and improves desorption. CO₂ is then discharged into the gas phase. The CO₂-free solvent is cooled and supplied back to the absorber column before a high-purity gaseous CO₂ stream is collected in the top of the desorber [124,127]. This method has several advantages and disadvantages. The main advantages include the efficient removal of certain contaminants from the biogas stream, like CO₂ and H₂S. Based on the properties of the impurity, the choice of absorbents can be optimized to achieve the appropriate level of purification. It is possible to regenerate and reuse the absorbents used in chemical absorption purification, which results in cost and resource savings. Disadvantages of this method include the cost of absorbents, regeneration agents, and possibly consumables, which can add to overall operating expenses. It also can be more complex than other biogas treatment methods, requiring additional equipment and maintenance requirements. The regeneration process can also be complex, energy-intensive, and require additional equipment or chemicals. Other aqueous alkaline salts, such as sodium, potassium, and calcium hydroxides, have also been utilized for the chemical reaction-based removal of CO₂ in addition to amine solutions [86,124,126,127].

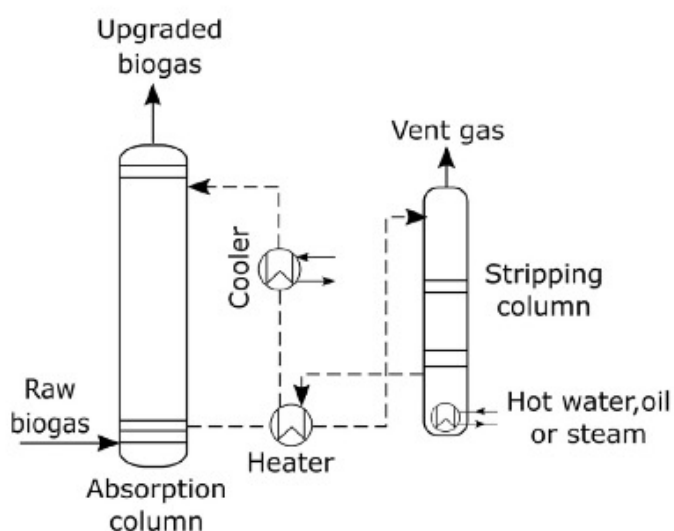


Figure 7. Chemical absorption scrubbing system [128].

VI.4. Membrane separation

One of the newest techniques for biogas upgrading, membrane-based gas permeation, has gained prominence recently, particularly over the past ten years. Due to their reduced cost, simple production, durability under high pressures, and simplicity of scaling, polymeric materials like cellulose acetate are preferred for the creation of membranes. The kind of membrane employed in this separation method matters significantly. There are numerous different membranes with various specifications that may be purchased commercially to permit or block the movement of particular chemicals. There are two fundamental membrane-based biogas purification systems, a low-pressure gas-liquid absorption separation where a liquid absorbs the molecules that diffuse through the membrane, and a high-pressure gas separation with gas phases on either side of the membrane. Most systems operate the high-pressure membrane separation process at a pressure of 20 bar, while others operate it at 8–10 bar [88,113,129]. The waste gases from the initial stages of the multi-stage membrane separation are recycled into the process to increase the CH₄ content (>96%) of the final gas output. Low pressure membrane systems function at pressures that are comparable to atmospheric pressure. In order to eliminate CH₄ losses, hybrid or multi-stage systems should be utilized. It has been discovered that using a capillary module with polyamide membranes enables membrane enrichment in a single module. The flow diagram for a single module and multi-stage membrane separation process is shown in the (Figure 8).

The procedure can be separated into dry (gas/gas separation) and wet (gas/liquid separation) techniques depending on the medium used for separation. CO₂ and CH₄ can be separated using polyimide and cellulose acetate-based membranes in a dry method. The mobility selectivity of these membranes is influenced by their permeation rate, which is influenced by the gas absorption coefficients and the membrane construction material. The hydrophobic qualities of microporous membranes were exploited in the wet process, which is where the difference between the dry and wet processes exists. The benefits of membrane separation and the absorption approach are combined by wet membrane technology. In real terms, the installed membrane divides the liquid from the gas input, allowing the gas molecules to pass through the membrane and be absorbed by the solvent flowing in the opposite direction [84,129].

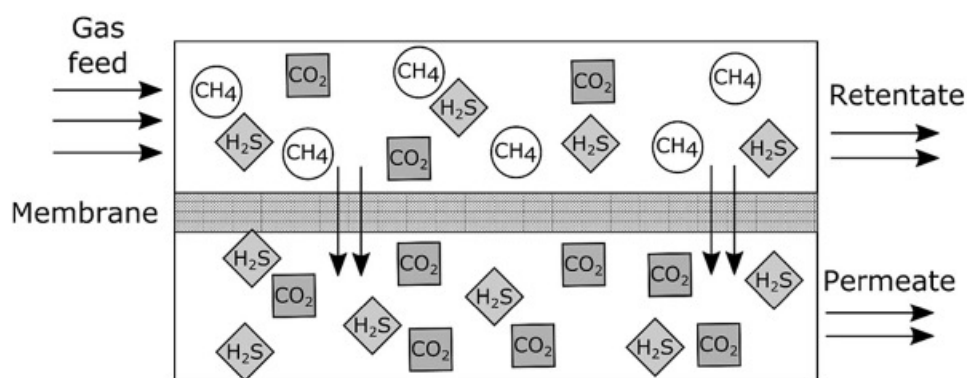


Figure 8. Principle of membrane separation [84].

Gas permeation technology offers biomethane purity of >99% with CH₄ recovery rates of up to 99.5% after considerable research and optimization. The process is generally recognized for security, flexibility in scaling up, robustness, simple operation and maintenance, and no need for hazardous chemicals. Above all, membrane technology is a molecular-scale separation technique. It has a number of advantages over traditional absorption-based biogas upgrading systems, including cheap cost, high energy efficiency, and simple use. However, like any technology, membrane separation also has its limitations and considerations. Membrane pollution, where contaminants accumulate on the membrane surface, can impair performance and call for periodic cleaning or pre-treatment.

It is essential to maintain the integrity of membranes since they may deteriorate over time as a result of chemical or biological attacks, necessitating monitoring and upkeep. Furthermore, it is crucial to choose the right membrane for a given separation task while taking into account aspects like pore size, charge selectivity, compatibility with feed streams, and cost-effectiveness [109,119].

In conclusion, membrane separation has transformed the purifying and separation industries by providing an effective, discerning, and sustainable method for producing high-quality products. It is a crucial tool for solving challenging separation problems because of its adaptability and extensive applicability across a variety of industries, including gas separation, food and beverage processing, pharmaceuticals, and water treatment [130].

VI.5. Cryogenic separation

In the separation and purification of gases at extremely low temperatures, an advanced and effective procedure is used known as cryogenic separation. This method enables the selective separation of gases based on their boiling points or vapor pressures by utilizing the distinct features of various gas components. Cryogenic separation has revolutionized the field of gas separation by enabling enhanced efficiency and precise separation capabilities by operating at extremely low temperatures [88,131]. CO₂ can be separated from CH₄ by condensation and distillation because the condensation temperatures of CH₄ and CO₂ are different. As methane has a boiling point of -160°C whereas CO₂ has a boiling temperature of -78°C, CO₂ can be separated from biogas by freezing the gas mixtures to high pressure. Pre-separating the water, SO₂, halogens, siloxanes, and H₂S is important to prevent freezing and other issues during the cryogenic process. This is accomplished by first compressing the raw biogas to 17–26 bar and then chilling it to approximately 260°C. The process of separation begins with the raw biogas being dried and compressed to 80 bars, then the temperature is gradually lowered to 110 °C. By lowering the temperature appropriately and gradually, one may regulate the product's purity (Figure 9) [84,132].

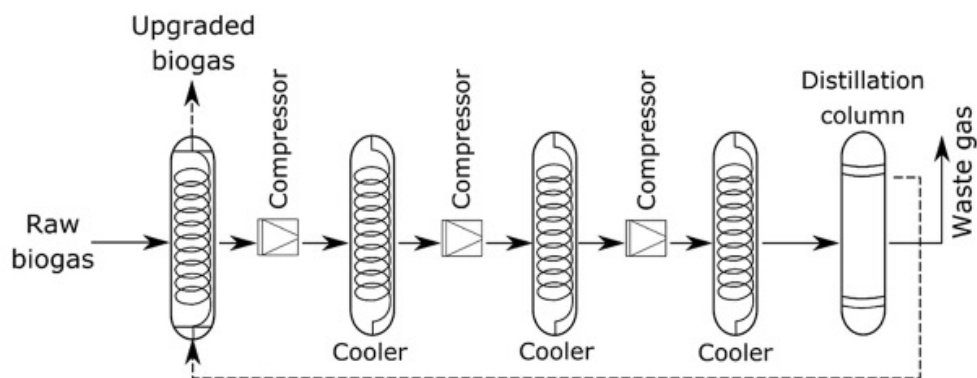


Figure 9. Cryogenic separation system [118].

Cryogenic separation has advantages due to its extraordinary efficacy, accuracy, and adaptability. It allows for the separation of gases with various physical qualities and produces highly pure gas streams by working at extremely low temperatures. Compared to other separation techniques, cryogenic separation offers increased energy efficiency, limiting energy consumption and lowering operational expenses. Additionally, the quality and purity

of gases are improved, satisfying the strict criteria of many industries, thanks to its ability to precisely separate some compounds [119]. In the end, cryogenic separation is a cutting-edge technique for the purification and separation of gases. It is an invaluable instrument in businesses that require high-purity gases, such as industrial gas production, natural gas processing, and impurity removal, due to its capacity to selectively separate gases based on their boiling points as well as its efficiency and precision. Cryogenic separation is continually developing as technology progresses, providing even more possibilities for the effective and long-lasting purification of gases in a variety of applications [88,131,132].

VI.6. Pressure swing adsorption (PSA)

The most common method for gas separation called pressure swing adsorption (PSA) focus on the selective adsorption of gases onto solid adsorbents. It provides an easy and inexpensive method to separate and clean gases in a variety of industries. Due to its adaptability to various gas combinations, versatility, and capacity for high levels of purity, PSA has experienced substantial growth in popularity. Considering the CH₄ molecule is larger than those of N₂, O₂, and CO₂, the PSA technology can be used for separating it from those gases. The molecular sieves material is regenerated during the process, which takes place in vertical columns packed with adsorbents under adsorption, depressurization, desorption, and pressurization sequences [114,133]. The purpose of PSA is the capacity for differential adsorption of gases to a suitable adsorbent material under varying pressure conditions. The process generally requires two main process steps: adsorption and desorption. The gas mixture is supplied into a vessel holding the adsorbent material during the adsorption process under high pressure, where it is ideally absorbed in large quantities and released when the pressure is reduced. The desired gas compounds are therefore successfully separated and concentrated. The schematic flow diagram for the PSA process is depicted in the Figure 10. In order to ensure a continuous operation, many adsorption columns (often four) are installed. The biogas is sent to a fresh column after one column has been saturated with CO₂, and the CO₂-saturated column is gradually depressurized (nearly to air pressure) to release the CO₂/CH₄ combination with high methane concentration, which is suction and recycled back to the PSA inlet.

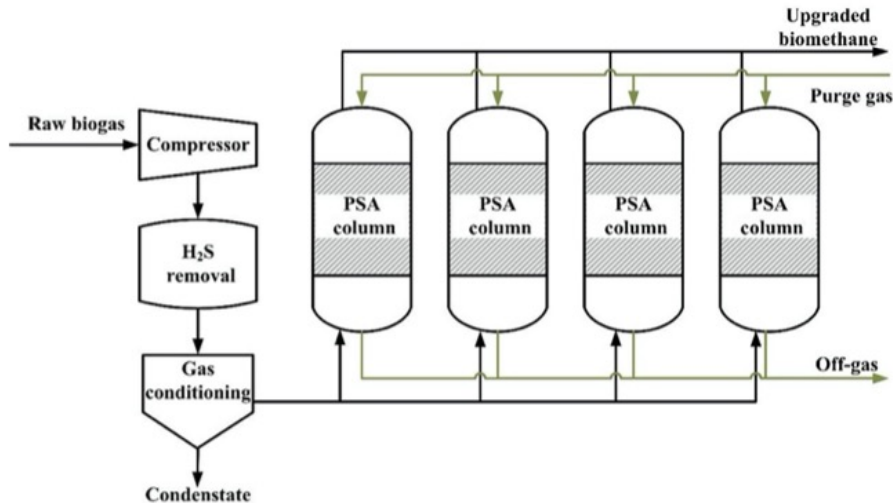


Figure 10. Pressure swing adsorption (PSA) [118].

Activated carbon, zeolites, and molecular sieves are the three adsorbents that are most frequently used in pressure swing adsorption (PSA). These materials are useful for gas separation applications because of their distinctive characteristics.

Due to its high porosity and substantial surface area, activated carbon offers plenty of places for gas molecules to bind. It has significant adsorption properties for a variety of gases, including odorous chemicals and volatile organic compounds (VOCs).

In PSA systems, activated carbon is frequently utilized for gas purification, impurity removal, and component recovery [84,88]. Flexibility, energy efficiency, and cost-effectiveness are some of PSA's advantages. By altering variables such as pressure, temperature, and adsorbent material, the process may be customized to fit various gas mixes and separation needs. Since PSA systems are often small and modular, they may be scaled easily and integrated into already-existing processes. Additionally, PSA uses almost ambient operating conditions and uses less energy than other separation techniques, which lowers operational expenses and has a smaller negative impact on the environment. Despite its advantages, PSA has a few disadvantages as well. In order to achieve effective gas release and reduce energy consumption, the regeneration step—where the adsorbed gases are desorbed from the adsorbent material—needs rigorous adjustment. Additionally, choosing the right adsorbent material and keeping it stable is essential for achieving good separation performance and preserving system longevity [22,133].

VI.7. Biological methods

Biogas purification using biological methods is a promising and environmentally friendly solution. These techniques use biological and microbial processes to transform and filter out pollutants found in the biogas stream. Utilizing microbial communities and enzymatic processes, biological processes can effectively convert or eliminate contaminants to produce purified biogas that is suited for a range of energy uses. This is caused by a number of things, including changes in electricity consumption, rising costs for renewable energy, combining the production of biomethane with the production of other high-value goods, and ultimately, as a result of numerous biotechnological process advancements. The various techniques for upgrading biological biogas based on chemoautotrophic or autotrophic bacteria and microbial electrochemical technologies (METs) are covered in the following sections [109,110,119].

VI.7.1. Chemoautotrophic biogas upgrading

Chemoautotrophic microorganisms have the capacity to use inorganic compounds as a source of energy as opposed to only utilizing organic substances. They use chemical processes to oxidize or reduce substances and produce energy for survival and growth.

Chemoautotrophic microorganisms can be crucial in the process of upgrading biogas because they can transform H_2S and other sulfur compounds into elemental sulfur or sulfate, which are less dangerous and can be easily isolated from the biogas [21,119].

The upgrading reactor is infused with the chosen chemoautotrophic microorganisms. Normally, to do this, a seed culture or biomass from an existing chemoautotrophic system is introduced. The creation of a stable microbial population capable of effective impurity conversion is ensured during the startup phase, which also entails acclimating the microorganisms to the biogas feedstock and adjusting operating parameters. The microorganisms in the chemoautotrophic biogas upgrading process change the targeted pollutants, like H_2S , into less dangerous forms. For instance, through biological processes, chemoautotrophic microorganisms can oxidize H_2S to elemental sulfur or sulfate. The metabolic activity of the microorganisms, the availability of nutrients, temperature, pH, and reactor design are only a few of the variables that have an impact on the effectiveness of impurity conversion [21,109,110].

The capacity of chemoautotrophic biogas upgrading to function in a variety of environmental circumstances is a fundamental advantage. These microorganisms can survive in a variety of settings, even harsh ones, and can produce large amounts of H₂S and biogas with a variety of compositions. Chemoautotrophic biogas upgrading is ideal for various biogas producing facilities and feedstock compositions because of its versatility.

Resource recovery is another advantage of chemoautotrophic biogas upgrading. Microorganisms can produce elemental sulfur or sulfate by the conversion of H₂S, which can then be processed and used in a variety of industries, including wastewater treatment, chemical manufacture, and agriculture. This increases the economic sustainability of the upgrading process by improving the quality of the biogas while also producing useful byproducts [113,119].

Nevertheless, chemoautotrophic biogas upgrading is still a new field of study, and research and development are currently ongoing. Some of the issues that need to be resolved include improving the effectiveness and performance of chemoautotrophic bacteria, assuring stable and sustainable biogas upgrading operations, and scaling up the procedure for commercial applications. Research, engineering, and industry stakeholders must work together to increase understanding of and actual use of chemoautotrophic biogas upgrading [84,119].

VI.7.2. Photosynthetic biogas upgrading

Nowadays, the only biotechnology capable of simultaneously relocating multiple biogas pollutants, such as CO₂, H₂S, and BTEX, is the upgrading of biogas based on symbiotic interactions between oxygenic photosynthetic or/and lithoautotrophic and heterotrophic microorganisms (microalgae and cyanobacteria). This innovative biotechnology for upgrading biogas depends on the solar-driven fixation of CO₂ through photosynthesis, concurrent with the bacterial oxidation of H₂S to SO₂ and BTEX to CO₂ and H₂O. The technique in biotechnology depends on the simultaneous bacterial oxidation of H₂S to SO₂ and BTEX to CO₂ and H₂O, as well as solar-driven fixation of CO₂ through photosynthesis. Algal-bacterial photobioreactors for upgrading biogas have typically been found to contain microalgae from the genus *Chlorella*, *Pseudanabaena*, and *Scenedesmus* as well as sulfur-oxidizing bacteria from the genus *Thiobacillus* [84,88].

The process of this method is started by the reactor system that is developed to give photosynthetic bacteria the best possible conditions for growth and metabolic activity. To

encourage photosynthesis and increase methane generation, variables like light intensity, temperature, pH, nutrient availability, and gas exchange are carefully regulated. The photosynthetic microorganisms in the reactor take CO₂ from the biogas stream and use photosynthesis to turn it into organic biomass. The fixation of CO₂ and the subsequent generation of oxygen are both fueled by sunlight in this process. The produced biomass acts as a source of carbon for the eventual creation of methane. As a result of anaerobic digestion, methanogenic microbes produce CH₄ and CO₂ from the photosynthesis-produced biomass. This methanogenesis process, which usually occurs in a different compartment of the reactor under anaerobic circumstances, is made possible by certain bacteria that produce methane. The upgraded biogas with a greater proportion of methane is separated from the reactor system following the methanogenesis stage. The methane gas can be cleaned up by using a variety of separation processes, including membrane separation, pressure swing adsorption, and gas scrubbing [110,119].

VI.7.3. Microbial electrochemical technologies (METs)

An innovative method for improving the quality and energy content of biogas is to use microbial electrochemical technologies (METs), which harness the power of electroactive bacteria. By harnessing the electrochemical activity of microorganisms to transform CO₂ and other pollutants into useful CH₄, it provides a sustainable and effective method for upgrading biogas. Through utilizing the distinctive qualities of electroactive microorganisms METs provide an alternative to conventional biogas upgrading techniques. These microorganisms can conduct electrochemical reactions because they have the ability to transfer electrons to or from solid electrodes. By taking advantage of this electrochemical activity, METs can help biogas contain more energy by converting CO₂ and other pollutants into usable CH₄. The biogas upgrading procedure in METs is carried out in a specifically constructed reactor system. A proton exchange membrane or an ion-selective membrane commonly separates the anode and cathode compartments of the reactor. The electroactive microorganisms oxidize the organic components in the biogas feedstock in the anode compartment, producing electrons and protons in the process [110,114,119]. While the protons move through the membrane to the cathode compartment, the electrons are transmitted to the anode electrode. The electrochemical reduction reaction takes place in the cathode compartment. Methane is

produced when protons produced during the anodic oxidation process combine with electrons from the cathode electrode. By increasing the amount of methane in the biogas, this electrochemical process upgrades the biogas. As a result of the continuous flow of electrons from the anode to the cathode enabled by the electrochemical circuit created by the anode and cathode electrodes, CO₂ and other pollutants can be converted into methane. Various separation processes, such as membrane separation or pressure swing adsorption, can be used to remove any leftover pollutants and purify the methane gas from the upgraded biogas, which has been enriched in methane content. Following its purification, biomethane can be used as a renewable energy source for many purposes, such as the production of electricity, heat, or fuel for vehicles. It can be disseminated for use in other industrial applications, added to the natural gas grid, or used on-site as energy, all of which help create a more ecologically friendly and sustainable energy system [86,88].

Biogas upgrading via METs provides several advantages, including increased methane production, lower greenhouse gas emissions, and the possibility of connection with current biogas production systems. There are still obstacles to solve, such as optimizing reactor design, improving electrode materials, and establishing long-term microbial community stability. For example, process scaling must be validated before commercialization; energy efficiency remains low, resulting in economic constraints; and new value compounds created by CO₂ could be studied [86,88,110,119].

VII. Economic and technological challenges of biogas upgrading

The economic and technological limitations connected with biogas upgrading, technologies are facing significant economic challenges, mainly due to the high operational cost of biogas creation, operation, maintenance and utilization. One of the most significant obstacles is the capital investment needed to upgrade equipment and infrastructure. Installing and operating upgrading technologies like as compression, adsorption, membrane separation, or chemical procedures can be costly. Finding economically viable alternatives to reduce capital investment and operating expenses is critical for widespread biogas upgrading adoption. Due to the initial cost-effectiveness of the plant installation, unsustainable and less suitable biogas upgrading technologies are frequently developed, which has unprecedented and extremely negative long-term effects. To ensure the long-term viability of biogas upgrading technology, process optimization [61,130]. The techno-economic and energy-economic issues associated

with biogas upgrading technologies are diverse, and they frequently lead to the deployment of less expensive but more energy-aggressive solutions, risking their long-term sustainability and relevance to the respective framework. Furthermore, there are concerns with the supply and stability of biogas feedstock. The content and quality of biogas might differ depending on the feedstock utilized, influencing the efficiency and efficacy of upgrading processes. Having a regular and reliable source of feedstock is critical for maintaining consistent biogas production and upgrading processes. Another major issue is the efficiency with which impurities are removed. Impurities in biogas such as CO₂, H₂S, and VOCs must be properly eliminated in order to achieve quality standards. Increasing impurity removal efficiency, particularly for trace contaminants or those needing specialized treatment procedures, provides continual technological problems [89,114].

Scalability and flexibility are essential factors to consider while developing biogas upgrading methods. Upgrading methods must be adaptive to various biogas production quantities and capable of dealing with fluctuations in feedstock availability and composition. To achieve the different requirements of biogas production, the ability to scale up or down and adapt to varying plant sizes and capacities is critical.

Besides from economic and technological problems, legal and policy frameworks are critical to the expansion of the biogas upgrading sector. Inconsistent rules, a lack of financial incentives, and ambiguous market structures can all stymie the development and profitability of biogas upgrading operations. Supportive regulations, feed-in tariffs, and market mechanisms can all be used to encourage investment, innovation, and the use of biogas upgrading systems.

Continuous technical developments, research, and stakeholder participation are required to address these challenges. Research activities aimed at improving the efficiency, dependability, and cost-effectiveness of upgrading technologies, as well as investigating novel ways for impurity removal and building integrated systems, it can propel biogas upgrading forward. Collaboration among technology developers, politicians, academics, and project financiers is critical for addressing economic and technological obstacles and providing a favorable climate for the biogas upgrading sector's long-term growth [61,110,119].

To overcome the shortcomings of environmental issues and the cost-effectiveness of upgrading technologies, many technologies have been tested and applied to remove impurities from biogas, such as water scrubbing, physical and chemical scrubbing, membrane

separation, pressure swing adsorption, biological methods, etc. however Physical absorption is considered a proper method that conforms to green technology and engineering standards [67,110,119].

Absorbents perform a crucial function by removing impurities from the biogas. Therefore, the development of novel absorbents with high absorption capacity and high recyclability is mandatory. The appropriate absorbent should moreover possess low viscosity, relatively low toxicity, low vapor pressure, high boiling point, high absorption capacity and low cost. Water, gathering all these characteristics, is typically used in biogas purification processes, mostly for CO₂ capture. However, as a majority of VOCs are hydrophobic, water is not the most appropriate solvent for these compounds. Consequently, substitute green solvents are searched to replace the currently used organic solvents. The first well-studied alternative solvents are ionic liquids (ILs), however, it was shown that ILs can be toxic and non-biodegradable and that their synthesis can be very costly and complicated. Recently, a new generation of green solvents, namely deep eutectic solvents (DESs), were also successfully used as absorption media and have been investigated in detail [134–139]. To comprehensively address these challenges, biogas upgrading has the potential to maximize the energy potential of biogas, reduce greenhouse gas emissions, increase the use of the circular economy, and help lead to a sustainable, low-carbon energy future.

VIII. Deep Eutectic Solvents (DES)

The development of an economical and ecologically friendly solvent is critical in the chemical industry. The desire for environmentally friendly, less toxic, biodegradable, natural, and low-cost solvents has gradually prompted the development of new alternative solvents. During the last decade, green solvents, such as supercritical fluids, biobased solvents, ionic liquids (ILs), and, more recently, DESs, have emerged as safe solvents. In recent years, DESs, a family of solvents with distinct characteristics and a wide range of applications, have attracted a lot of attention [140]. The name “eutectic” is derived from the Greek terms “eu” (which means “well or good”) and “tēktos” (which means “melted”). “A liquefaction temperature lower than that provided by any other proportions” is what the term “eutectic” refers to [141,142].

Abbott et al. developed the concept of DESs in 2003 and describe the eutectic combinations with different properties identified throughout their investigation. DESs are obtained by combining two or more chemicals with high affinity for each other with specific non-covalent interactions, thus, allowing for the formation of a eutectic mixture [143,144]. In order to develop a DES, the right components must be chosen, typically a hydrogen bond acceptor (HBA) and a hydrogen bond donor (HBD). The HBA is often a molecule capable of acting as a Lewis acid or forming coordination complexes, whereas the HBD is a compound composed of hydrogen atoms [143–145].

DESs exhibit a eutectic point, which is the particular composition and temperature where their lowest melting point is reached. The DES reaches an ideal composition at the eutectic point, maximizing interactions between the components, resulting in unique molecular structures and a lower melting point than the individual components (Figure 11) [142,143].

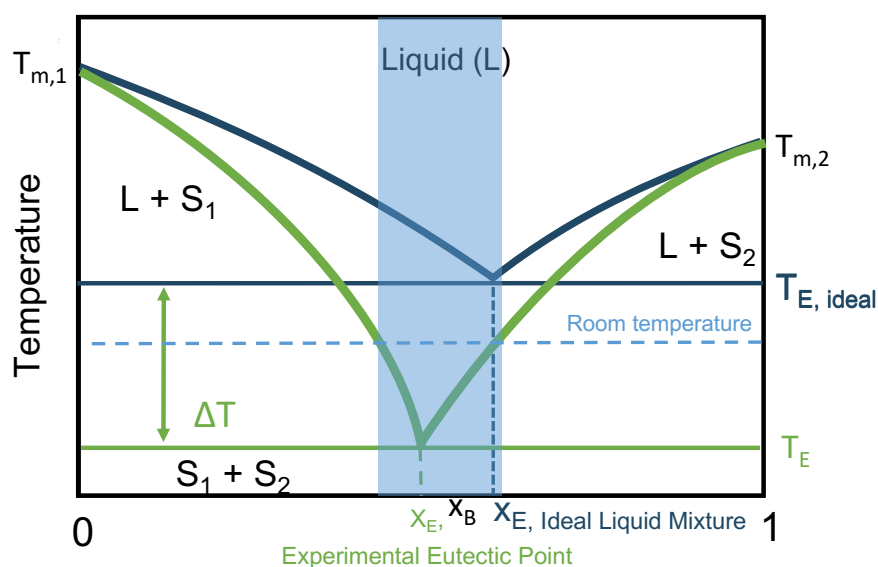


Figure 11. Liquid-solid phase diagram of a binary mixture.

The solid-liquid equilibrium representation of a deep eutectic mixture shows that the transition from solid to liquid is not as sharp as in an ideal eutectic combination. The increased melting range in a deep eutectic mixture is due to interactions between the components, which influence the molecular preparation and the energy required for phase transition. The comparison between the solid-liquid equilibrium of a simple ideal eutectic mixture and a deep eutectic mixture highlights the different behavior and phase transitions observed in these

systems. Therefore, as shown in Figure 11, the Deep attribute is determined by comparing the ideal eutectic temperature ($T_{E,ideal}$) with the experimental mixing temperature (T_E). Consequently, we can classify the mixture as "Deep" or eutectic by determining this difference temperature (ΔT), which can be linked to the non-ideality of the mixture. Nevertheless, the liquefaction curves of the two compounds intersect at the eutectic point with a composition X_E or $X_{E,ideal}$. Thus, the liquid mixtures can also be obtained by compositions far from the eutectic point, depending on the temperature applied to the mixture. In these cases, eutectic mixtures are obtained which are liquid at a higher temperature than the liquefaction curves of the pure compounds.

The deep melting can vary allowing for greater temperature control and stability, which can be helpful in some applications. Understanding the eutectic point is critical for adjusting DES properties for various applications since it enables for changes in melting temperature, viscosity, conductivity, and other essential properties.

The formation of hydrogen bonds between the compounds is one of the theories advanced in the literature by several groups to explain this deviation from the eutectic ideal. This started after Abbot was looking for liquids that could overcome the moisture sensitivity and high cost of some common IIs [142,146–149]. DESs were developed based on quaternary salts with non-hydrate metal chloride and hydrate metal chloride, such as choline chloride (ChCl) and zinc chloride ($ZnCl_2$) that fits into the category of type 1 and 2 (figure 12). Subsequently, many other DES were developed, thus developing type 3. These are formed by combining ChCl as HBA with carboxylic acids, alcohol, amine, sugar, or amide as HBD. Thereafter, group 4 was created, which are solvents formed by transition metals ($ZnCl_2$) mixed with organic molecules, such as urea, acetamide, ethylene glycol and 1,6-hexanediol [148,150–154]. Furthermore, type 5 is a new class of sustainable solvents. They are obtained by mixing solid non-ionic compounds, which show significant negative deviations from thermodynamic ideality. Therefore, asymmetric HBDs (strong HBD but weak HBA sites) and lone HBAs are considered viable options for the development of type 5 DESs. As example we can cite the DESs obtained with thymol and menthol, thymol and trioctylphosphine oxide (TOPO) or nonanoic acid (C_9) and TOPO [155–157].

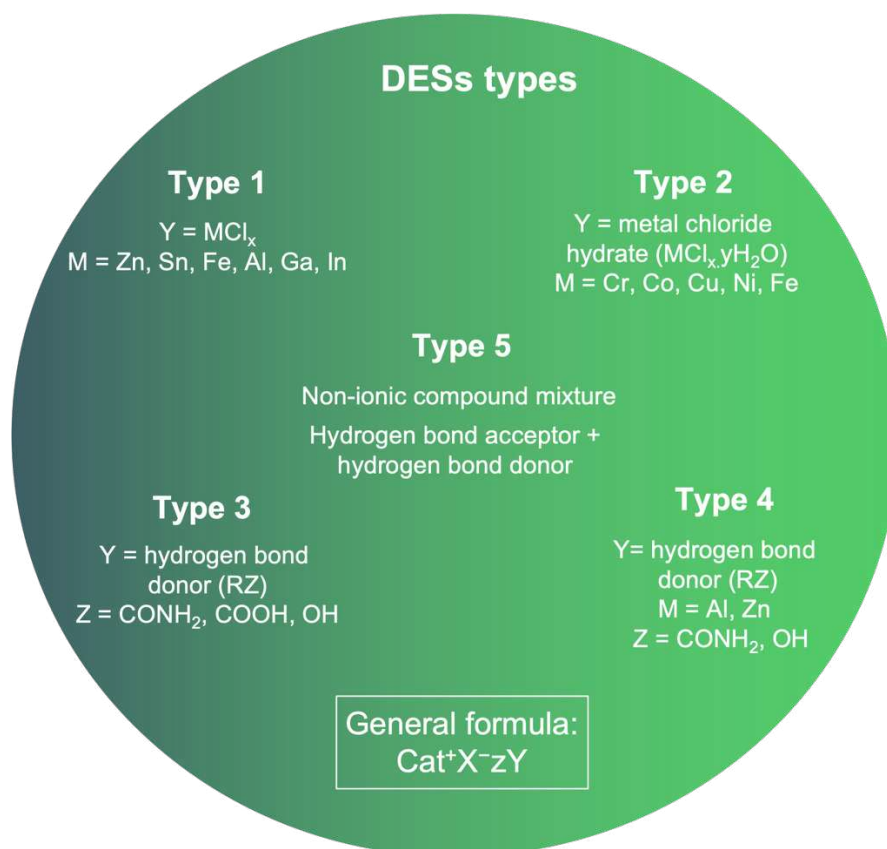


Figure 12. Deep eutectic solvents classification.

Besides this classification based on the structure of the DES components, several DES families have emerged in the literature. Natural Deep Eutectic Solvents (NADES) are a specific type of deep eutectic solvents derived from natural compounds such as organic acids and sugars and might combine to generate eutectic-type mixtures with qualities similar to synthetic DES. Thus, DESs formed using an active principle as a component are called THEDES for therapeutic DESs [145,158,159]. Hydrophobic DES (HDES) have recently been described. In the presence of water, they have the ability to establish a stable two-phase system. They can be prepared using quaternary ammonium salts and decanoic acid or with menthol and other carboxylic acids [153,154]. More recently, supramolecular mixtures known as SUPRADES have emerged [160]. They have been developed by using cyclodextrins (CD). It is noteworthy to mention that CD are natural cyclic oligosaccharides derived from the enzymatic degradation of starch [161,162]. CDs are of particular interest because of their hydrophobic inner cavity that can easily form an inclusion complex with various hydrophobic guest molecules in order to improve their physicochemical properties [161].

Native CD are the α -CD, β -CD, and γ -CD, made up of six, seven or eight (α -1.4)-linked α -D-glucopyranose units, respectively. Afterwards, scientists synthesized chemically modified CD in order to improve their properties, like for example the Randomly methylated β -CD (RAMEB) [160,163]. SUPRADES have been developed by combining CD with HBD or by dissolving CD in already prepared DES [163]. As example, β -CD was found to have a much higher solubility in choline chloride:urea DES (1 g.mL^{-1}) compared to water (0.018 g.mL^{-1}) [164]. The SUPRADES have been shown to form inclusion complexes with a variety of guest molecules [160,165,166].

VIII.1. DES characterization

The selection of compounds that form DES creates a new generation of solvents with many different types of materials and a huge number of combinations. The characteristics and behaviors exhibited by these specific liquid mixtures set DESs apart from conventional solvents and explain why they are becoming increasingly popular in a wide range of applications. DESs have a variety of physico-chemical characteristics, including viscosities, densities, water contents, melting and freezing points, and surface tension, etc. (table 5) [149,167,168].

The low melting point of DESs is one of their important physico-chemical characteristics. Because of this characteristic, some DESs may operate as liquids at room temperature or in moderate circumstances, making them energy-efficient and environmentally friendly solvents. Therefore, to achieve the criteria of green chemistry and engineering, the toxicity, vapor pressure, and biodegradability of DES must also be determined [169,170].

VIII.1.1. Viscosity

Viscosity is a crucial parameter for DES characterization and also an important property for industrial applications. The viscosity of DESs can be tuned in order to meet certain application requirements, such as gas absorption, by choosing various combinations and ratios of HBDs and HBAs. DESs have an affinity for absorbing some components more than others due to their selectivity towards particular gases. Another viscosity impact is how quickly mass is transferred in DES-based processes. The efficiency and kinetics of numerous processes, including absorption, can be impacted by higher viscosity. During the absorption process, high dynamic viscosity of DES can result in delayed gas diffusion through the gas-liquid interface. Due to the high energy requirements, the absorption column produces large gas bubbles which reduces the gas-liquid interaction, and it affects factors such as fluid flow, pressure drop and mixture behavior [149,160]. Adding water to DES is one way to reduce its viscosity. Water addition may significantly change other physicochemical parameters, resulting in a decrease the absorption capacity of the DESs. Temperature has a significant impact on viscosity. DES viscous at room temperature, can be therefore used in industrial operations at higher temperatures. On the other hand, due to the exothermic nature of the absorption process, increasing the temperature of the absorption process is not efficient. Thus, it is preferable to select DES, which has a low viscosity at low temperatures. Moreover, using low viscosity solvents in the gas upgrading can save energy on the whole dynamics process, such as mixing, pumping, heat transfer and solvent regeneration. Understanding the viscosity of DESs facilitates the optimization of process parameters to enable effective mass transfer.

As shown in table 5, there are various type of DES with low and high viscosities, including hydrophobic, hydrophilic, cyclodextrins-based, ChCl-based, and non-ionic DES. However, every single DES are utilized for a specific purpose. Viscosity is a key factor when scaling up DES-based operations from the laboratory to industrial scale. By considering viscosity as an important factor in industrial DES applications, researchers and engineers can improve the entire process to successfully scale up DES-based processes to commercial production [143,167,171].

Table 5. Physicochemical properties of DES used for VOCs absorption.

DESs	Molar ratio	Viscosity at 20 °C (mPa·s)	Density at 20 °C (g/cm ³)
Choline chloride: urea	1:2	1618	1.17
Choline chloride: levulinic acid	1:2	362	1.14
Rameb: Levulinic acid	1:27	212	1.184
Carvone: decanoic acid	1:1	5	0.93
Tetrabutylammonium bromide: decanoic acid	1:2	548	0.904
Tetrabutylphosphonium bromide: Levulinic acid	1:6	118	1.09

Ref. [136,169,172–175].

VIII.1.2. Density

Another important characterization is density. It may provide important information about the composition. Considering DESs are formed by combining two or more components, the density can be used to determine the concentration of the individual components as well as their total proportion in the mixture. However, the density of DESs is directly linked to their phase behavior. It describes liquid-liquid phase transitions, solid-liquid phase transitions, and temperature-dependent density variations. In industrial contexts, density is a crucial characteristic for quality control. It provides a measure of the reliability and purity of DESs [167,169]. A DES's efficiency in industrial processes may be impacted by differences in its composition or the presence of contaminants, which may be indicated by variations in density. However, the impact of this parameter on the absorption process is minor. In separation procedures, density discrepancies between components in a DES can be used. Components can be separated based on the changes in their densities using procedures like liquid-liquid extraction, centrifugation, or distillation. The selection of the DES regeneration procedure can be influenced by DES density values. Extraction can be used to regenerate deep eutectic solvents, whose densities are dramatically different from those of common solvents like water [175].

VIII.1.3. Polarity

DESs characterization include polarity as an important parameter. The distribution of charge within a molecule is known as polarity, and it affects the interactions, behavior, and solubility of DESs in a variety of applications. The polarity influences DES solubility in different solvents as well as their capacity to dissolve other compounds. DESs with higher polarity have a stronger affinity for polar substances. Due to the presence of comparable intermolecular interactions, they can effectively solvate and dissolve polar solutes or gases. The polar nature of the DES increases polar chemical solubility and absorption capacity. However, non-polar DESs with lower polarity are better suited to dissolve non-polar substances or gases as well. Lower polarity decreases affinity for polar solutes while increasing solubility and absorption capacity for non-polar compounds. The selectivity of the absorbent is crucial depending on the application. In the case of absorption, the polarity of the DES can also have an effect. Based on their polarity or chemical properties, DESs with specific polarities may preferentially absorb certain chemicals [145,176–178]. This selectivity might be useful in separation or purification operations where specific chemical absorption is sought. However, the desorption and release of absorbed compounds can be affected by the polarity of the DES. Due to the intensity of interactions between the DES and compounds absorbed. Higher polarity might cause stronger interactions, slowing desorption kinetics and potentially changing the release or recovery of absorbed chemicals. In the case of temperature, the polarity is able to change by increasing or decreasing the DES temperature. The decrease in temperature often increases the polarity of the DES. The change is affected by an increase in the hydrogen-bond donating acidity of the absorbent and the development of stronger interactions between HBA and HBD. When setting up absorption procedures or selecting a DES for a given application, the polarity of the DES must be taken into account. By matching the polarity of the DES with the necessary solutes or gases, one of them can enhance absorption capacity and selectivity, therefore increasing the absorption capacity of the DES [158,172,177].

VIII.1.4. Surface tension

The surface tension of DES influences the mass transfer process as well. Surface tension is a liquid property that defines the force at the interface of a liquid and a gas or another immiscible liquid. It is the force that tends to reduce a liquid's surface area. However, the type of DES (hydrophilic and hydrophobic), temperature, presence of additional solvents, HBA and HBD, all have an impact on the surface tension of DESs [175]. DESs often have higher surface tension, however some DESs are lower than water and conventional solvents. This is because the DES's constituent parts interact strongly via hydrogen bonds. Therefore, they are more likely to disperse and create foams on surfaces. This can improve the surface area available for mass transfer during absorption processes. The effectiveness of VOC absorption is positively impacted by low surface tension levels. When forming DES, HBA or HBD with a longer alkyl chain should be utilized to lower the surface tension of absorbents [179–184].

VIII.2. DESs preparation

DESs are often prepared by mixing two or more compounds with the appropriate molar ratio of HBD to HBA and heating the mixture under stirring to a reasonably high temperature, usually between 60 and 100 °C until a homogeneous liquid is formed [185,186]. In case single components are liquid at room temperature, the mixture can be formed without heating, as in the case of DES based on choline chloride and levulinic acid (1:2). Instead of heating the compounds, DESs can also be prepared by grinding, which involves combining them at room temperature and pounding them with a mortar and pestle until a clear liquid is formed [187]. A different method is dissolving the compounds in water to form an aqueous solution, and then using freeze-drying cycles to remove the water. After that, a desiccator is used to dry the resulting viscous liquid DES [145,188,189].

VIII.3. DESs application

DESs have become a class of adaptable solvents with several uses in a variety of industries. Researchers have begun to think about using these new solvents in a variety of domains of application due to the exceptional and adaptable qualities of DESs as well as the growing need for environmentally friendly processes and the desire to replace traditional organic solvents.

DESs are used in a variety of applications, such as, extraction, microextraction, pharmacy, solubilization and gas purification process by absorption (figure 13) [121–123,136].

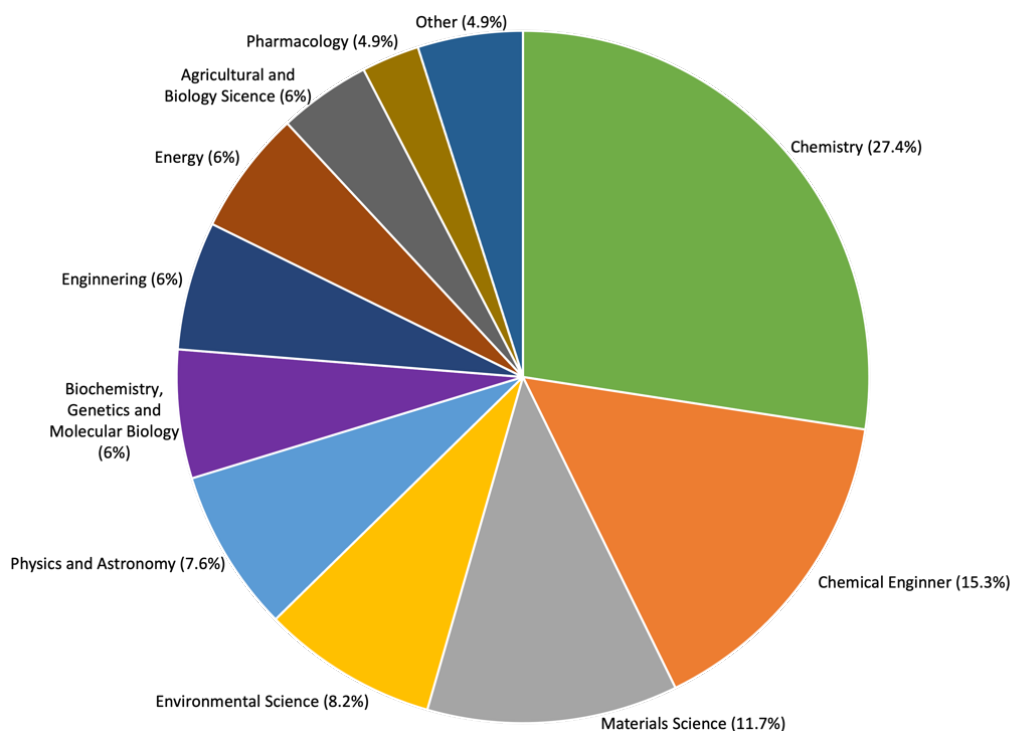


Figure 13. Distribution of publications on DES in the various domains (Scopus-consulted July 2023).

VIII.3.1. Extraction

Water and conventional organic solvents have long been studied for applications involving extraction. However, researchers were driven to investigate DESs as extraction solvents due to their more environmentally friendly nature, variables and exceptional solubilization capacity compared to the toxicity of organic solvents and the unique water based polar compounds. It allows the selective extraction of desire components from complicated conditions, due to their capacity to dissolve both polar and non-polar compounds. Thus, DESs in extraction procedures has drawn considerable interest from a variety of industries [190,191].

DESs have showed potential in effectively isolating bioactive components from plant materials and fermentation broths for natural product extraction. The isolation of high-value natural compounds for use in pharmaceutical, nutraceutical, and cosmetic applications is made possible by their ability to adapt qualities, which permit improved solubility and

extraction effectiveness. Also, DESs are useful in the extraction of lipids and biofuels from biomass sources like microalgae, which is a crucial step in the biofuel manufacturing process. High extraction efficacy, selectivity, and compatibility with downstream processing are all provided by DESs, aiding in the emergence of clean, renewable energy sources. Additionally, DESs can be applied to analytical chemistry solid-phase extraction techniques as sample preparation solvents. Technologies for solid-phase extraction based on DES enhance the sensitivity and accuracy of analytical processes. DES-based extraction techniques could become more effective, selective, and environmentally benign with more study and development [148,192,193].

VIII.3.2. Solubilization

Following their unique features and tunability, DESs have gained a lot of attention in the field of solubilization. DES's solubilizing ability is a high desirable quality that these solvents offer advantages such as great solvation capacity, adaptability, and environmental sustainability, making them appropriate for a wide range of field solubilization applications. DESs have shown potential to improve the solubility of a variety of compounds, which is a highly attractive feature that has contributed greatly to their consideration, including drug delivery, bioactive chemicals, extraction, biomass, and others [194–199]. Their ability to dissolve polar and non-polar molecules allows for the solubilization of most components, enabling its effective use in a variety of applications. DESs have been investigated in the pharmaceutical industry as drugs solubilizers for insoluble substances. These solvents can make drugs more soluble and bioavailable, enabling more efficient drug delivery and better therapeutic results. Low solubility and slow dissolution rates of certain drugs present a barrier, but DES-based solubilization techniques present a possible answer [163,200–203]. When compared to other DES and conventional solvents, NADES and THEDES offer various advantages for solubilization, such as some bioactive chemicals and biological macromolecules. It is possible to tune the solubilization properties of the desirable component in DESs by adjusting the DES's composition and structure. Utilizing DESs for solubilization has several benefits, including the possibility for low energy consumption and minimal environmental effect [204–207].

VIII.3.3. Absorption

VIII.3.3.1. Carbon dioxide (CO₂)

One of the pollutants that is most frequently studied is CO₂, which is typically found in industrial flue gases, power plant emissions, and other sources. One of the main causes of global warming and climate change is the rising of CO₂ concentration in the Earth's atmosphere, which primarily comes on by human activities such the burning of fossil fuels, deforestation, and industrial operations. In order to control the rise in global temperatures and the related negative effects, CO₂ emissions must be reduced. One of the primary methods for trapping CO₂ is absorption. From industrial flue gases, power station emissions and other sources, CO₂ is absorbed before being released into the environment, therefore the absorbent must be carefully chosen. In the early days of CO₂ absorption, conventional solvents such as water and aqueous amine solutions were used. Due to its abundance, water was one of the first solvents to be used. However, its absorption capacity was limited. It also required energy-intensive regeneration. Aqueous solutions of amines were a significant improvement, as they were able to react chemically with the CO₂ to form stable compounds, thereby increasing the absorption capacity. Despite that, these solvents had disadvantages such as corrosion, foaming and high energy requirements for regeneration [196–199].

To address the limitations of traditional solvents, DESs have been studied for this purpose. DESs can achieve better CO₂ absorption compared to conventional solvents. They can also be regenerated with less energy, thus, reducing operating costs. In addition, by selecting specific HBDs and HBAs, DESs can be tuned to the characteristics of the gases to be absorbed. Some DESs are intended to be less hazardous and more environmentally friendly than conventional solvents. Scientists and researchers began researching DES to better understand its behavior and improve its efficiency once they realized how effective it could be at capturing CO₂. Scientists and researchers have begun to investigate DES in order to better understand how it behaves and improve its efficiency. In brief, the replacement of traditional solvents with DES for CO₂ absorption started out as a response to the need for more efficient, economical and environmentally acceptable methods of carbon capture [208–212].

VIII.3.3.2. Volatile organic compounds (VOCs)

While some conventional solvents are characterized by their low absorption capacity, DESs can be used in absorption processes to capture and remove certain desired components from gas streams such as VOCs that are the most often found in industrial and waste gas pollutants. The presence of VOCs in air and waste gas streams is hazardous from an ecological, public health, and industrial viewpoint. They are characterized by high toxicity and organism-damaging. In order to reduce air pollution and satisfy the air quality requirements and regulations, VOCs emissions must be under control. Additionally, the presence of VOCs in biogas and natural gas production may have an impact on engine system corrosion, pollution, and clogging. However, DESs have a high affinity for specific compounds and can increase the selectivity and effectiveness of the absorption process. DESs can be designed according to the required solute-solvent interactions, allowing for efficient absorption. Therefore, The DES must be regenerated after becoming saturated with VOCs before it can be reused. Changing the parameters, such as temperature or pressure, usually leads to the release of the captured VOCs from the DES. Usually, they adapt to different conditions to facilitate regeneration. [122,138,213,214].

Many studies have shown that the VOCs and impurities from exhaust gas can be absorbed by DES with great absorption compared to conventional solvents. The efficiency of a number of well-known ionic eutectic combinations based on quaternary ammonium and phosphonium salts, including ChCl:U (1:2), ChCl:EG (1:2), ChCl:Gly (1:2), ChCl:Lev (1:2), TBPB:Gly (1:1), TBPB:Lev (1:6), and TBAB:DA (1:2), was investigated. Different DES based on cyclodextrins (CD) were also evaluated and demonstrated better absorption than conventional solvents. These included Captisol:Lev (1:44), CRYSMEB:Lev (1:25), HP-CD:Lev (1:32), and RAMEB:Lev (1:27) [136,161,165,215]. DES provide a flexible and sustainable ability to selectively capture VOCs from gas streams. Furthermore, to the experimental process, theoretical research has provided methods such as COSMO-SAC, ASPEN, and PC-SAFT to predict the absorption of these impurities in DESs in order to simulate the condition.

We outline many DES characteristics and the various applications for these novel solvents in this brief literature review. Ionic liquids have a high VOC absorption capacity, according to recent studies [194,216–218]. However, the cost and toxicity of their industrial application

presents challenges. The effectiveness and viability of DES are being improved through current research and development in this area.

VIII.3.3.3. Biogas upgrading

As we have seen before, biogas production is becoming increasingly important due to its economic and environmental benefits. Biogas is rich in CH₄ and CO₂ and is produced from organic materials such as agricultural waste, sewage, and food scraps. However, it contains the most technologically challenging chemical component groupings, such as VOCs and other impurities. Biogas must be purified to meet certain quality requirements before it can be introduced into the natural gas network or used as an alternative transportation fuel. However, there is a current need to develop an efficient and cost-effective biogas treatment method to optimize the properties of high-methane gas (natural gas and compressed natural gas) [17,78,81].

DESs are finally coming to be known as a potential and sustainable biogas absorption process. They have unique characteristics, such as a chemical composition that can be adjusted, which makes them useful for selective gas absorption. DESs are absorbents that can be used in the biogas upgrading to remove specific contaminants from biogas stream. The advantages of DES for biogas upgrading include high VOCs selectivity and other impurities, the possibility of adjusting to different biogas compositions and potential energy efficiency during the desorption (regeneration) process. In comparison to conventional solvents, they showed low absorption capacity, and it can also reduce operational costs. DES-based biogas absorption is useful in a variety of industries, including wastewater treatment plants, agricultural facilities, and biogas upgrading plants. Research in this area is still focusing on enhancing DES compositions, absorption processes, and scalability for larger biogas purification use.

Some studies have demonstrated that contaminants in biogas and exhaust gas can be absorbed by DES with more efficiency than traditional solvents such as syringol (Syr):levulinic acid (Lev), carvone (C): decanoic acid, ChCl:U, ChCl:Lev, (C):guaiacol (G):(Lev), and many others.

In conclusion, the selective removal of impurities from biogas by the use of DESs for absorption is a promising and sustainable process [122,123,219–222]. Biogas upgrading using DESs is expected to have a crucial part in expanding the use of biogas as a renewable and

sustainable energy source as research and development efforts proceed. Therefore, to solve these limitations of conventional solvents, we evaluated the use of DESs for the absorption of various groups of VOCs and other impurities found in biogas.

IX. Research overview

Due to the limitations of scrubbing solvents, the absorption of gaseous effluents is yet to be extensively investigated despite having numerous benefits, such as a high absorption capacity, adaptability to various industrial sectors, and others. The use of water, conventional solvents and amine scrubbers has been the oldest and most popular method of biogas upgrading due to the lack of flexible and economical scrubbing solvents. However, since most VOC contaminants are hydrophobic, some solvents are not the best for these compounds. Therefore, they are not effective enough to remove VOCs. In addition, to avoid undesirable events such as costly solvents, engine failure, low impurity absorption capacity, etc., biogas must be upgraded to remove impurities from raw biogas and meet biomethane quality requirements. Moreover, the appropriate absorbent developed shall have low viscosity, relatively low toxicity, low vapor pressure, high boiling point, high absorption capacity and low cost. These physicochemical properties are attractive from an industrial point of view. DES have physicochemical properties such as viscosity and polarity that can be tuned to meet these requirements. The purpose of this study is to evaluate hydrophobic DESs and conventional green solvents as VOC and CO₂ absorbents for biogas upgrading. The research is conducted in collaboration with our industrial partner (Terrao®), which is committed to driving innovation and addressing important global issues, thereby contributing to real-world applications.

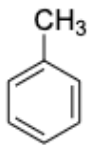
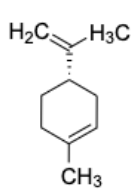
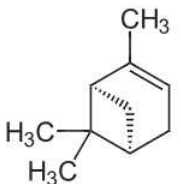
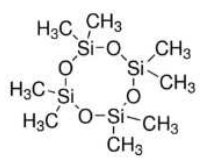
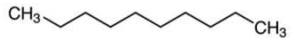
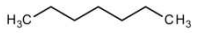
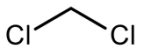
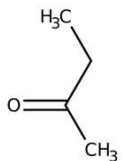
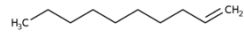
IX.1. Choice of biogas impurities

The composition of biogas varies depending on the kind of biogas feedstock and the relative amount of each feedstock. Impurities found in biogas include carbon monoxide, hydrogen, hydrogen sulfide, oxygen, nitrogen, and a variety of VOCs (alkanes, alkenes, siloxanes, terpenes, halogenated and aromatic hydrocarbons). We chose VOCs with a variety of physical and chemical properties that are found in biogas. Table 6 shows the impurities of biogas selected for our study.

IX.2. Choice of DESs and conventional solvents

The combinations that form the DES have been developed using components that can be produced on an industrial scale. However, there were two options for producing chemicals: chemical synthesis and natural extraction. For example, hydrophobic DESs with long chain fatty acids (caprylic, pelargonic, capric, and lauric acid) are widely used in many applications such as the flavor and fragrance industry, cosmetics and personal care products, pharmaceuticals, and furthermore, while choline chloride and cyclodextrins are usually used in the food industry and drug delivery. Nonetheless, conventional solvents are currently used in a wide range of applications. As a result, these components are available, facilitating their industrial application. Table 7 and 8 shows the structures of the DES and conventional solvents components.

Table 6. Structures and characteristics of selected VOCs.

VOCs	Toluene	Limonene	Pinene	Siloxane D4	Decane	Heptane	Dichloro methane	Methyl ethyl ketone	Decene
Structure									
Family	Aromatic	Terpene		Siloxane	Alkane		Halogenated	Ketone	Alkene
Water solubility (mg L ⁻¹) 25 C	526	7.57	2.5	0.056	0.052	3.4	13	220000	0.1

Ref. [<https://pubchem.ncbi.nlm.nih.gov/>].

Table 7. Selected DES component structures.

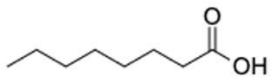
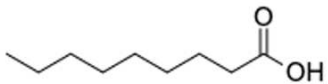
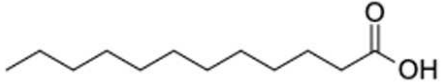
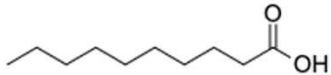
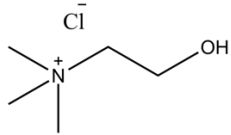
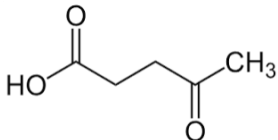
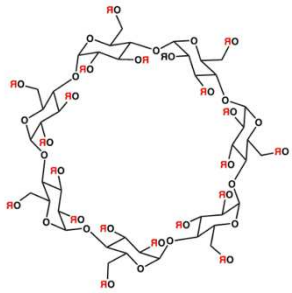
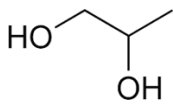
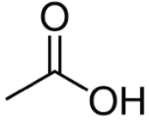
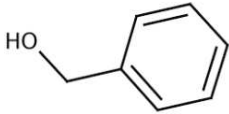
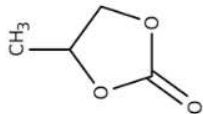
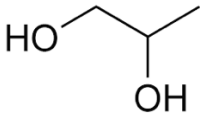
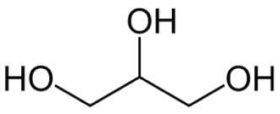
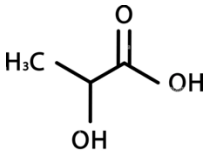
Deep Eutectic Solvents		Molar ratio	Abbreviation
HBA	HBD	-	-
Octanoic acid			
		3:1	C ₈ :C ₁₂
Nonanoic acid	Dodecanoic acid		
		3:1	C ₉ :C ₁₂
Decanoic acid			
		2:1	C ₁₀ :C ₁₂
ChCl	Levulinic acid		
		2:1	CL
Rameb	Propylene glycol		
		7:3	RL
R= -H or -CH ₃ , DS=12.9		1:30	RPG

Table 8. Selected conventional solvent's structure.

Conventional Solvents	Abbreviation	Water content (%)
Acetic acid		
	AA	0.05
Benzyl alcohol		
	BA	0.08
Cooking oil	CO	0.06
Propylene carbonate		
	PC	0.07
Propylene glycol		
	PG	0.52
	PG16	16
Glycerol		
	G	0.36
Lactic acid		
	LA	9

1. Aim of the study

The purpose of this study was to evaluate DESs and conventional green solvents as new absorbents for biogas upgrading and to select the most promising for upscaling (Figure 14). Indeed, this study was performed in collaboration with an industrial partner (Terrao®) who developed new mass and heat exchanger.

- Objective 1: Selection, preparation and characterization (density, viscosity, IR and water content) of DESs and conventional solvents.
- Objective 2: Evaluation of absorption capacities by using static headspace gas chromatography (SH-GC) to identify the DESs/solvents with the best VOC affinity. The effect of various factors including temperature, water content and initial VOC concentration were evaluated as they can influence the absorption process. Also, the absorption of VOC mixtures by DES was tested. Finally, we evaluated the regeneration of the studied solvents.
- Objective 3: Validation of the absorption capacities of DES and conventional solvents in a laboratory-scale dynamic absorption device (mimicking an industrial dynamic scrubber). Analyzing the effect of temperature, flow rate and water content on the absorption capacity of these solvents. Applying the device to synthetic biogas.
- Objective 4: Comparison of the performance of selected absorbent at industrial scale.

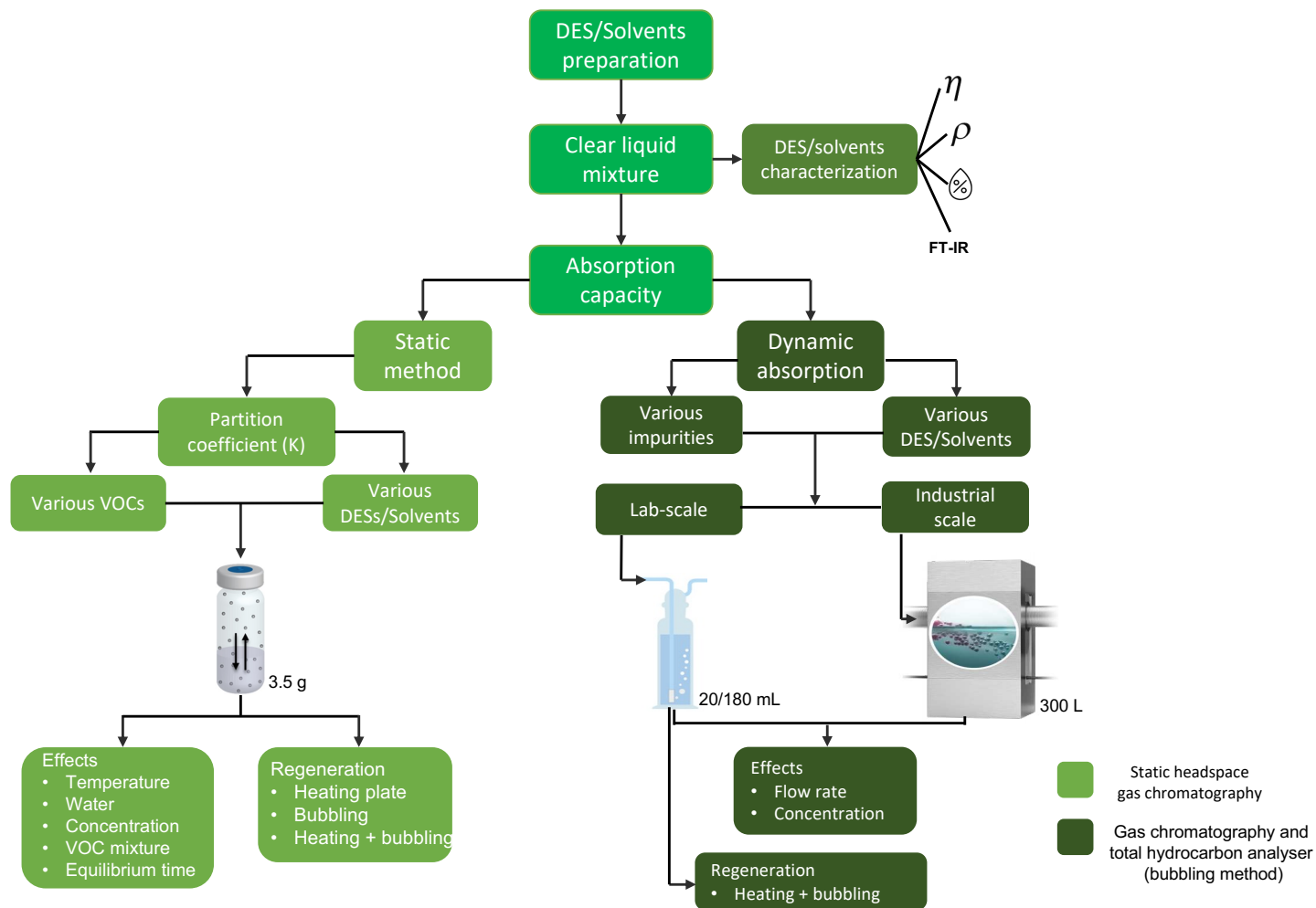


Figure 14. Methodology used in our study to evaluate DESs and conventional solvents as absorbents for biogas upgrading.

X. References

- [1] I. Angelidaki, L. Treu, P. Tsapekos, G. Luo, S. Campanaro, H. Wenzel, P.G. Kougias, Biogas upgrading and utilization: Current status and perspectives, *Biotechnol Adv.* 36 (2018) 452–466. <https://doi.org/10.1016/j.biotechadv.2018.01.011>.
- [2] V. Nallathambi Gunaseelan, *ANAEROBIC DIGESTION OF BIOMASS FOR METHANE PRODUCTION: A REVIEW*, 1997.
- [3] T. Bond, M.R. Templeton, History and future of domestic biogas plants in the developing world, *Energy for Sustainable Development.* 15 (2011) 347–354. <https://doi.org/10.1016/j.esd.2011.09.003>.
- [4] L.C.M. das Neves, A. Converti, T.C.V. Penna, Biogas production: New trends for alternative energy sources in rural and urban zones, *Chem Eng Technol.* 32 (2009) 1147–1153. <https://doi.org/10.1002/ceat.200900051>.
- [5] R. Bailis, V. Berrueta, C. Chengappa, K. Dutta, R. Edwards, O. Masera, D. Still, K.R. Smith, Performance testing for monitoring improved biomass stove interventions: experiences of the Household Energy and Health Project This paper is one of six describing work done as part of the Household Energy and Health (HEH) Project, *Energy for Sustainable Development.* 11 (2007) 57–70. [https://doi.org/10.1016/S0973-0826\(08\)60400-7](https://doi.org/10.1016/S0973-0826(08)60400-7).
- [6] H.N. Chanakya, S. Bhogle, R.S. Arun, Field experience with leaf litter-based biogas plants, *Energy for Sustainable Development.* 9 (2005) 49–62. [https://doi.org/10.1016/S0973-0826\(08\)60492-5](https://doi.org/10.1016/S0973-0826(08)60492-5).
- [7] J. Clemens, M. Trimborn, P. Weiland, B. Amon, Mitigation of greenhouse gas emissions by anaerobic digestion of cattle slurry, in: *Agric Ecosyst Environ*, 2006: pp. 171–177. <https://doi.org/10.1016/j.agee.2005.08.016>.
- [8] T. Horschig, A. Welfle, E. Billig, D. Thrän, From Paris agreement to business cases for upgraded biogas: Analysis of potential market uptake for biomethane plants in Germany using biogenic carbon capture and utilization technologies, *Biomass Bioenergy.* 120 (2019) 313–323. <https://doi.org/10.1016/j.biombioe.2018.11.022>.
- [9] H. Niu, Correlations between crude oil and stocks prices of renewable energy and technology companies: A multiscale time-dependent analysis, *Energy.* 221 (2021) 119800. <https://doi.org/10.1016/j.energy.2021.119800>.
- [10] J. Inchauspe, R.D. Ripple, S. Trück, The dynamics of returns on renewable energy companies: A state-space approach, *Energy Econ.* 48 (2015) 325–335. <https://doi.org/10.1016/j.eneco.2014.11.013>.
- [11] S. Managi, T. Okimoto, Does the price of oil interact with clean energy prices in the stock market?, *Japan World Econ.* 27 (2013) 1–9. <https://doi.org/10.1016/j.japwor.2013.03.003>.
- [12] PANORAMA DU GAZ RENOUVELABLE EN 2020, n.d.
- [13] A.K.P. Meyer, E.A. Ehimen, J.B. Holm-Nielsen, Future European biogas: Animal manure, straw and grass potentials for a sustainable European biogas production, *Biomass Bioenergy.* 111 (2018) 154–164. <https://doi.org/10.1016/j.biombioe.2017.05.013>.
- [14] A. Barragán-Escandón, J.M. Olmedo Ruiz, J.D. Curillo Tigre, E.F. Zalamea-León, Assessment of Power Generation Using Biogas from Landfills in an Equatorial Tropical Context, *Sustainability.* 12 (2020) 2669. <https://doi.org/10.3390/su12072669>.

- [15] T. Zhu, J. Curtis, M. Clancy, Promoting agricultural biogas and biomethane production: Lessons from cross-country studies, *Renewable and Sustainable Energy Reviews*. 114 (2019) 109332. <https://doi.org/10.1016/j.rser.2019.109332>.
- [16] M.U. Khan, J.T.E. Lee, M.A. Bashir, P.D. Dissanayake, Y.S. Ok, Y.W. Tong, M.A. Shariati, S. Wu, B.K. Ahring, Current status of biogas upgrading for direct biomethane use: A review, *Renewable and Sustainable Energy Reviews*. 149 (2021) 111343. <https://doi.org/10.1016/j.rser.2021.111343>.
- [17] L. Deng, Y. Liu, W. Wang, *Biogas Technology*, Springer Singapore, Singapore, 2020. <https://doi.org/10.1007/978-981-15-4940-3>.
- [18] D. Liu, B. Li, J. Wu, Y. Liu, Sorbents for hydrogen sulfide capture from biogas at low temperature: a review, *Environ Chem Lett*. 18 (2020) 113–128. <https://doi.org/10.1007/s10311-019-00925-6>.
- [19] P.C. Chan, Q. Lu, R.A. de Toledo, J.D. Gu, H. Shim, Improved anaerobic co-digestion of food waste and domestic wastewater by copper supplementation – Microbial community change and enhanced effluent quality, *Science of the Total Environment*. 670 (2019) 337–344. <https://doi.org/10.1016/j.scitotenv.2019.03.081>.
- [20] L.N. Nguyen, J. Kumar, M.T. Vu, J.A.H. Mohammed, N. Pathak, A.S. Commault, D. Sutherland, J. Zdarta, V.K. Tyagi, L.D. Nghiem, Biomethane production from anaerobic co-digestion at wastewater treatment plants: A critical review on development and innovations in biogas upgrading techniques, *Science of the Total Environment*. 765 (2021) 142753. <https://doi.org/10.1016/j.scitotenv.2020.142753>.
- [21] V. Kumar Gupta, M.G. Tuohy, *Biogas Fundamentals, Process and Operation*, 2018. <https://doi.org/https://doi.org/10.1007/978-3-319-77335-3>.
- [22] Adnan, Ong, Nomanbhay, Chew, Show, *Technologies for Biogas Upgrading to Biomethane: A Review*, *Bioengineering*. 6 (2019) 92. <https://doi.org/10.3390/bioengineering6040092>.
- [23] J. Niesner, D. Jecha, P. Stehlík, Biogas upgrading technologies: State of art review in european region, in: *Chem Eng Trans, Italian Association of Chemical Engineering - AIDIC, 2013*: pp. 517–522. <https://doi.org/10.3303/CET1335086>.
- [24] M.A. Goossens, *LANDFILL GAS POWER PLANTS*, 1996. [https://doi.org/https://doi.org/10.1016/0960-1481\(96\)88452-7](https://doi.org/https://doi.org/10.1016/0960-1481(96)88452-7).
- [25] US EPA, Chapter 2: Landfill Gas Basics. In *Landfill Gas Primer - An Overview for Environmental Health Professionals*, 2008. https://www.atsdr.cdc.gov/HAC/landfill/PDFs/Landfill_2001_ch2mod.pdf (accessed July 31, 2023).
- [26] H.W. Kim, J.Y. Nam, H.S. Shin, A comparison study on the high-rate co-digestion of sewage sludge and food waste using a temperature-phased anaerobic sequencing batch reactor system, *Bioresour Technol*. 102 (2011) 7272–7279. <https://doi.org/10.1016/j.biortech.2011.04.088>.
- [27] A. Converti, R.P.S. Oliveira, B.R. Torres, A. Lodi, M. Zilli, Biogas production and valorization by means of a two-step biological process, *Bioresour Technol*. 100 (2009) 5771–5776. <https://doi.org/10.1016/j.biortech.2009.05.072>.
- [28] D. Nagarajan, D.J. Lee, J.S. Chang, Integration of anaerobic digestion and microalgal cultivation for digestate bioremediation and biogas upgrading, *Bioresour Technol*. 290 (2019) 1218004. <https://doi.org/10.1016/j.biortech.2019.121804>.

- [29] J.N. Meegoda, B. Li, K. Patel, L.B. Wang, A review of the processes, parameters, and optimization of anaerobic digestion, *Int J Environ Res Public Health*. 15 (2018) 2224. <https://doi.org/10.3390/ijerph15102224>.
- [30] R.L. da Silva Pinto, A.C. Vieira, A. Scarpetta, F.S. Marques, R.M.M. Jorge, A. Bail, L.M.M. Jorge, M.L. Corazza, L.P. Ramos, An overview on the production of synthetic fuels from biogas, *Bioresour Technol Rep.* 18 (2022) 101104. <https://doi.org/10.1016/j.biteb.2022.101104>.
- [31] C. Li, P. He, L. Hao, F. Lü, L. Shao, H. Zhang, Diverse acetate-oxidizing syntrophs contributing to biogas production from food waste in full-scale anaerobic digesters in China, *Renew Energy*. 193 (2022) 240–250. <https://doi.org/10.1016/j.renene.2022.04.143>.
- [32] Trace Organic Compounds in Landfill Gas at Seven U.K. Waste Disposal Sites, *U.K. Waste Disposal Sites, Environ. Sci. Technol.* 31 (1997) 1054–1061. <https://doi.org/https://doi.org/10.1021/es9605634>.
- [33] L. Pizzuti, C.A. Martins, P.T. Lacava, Laminar burning velocity and flammability limits in biogas: A literature review, *Renewable and Sustainable Energy Reviews*. 62 (2016) 856–865. <https://doi.org/10.1016/j.rser.2016.05.011>.
- [34] F. Daniel, M. Sekar, B. Gavurová, C. Govindasamy, K. Moorthy R, B. P, P. T R, Recovering biogas and nutrients via novel anaerobic co-digestion of pre-treated water hyacinth for the enhanced biogas production, *Environ Res.* 231 (2023) 116216. <https://doi.org/10.1016/j.envres.2023.116216>.
- [35] S. Manigandan, P. T R, A. Anderson, A.M. Maryam, E. Mahmoud, Benefits of pretreated water hyacinth for enhanced anaerobic digestion and biogas production, *International Journal of Thermofluids*. 19 (2023) 100369. <https://doi.org/10.1016/j.ijft.2023.100369>.
- [36] P. Wang, H. Wang, Y. Qiu, L. Ren, B. Jiang, Microbial characteristics in anaerobic digestion process of food waste for methane production—A review, *Bioresour Technol.* 248 (2018) 29–36. <https://doi.org/10.1016/j.biortech.2017.06.152>.
- [37] L.N. Nguyen, A.Q. Nguyen, L.D. Nghiem, Microbial Community in Anaerobic Digestion System: Progression in Microbial Ecology, in: *Energy, Environment, and Sustainability*, Springer Nature, 2019: pp. 331–355. https://doi.org/10.1007/978-981-13-3259-3_15.
- [38] M.R. Atelge, H. Senol, D. Mohammed, T.A. Hansu, D. Krisa, A. Atabani, C. Eskicioglu, H. Muratçobanoğlu, S. Unalan, K. Slimane, N. Azbar, H.D. Kivrak, A critical overview of the state-of-the-art methods for biogas purification and utilization processes, *Sustainability (Switzerland)*. 13 (2021) 11515. <https://doi.org/10.3390/su132011515>.
- [39] X. Guo, C. Wang, F. Sun, W. Zhu, W. Wu, A comparison of microbial characteristics between the thermophilic and mesophilic anaerobic digesters exposed to elevated food waste loadings, *Bioresour Technol.* 152 (2014) 420–428. <https://doi.org/10.1016/j.biortech.2013.11.012>.
- [40] A. Anukam, A. Mohammadi, M. Naqvi, K. Granström, A review of the chemistry of anaerobic digestion: Methods of accelerating and optimizing process efficiency, *Processes*. 7 (2019) 1–19. <https://doi.org/10.3390/PR7080504>.
- [41] M. Schweigkofler, R. Niessner, Determination of siloxanes and VOC in landfill gas and sewage gas by canister sampling and GC-MS/AES analysis, *Environ Sci Technol.* 33 (1999) 3680–3685. <https://doi.org/10.1021/es9902569>.
- [42] A.C. Elwell, N.H. Elsayed, J.N. Kuhn, B. Joseph, Design and analysis of siloxanes removal by adsorption from landfill gas for waste-to-energy processes, *Waste Management*. 73 (2018) 189–196. <https://doi.org/10.1016/j.wasman.2017.12.021>.

- [43] M.D. Vaverková, Landfill impacts on the environment— review, *Geosciences* (Switzerland). 9 (2019) 431. <https://doi.org/10.3390/geosciences9100431>.
- [44] M.S. Ghafoori, K. Loubar, M. Marin-Gallego, M. Tazerout, Techno-economic and sensitivity analysis of biomethane production via landfill biogas upgrading and power-to-gas technology, *Energy*. 239 (2022) 122086. <https://doi.org/10.1016/j.energy.2021.122086>.
- [45] R. Chiriac, J. Carre, Y. Perrodin, L. Fine, J.M. Letoffe, Characterisation of VOCs emitted by open cells receiving municipal solid waste, *J Hazard Mater*. 149 (2007) 249–263. <https://doi.org/10.1016/j.jhazmat.2007.07.094>.
- [46] Y. Chhiti, M. Kemiha, Thermal Conversion of Biomass, Pyrolysis and Gasification: A Review, 2013. www.theijes.com.
- [47] A.S. Calbry-Muzyka, A. Gantenbein, J. Schneebeli, A. Frei, A.J. Knorpp, T.J. Schildhauer, S.M.A. Biollaz, Deep removal of sulfur and trace organic compounds from biogas to protect a catalytic methanation reactor, *Chemical Engineering Journal*. 360 (2019) 577–590. <https://doi.org/10.1016/j.cej.2018.12.012>.
- [48] J. Witte, A. Calbry-Muzyka, T. Wieseler, P. Hottinger, S.M.A. Biollaz, T.J. Schildhauer, Demonstrating direct methanation of real biogas in a fluidised bed reactor, *Appl Energy*. 240 (2019) 359–371. <https://doi.org/10.1016/j.apenergy.2019.01.230>.
- [49] J. Kopyscinski, T.J. Schildhauer, S.M.A. Biollaz, Production of synthetic natural gas (SNG) from coal and dry biomass - A technology review from 1950 to 2009, *Fuel*. 89 (2010) 1763–1783. <https://doi.org/10.1016/j.fuel.2010.01.027>.
- [50] K. Koido, T. Iwasaki, Biomass Gasification: A Review of Its Technology, Gas Cleaning Applications, and Total System Life Cycle Analysis, in: *Lignin - Trends and Applications*, InTech, 2018: pp. 161–180. <https://doi.org/10.5772/intechopen.70727>.
- [51] M. Hervy, D. Pham Minh, C. Gérente, E. Weiss-Hortala, A. Nzihou, A. Villot, L. Le Coq, H₂S removal from syngas using wastes pyrolysis chars, *Chemical Engineering Journal*. 334 (2018) 2179–2189. <https://doi.org/10.1016/j.cej.2017.11.162>.
- [52] P. Devi, A.K. Dalai, Occurrence, distribution, and toxicity assessment of polycyclic aromatic hydrocarbons in biochar, biocrude, and biogas obtained from pyrolysis of agricultural residues, *Bioresour Technol*. 384 (2023) 129293. <https://doi.org/10.1016/j.biortech.2023.129293>.
- [53] J. Luo, R. Ma, J. Lin, S. Sun, G. Gong, J. Sun, Y. Chen, N. Ma, Review of microwave pyrolysis of sludge to produce high quality biogas: Multi-perspectives process optimization and critical issues proposal, *Renewable and Sustainable Energy Reviews*. 173 (2023) 113107. <https://doi.org/10.1016/j.rser.2022.113107>.
- [54] A. Miyamoto, C. Ishiguro, The outlook for natural gas and LNG in China in the war against air pollution, Oxford, United Kingdom, 2018. <https://doi.org/10.26889/9781784671242>.
- [55] B.R. Singh, O. Singh, Global Trends of Fossil Fuel Reserves and Climate Change in the 21st Century, 2012. <https://doi.org/https://doi.org/10.5772/38655>.
- [56] K.A. Lyng, A.E. Stensgård, O.J. Hanssen, I.S. Modahl, Relation between greenhouse gas emissions and economic profit for different configurations of biogas value chains: A case study on different levels of sector integration, *J Clean Prod*. 182 (2018) 737–745. <https://doi.org/10.1016/j.jclepro.2018.02.126>.
- [57] D. Divya, L.R. Gopinath, P. Merlin Christy, A review on current aspects and diverse prospects for enhancing biogas production in sustainable means, *Renewable and*

- Sustainable Energy Reviews. 42 (2015) 690–699. <https://doi.org/10.1016/j.rser.2014.10.055>.
- [58] V. Esen, B. Oral, Natural gas reserve/production ratio in Russia, Iran, Qatar and Turkmenistan: A political and economic perspective, *Energy Policy*. 93 (2016) 101–109. <https://doi.org/10.1016/j.enpol.2016.02.037>.
- [59] F.P. Vahl, N.C. Filho, Energy transition and path creation for natural gas in the Brazilian electricity mix, *J Clean Prod*. 86 (2015) 221–229. <https://doi.org/10.1016/j.jclepro.2014.08.033>.
- [60] A. Pertl, P. Mostbauer, G. Obersteiner, Climate balance of biogas upgrading systems, *Waste Management*. 30 (2010) 92–99. <https://doi.org/10.1016/j.wasman.2009.08.011>.
- [61] A. Golmakani, S. Ali Nabavi, B. Wadi, V. Manovic, Advances, challenges, and perspectives of biogas cleaning, upgrading, and utilisation, *Fuel*. 317 (2022) 123085. <https://doi.org/10.1016/j.fuel.2021.123085>.
- [62] M.M. Maroneze, L.Q. Zepka, J.G. Vieira, M.I. Queiroz, E. Jacob-Lopes, A tecnologia de remoção de fósforo: Gerenciamento do elemento em resíduos industriais, *Revista Ambiente e Agua*. 9 (2014) 445–458. <https://doi.org/10.4136/1980-993X>.
- [63] R. Strzalka, D. Schneider, U. Eicker, Current status of bioenergy technologies in Germany, *Renewable and Sustainable Energy Reviews*. 72 (2017) 801–820. <https://doi.org/10.1016/j.rser.2017.01.091>.
- [64] M. Zupančič, V. Možic, M. Može, F. Cimerman, I. Golobič, Current Status and Review of Waste-to-Biogas Conversion for Selected European Countries and Worldwide, Sustainability (Switzerland). 14 (2022) 1823. <https://doi.org/10.3390/su14031823>.
- [65] S. Xue, J. Song, X. Wang, Z. Shang, C. Sheng, C. Li, Y. Zhu, J. Liu, A systematic comparison of biogas development and related policies between China and Europe and corresponding insights, *Renewable and Sustainable Energy Reviews*. 117 (2020) 109474. <https://doi.org/10.1016/j.rser.2019.109474>.
- [66] S. Bourdin, A. Chassy, Are citizens ready to make an environmental effort? A study of the social acceptability of biogas in France, *Environ Manage*. 71 (2023) 1228–1239. <https://doi.org/10.1007/s00267-022-01779-5>.
- [67] J. Pavičić, K.N. Mavar, V. Brkić, K. Simon, Biogas and Biomethane Production and Usage: Technology Development, Advantages and Challenges in Europe, *Energies (Basel)*. 15 (2022) 2940. <https://doi.org/10.3390/en15082940>.
- [68] F. Levavasseur, L. Martin, L. Boros, J. Cadiou, M. Carozzi, P. Martin, S. Houot, Land cover changes with the development of anaerobic digestion for biogas production in France, *GCB Bioenergy*. 15 (2023) 630–641. <https://doi.org/10.1111/gcbb.13042>.
- [69] S.S. Cordova, M. Gustafsson, M. Eklund, N. Svensson, Potential for the valorization of carbon dioxide from biogas production in Sweden, *J Clean Prod*. 370 (2022) 133498. <https://doi.org/10.1016/j.jclepro.2022.133498>.
- [70] R. González, J. García-Cascallana, X. Gómez, Energetic valorization of biogas. A comparison between centralized and decentralized approach, *Renew Energy*. 215 (2023) 119013. <https://doi.org/10.1016/j.renene.2023.119013>.
- [71] B. Comesaña-Gándara, O. García-Depraect, F. Santos-Beneit, S. Bordel, R. Lebrero, R. Muñoz, Recent trends and advances in biogas upgrading and methanotrophs-based valorization, *Chemical Engineering Journal Advances*. 11 (2022) 100325. <https://doi.org/10.1016/j.cej.2022.100325>.

- [72] F. Pasciucco, G. Francini, I. Pecorini, A. Baccioli, L. Lombardi, L. Ferrari, Valorization of biogas from the anaerobic co-treatment of sewage sludge and organic waste: Life cycle assessment and life cycle costing of different recovery strategies, *J Clean Prod.* 401 (2023) 136762. <https://doi.org/10.1016/j.jclepro.2023.136762>.
- [73] N.K. Agarwal, M. Kumar, P. Ghosh, S.S. Kumar, L. Singh, V.K. Vijay, V. Kumar, Anaerobic digestion of sugarcane bagasse for biogas production and digestate valorization, *Chemosphere.* 295 (2022) 133893. <https://doi.org/10.1016/j.chemosphere.2022.133893>.
- [74] F. Monlau, S. Suarez-Alvarez, A. Lallement, G. Vaca-Medina, G. Giacinti, M. Munarriz, I. Urreta, C. Raynaud, C. Ferrer, S. Castañón, A cascade biorefinery for the valorization of microalgal biomass: biodiesel, biogas, fertilizers and high valuable compounds, *Algal Res.* 59 (2021) 102433. <https://doi.org/10.1016/j.algal.2021.102433>.
- [75] S.A. Alavi-Borazjani, I. Capela, L.A.C. Tarelho, Valorization of biomass ash in biogas technology: Opportunities and challenges, in: *Energy Reports*, Elsevier Ltd, 2020: pp. 472–476. <https://doi.org/10.1016/j.egyr.2019.09.010>.
- [76] R. Kapoor, P. Ghosh, B. Tyagi, V.K. Vijay, V. Vijay, I.S. Thakur, H. Kamyab, D.D. Nguyen, A. Kumar, Advances in biogas valorization and utilization systems: A comprehensive review, *J Clean Prod.* 273 (2020) 123052. <https://doi.org/10.1016/j.jclepro.2020.123052>.
- [77] S. Dahiya, T.K. Vanitha, S. Venkata Mohan, Synergistic impact of gas-looping, biocatalyst and co-substrate on acidogenic distributed metabolism of spent wash: Volatile fatty acid enrichment and in situ biogas upgradation, *Chemical Engineering Journal.* 444 (2022) 136372. <https://doi.org/10.1016/j.cej.2022.136372>.
- [78] I. Bragança, F. Sánchez-Soberón, G.F. Pantuzza, A. Alves, N. Ratola, Impurities in biogas: Analytical strategies, occurrence, effects and removal technologies, *Biomass Bioenergy.* 143 (2020) 105878. <https://doi.org/10.1016/j.biombioe.2020.105878>.
- [79] A.I. Osman, M. Hefny, M.I.A. Abdel Maksoud, A.M. Elgarahy, D.W. Rooney, Recent advances in carbon capture storage and utilisation technologies: a review, *Environ Chem Lett.* 19 (2021) 797–849. <https://doi.org/10.1007/s10311-020-01133-3>.
- [80] Z.-F. Sun, L. Zhao, K.-K. Wu, Z.-H. Wang, J. Wu, C. Chen, S.-S. Yang, A.-J. Wang, N.-Q. Ren, Overview of recent progress in exogenous hydrogen supply biogas upgrading and future perspective, *Science of The Total Environment.* 848 (2022) 157824. <https://doi.org/10.1016/j.scitotenv.2022.157824>.
- [81] E. Privalova, S. Rasi, P. Mäki-Arvela, K. Eränen, J. Rintala, D.Y. Murzin, J.P. Mikkola, CO₂ capture from biogas: Absorbent selection, *RSC Adv.* 3 (2013) 2979–2994. <https://doi.org/10.1039/c2ra23013e>.
- [82] J.G. Lu, X. Li, Y.X. Zhao, H.L. Ma, L.F. Wang, X.Y. Wang, Y.F. Yu, T.Y. Shen, H. Xu, Y.T. Zhang, CO₂ capture by ionic liquid membrane absorption for reduction of emissions of greenhouse gas, *Environ Chem Lett.* 17 (2019) 1031–1038. <https://doi.org/10.1007/s10311-018-00822-4>.
- [83] Y. Zhang, Z. Zhu, Y. Zheng, Y. Chen, F. Yin, W. Zhang, H. Dong, H. Xin, Characterization of volatile organic compound (VOC) emissions from swine manure biogas digestate storage, *Atmosphere (Basel).* 10 (2019) 411. <https://doi.org/10.3390/atmos10070411>.
- [84] M. Struk, I. Kushkevych, M. Vítězová, Biogas upgrading methods: recent advancements and emerging technologies, *Rev Environ Sci Biotechnol.* 19 (2020) 651–671. <https://doi.org/10.1007/s11157-020-09539-9>.

- [85] R. Noorain, T. Kindaichi, N. Ozaki, Y. Aoi, A. Ohashi, Biogas purification performance of new water scrubber packed with sponge carriers, *J Clean Prod.* 214 (2019) 103–111. <https://doi.org/10.1016/j.jclepro.2018.12.209>.
- [86] I. Angelidaki, L. Xie, G. Luo, Y. Zhang, H. Oechsner, A. Lemmer, R. Munoz, P.G. Kougias, Biogas upgrading: Current and emerging technologies, in: *Biomass, Biofuels, Biochemicals: Biofuels: Alternative Feedstocks and Conversion Processes for the Production of Liquid and Gaseous Biofuels*, Elsevier, 2019: pp. 817–843. <https://doi.org/10.1016/B978-0-12-816856-1.00033-6>.
- [87] M. Struk, I. Kushkevych, M. Vítězová, Biogas upgrading methods: recent advancements and emerging technologies, *Rev Environ Sci Biotechnol.* 19 (2020) 651–671. <https://doi.org/10.1007/s11157-020-09539-9>.
- [88] M.E. López, E.R. Rene, M.C. Veiga, C. Kennes, Biogas technologies and cleaning techniques, in: *Environmental Chemistry for a Sustainable World*, Springer Netherlands, 2012: pp. 347–377. https://doi.org/10.1007/978-94-007-2439-6_9.
- [89] O. Wesley Awe, Y. Zhao, A. Nzihou, D. Pham Minh, N. Lyczko, A Review of Biogas Utilisation, Purification and Upgrading Technologies A Review of Biogas Utilisation, Purification and Upgrading Technologies: Review. *Waste and Biomass Valorization A Review of Biogas Utilisation, Purification and Upgrading Technologies*, 3311 GZ DORDRECHT. 30 (2017) 267–283. <https://doi.org/10.1007/s12649-016-9826-4>.
- [90] P. Arora, R. Chance, H. Hendrix, M.J. Realff, V.M. Thomas, Y. Yuan, Life cycle greenhouse gas emissions of different CO₂ supply options for an algal biorefinery, *Journal of CO₂ Utilization.* 40 (2020) 101213. <https://doi.org/10.1016/j.jcou.2020.101213>.
- [91] G.G. Esquivel-Patiño, F. Nápoles-Rivera, Environmental and energetic analysis of coupling a biogas combined cycle power plant with carbon capture, organic Rankine cycles and CO₂ utilization processes, *J Environ Manage.* 300 (2021) 113746. <https://doi.org/10.1016/j.jenvman.2021.113746>.
- [92] Z. Zhao, Y. Huang, Z. Zhang, W. Fei, M. Luo, Y. Zhao, Experimental and simulation study of CO₂ and H₂S solubility in propylene carbonate, imidazolium-based ionic liquids and their mixtures, *J Chem Thermodyn.* 142 (2020) 106017. <https://doi.org/10.1016/j.jct.2019.106017>.
- [93] T. Keipi, V. Hankalin, J. Nummelin, R. Raiko, Techno-economic analysis of four concepts for thermal decomposition of methane: Reduction of CO₂ emissions in natural gas combustion, *Energy Convers Manag.* 110 (2016) 1–12. <https://doi.org/10.1016/j.enconman.2015.11.057>.
- [94] X. Lu, Y. Liu, Q. Zhang, Y. Chen, J. Yao, Online detection and source tracing of VOCs in the air, *Opt Laser Technol.* 149 (2022). <https://doi.org/10.1016/j.optlastec.2021.107826>.
- [95] B. Ozturk, C. Kuru, H. Aykac, S. Kaya, VOC separation using immobilized liquid membranes impregnated with oils, *Sep Purif Technol.* 153 (2015) 1–6. <https://doi.org/10.1016/j.seppur.2015.08.032>.
- [96] M. Tomatis, M.T. Moreira, H. Xu, W. Deng, J. He, A.M. Parvez, Removal of VOCs from waste gases using various thermal oxidizers: A comparative study based on life cycle assessment and cost analysis in China, *J Clean Prod.* 233 (2019) 808–818. <https://doi.org/10.1016/j.jclepro.2019.06.131>.
- [97] G. Carriero, L. Neri, D. Famulari, S. Di Lonardo, D. Piscitelli, A. Manco, A. Esposito, A. Chirico, O. Facini, S. Finardi, G. Tinarelli, R. Prandi, A. Zaldei, C. Vagnoli, P. Toscano, V.

- Magliulo, P. Ciccioli, R. Baraldi, Composition and emission of VOC from biogas produced by illegally managed waste landfills in Giugliano (Campania, Italy) and potential impact on the local population, *Science of the Total Environment*. 640–641 (2018) 377–386. <https://doi.org/10.1016/j.scitotenv.2018.05.318>.
- [98] J.I. Salazar Gómez, H. Lohmann, J. Krassowski, Determination of volatile organic compounds from biowaste and co-fermentation biogas plants by single-sorbent adsorption, *Chemosphere*. 153 (2016) 48–57. <https://doi.org/10.1016/j.chemosphere.2016.02.128>.
- [99] G. Piechota, Removal of siloxanes from biogas upgraded to biomethane by Cryogenic Temperature Condensation System, *J Clean Prod*. 308 (2021) 127404. <https://doi.org/10.1016/j.jclepro.2021.127404>.
- [100] A. Manco, P. Ciccioli, D. Famulari, F. Brillì, P. Ciccioli, P. Di Tommasi, P. Toscano, B. Gioli, A. Esposito, V. Magliulo, Real-time air concentrations and turbulent fluxes of volatile organic compounds (VOCs) over historic closed landfills to assess their potential environmental impact, *Environmental Pollution*. 309 (2022) 119748. <https://doi.org/10.1016/j.envpol.2022.119748>.
- [101] A. Randazzo, F. Zorzi, S. Venturi, G. Bicocchi, G. Viti, F. Tatàno, F. Tassi, Degradation of biogas in a simulated landfill cover soil at laboratory scale: Compositional changes of main components and volatile organic compounds, *Waste Management*. 157 (2023) 229–241. <https://doi.org/10.1016/j.wasman.2022.12.027>.
- [102] E. Santos-Clotas, A. Cabrera-Codony, E. Boada, F. Gich, R. Muñoz, M.J. Martín, Efficient removal of siloxanes and volatile organic compounds from sewage biogas by an anoxic biotrickling filter supplemented with activated carbon, *Bioresour Technol*. 294 (2019) 122136. <https://doi.org/10.1016/j.biortech.2019.122136>.
- [103] Gang Wang, Zhongshen Zhang, Zhengping Hao, Recent advances in technologies for the removal of volatile methylsiloxanes: A case in biogas purification process, *Crit Rev Environ Sci Technol*. (2019). <https://doi.org/https://doi.org/10.1080/10643389.2019.1607443>.
- [104] A.N. Arias, R. Girón-Navarro, I. Linares-Hernández, V. Martínez-Miranda, E.A. Teutli-Sequeira, J. Lobato, M.A. Rodrigo, Removal of VOCs using electro-Fenton assisted absorption process, *J Environ Chem Eng*. 11 (2023) 110041. <https://doi.org/10.1016/j.jece.2023.110041>.
- [105] K. Starr, X. Gabarrell, G. Villalba, L. Talens, L. Lombardi, Life cycle assessment of biogas upgrading technologies, *Waste Management*. 32 (2012) 991–999. <https://doi.org/10.1016/j.wasman.2011.12.016>.
- [106] L. Lombardi, G. Francini, Techno-economic and environmental assessment of the main biogas upgrading technologies, *Renew Energy*. 156 (2020) 440–458. <https://doi.org/10.1016/j.renene.2020.04.083>.
- [107] A. Carranza-Abaid, R.R. Wanderley, H.K. Knuutila, J.P. Jakobsen, Analysis and selection of optimal solvent-based technologies for biogas upgrading, *Fuel*. 303 (2021). <https://doi.org/10.1016/j.fuel.2021.121327>.
- [108] J. Zhao, Y. Li, R. Dong, Recent progress towards in-situ biogas upgrading technologies, *Science of the Total Environment*. 800 (2021). <https://doi.org/10.1016/j.scitotenv.2021.149667>.
- [109] S. Koonaphapdeelert, P. Aggarangsi, J. Moran, Green Energy and Technology Biomethane Production and Applications, 2020. <https://doi.org/https://doi.org/10.1007/978-981-13-8307-6>.

- [110] L. Deng, Y. Liu, W. Wang, *Biogas technology*, Springer Singapore, 2020. <https://doi.org/10.1007/978-981-15-4940-3>.
- [111] F.M. Baena-Moreno, E. le Saché, L. Pastor-Pérez, T.R. Reina, Membrane-based technologies for biogas upgrading: a review, *Environ Chem Lett.* 18 (2020) 1649–1658. <https://doi.org/10.1007/s10311-020-01036-3>.
- [112] R. Kapoor, P. Ghosh, M. Kumar, V.K. Vijay, *Evaluation of biogas upgrading technologies and future perspectives: a review*, Springer Verlag, 2019. <https://doi.org/10.1007/s11356-019-04767-1>.
- [113] P. Gkotsis, P. Kougiyas, M. Mitrakas, A. Zouboulis, Biogas upgrading technologies – Recent advances in membrane-based processes, *Int J Hydrogen Energy.* 48 (2023) 3965–3993. <https://doi.org/10.1016/j.ijhydene.2022.10.228>.
- [114] H. Karne, U. Mahajan, U. Ketkar, A. Kohade, P. Khadilkar, A. Mishra, A review on biogas upgradation systems, *Mater Today Proc.* 72 (2023) 775–786. <https://doi.org/10.1016/j.matpr.2022.09.015>.
- [115] E. Wantz, D. Benizri, N. Dietrich, G. Hébrard, Rate-based modeling approach for High Pressure Water Scrubbing with unsteady gas flowrate and multicomponent absorption applied to biogas upgrading, *Appl Energy.* 312 (2022) 118754. <https://doi.org/10.1016/j.apenergy.2022.118754>.
- [116] R. Kapoor, P.M.V. Subbarao, V.K. Vijay, Integration of flash vessel in water scrubbing biogas upgrading system for maximum methane recovery, *Bioresour Technol Rep.* 7 (2019) 100251. <https://doi.org/10.1016/j.biteb.2019.100251>.
- [117] H. Wang, C. Ma, Z. Yang, X. Lu, X. Ji, Improving high-pressure water scrubbing through process integration and solvent selection for biogas upgrading, *Appl Energy.* 276 (2020) 115462. <https://doi.org/10.1016/j.apenergy.2020.115462>.
- [118] F.M. Baena-Moreno, M. Rodríguez-Galán, F. Vega, L.F. Vilches, B. Navarrete, Z. Zhang, Biogas upgrading by cryogenic techniques, *Environ Chem Lett.* 17 (2019) 1251–1261. <https://doi.org/10.1007/s10311-019-00872-2>.
- [119] A.I. Adnan, M.Y. Ong, S. Nomanbhay, K.W. Chew, P.L. Show, Technologies for biogas upgrading to biomethane: A review, *Bioengineering.* 6 (2019) 6–92. <https://doi.org/10.3390/bioengineering6040092>.
- [120] P. Xu, Z. Shang, G. Li, Z. Chen, W. Zhang, Efficient purification of biogas using ionic liquid as absorbent: Molecular thermodynamics, dynamics and experiment, *J Environ Chem Eng.* 11 (2023) 110083. <https://doi.org/10.1016/j.jece.2023.110083>.
- [121] E. Słupek, P. Makoś, J. Gębicki, Theoretical and economic evaluation of low-cost deep eutectic solvents for effective biogas upgrading to bio-methane, *Energies (Basel).* 13 (2020) 3390. <https://doi.org/10.3390/en13133379>.
- [122] E. Słupek, P. Makoś-Chełstowska, J. Gębicki, Removal of siloxanes from model biogas by means of deep eutectic solvents in absorption process, *Materials.* 14 (2021) 1–20. <https://doi.org/10.3390/ma14020241>.
- [123] P. Makoś-Chełstowska, E. Słupek, A. Kramarz, J. Gębicki, New carvone-based deep eutectic solvents for siloxanes capture from biogas, *Int J Mol Sci.* 22 (2021) 9551. <https://doi.org/10.3390/ijms22179551>.
- [124] A. Ahmad, D. Andrio, T.Y. Putra, U. Seprizal, Determination of mass transfer coefficient from biogas purification process by mono ethanol amine (MEA), *Mater Today Proc.* 63 (2022) S231–S236. <https://doi.org/10.1016/j.matpr.2022.02.430>.

- [125] A.A. Werkneh, Biogas impurities: environmental and health implications, removal technologies and future perspectives, *Heliyon*. 8 (2022) e10929. <https://doi.org/10.1016/j.heliyon.2022.e10929>.
- [126] R.S. Cavaignac, N.L. Ferreira, R. Guardani, Techno-economic and environmental process evaluation of biogas upgrading via amine scrubbing, *Renew Energy*. 171 (2021) 868–880. <https://doi.org/10.1016/j.renene.2021.02.097>.
- [127] F. Meng, T. Ju, S. Han, L. Lin, J. Li, K. Chen, J. Jiang, Novel monoethanolamine absorption using ionic liquids as phase splitter for CO₂ capture in biogas upgrading: High CH₄ purity and low energy consumption, *Chemical Engineering Journal*. 462 (2023) 142296. <https://doi.org/10.1016/j.cej.2023.142296>.
- [128] R. Muñoz, L. Meier, I. Diaz, D. Jeison, A review on the state-of-the-art of physical/chemical and biological technologies for biogas upgrading, *Rev Environ Sci Biotechnol*. 14 (2015) 727–759. <https://doi.org/10.1007/s11157-015-9379-1>.
- [129] A. Roozitalab, F. Hamidavi, A. Kargari, A review of membrane material for biogas and natural gas upgrading, *Gas Science and Engineering*. 114 (2023) 204969. <https://doi.org/10.1016/j.jgsce.2023.204969>.
- [130] N. Fajrina, N. Yusof, A.F. Ismail, F. Aziz, M.R. Bilad, M. Alkahtani, A crucial review on the challenges and recent gas membrane development for biogas upgrading, *J Environ Chem Eng*. 11 (2023) 110235. <https://doi.org/10.1016/j.jece.2023.110235>.
- [131] A. Naquash, M.A. Qyyum, J. Haider, A. Bokhari, H. Lim, M. Lee, State-of-the-art assessment of cryogenic technologies for biogas upgrading: Energy, economic, and environmental perspectives, *Renewable and Sustainable Energy Reviews*. 154 (2022) 111826. <https://doi.org/10.1016/j.rser.2021.111826>.
- [132] L.A. Pellegrini, G. De Guido, S. Langé, Biogas to liquefied biomethane via cryogenic upgrading technologies, *Renew Energy*. 124 (2018) 75–83. <https://doi.org/10.1016/j.renene.2017.08.007>.
- [133] A.A. Abd, M.R. Othman, Z. Helwani, J. Kim, Waste to wheels: Performance comparison between pressure swing adsorption and amine-absorption technologies for upgrading biogas containing hydrogen sulfide to fuel grade standards, *Energy*. 272 (2023) 127060. <https://doi.org/10.1016/j.energy.2023.127060>.
- [134] A.-S. Rodriguez Castillo, P.-F. Biard, S. Guihéneuf, L. Paquin, A. Amrane, A. Couvert, Assessment of VOC absorption in hydrophobic ionic liquids: Measurement of partition and diffusion coefficients and simulation of a packed column, *Chemical Engineering Journal*. 360 (2019) 1416–1426. <https://doi.org/10.1016/j.cej.2018.10.146>.
- [135] W. Wang, X. Ma, S. Grimes, H. Cai, M. Zhang, Study on the absorbability, regeneration characteristics and thermal stability of ionic liquids for VOCs removal, *Chemical Engineering Journal*. 328 (2017) 353–359. <https://doi.org/10.1016/j.cej.2017.06.178>.
- [136] L. Moura, T. Moufawad, M. Ferreira, H. Bricout, S. Tilloy, E. Monflier, M.F. Costa Gomes, D. Landy, S. Fourmentin, Deep eutectic solvents as green absorbents of volatile organic pollutants, *Environ Chem Lett*. 15 (2017) 747–753. <https://doi.org/10.1007/s10311-017-0654-y>.
- [137] S. Fourmentin, D. Landy, L. Moura, S. Tilloy, H. Bricout, Ferreira M., Process for Purifying a Gaseous Effluent, WO 2018/091379 A1, 2018.
- [138] P. Makoś-Chełstowska, E. Słupek, J. Gębicki, Deep eutectic solvent-based green absorbents for the effective removal of volatile organochlorine compounds from biogas, *Green Chemistry*. 23 (2021) 4814–4827. <https://doi.org/10.1039/D1GC01735G>.

- [139] C.-C. Chen, Y.-H. Huang, S.-M. Hung, C. Chen, C.-W. Lin, H.-H. Yang, Hydrophobic deep eutectic solvents as attractive media for low-concentration hydrophobic VOC capture, *Chemical Engineering Journal*. 424 (2021) 130420. <https://doi.org/10.1016/j.cej.2021.130420>.
- [140] C. Florindo, F. Lima, B.D. Ribeiro, I.M. Marrucho, Deep eutectic solvents: overcoming 21st century challenges, *Curr Opin Green Sustain Chem*. 18 (2019) 31–36. <https://doi.org/10.1016/j.cogsc.2018.12.003>.
- [141] J.A.P. Coutinho, S.P. Pinho, Special Issue on Deep Eutectic Solvents: A foreword, *Fluid Phase Equilib*. 448 (2017) 1. <https://doi.org/10.1016/j.fluid.2017.06.011>.
- [142] M.A.R. Martins, S.P. Pinho, J.A.P. Coutinho, Insights into the Nature of Eutectic and Deep Eutectic Mixtures, *J Solution Chem*. 48 (2019) 962–982. <https://doi.org/10.1007/s10953-018-0793-1>.
- [143] A.P. Abbott, G. Capper, D.L. Davies, R.K. Rasheed, V. Tambyrajah, Novel solvent properties of choline chloride/urea mixtures, *Chemical Communications*. (2003) 70–71. <https://doi.org/10.1039/b210714g>.
- [144] A.P. Abbott, G. Capper, D.L. Davies, H.L. Munro, R.K. Rasheed, V. Tambyrajah, Preparation of novel, moisture-stable, lewis-acidic ionic liquids containing quaternary ammonium salts with functional side chains, *Chemical Communications*. 1 (2001) 2010–2011. <https://doi.org/10.1039/b106357j>.
- [145] Y. Dai, J. van Spronsen, G.J. Witkamp, R. Verpoorte, Y.H. Choi, Natural deep eutectic solvents as new potential media for green technology, *Anal Chim Acta*. 766 (2013) 61–68. <https://doi.org/10.1016/j.aca.2012.12.019>.
- [146] A. Paiva, R. Craveiro, I. Aroso, M. Martins, R.L. Reis, A.R.C. Duarte, Natural deep eutectic solvents - Solvents for the 21st century, *ACS Sustain Chem Eng*. 2 (2014) 1063–1071. <https://doi.org/10.1021/sc500096j>.
- [147] S.E.E. Warrag, C.J. Peters, M.C. Kroon, Deep eutectic solvents for highly efficient separations in oil and gas industries, *Curr Opin Green Sustain Chem*. 5 (2017) 55–60. <https://doi.org/10.1016/j.cogsc.2017.03.013>.
- [148] C. Florindo, L.C. Branco, I.M. Marrucho, Quest for Green-Solvent Design: From Hydrophilic to Hydrophobic (Deep) Eutectic Solvents, *ChemSusChem*. 12 (2019) 1549–1559. <https://doi.org/10.1002/cssc.201900147>.
- [149] E.L. Smith, A.P. Abbott, K.S. Ryder, Deep Eutectic Solvents (DESS) and Their Applications, *Chem Rev*. 114 (2014) 11060–11082. <https://doi.org/10.1021/cr300162p>.
- [150] I.M. Aroso, J.C. Silva, F. Mano, A.S.D. Ferreira, M. Dionísio, I. Sá-Nogueira, S. Barreiros, R.L. Reis, A. Paiva, A.R.C. Duarte, Dissolution enhancement of active pharmaceutical ingredients by therapeutic deep eutectic systems, *European Journal of Pharmaceutics and Biopharmaceutics*. 98 (2016) 57–66. <https://doi.org/10.1016/j.ejpb.2015.11.002>.
- [151] A.R.C. Duarte, A.S.D. Ferreira, S. Barreiros, E. Cabrita, R.L. Reis, A. Paiva, A comparison between pure active pharmaceutical ingredients and therapeutic deep eutectic solvents: Solubility and permeability studies, *European Journal of Pharmaceutics and Biopharmaceutics*. 114 (2017) 296–304. <https://doi.org/10.1016/j.ejpb.2017.02.003>.
- [152] I.M. Aroso, R. Craveiro, Â. Rocha, M. Dionísio, S. Barreiros, R.L. Reis, A. Paiva, A.R.C. Duarte, Design of controlled release systems for THEDES - Therapeutic deep eutectic solvents, using supercritical fluid technology, *Int J Pharm*. 492 (2015) 73–79. <https://doi.org/10.1016/j.ijpharm.2015.06.038>.

- [153] D.J.G.P. Van Osch, L.F. Zubeir, A. Van Den Bruinhorst, M.A.A. Rocha, M.C. Kroon, Hydrophobic deep eutectic solvents as water-immiscible extractants, *Green Chemistry*. 17 (2015) 4518–4521. <https://doi.org/10.1039/c5gc01451d>.
- [154] B.D. Ribeiro, C. Florindo, L.C. Iff, M.A.Z. Coelho, I.M. Marrucho, Menthol-based eutectic mixtures: Hydrophobic low viscosity solvents, *ACS Sustain Chem Eng*. 3 (2015) 2469–2477. <https://doi.org/10.1021/acssuschemeng.5b00532>.
- [155] D.O. Abranches, J.A.P. Coutinho, Type V deep eutectic solvents: Design and applications, *Curr Opin Green Sustain Chem*. 35 (2022) 100612. <https://doi.org/10.1016/j.cogsc.2022.100612>.
- [156] N. Schaeffer, J.H.F. Conceição, M.A.R. Martins, M.C. Neves, G. Pérez-Sánchez, J.R.B. Gomes, N. Papaiconomou, J.A.P. Coutinho, Non-ionic hydrophobic eutectics-versatile solvents for tailored metal separation and valorisation, *Green Chemistry*. 22 (2020) 2810–2820. <https://doi.org/10.1039/d0gc00793e>.
- [157] D.O. Abranches, M.A.R. Martins, L.P. Silva, N. Schaeffer, S.P. Pinho, J.A.P. Coutinho, Phenolic hydrogen bond donors in the formation of non-ionic deep eutectic solvents: The quest for type v des, *Chemical Communications*. 55 (2019) 10253–10256. <https://doi.org/10.1039/c9cc04846d>.
- [158] Y. Liu, J.B. Friesen, J.B. McAlpine, D.C. Lankin, S.N. Chen, G.F. Pauli, Natural Deep Eutectic Solvents: Properties, Applications, and Perspectives, *J Nat Prod*. 81 (2018) 679–690. <https://doi.org/10.1021/acs.jnatprod.7b00945>.
- [159] K. Bica, J. Shamshina, W.L. Hough, D.R. MacFarlane, R.D. Rogers, Liquid forms of pharmaceutical co-crystals: Exploring the boundaries of salt formation, *Chemical Communications*. 47 (2011) 2267–2269. <https://doi.org/10.1039/c0cc04485g>.
- [160] T. El Achkar, T. Moufawad, S. Ruellan, D. Landy, H. Greige-Gerges, S. Fourmentin, Cyclodextrins: From solute to solvent, *Chemical Communications*. 56 (2020) 3385–3388. <https://doi.org/10.1039/d0cc00460j>.
- [161] S. Panda, S. Fourmentin, Cyclodextrin-based supramolecular low melting mixtures: efficient absorbents for volatile organic compounds abatement, *Environmental Science and Pollution Research*. 29 (2022) 264–270. <https://doi.org/10.1007/s11356-021-16279-y>.
- [162] M. Kfoury, D. Landy, S. Fourmentin, Combination of DES and macrocyclic host molecules: Review and perspectives, *Curr Opin Green Sustain Chem*. 36 (2022) 100630. <https://doi.org/10.1016/j.cogsc.2022.100630>.
- [163] T. El Achkar, L. Moura, T. Moufawad, S. Ruellan, S. Panda, S. Longuemart, F.X. Legrand, M. Costa Gomes, D. Landy, H. Greige-Gerges, S. Fourmentin, New generation of supramolecular mixtures: Characterization and solubilization studies, *Int J Pharm*. 584 (2020) 119443. <https://doi.org/10.1016/j.ijpharm.2020.119443>.
- [164] J.A. McCune, S. Kunz, M. Olesińska, O.A. Scherman, DESolution of CD and CB Macrocycles, *Chemistry - A European Journal*. 23 (2017) 8601–8604. <https://doi.org/10.1002/chem.201701275>.
- [165] T. Moufawad, L. Moura, M. Ferreira, H. Bricout, S. Tilloy, E. Monflier, M. Costa Gomes, D. Landy, S. Fourmentin, First Evidence of Cyclodextrin Inclusion Complexes in a Deep Eutectic Solvent, *ACS Sustain Chem Eng*. 7 (2019) 6345–6351. <https://doi.org/10.1021/acssuschemeng.9b00044>.
- [166] T. Moufawad, S. Fourmentin, M.C. Gomes, Solvants eutectiques profonds Vers des procédés plus durables, 2021. <https://doi.org/https://doi.org/10.51257/a-v1-chv4002>.

- [167] P. Makoś, E. Słupek, J. Gębicki, Hydrophobic deep eutectic solvents in microextraction techniques—A review, *Microchemical Journal*. 152 (2020) 104384. <https://doi.org/10.1016/j.microc.2019.104384>.
- [168] P. Makoś-Chełstowska, M. Kaykhaii, J. Płotka-Wasyłka, M. de la Guardia, Magnetic deep eutectic solvents – Fundamentals and applications, *J Mol Liq*. 365 (2022) 120158. <https://doi.org/10.1016/j.molliq.2022.120158>.
- [169] T. El Achkar, H. Greige-Gerges, S. Fourmentin, Basics and properties of deep eutectic solvents: a review, *Environ Chem Lett*. 19 (2021) 3397–3408. <https://doi.org/10.1007/s10311-021-01225-8>.
- [170] L.S. Bobrova, F.I. Danilov, V.S. Protsenko, Effects of temperature and water content on physicochemical properties of ionic liquids containing CrCl₃·xH₂O and choline chloride, *J Mol Liq*. 223 (2016) 48–53. <https://doi.org/10.1016/j.molliq.2016.08.027>.
- [171] F. Fahri, K. Bacha, F.F. Chiki, J.P. Mbakidi, S. Panda, S. Bouquillon, S. Fourmentin, Air pollution: new bio-based ionic liquids absorb both hydrophobic and hydrophilic volatile organic compounds with high efficiency, *Environ Chem Lett*. 18 (2020) 1403–1411. <https://doi.org/10.1007/s10311-020-01007-8>.
- [172] K.A. Omar, R. Sadeghi, Physicochemical properties of deep eutectic solvents: A review, *J Mol Liq*. 360 (2022) 119524. <https://doi.org/10.1016/j.molliq.2022.119524>.
- [173] T. Moufawad, M. Costa Gomes, S. Fourmentin, Deep eutectic solvents as absorbents for VOC and VOC mixtures in static and dynamic processes, *Chemical Engineering Journal*. 448 (2022) 137619. <https://doi.org/10.1016/j.cej.2022.137619>.
- [174] B.-Y. Zhao, P. Xu, F.-X. Yang, H. Wu, M.-H. Zong, W.-Y. Lou, Biocompatible Deep Eutectic Solvents Based on Choline Chloride: Characterization and Application to the Extraction of Rutin from *Sophora japonica*, 2015. <http://library.cmich.edu>.
- [175] P. Makoś-Chełstowska, VOCs absorption from gas streams using deep eutectic solvents – A review, *J Hazard Mater*. 448 (2023) 130957. <https://doi.org/10.1016/j.jhazmat.2023.130957>.
- [176] A.R.R. Teles, E. V. Capela, R.S. Carmo, J.A.P. Coutinho, A.J.D. Silvestre, M.G. Freire, Solvatochromic parameters of deep eutectic solvents formed by ammonium-based salts and carboxylic acids, *Fluid Phase Equilib*. 448 (2017) 15–21. <https://doi.org/10.1016/j.fluid.2017.04.020>.
- [177] M. Zhang, X. Zhao, S. Tang, K. Wu, B. Wang, Y. Liu, Y. Zhu, H. Lu, B. Liang, Structure–properties relationships of deep eutectic solvents formed between choline chloride and carboxylic acids: Experimental and computational study, *J Mol Struct*. 1273 (2023) 134283. <https://doi.org/10.1016/j.molstruc.2022.134283>.
- [178] C. Reichardt, *Solvatochromic Dyes as Solvent Polarity Indicators*, 1994. <https://doi.org/10.1021/cr00032a005>.
- [179] A.P. Abbott, R.C. Harris, K.S. Ryder, C. D’Agostino, L.F. Gladden, M.D. Mantle, Glycerol eutectics as sustainable solvent systems, *Green Chemistry*. 13 (2011) 82–90. <https://doi.org/10.1039/c0gc00395f>.
- [180] Y. Chen, W. Chen, L. Fu, Y. Yang, Y. Wang, X. Hu, F. Wang, T. Mu, Surface Tension of 50 Deep Eutectic Solvents: Effect of Hydrogen-Bonding Donors, Hydrogen-Bonding Acceptors, Other Solvents, and Temperature, *Ind Eng Chem Res*. 58 (2019) 12741–12750. <https://doi.org/10.1021/acs.iecr.9b00867>.
- [181] E. Jiménez, M. Cabanas, L. Segade, S. García-Garabal, H. Casas, Excess volume, changes of refractive index and surface tension of binary 1,2-ethanediol + 1-propanol or 1-butanol mixtures at several temperatures, 2001.

- [182] G. García, S. Aparicio, R. Ullah, M. Atilhan, Deep eutectic solvents: Physicochemical properties and gas separation applications, *Energy and Fuels*. 29 (2015) 2616–2644. <https://doi.org/10.1021/ef5028873>.
- [183] K. Shahbaz, F.S. Mjalli, M.A. Hashim, I.M. AlNashef, Prediction of the surface tension of deep eutectic solvents, *Fluid Phase Equilib.* 319 (2012) 48–54. <https://doi.org/10.1016/j.fluid.2012.01.025>.
- [184] M. Tariq, M.G. Freire, B. Saramago, J.A.P. Coutinho, J.N.C. Lopes, L.P.N. Rebelo, Surface tension of ionic liquids and ionic liquid solutions, *Chem Soc Rev.* 41 (2012) 829–868. <https://doi.org/10.1039/c1cs15146k>.
- [185] A.P. Abbott, D. Boothby, G. Capper, D.L. Davies, R.K. Rasheed, Deep Eutectic Solvents formed between choline chloride and carboxylic acids: Versatile alternatives to ionic liquids, *J Am Chem Soc.* 126 (2004) 9142–9147. <https://doi.org/10.1021/ja048266j>.
- [186] N. Rodriguez Rodriguez, A. Van Den Bruinhorst, L.J.B.M. Kollau, M.C. Kroon, K. Binnemans, Degradation of Deep-Eutectic Solvents Based on Choline Chloride and Carboxylic Acids, *ACS Sustain Chem Eng.* 7 (2019) 11521–11528. <https://doi.org/10.1021/acssuschemeng.9b01378>.
- [187] C. Florindo, F.S. Oliveira, L.P.N. Rebelo, A.M. Fernandes, I.M. Marrucho, Insights into the synthesis and properties of deep eutectic solvents based on cholinium chloride and carboxylic acids, *ACS Sustain Chem Eng.* 2 (2014) 2416–2425. <https://doi.org/10.1021/sc500439w>.
- [188] M.C. Gutiérrez, M.L. Ferrer, C.R. Mateo, F. Del Monte, Freeze-drying of aqueous solutions of deep eutectic solvents: A suitable approach to deep eutectic suspensions of self-assembled structures, *Langmuir.* 25 (2009) 5509–5515. <https://doi.org/10.1021/la900552b>.
- [189] R. Craveiro, I. Aroso, V. Flammia, T. Carvalho, M.T. Viciosa, M. Dionísio, S. Barreiros, R.L. Reis, A.R.C. Duarte, A. Paiva, Properties and thermal behavior of natural deep eutectic solvents, *J Mol Liq.* 215 (2016) 534–540. <https://doi.org/10.1016/j.molliq.2016.01.038>.
- [190] M. de los Á. Fernández, J. Boiteux, M. Espino, F.J.V. Gomez, M.F. Silva, Natural deep eutectic solvents-mediated extractions: The way forward for sustainable analytical developments, *Anal Chim Acta.* 1038 (2018) 1–10. <https://doi.org/10.1016/j.aca.2018.07.059>.
- [191] M. de los Á. Fernández, M. Espino, F.J.V. Gomez, M.F. Silva, Novel approaches mediated by tailor-made green solvents for the extraction of phenolic compounds from agro-food industrial by-products, *Food Chem.* 239 (2018) 671–678. <https://doi.org/10.1016/j.foodchem.2017.06.150>.
- [192] T. El Achkar, S. Fourmentin, H. Greige-Gerges, Deep eutectic solvents: An overview on their interactions with water and biochemical compounds, *J Mol Liq.* 288 (2019) 111028. <https://doi.org/10.1016/j.molliq.2019.111028>.
- [193] S.C. Cunha, J.O. Fernandes, Extraction techniques with deep eutectic solvents, *TrAC - Trends in Analytical Chemistry.* 105 (2018) 225–239. <https://doi.org/10.1016/j.trac.2018.05.001>.
- [194] C.H.J.T. Dietz, D.J.G.P. van Osch, M.C. Kroon, G. Sadowski, M. van Sint Annaland, F. Gallucci, L.F. Zubeir, C. Held, PC-SAFT modeling of CO₂ solubilities in hydrophobic deep eutectic solvents, *Fluid Phase Equilib.* 448 (2017) 94–98. <https://doi.org/10.1016/j.fluid.2017.03.028>.

- [195] L.F. Zubeir, D.J.G.P. Van Osch, M.A.A. Rocha, F. Banat, M.C. Kroon, Carbon Dioxide Solubilities in Decanoic Acid-Based Hydrophobic Deep Eutectic Solvents, *J Chem Eng Data*. 63 (2018) 913–919. <https://doi.org/10.1021/acs.jced.7b00534>.
- [196] R.B. Leron, M.H. Li, Solubility of carbon dioxide in a choline chloride-ethylene glycol based deep eutectic solvent, *Thermochim Acta*. 551 (2013) 14–19. <https://doi.org/10.1016/j.tca.2012.09.041>.
- [197] M. Lu, G. Han, Y. Jiang, X. Zhang, D. Deng, N. Ai, Solubilities of carbon dioxide in the eutectic mixture of levulinic acid (or furfuryl alcohol) and choline chloride, *Journal of Chemical Thermodynamics*. 88 (2015) 72–77. <https://doi.org/10.1016/j.jct.2015.04.021>.
- [198] R.B. Leron, M.H. Li, Solubility of carbon dioxide in a eutectic mixture of choline chloride and glycerol at moderate pressures, *Journal of Chemical Thermodynamics*. 57 (2013) 131–136. <https://doi.org/10.1016/j.jct.2012.08.025>.
- [199] R.B. Leron, A. Caparanga, M.H. Li, Carbon dioxide solubility in a deep eutectic solvent based on choline chloride and urea at T = 303.15–343.15K and moderate pressures, *J Taiwan Inst Chem Eng*. 44 (2013) 879–885. <https://doi.org/10.1016/j.jtice.2013.02.005>.
- [200] H.G. Morrison, C.C. Sun, S. Neervannan, Characterization of thermal behavior of deep eutectic solvents and their potential as drug solubilization vehicles, *Int J Pharm*. 378 (2009) 136–139. <https://doi.org/10.1016/j.ijpharm.2009.05.039>.
- [201] Y.H. Choi, J. van Spronsen, Y. Dai, M. Verberne, F. Hollmann, I.W.C.E. Arends, G.J. Witkamp, R. Verpoorte, Are natural deep eutectic solvents the missing link in understanding cellular metabolism and physiology?, *Plant Physiol*. 156 (2011) 1701–1705. <https://doi.org/10.1104/pp.111.178426>.
- [202] S. El Masri, S. Ruellan, M. Zakhour, L. Auezova, S. Fourmentin, Cyclodextrin-based low melting mixtures as a solubilizing vehicle: Application to non-steroidal anti-inflammatory drugs, *J Mol Liq*. 353 (2022) 118827. <https://doi.org/10.1016/j.molliq.2022.118827>.
- [203] L. Nakhle, M. Kfoury, H. Greige-Gerges, S. Fourmentin, Effect of dimethylsulfoxide, ethanol, α - and β -cyclodextrins and their association on the solubility of natural bioactive compounds, *J Mol Liq*. 310 (2020) 113156. <https://doi.org/10.1016/j.molliq.2020.113156>.
- [204] E. Silva, F. Oliveira, J.M. Silva, R.L. Reis, A.R.C. Duarte, Untangling the bioactive properties of therapeutic deep eutectic solvents based on natural terpenes, *Current Research in Chemical Biology*. 1 (2021) 100003. <https://doi.org/10.1016/j.crchbi.2021.100003>.
- [205] J. Pereira, M. Miguel Castro, F. Santos, A. Rita Jesus, A. Paiva, F. Oliveira, A.R.C. Duarte, Selective terpene based therapeutic deep eutectic systems against colorectal cancer, *European Journal of Pharmaceutics and Biopharmaceutics*. 175 (2022) 13–26. <https://doi.org/10.1016/j.ejpb.2022.04.008>.
- [206] V. Huber, L. Muller, P. Degot, D. Touraud, W. Kunz, NADES-based surfactant-free microemulsions for solubilization and extraction of curcumin from *Curcuma Longa*, *Food Chem*. 355 (2021) 129624. <https://doi.org/10.1016/j.foodchem.2021.129624>.
- [207] M.M. Abdelquader, S. Li, G.P. Andrews, D.S. Jones, Therapeutic deep eutectic solvents: A comprehensive review of their thermodynamics, microstructure and drug delivery applications, *European Journal of Pharmaceutics and Biopharmaceutics*. 186 (2023) 85–104. <https://doi.org/10.1016/j.ejpb.2023.03.002>.

- [208] M. Farsi, E. Soroush, CO₂ absorption by ionic liquids and deep eutectic solvents, in: *Advances in Carbon Capture: Methods, Technologies and Applications*, Elsevier, 2020: pp. 89–105. <https://doi.org/10.1016/B978-0-12-819657-1.00004-9>.
- [209] G. Siani, M. Tiecco, P. Di Profio, S. Guernelli, A. Fontana, M. Ciulla, V. Canale, Physical absorption of CO₂ in betaine/carboxylic acid-based Natural Deep Eutectic Solvents, *J Mol Liq.* 315 (2020) 113708. <https://doi.org/10.1016/j.molliq.2020.113708>.
- [210] J. Sun, Y. Sato, Y. Sakai, Y. Kansha, A review of ionic liquids and deep eutectic solvents design for CO₂ capture with machine learning, *J Clean Prod.* 414 (2023) 137695. <https://doi.org/10.1016/j.jclepro.2023.137695>.
- [211] A. Gutiérrez, S. Rozas, P. Hernando, R. Alcalde, M. Atilhan, S. Aparicio, A theoretical study of CO₂ capture by highly hydrophobic type III deep eutectic solvents, *J Mol Liq.* 366 (2022) 120285. <https://doi.org/10.1016/j.molliq.2022.120285>.
- [212] J. Jo, J. Park, S. Kwon, M. Park, J. Jung, Y. Yoo, D. Kang, Revolutionizing CO₂ capture: Molecular complexes of deep eutectic solvents with enhanced hydrogen bond accepting interaction for superior absorption performance, *J Environ Chem Eng.* 11 (2023) 110108. <https://doi.org/10.1016/j.jece.2023.110108>.
- [213] C. Li, L. He, X. Yao, Z. Yao, Recent advances in the chemical oxidation of gaseous volatile organic compounds (VOCs) in liquid phase, *Chemosphere.* 295 (2022) 133868. <https://doi.org/10.1016/j.chemosphere.2022.133868>.
- [214] S. Zhang, H. He, Q. Zhou, X. Zhang, X. Lu, Y. Tian, Principles and strategies for green process engineering, *Green Chemical Engineering.* 3 (2022) 1–4. <https://doi.org/10.1016/j.gce.2021.11.008>.
- [215] G. Xu, M. Shi, P. Zhang, Z. Tu, X. Hu, X. Zhang, Y. Wu, Tuning the composition of deep eutectic solvents consisting of tetrabutylammonium chloride and n-decanoic acid for adjustable separation of ethylene and ethane, *Sep Purif Technol.* 298 (2022) 121680. <https://doi.org/10.1016/j.seppur.2022.121680>.
- [216] C. Gui, G. Li, M. Song, Z. Lei, Absorption of dichloromethane in deep eutectic solvents: Experimental and computational thermodynamics, *Sep Purif Technol.* 311 (2023) 123281. <https://doi.org/10.1016/j.seppur.2023.123281>.
- [217] C. Zhang, J. Wu, R. Wang, E. Ma, L. Wu, J. Bai, J. Wang, Study of the toluene absorption capacity and mechanism of ionic liquids using COSMO-RS prediction and experimental verification, *Green Energy and Environment.* 6 (2021) 339–349. <https://doi.org/10.1016/j.gee.2020.08.001>.
- [218] Y. Zhao, J. Zhao, Y. Huang, Q. Zhou, X. Zhang, S. Zhang, Toxicity of ionic liquids: Database and prediction via quantitative structure-activity relationship method, *J Hazard Mater.* 278 (2014) 320–329. <https://doi.org/10.1016/j.jhazmat.2014.06.018>.
- [219] E. Supek, P. Makoś, J. Gębicki, A. Rogala, Purification of model biogas from toluene using deep eutectic solvents, in: *E3S Web of Conferences*, EDP Sciences, 2019: p. 00078. <https://doi.org/10.1051/e3sconf/201911600078>.
- [220] E. Słupek, P. Makoś, J. Gębicki, Deodorization of model biogas by means of novel non-ionic deep eutectic solvent, *Archives of Environmental Protection.* 46 (2020) 41–46. <https://doi.org/10.24425/aep.2020.132524>.
- [221] E. Słupek, P. Makoś, Absorptive desulfurization of model biogas stream using choline chloride-based deep eutectic solvents, *Sustainability (Switzerland).* 12 (2020) 1619. <https://doi.org/10.3390/su12041619>.
- [222] P. Makoś-Chełstowska, E. Słupek, A. Kramarz, D. Dobrzyniewski, B. Szulczyński, J. Gębicki, Green monoterpenes based deep eutectic solvents for effective BTEX

absorption from biogas, *Chemical Engineering Research and Design*. 188 (2022) 179–196. <https://doi.org/10.1016/j.cherd.2022.09.047>.

Chapter 2- Preparation and physicochemical characterization of the DESs and conventional solvents

In this chapter, we have studied the physicochemical properties of the DES and conventional solvents tested for the removal of biogas impurities. We present the techniques and methods used to characterize the absorbents, such as viscosity, density. Furthermore, the interaction between DES components and between DES and volatile organic compounds were investigated using FT-IR.

I. Preparation of the studied DES

During this study various DES were prepared using octanoic acid (C_8), nonanoic acid (C_9), decanoic acid (C_{10}), choline chloride (ChCl) and randomly methylated β -CD (RAMEB) as HBA, and dodecanoic acid (C_{12}), levulinic acid (Lev), and propylene glycol (PG) as HBD. The composition of the evaluated DES as well as their water content is given in table 9. The DESs were prepared by stirring the two components (HBA and HBD) at the desired molar ratio at 60 °C until a clear homogeneous liquid was formed. All compounds were used without pre-treatment to prepare the DES, except for choline chloride (ChCl), which is dried in an oven at 60 °C for at least two weeks to reduce the amount of water [1–3].

Table 9. Composition of the studied DES and their water content (%).

Solvents		Ratio	Abbreviation	Water content (%)
HBA	HBD			
Octanoic acid		3:1	$C_8:C_{12}$	0.11
Nonanoic acid	Dodecanoic acid	3:1	$C_9:C_{12}$	0.07
Decanoic acid		2:1	$C_{10}:C_{12}$	0.05
ChCl	Levulinic acid	1:2	CL	0.06
Rameb	Propylene glycol	1:30	RL RPG	2.00 2.30
Propylene carbonate		-	PC	0.07
Propylene glycol		-	PG	0.52
		-	PG16	16.00
Glycerol		-	G	0.36

Lactic acid	-	LA	9.00
Acetic acid	-	AA	0.05
Benzyl alcohol	-	BA	0.06
Cooking oil	-	CO	0.04

II. Characterization of the DESs and conventional solvents

Physicochemical properties like density and viscosity are important parameters that can affect mass transport processes thus, influencing their performance. We studied the physicochemical properties of the DESs and traditional solvents used to evaluate their capacity to absorb impurities from biogas. In order to characterize DES and traditional solvents, we present the methodologies and methods used to measure the viscosity, density, Infrared spectroscopy, and water content. The viscosity and density of the studied solvents were measured using SVM 3001 (Anton Paar), FT-IR spectra were recorded with an ATR (Attenuated Total Reflection) module on a Thermo Scientific™ Nicolet iS5 spectrometer, and the water content was determined by Karl Fischer titration (Mettler Toledo C20S KF Titrator).

II.1. Water content %

Water content is a critical factor that can have a significant effect on solvent characterization such as viscosity, thus, changing the process efficiency. It is a fundamental tool for determining the properties of DES and conventional solvents. Karl Fisher titration provides accurate information on water content, enabling the development and optimization of these solvents for specific applications. Accuracy is therefore required in the transition from laboratory to industrial scale. Indeed, in many industrial processes, choosing the right absorbent is a crucial step, especially in situations such as gas absorption where performance can be greatly impacted by water content as some compounds contain water content that may be naturally present in DES. A high-water content level might limit the absorption performance. The water content present in six DESs and eight conventional solvents are given in Table 9.

The values obtained for all DES and conventional solvents range from 0.05 to 16 wt%. The lowest wt% were obtained for the DES based on fatty acid certainly linked with the hydrophobic properties of the long alkyl chain fatty acid. The DES based on cyclodextrins contain more water than conventional DES. This could be explained by the presence of water in the cyclodextrin cavity. These values are in good agreement with the one obtained in previous studies with SUPRADES. The obtained values for ChCl:Lev showed a similar water content (0.06%) compared to the literature which showed a 0.05 wt% water content [2,4,5]

II.2. Melting point

The depressed melting point of deep eutectic solvents can be used to identify them. The melting point of DESs is significantly influenced by the molar ratio, alkyl chain length, and hydrogen bond donor, as shown in Table 10. According to Florindo et al. [1] the melting point of the hydrophobic DES based on long alkyl chain fatty acid is lower than that of their pure constituents. There is a significant drop in melting point of more than 10 °C compared to the individual materials [1]. Nevertheless, for SUPRADES several studies report that these DESs showed only a glass transition and no melting point with a temperature in the range from -13 to -75 °C [2,6]. Meanwhile it is clear that these novel neutral eutectic solvents do not exhibit the same melting point depressions as ionic compounds, which may reach 178 °C in the case of choline chloride and urea [3,7–9].

Table 10. Melting temperatures and molecular weight (MW) of fatty acid-based DESs, individual materials and conventional solvents used in this work.

	MW (g/mol)	Melting point (°C)
C ₁₂	200.32	43.2 ^a
C ₁₀	172.26	31.6 ^a
C ₉	158.23	12.6 ^a
C ₈	144.21	16.7 ^a
C ₈ :C ₁₂ (3:1)	162.91	9 ^a
C ₉ :C ₁₂ (3:1)	168.75	9 ^a
C ₁₀ :C ₁₂ (2:1)	179.28	18 ^a
PC	102.09	-55 ^b

PG	76.09	-60 ^b
G	92.09	
LA		
AA	60.05	16 ^b
BA	108.13	-15 ^b
CO	-	-17 ^b

^a [1] ^b [<https://pubchem.ncbi.nlm.nih.gov/>].

II.3. Viscosity

The Anton Paar SVM 3001 viscometer measures the torque needed to overcome the resistance provided by the viscosity of a liquid sample by rotating a spindle inside the liquid sample. This measurement makes it possible to determine viscosity accurately and reliably. It also provides temperature guidance benefits, such as within-range control and repeatability (0.005 °C). A certified viscosity and density reference standard was used for calibration. All studied solvents were measured at temperatures between 20 and 60 °C at atmospheric pressure. The experimental viscosity values were fitted as a function of temperature, using the Vogel – Fulcher – Tammann (VFT) model (Eq.1):

$$\eta = A' e^{B/(T-T_0)} \quad (\text{Eq.1})$$

where A' (mPa·s) quantifies the viscosity at infinite temperature, and B (K) and T_0 (K) are empirical constants.

The experimental viscosity results of DESs and conventional solvents as a function of temperature are presented in Table 11. The experimental viscosity values could be fitted as a function of temperature, using the Vogel – Fulcher – Tammann (VFT). The fitting parameter for each solvent are presented in Table 12. For all the samples, a decrease in viscosity with increasing temperature was observed (Figure 15). This behavior is similar to the one reported for most of the described DESs [1,5,10–12]. The same behavior was observed in the case of conventional solvents. As the DES based on fatty acid present a low viscosity at room temperature, they undergo a flat decay at elevated temperatures compared to highly viscous solvents. The obtained viscosities of the hydrophobic fatty acids DESs are quite low, ranging

between 6 and 9 mPa·s at 30 °C. Moreover, the viscosity is influenced by the length of the alkyl chain of the fatty acids. In fact, the following order was observed: C₈:C₁₂ < C₉:C₁₂ < C₁₀:C₁₂. These values and observations are in good agreement with those obtained in previous studies for these three hydrophobic DES [1]. These values are lower than those measured for hydrophilic and cyclodextrin-based DES, which range from 206.17 mPa·s to 300.9 mPa·s at 30 °C, respectively [13]. These values are consistent with the values of the most DES described in literature such as tetrapropylammonium bromide: tetraethylene glycol and choline chloride: resorcinol, which typically range from 84.6 to 326 mPa·s respectively. The viscosity values are affected by the presence of water and other contaminants [14–16]. Among the conventional physical absorbent PC present the lowest viscosity, but still the viscosity values are quite small except for glycerol (550 mPa·s at 30°C).

Mass transfer and the dynamics of the liquid phase in a system are determined by viscosity. However, by reducing viscosity, gas-phase compounds can absorb faster because molecules will diffuse into the liquid medium more readily. The use of less viscous liquids, where absorption and desorption are quicker and less energy-intensive for operations based on an absorption column, is more desirable from an industrial perspective.

Table 11. Experimental DESs and conventional solvents values of the dynamic viscosity as a function of temperature for the studied absorbent.

Absorbents	(η / mPa·s)				
	T °C				
	20	30	40	50	60
C ₈ :C ₁₂ (3:1)	-	6.08	4.69	3.72	3.01
C ₉ :C ₁₂ (3:1)	-	7.35	5.58	4.36	3.49
C ₁₀ :C ₁₂ (2:1)	-	9.09	6.79	5.25	4.16
Rameb:PG (1:30)	-	215.43	116.90	60.60	37.50
Rameb:Lev (1:30)	-	208.45	108.17	61.92	38.16
ChCl:Lev (1:2)	-	206.17	114.8	69.30	45.13
Propylene carbonate	2.69	2.19	1.84	1.56	1.35
Propylene glycol	54.02	30.59	18.37	11.78	7.82
Propylene glycol 16	34.16	20.23	12.74	8.50	5.94

Benzyl alcohol	6.4462	4.6763	3.5073	2.7103	2.1495
Glycerol	1281.1	550.18	261.72	136.34	76.716
Cooking oil	79.93	51.56	34.84	24.64	18.1

Table 12. Fitted parameters of Vogel–Fulcher–Tammann (VFT) model given by Equation (1) for the studied absorbents.

Absorbent	Parameters		
	A (mPa·s)	B (K)	T ₀ (K)
C ₈ :C ₁₂ (3:1)	0.84	922.07	112.29
C ₉ :C ₁₂ (3:1)	0.76	968.19	113.78
C ₁₀ :C ₁₂ (2:1)	1.74	694.85	149.01
Rameb:PG (1:30)	1.19	928.36	188.30
Rameb:Lev (1:30)	1.19	928.34	187
ChCl:Lev (1:2)	1.94	928.45	188.56
Propylene carbonate	1.96	508.95	131.93
Propylene glycol	0.11	1369.62	40.70
Propylene glycol 16	0.38	980.22	159.29

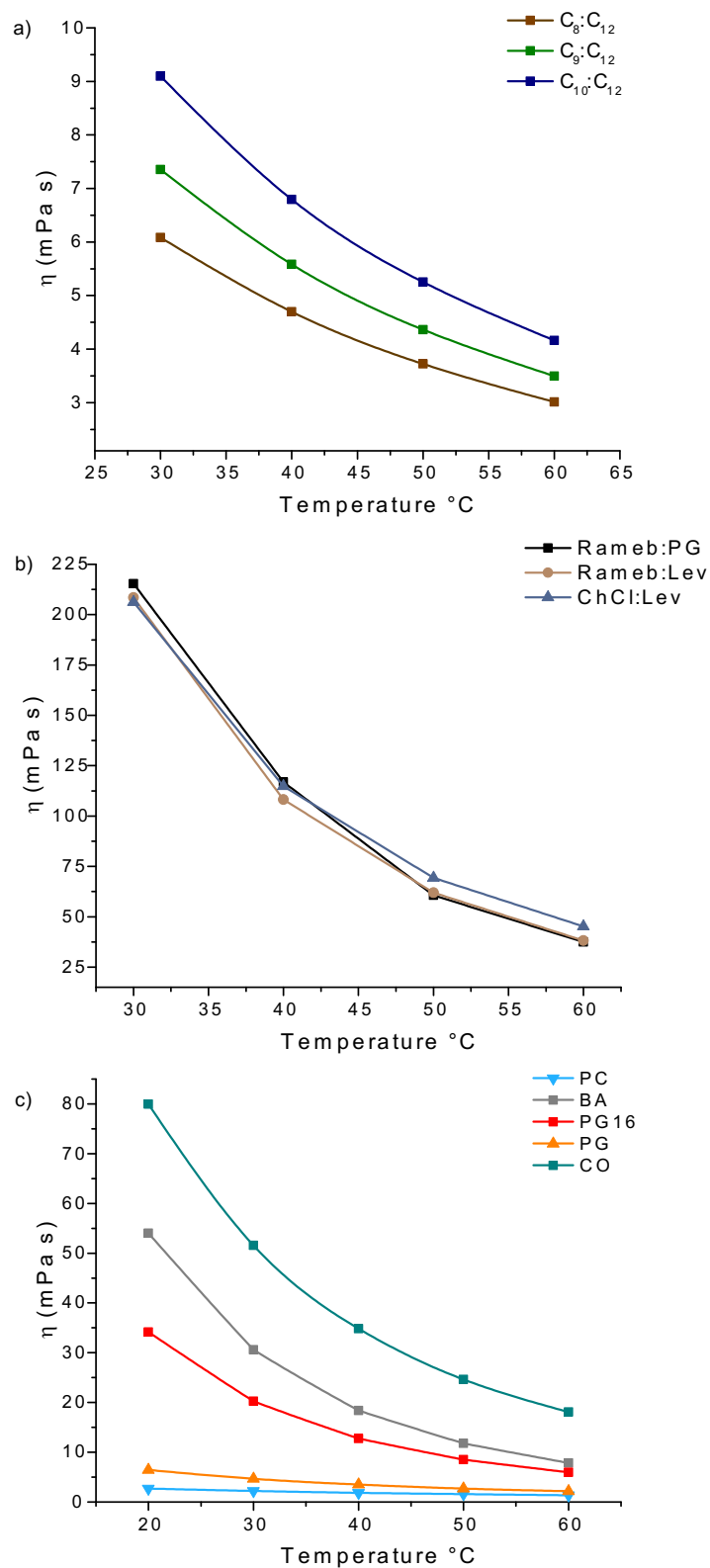


Figure 15. Experimental viscosity of the studied DESs (a and b) and conventional solvents (c) as a function of temperature.

II.4. Density

The Anton Paar SVM 3001 Viscometer is primarily designed to measure viscosity, but it can also be equipped with a density cell to measure density at the same time. This cell uses the oscillating U-tube principle. Standing waves are generated within the U-tube as a result of these oscillations. This approach is often used for accurate density measurements and is based on the idea of resonance frequency. Temperature control, like with viscosity measurements, is critical for precise density measurements. The SVM 3001 uses a temperature control system in order for the sample temperature to remain constant during the measurement. All solvents studied were measured at temperatures between 20 and 60 °C at atmospheric pressure. In order to fit the experimental density values, a linear fit was adopted using the following equation (Eq.2):

$$\rho = A_0 + A_1T \quad (\text{Eq.2})$$

where the density ρ is expressed in terms of: A_0 the intercept of the linear fit, A_1 the slope of the linear fit, and T (K) the ideal glass-transition temperature.

The experimental density results of DES and conventional solvents as a function of temperature are presented in Table 13. The experimental viscosity values could be fitted as a function of temperature with the equation (2) presented in Table 14. The density of all DESs and conventional solvents decreased linearly with temperature as shown in Figure 16. The experimental values at 30 °C ranged between 0.8901 to 0.8972 g.cm³ for hydrophobic DESs, 1.11 and 1.18 g.cm³ for hydrophilic DES and 1.02 to 1.19 g.cm³ for conventional solvents [13]. The obtained density of hydrophobic DESs at 30 °C are lower compared to most of the described hydrophilic DESs, like tetrabutylammonium:propylene glycol and tetrabutylphosphonium bromide: levulinic acid, that range between 1.05 to 1.11 g.cm⁻³ [5,17].

Table 13. Experimental densities of the studied absorbents as function of temperature.

Absorbents	Density (ρ / g.cm ³)				
	T °C				
	20	30	40	50	60
C ₈ :C ₁₂ (3:1)	-	0.89	0.88	0.88	0.87
C ₉ :C ₁₂ (3:1)	-	0.89	0.88	0.87	0.87
C ₁₀ :C ₁₂ (2:1)		0.89	0.88	0.87	0.86
Rameb:PG (1:30)	1.12	1.11	1.11	1.10	1.09
Rameb:Lev (1:30)	1.19	1.18	1.17	1.16	1.15
ChCl:Lev (1:2)	1.14	1.13	1.12	1.12	1.11
Propylene carbonate	1.20	1.19	1.18	1.17	1.16
Propylene glycol	1.03	1.02	1.02	1.01	1
Propylene glycol 16	1.08	1.07	1.06	1.05	1.05
Benzyl alcohol	1.04	1.03	1.03	1.02	1.01
Cooking oil	0.91	0.90	0.90	0.89	0.88

Table 14. Parameters, A_0 and A_1 , of Equation (2) describing temperature dependence of density of the studied absorbents.

Absorbent	Parameters	
	A_0 (g.cm ⁻³)	A_1 (x10 ⁻⁴) (g.cm ⁻³)
C ₈ :C ₁₂	1.132	-7.77
C ₉ :C ₁₂	1.125	-7.64
C ₁₀ :C ₁₂	1.116	-7.47
Propylene carbonate	1.514	-10.58
Propylene glycol	1.260	-7.63
Propylene glycol 16	1.297	-7.39

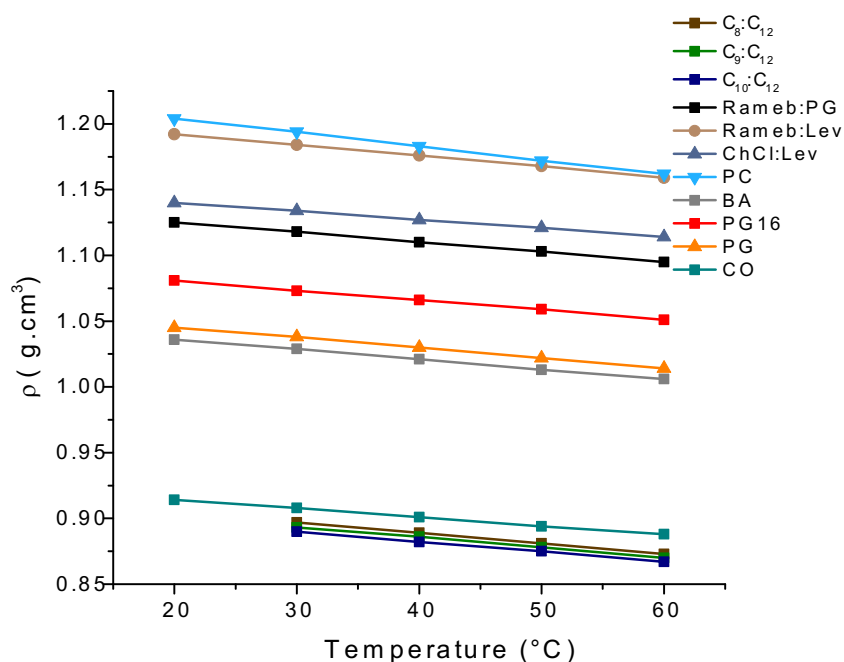


Figure 16. Experimental density of the studied DESs and conventional solvents as a function of temperature.

II.5. Infrared spectroscopy (FT-IR)

The FT-IR analysis provided many important insights into the structure, thus, understanding better the molecular interactions between absorbents components and their mixtures. It was possible, on the basis of the peak shifts, to find out which groups of individual compounds were involved in the formation of the DES, and to determine if any by-products were made during the preparation process. FT-IR (Fourier Transform Infrared Spectroscopy) spectra were recorded with an ATR (Attenuated Total Reflection) module on a Thermo Scientific™ Nicolet iS5 spectrometer between frequencies 4000 and 500 cm^{-1} .

Figure 17 shows the FT-IR spectra of the individual compounds of the C₁₀:C₁₂ and the prepared C₁₀:C₁₂ DES. In addition, individual toluene, limonene, siloxane D4 and their mixture (TLS) were evaluated in order to observe the behavior on absorption of individual VOCs and TLS mixture in C₁₀:C₁₂. Figure 17a displays the FT-IR spectra of C₁₀, C₁₂ individual compounds and C₁₀:C₁₂ DES. The peaks observed at 2900 cm^{-1} and 2800 cm^{-1} correlate to the -CH₃ and -CH₂ stretching vibrations, correspondingly. The peaks of the mixtures at 1689 to 1705 cm^{-1} is attributed to the characteristic C=O stretching mode, also the absorption band found between 3000 cm^{-1} and 3500 cm^{-1} is attributed to the hydroxyl group of the fatty acids.

Comparing the spectra of all DES mixtures and their individual components, it can be seen that all show the same characteristic peaks, indicating that no chemical reaction has occurred between the C₁₀ and C₁₂, components. These values and observations are in good agreement with the literature [18–20].

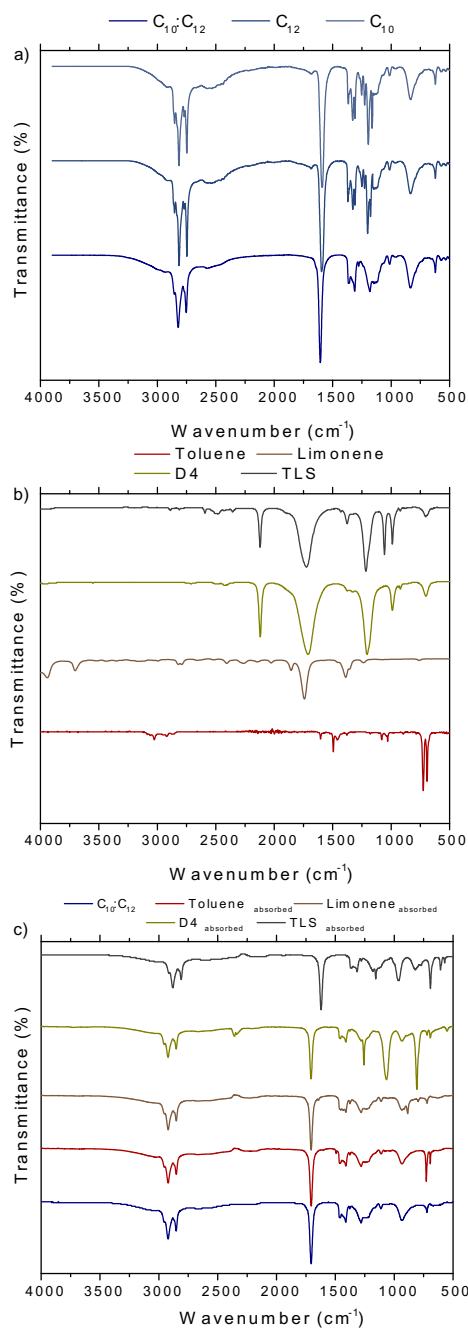


Figure 17. FT-IR of the prepared a) DES mixtures and their individual components: C₁₀:C₁₂, C₁₂ and C₁₀. b) VOCs alone and VOCs mixture c) DES mixture, VOCs alone absorbed by DES and VOCs mixture absorbed by DES C₁₀:C₁₂.

The figure 17b and c shows the spectra of the DES after the absorption of VOCs, for toluene, limonene, and siloxane D4 individually and for their mixture in C₁₀:C₁₂. For individual toluene, the C-H bending is visible as medium-intensity peaks in the 700–1000 cm⁻¹ range, which are the result of the C–H bonds in toluene bending vibrations. The stretching vibration of the carbon-carbon (C-C) bonds in the benzene ring is represented as a high peak in the aromatic characteristic at about 1500 cm⁻¹. An indication of an aromatic chemical is this peak. Regarding for toluene absorbed by C₁₀:C₁₂, the peak at 730 cm⁻¹ is characteristic of the pattern aromatics substitution. Furthermore, the strength of the C=O Stretch vibration at 1689-1706 cm⁻¹ in the DES increases considerably after the absorption of toluene. This may be due to an enhanced π - π interaction between the C=O bond in the fatty acids and the aromatic ring of toluene, since a similar C=O stretching vibration is observed in DES with a high efficiency of liquid-liquid extraction of toluene from mixed solvents. Negligible changes were observed in the peaks associated with CH₃, CH₂ and hydroxyl groups after toluene absorption [18–21].

In addition, when limonene is studied by FT-IR, several distinctive peaks in the IR spectrum can be seen in Figure 17b, each corresponding to specific vibrational modes of the molecule. Bending of the C-C and C-H vibrations cause peaks in the 750 to 1000 cm⁻¹ range. Terpene-related bands in limonene are frequently connected with skeletal vibrations and display bands in the 1100 to 1250 cm⁻¹ area. A carbon-carbon double bond (C=C) is found in limonene. The stretching vibration of this double bond often manifests as a prominent peak in the 1650-1750 cm⁻¹ region. The peaks between 2000 and 2500 cm⁻¹ are where the C-H stretching vibrations sequence. Individual peaks of limonene can be observed corresponding to the exact same peak for limonene absorbed by the C₁₀:C₁₂ as shown in Figure 17c [22–24].

For siloxane D4, when analyzed by infrared (IR) spectroscopy, several peaks can be observed as shown in Figure 17b. In the 500-600 cm⁻¹ range, bending vibrations connected to the Si-O-Si bonds may be observed. Due to the Si-C bonds in siloxane D4, stretching vibrations are frequently seen between 700 and 900 cm⁻¹. However, the strongest peaks in the IR spectra, which typically occur between 1000 and 1200 cm⁻¹, are linked to Si-O stretching vibrations. Peaks associated with C-H stretching vibrations may be visible in the 2800–3000 cm⁻¹ range, especially if the molecule contains methyl (CH₃) groups. For each siloxane D4 peak is associated with an individual bond due to siloxane absorption by the DES as shown in Figure

17c [25–28]. Finally, the TLS mixtures showed the individual peak as observed for each VOC separately, while the absorbed TLS DES again showed the same peaks as TLS mixture as can be seen in Figure 17c. Altogether, the observed results suggest that the studied VOCs are mainly absorbed physically by the DES, with no formation of new chemical bonds.

In this chapter, we have determined several physicochemical parameters of DES and conventional solvents (water content wt%, viscosity, and density). Also, in order to determine the functional groups of the molecules involved in the obtention of DES, the infrared spectra of DES and of its individual components have been determined. Once the solvents obtained have been characterized, the purpose of the next chapter is to determine the absorption capacity of DES and conventional solvents for the biogas impurities.

III. References

- [1] C. Florindo, L. Romero, I. Rintoul, L.C. Branco, I.M. Marrucho, From Phase Change Materials to Green Solvents: Hydrophobic Low Viscous Fatty Acid-Based Deep Eutectic Solvents, *ACS Sustain Chem Eng.* 6 (2018) 3888–3895. <https://doi.org/10.1021/acssuschemeng.7b04235>.
- [2] T. El Achkar, L. Moura, T. Moufawad, S. Ruellan, S. Panda, S. Longuemart, F.X. Legrand, M. Costa Gomes, D. Landy, H. Greige-Gerges, S. Fourmentin, New generation of supramolecular mixtures: Characterization and solubilization studies, *Int J Pharm.* 584 (2020) 119443. <https://doi.org/10.1016/j.ijpharm.2020.119443>.
- [3] T. El Achkar, T. Moufawad, S. Ruellan, D. Landy, H. Greige-Gerges, S. Fourmentin, Cyclodextrins: From solute to solvent, *Chemical Communications.* 56 (2020) 3385–3388. <https://doi.org/10.1039/d0cc00460j>.
- [4] T. El Achkar, S. Fourmentin, H. Greige-Gerges, Deep eutectic solvents: An overview on their interactions with water and biochemical compounds, *J Mol Liq.* 288 (2019) 111028. <https://doi.org/10.1016/j.molliq.2019.111028>.
- [5] L. Moura, T. Moufawad, M. Ferreira, H. Bricout, S. Tilloy, E. Monflier, M.F. Costa Gomes, D. Landy, S. Fourmentin, Deep eutectic solvents as green absorbents of volatile organic pollutants, *Environ Chem Lett.* 15 (2017) 747–753. <https://doi.org/10.1007/s10311-017-0654-y>.
- [6] M. Francisco, A. Van Den Bruinhorst, M.C. Kroon, New natural and renewable low transition temperature mixtures (LTTMs): Screening as solvents for lignocellulosic biomass processing, *Green Chemistry.* 14 (2012) 2153–2157. <https://doi.org/10.1039/c2gc35660k>.
- [7] P. Janicka, M. Kaykhaii, J. Płotka-Wasyłka, J. Gębicki, Supramolecular deep eutectic solvents and their applications, *Green Chemistry.* 24 (2022) 5035–5045. <https://doi.org/10.1039/d2gc00906d>.
- [8] S. Panda, S. Fourmentin, Cyclodextrin-based supramolecular low melting mixtures: efficient absorbents for volatile organic compounds abatement, *Environmental Science and Pollution Research.* 29 (2022) 264–270. <https://doi.org/10.1007/s11356-021-16279-y>.
- [9] T. El Achkar, H. Greige-Gerges, S. Fourmentin, Basics and properties of deep eutectic solvents: a review, *Environ Chem Lett.* 19 (2021) 3397–3408. <https://doi.org/10.1007/s10311-021-01225-8>.
- [10] J.N. Al-Dawsari, A. Bessadok-Jemai, I. Wazeer, S. Mokraoui, M.A. AlMansour, M.K. Hadj-Kali, Fitting of experimental viscosity to temperature data for deep eutectic solvents, *J Mol Liq.* 310 (2020) 113127. <https://doi.org/10.1016/j.molliq.2020.113127>.
- [11] R. Haghbakhsh, K. Parvaneh, S. Raeissi, A. Shariati, A general viscosity model for deep eutectic solvents: The free volume theory coupled with association equations of state, *Fluid Phase Equilib.* 470 (2018) 193–202. <https://doi.org/10.1016/j.fluid.2017.08.024>.
- [12] P. Makoś-Chełstowska, VOCs absorption from gas streams using deep eutectic solvents – A review, *J Hazard Mater.* 448 (2023). <https://doi.org/10.1016/j.jhazmat.2023.130957>.
- [13] P. Villarim, E. Genty, J. Zemmouri, S. Fourmentin, Deep eutectic solvents and conventional solvents as VOC absorbents for biogas upgrading: A comparative study,

- Chemical Engineering Journal. 446 (2022) 136875.
<https://doi.org/10.1016/j.cej.2022.136875>.
- [14] E. Słupek, P. Makoś-Chełstowska, J. Gębicki, Removal of siloxanes from model biogas by means of deep eutectic solvents in absorption process, *Materials*. 14 (2021) 1–20. <https://doi.org/10.3390/ma14020241>.
- [15] Y. Song, S. Chen, F. Luo, L. Sun, Absorption of Toluene Using Deep Eutectic Solvents: Quantum Chemical Calculations and Experimental Investigation, *Ind Eng Chem Res*. 59 (2020) 22605–22618. <https://doi.org/10.1021/acs.iecr.0c04986>.
- [16] C.C. Chen, Y.H. Huang, J.Y. Fang, Hydrophobic deep eutectic solvents as green absorbents for hydrophilic VOC elimination, *J Hazard Mater*. 424 (2022) 127366. <https://doi.org/10.1016/j.jhazmat.2021.127366>.
- [17] R. Yusof, E. Abdulmalek, K. Sirat, M.B.A. Rahman, Tetrabutylammonium bromide (TBABr)-Based deep eutectic solvents (DESSs) and their physical properties, *Molecules*. 19 (2014) 8011–8026. <https://doi.org/10.3390/molecules19068011>.
- [18] C.C. Chen, Y.H. Huang, S.M. Hung, C. Chen, C.W. Lin, H.H. Yang, Hydrophobic deep eutectic solvents as attractive media for low-concentration hydrophobic VOC capture, *Chemical Engineering Journal*. 424 (2021) 130420. <https://doi.org/10.1016/j.cej.2021.130420>.
- [19] D.P. Arcon, F.C. Franco, All-fatty acid hydrophobic deep eutectic solvents towards a simple and efficient microextraction method of toxic industrial dyes, *J Mol Liq*. 318 (2020) 114220. <https://doi.org/10.1016/j.molliq.2020.114220>.
- [20] H. He, Q. Yue, B. Gao, X. Zhang, Q. Li, Y. Wang, The effects of compounding conditions on the properties of fatty acids eutectic mixtures as phase change materials, *Energy Convers Manag*. 69 (2013) 116–121. <https://doi.org/10.1016/j.enconman.2013.01.026>.
- [21] E. Supek, P. Makoś, J. Gębicki, A. Rogala, Purification of model biogas from toluene using deep eutectic solvents, in: *E3S Web of Conferences*, EDP Sciences, 2019: p. 00078. <https://doi.org/10.1051/e3sconf/201911600078>.
- [22] E.R.M. de Oliveira, R.P. Vieira, Synthesis and Characterization of Poly(limonene) by Photoinduced Controlled Radical Polymerization, *J Polym Environ*. 28 (2020) 2931–2938. <https://doi.org/10.1007/s10924-020-01823-7>.
- [23] F. Partal Ureña, J.R.A. Moreno, J.J. López González, Conformational study of (R)-(+)-limonene in the liquid phase using vibrational spectroscopy (IR, Raman, and VCD) and DFT calculations, *Tetrahedron Asymmetry*. 20 (2009) 89–97. <https://doi.org/10.1016/j.tetasy.2009.01.024>.
- [24] D. Cava, R. Catala, R. Gavara, J.M. Lagaron, Testing limonene diffusion through food contact polyethylene by FT-IR spectroscopy: Film thickness, permeant concentration and outer medium effects, *Polym Test*. 24 (2005) 483–489. <https://doi.org/10.1016/j.polymertesting.2004.12.003>.
- [25] E. Słupek, P. Makoś-Chełstowska, J. Gębicki, Removal of siloxanes from model biogas by means of deep eutectic solvents in absorption process, *Materials*. 14 (2021) 1–20. <https://doi.org/10.3390/ma14020241>.
- [26] P. Makoś-Chełstowska, E. Słupek, J. Gębicki, Deep eutectic solvent-based green absorbents for the effective removal of volatile organochlorine compounds from biogas, *Green Chemistry*. 23 (2021) 4814–4827. <https://doi.org/10.1039/D1GC01735G>.

- [27] S.C. Nunes, V. De Zea Bermudez, D. Ostrovskii, L.D. Carlos, FT-IR and Raman spectroscopic study of di-urea cross-linked poly(oxyethylene)/siloxane ormolytes doped with Zn²⁺ ions, *Vib Spectrosc.* 40 (2006) 278–288. <https://doi.org/10.1016/j.vibspec.2005.11.003>.
- [28] V.T.L. Tran, P. Gélin, C. Ferronato, L. Fine, J.M. Chovelon, G. Postole, Exploring the potential of infrared spectroscopy on the study of the adsorption/desorption of siloxanes for biogas purification, *Catal Today.* 306 (2018) 191–198. <https://doi.org/10.1016/j.cattod.2017.01.006>.

Chapter 3 - Deep eutectic solvents and conventional solvents as absorbents for the removal of biogas impurities in static and dynamic processes

This chapter describes the methods and conditions used to determine the absorption capacity of the biogas impurities in the absorbents. The effects of various factors have been evaluated. These include temperature, water content, initial VOC concentration and VOCs mixtures, as these can affect the absorption capacity. Three experimental methods were used to determine the efficiency of DES and conventional solvents as biogas impurities absorbents at laboratory and industrial scale *i)* determination of the partition coefficients of VOCs and CO₂ in the absorbents by static headspace gas chromatography, *ii)* determination of the absorption capacities of absorbents in dynamic process and *iii)* using an exchanger developed by our industrial partner (Terrao®). We also tried to explain the absorption mechanism of some solvents by COSMO-RS calculation. Additionally, the regeneration of the studied solvents was evaluated.

I. Determination the vapor-liquid partition coefficients (K) of VOCs

The vapor-liquid partition coefficient (K) is a fundamental parameter that expresses the mass distribution between two phases (gas and liquid) in equilibrium, the liquid phase being either water or solvents. It depends on the solubility of the analyte in the liquid phase and is defined as the ratio of the concentrations of the component in each phase. The use of appropriately diluted VOC solutions enables us to compare the K values obtained with Henry's law constants (H_c) in aqueous solution. K values were measured by static headspace gas chromatography (SH-GC), following a combination of two methods the phase ratio variation and vapor phase calibration. The K is defined by the following equation (Eq.3) [1–3].

$$K = \frac{C_G}{C_L} \quad (\text{Eq.3})$$

where C_G and C_L are the respective concentrations of the solute in gas and liquid phase at equilibrium.

I.1. Static headspace-gas chromatography (SH-GC)

In the present study, we obtained K values using gas chromatography connect to a static headspace. This method is based on gas extraction to analyze the vapor phase of a sample. The sample (liquid or solid) is first placed in a vial before being tightly sealed. The vial is then placed under a temperature control until equilibrium is reached between the two phases. Consequently, the gas phase in the sample is then collected and transferred to the carrier gas, which is sent to the column for gas chromatographic analysis. We can analyze the volatile components by collecting the gas phase sample. A vial used in our studies is shown in Figure 18, where a volatile component is in equilibrium with the two phases already present. All measurements were performed with a Thermo Scientific TriPlus™ 500 headspace autosampler coupled to a Trace 1300 gas chromatograph equipped with a flame ionization detector and a DB 624 column using nitrogen as carrier gas.

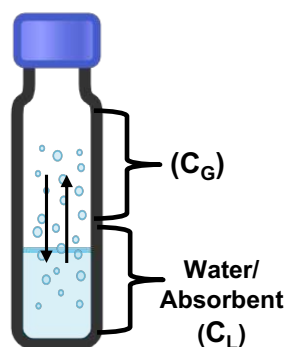


Figure 18. Vial used for headspace analysis with different phases.

I.2. K-value of VOC in water using phase ratio variation method (PRV)

The PRV method was used to determine the K value in water as described by Kolb and Ettre [4]. As shown in Figure 19 the same amount of VOC was added to several vials containing different amounts of water. The vapor/liquid volumetric ratio and the ratio between the corresponding chromatographic peak areas were used to calculate the K values. Using the previously obtained vapor-liquid partition coefficients of the VOCs in water, it is possible to be able to draw the calibration curve linking the VOC concentration in the vapor phase to the area under the chromatographic peak area.

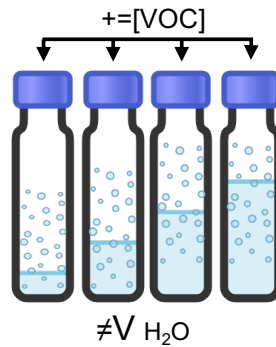


Figure 19. Several vials containing different amounts of water with the same amount of VOC [5].

In order to determine the K values of VOCs in water, stock solutions of the various VOCs were prepared in ethanol or water at 10,000 ppm. Then a precise volume of this stock solution is added to different water volume. As shown by Grossett et al., who noted a drop in the Henry's law constant (H_c) of tetrachloroethylene for methanol levels above 5%, the final concentration of ethanol is less than 0.1% and has no effect on the K values [6].

The partition coefficient K is measured at thermodynamic equilibrium between the two phases (gas and liquid). The vials containing VOCs in water were placed in a chamber thermostatically controlled at 30 °C for 30 minutes. The vials were then analyzed by GC. The K values were determined by the ratio between the respective chromatographic peak areas and the vapor-liquid volumetric ratio (Eq.4) [2,4].

$$C_{L0} \times V_L = \left(\frac{C_G}{K} \times V_L \right) + (C_G \times V_G) \quad (\text{Eq.4})$$

Where C_{L0} : Initial concentration of solute in solution (mol.L^{-1})

V_L : Volume of aqueous solution in vial (mL)

C_G : Concentration of solute in gas phase at equilibrium (mol.L^{-1})

V_G : Volume of gas phase in vial (mL)

The concentration of the gas phase is proportional to the area of the chromatographic peak (A):

$$A = \alpha C_G \quad (\text{Eq.5})$$

$$C_{L0} \times V_L = \left(\frac{A}{\alpha K} \times V_L \right) + \left(\frac{A}{\alpha} \times V_G \right) \quad (\text{Eq.6})$$

Where A: Chromatographic peak area

α : Constant combining various parameters related to the apparatus used

$$\frac{1}{AV_L} = \frac{1}{\alpha} \frac{V_G}{V_L} + \frac{1}{\alpha K} \quad (\text{Eq.7})$$

where A is the peak area, α is a constant incorporating several parameters, V_G is the vapor volume and V_L is the liquid volume. By plotting the graph $1/A.V_L$ as a function of the ratio between the volume of the gas and liquid phase (V_G/V_L), the value of K is obtained by the ratio between the slope and the y-intercept of the straight line obtained. The experimental conditions for the determination of K using gas chromatography are shown in Table 15.

Table 15. Experimental conditions used in gas chromatography for measurements of VOCs individually.

VOCs	GC Parameters		
	Column temperature °C	Analysis time / min	Retention time / min
Toluene	80	6	4.3
Heptane	80	4	2.6
Methyl ethyl ketone (MEK)	80	5	3.16
Limonene	120	8	6.15
Siloxane D4	120		4.21
Decane	120		4.8
Decene	120	6	4.7
Pinene	120		4.06
Dichloromethane	40	4	2.6

I.3 K-value of VOC in solvents using the vapor phase calibration method (VPC)

In order to determine the K values of VOC in absorbents the VPC method was used to determine the co-relation between area and concentration in the gas phase. As shown in Figure 20 different concentrations of VOCs were added to vials containing the same amount of water.

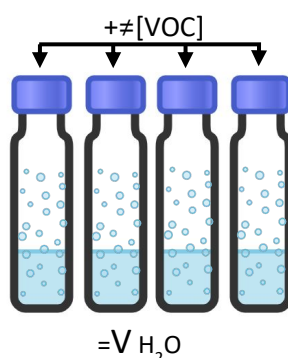


Figure 20. Several vials containing same amounts of water with the different amount of VOC.

In this method, the areas obtained in the solvent vials are compared with the areas obtained in the water vials to determine the K in the DES, as shown in Figure 21, following a combination of two methods as described previously. The experimental chromatographic peak areas allowed estimation of C_G and mass balance was used for determination of VOC concentration in absorbents [2,4].

$$C_G = \frac{n_{VOC}K}{V_L + KV_G} \quad (\text{Eq.8})$$

where n_{VOC} is the total mole amount of VOC added to each vial. Since C_G is proportional to the area under the chromatographic peak (A), we can draw the calibration curve between the area and the gas concentration.

Different concentrations of VOCs were added to vials containing the same amount of DES (3.5 g) placed in 20mL vials using stock solutions prepared from ethanol at 100,000 ppm. These vials were sealed and incubated at different temperatures for 24 h under magnetic stirring to

reach equilibrium before SH-GC analysis. They were then placed in a headspace oven for two hours at studied temperature.

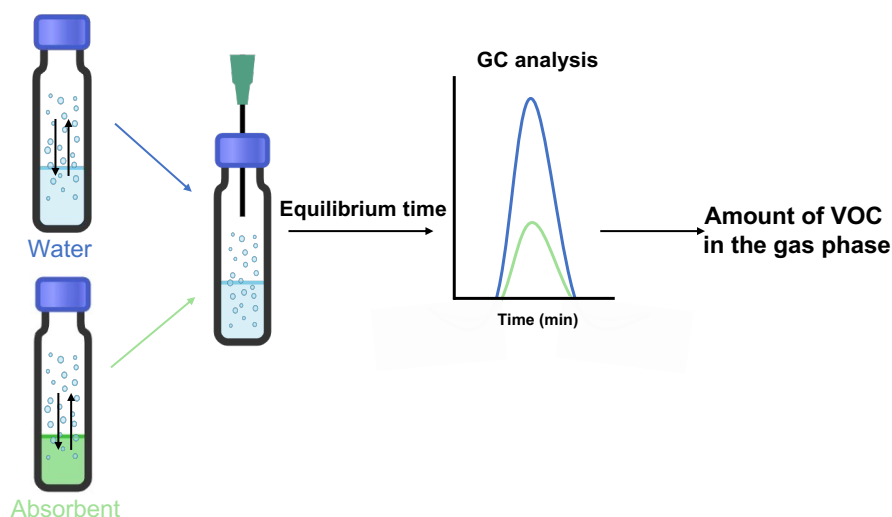


Figure 21. Representation of the measurement of vapor–liquid partition coefficients (K) using static-headspace-gas chromatography (SH-GC).

1.4. Results and discussion

1.4.1. Effect of equilibrium time

Gases and liquids often interact in a variety of applications, resulting in a state of equilibrium where the concentrations of gases dissolved in the liquid phase and present in the gas phase remain nearly constant. Gas-liquid equilibrium is essential for many processes, including gas absorption, chemical reactions, and environmental activities.

The time required to reach gas-liquid equilibrium can vary depending on a number of factors, including the type of the absorbents and gas, solubility of the gas, and temperature. While some systems may reach equilibrium quickly, others may take longer. As a result, several equilibrium times were evaluated in order to study the absorption behavior of toluene (295 ppm) in the DES based on fatty acid ($C_9:C_{12}$) and propylene carbonate (PC).

As can be seen in Figure 22, in the case of PC the areas ranged between 610, 455, 425, 335 and 339, respectively. 24 hours are necessary to reach the equilibrium. For $C_9:C_{12}$, there was quite no variation in the area, which remained around 165, meaning that toluene is absorbed fairly quickly after the VOC comes into contact with $C_9:C_{12}$. Previous studies with other DESs

have also underlined the necessity of 24h equilibrium. Therefore, all the partition coefficient measurements were performed after 24h equilibrium.

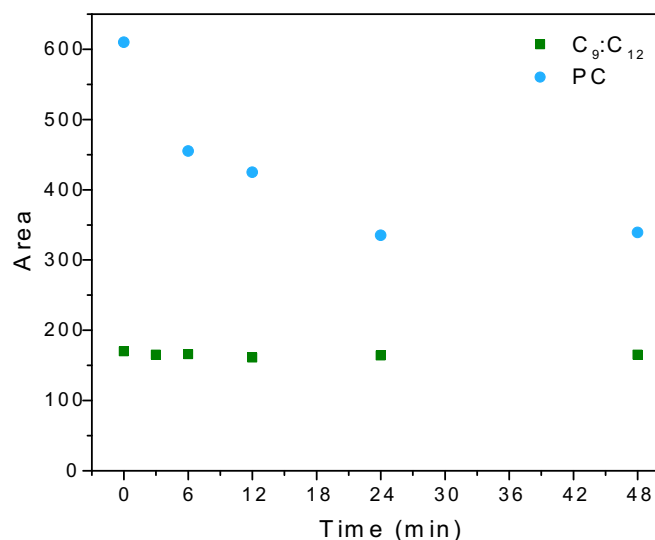


Figure 22. Areas of toluene in C₉:C₁₂ and PC at 30 °C for different equilibrium times.

I.4.2. Determination of K-values of VOC at 30 °C

The obtained partition coefficients (K) of all VOCs in water, DESs and conventional solvents at 30 °C are given in Table 16. The values in water are close to the one from literature [7–11]. Concerning siloxane D4, we can observe large variations in literature depending on the used method or equilibrium time. However, the value obtained for 24H equilibrium is close to our value. Moreover, all the experiments were performed at the same equilibrium time and therefore the obtained K values in solvents could be compared to the one in water. The decrease of K values observed for all VOCs in all the solvents in comparison to water indicated that a greater amount of VOC was absorbed in these solvents. Moreover, the K values of VOCs in hydrophobic DESs are lower compared to other studied DESs. Among the studied physical solvents, glycerol showed the lowest VOCs absorption capacity. Furthermore, propylene carbonate, cooking oil, benzyl alcohol, acetic acid and lactic acid exhibited good to moderate VOCs absorption capacities. However, due to their high viscosity we decided to discard lactic acid and glycerol. The commercial aqueous solution of propylene glycol showed highest K value compared to the pure one. This result could be attributed to the amount of water (16%) that lower the absorption efficiency of the solvent [12].

Table 16. Partition coefficients (K) of VOCs at 30 °C in the different DES.

Absorbent	Toluene	Limonene	Siloxane D4	Decene	Decane	Pinene	Heptane	Dichloro- methane	MEK
Water	0.294 ^a	2.32 ^a	4 ^a	18 ^a	21 ^a	6.35 ^a	29 ^a	0.13 ^a	0.005 ^a
	0.251 ^b		5 ^e (20 °C)						
	0.268 ^c	1.94 ^d	23, 9.6, 5.6, 3.4 ^f	25 ^g		11 ^h	27 ^g	0.14 ^g	0.003 ^g
C₈:C₁₂	4.75E-04	1.19E-04	2.97E-04	1.26E-04	1.15E-04	1.86E-04	1.64E-03	7.94E-03	6.59E-04
C₉:C₁₂	4.55E-04	1.22E-04	2.92E-04	1.24E-04	1.27E-04	1.91E-04	1.65E-03	7.34E-03	6.75E-04
C₁₀:C₁₂	5.14E-04	1.13E-04	3.14E-04	1.23E-04	1.11E-04	1.89E-04	1.65E-03	9.34E-03	7.27E-04
ChCl:Lev	4.15E-03	-	-	-	-	-	-	-	-
Rameb:Lev	1.80E-03	6.18E-04	1.36E-02	-	6.42E-03	-	-	-	-
Rameb:PG	1.62E-03	6.21E-04	7.22E-03	-	2.57E-03	-	-	-	-
Propylene carbonate	1.20E-03	6.29E-04	5.54E-03	2.14E-03	4.12E-03	2.01E-03	2.06E-02	3.03E-03	3.30E-04
Propylene glycol	3.31E-03	1.42E-03	1.23E-02	4.14E-03	6.19E-03	3.09E-03	2.96E-02	7.25E-03	8.48E-04
Propylene glycol 16	1.48E-02	1.17E-02	2.81E-02	5.57E-02	3.97E-02	2.80E-02	1.64E-01	1.80E-02	1.05E-03
Glycerol	4.06E-02	6.56E-02	8.42E-02	-	-	-	-	-	-

Benzyl acohol	6.04E-04	2.69E-04	1.61E-03	-	8.20E-04	-	-	4.45E-03	2.94E-04
Acetic acid (glacial)	9.34E-05	-	-	-	-	-	-	-	-
Lactic acid	6.05E-04	-	-	-	-	-	-	-	-
Cooking oil	4.48E-04	9.73E-05	4.45E-04	-	1.01E-04	-	-	1.05E-02	1.15E-03

^a This work, ^b Ref. [3], ^c Ref. [8], ^d Ref. [9], ^e Ref. [7], ^f Ref. [13], ^g Ref. [10], ^h [<https://pubchem.ncbi.nlm.nih.gov/>].

One of the most studied VOCs in the literature is toluene. In the case of hydrophobic VOCs, it serves as a model VOC. We have found that the toluene affinities of DESs vary. The obtained K values for toluene in the six studied DESs and eight conventional solvents ranged between $4.55\text{E-}04$ and $4.06\text{E-}02$ (up to 646-fold lower than in water). Among the six DESs, $\text{C}_9\text{:C}_{12}$ presents the lowest K value and among the eight conventional solvents, AA showed the lowest K value and corresponds to a 4.8-fold greater absorption than the best DES physical absorbent, $\text{C}_9\text{:C}_{12}$, at $30\text{ }^\circ\text{C}$. Nevertheless, we decided not to continue using acetic acid due to its corrosiveness and safety considerations. Therefore, the obtained values for hydrophobic DES are among the lowest that could be found in the literature for DESs, ionic liquids, or oil such as TBPBr:Dec ($9\text{E-}04$) and TBPBr:Lev ($1.3\text{E-}03$), these values and observations are in good agreement with hydrophobic DES [10,14–19].

Concerning limonene, the K values in hydrophobic DESs ranged between $1.13\text{E-}04$ and $1.19\text{E-}04$ corresponding to an up-to 20531-fold decrease compared to water [18,20]. DESs showed once more the greatest capacity to absorb limonene compared to the other solvents, except for cooking oil which was $9.73\text{E-}05$. In addition, the K value in benzyl alcohol ($2.69\text{E-}04$) was one of the lowest among the conventional solvents. Furthermore, since pinene belongs to the same class as limonene (terpene), the same affinity profiles are observed.

K values of siloxane D4 ranged between from $2.92\text{E-}04$ to $3.14\text{E-}04$ in DESs and from $8.42\text{E-}02$ to $4.45\text{E-}04$ in conventional solvents. This makes again hydrophobic DESs the most effective absorbent and cooking oil and propylene carbonate the most promising conventional absorbent. Few studies were dedicated to the evaluation of solvents (DESs or ionic liquids) for siloxanes absorption [18,21–23]. However, no partition coefficients were determined in these studies. Słupek et al. evaluated several DESs based on tetrapropylammonium bromide and glycols and based on carvone as absorbents for the removal of siloxanes from model biogas stream using COSMO-RS studies. Their results underlined that DESs composed of carvone, and carboxylic acids presented a high affinity for siloxanes [22]. This finding is in good agreement with the high affinity observed in our case between the carboxylic acids-based DESs and siloxane D4 compared to the conventional solvents. Due to the higher K values of VOCs in glycerol, as well as its high viscosity, no further evaluation of this solvent was performed.

The VOC with the highest solubility in water is methyl ethyl ketone. This may be the reason for the low K value in water in comparison to other VOCs. However, it is one of the VOC that water can absorb more effectively than certain DES described in the literature, such as ChCl:U and ChCl:G [10]. Hydrophobic DES and PG still show better absorption while BA and PC show moderate absorption. However, they are in the same order of magnitude than hydrophobic DES [5,10].

In the case of dichloromethane, we note similar capture in PC than the DES composed of fatty acids and other conventional solvents. However, compared to the literature PC is the same range as TBPBr:EG and TPBPBr:Dec based on quaternary salts substituted by long alkyl chains. These observations are confirmed in the literature as Rodriguez Castillo et al. noted the decrease in K values for several ionic liquids (ILs), silicone, and mineral oils [11]. A stronger affinity for dichloromethane was also noticed by the authors for LIs with longer alkyl chains [10,11,17].

The most suitable absorbent for long-chain linear hydrocarbons, such as heptane and decene, are the fatty acids with long alkyl chains such as C₈:C₁₂, C₉:C₁₂ and C₁₀:C₁₂ compared to conventional solvents and some DES in the literature. Considering the structural similarities between heptane and decene, it is also found that the affinity profiles between the different DES/VOCs are the same. The best absorption capacity for both heptane and decene can be explained by the apolar environments of the DES alkyl chains. In comparison to water, our results are more than 146,000 fold better, and they are 3-fold better than those for TBABr:Dec found in the literature [10].

The good agreement between our values and those from the literature in the case of C₁₀:C₁₂ DESs validates the results obtained in this study for limonene and siloxane, as these VOCs were not previously studied. The results obtained by the cooking oil could be explained by the fact that cooking oil contains triglyceride (ester of glycerol and fatty acid).

Table 17 gathers the K values of toluene, methyl ethyl ketone and dichloromethane obtained in the literature for various solvents. DES composed of fatty acids with long alkyl chains, as both components, exhibited lower K values for toluene in comparison to the other studied solvents.

Table 17. Comparison of partition coefficient (K) for VOC in various solvents.

Absorbents	T °C	K (dimensionless)	K (dimensionless)	K (dimensionless)
		Toluene	MEK	Dichloromethane
C ₈ :C ₁₂	30	4.75E-04 ^a	6.59E-04 ^a	7.94E-03 ^a
C ₉ :C ₁₂		4.55E-04 ^a	6.75E-04 ^a	7.34E-03 ^a
C ₁₀ :C ₁₂		5.14E-04 ^a	7.27E-04 ^a	9.34E-03 ^a
		3.14E-04 ^b		
ChCl:lev		4.00E-03 ^c	6.50E-3 ^d	8.00E-03 ^d
		5.00E-03 ^d		
ChCl:U		2.60E-02 ^e		5.20E-02 ^e
RAMEB:Lev		1.00E-03 ^c	-	9.00E-03 ^c
TBABr:Dec		9.00E-04 ^d	4.00E-03 ^d	5.00E-04 ^d
TBPBr:Lev		1.30E-03 ^d	4.00E-03 ^d	6.00E-04 ^d
Captisol:Lev	3.00E-03 ^c	-	1.30E-02 ^c	
Silicone Oil	25	8.90E-04 ^f	4.60E-03 ^f	8.70E-03 ^f
C ₄ mim:PF ₆		9.60E-04 ^g	-	-

^a This work ^b Ref. [15] ^c Ref. [3] ^d Ref. [10] ^e Ref. [24] ^f Ref. [17] ^g Ref. [25].

I.4.3. Effect of temperature

Temperature is one critical factor that could affect the absorption of VOCs. The influence of temperature on VOCs absorption was investigated at -20, 0, 30, 45 and 60 °C (except for the DESs that are solid at 0 °C). As shown in Figure 23 the K values of all studied VOCs increased with temperature whatever the studied solvent. This observation reflects a better absorption of VOCs at low temperatures [18].

The K value of toluene in C₈:C₁₂ is 4.75E-04 at 30 °C, while it increases to 2.60E-03 at 60 °C. Concerning the conventional solvents, the lowering of temperature allows them to reach values close to the one obtained at 30 °C for the hydrophobic DESs. Indeed, for propylene carbonate the K value decreases from 3.08E-03 at 60 °C to 2.65E-04 at -20 °C, the later value being in the same range as the one obtained with the DESs (4.55-5.14E-04 at 30 °C).

These observations are similar for limonene and siloxane D4. It is very clear from the results that lowering the temperature had a beneficial effect on the absorption of studied VOCs and could be used as a parameter to tune the efficiency of solvents.

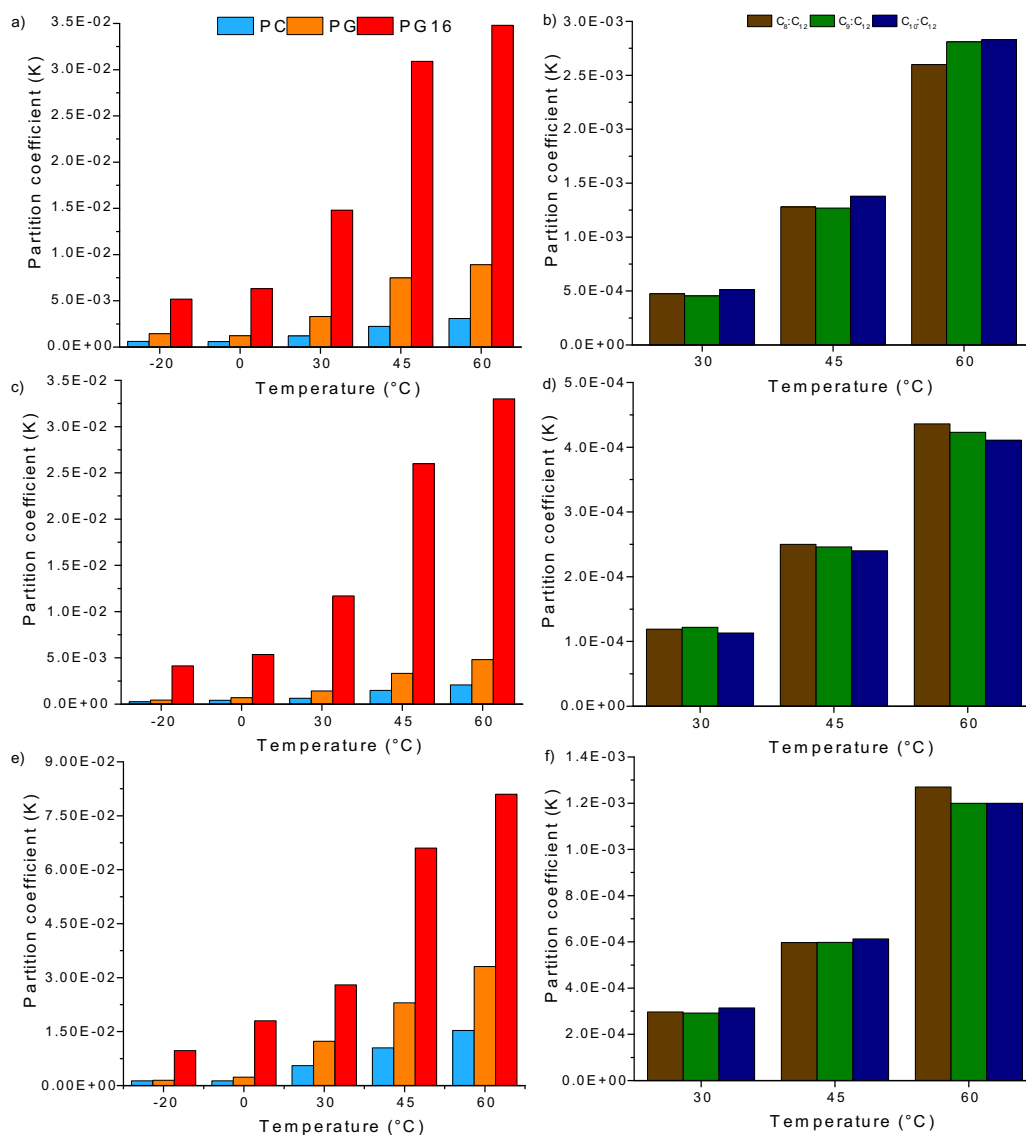


Figure 23. Partition coefficient (K) of a, b) toluene, c, d) limonene and e, f) siloxane D4 in the studied solvents at different temperatures.

As the VOC absorption in the studied solvents presented a high-temperature dependence, the absorption thermodynamic models were investigated. Therefore, the enthalpy change (ΔH), entropy change (ΔS), and Gibbs free energy change (ΔG), were determined in order to provide more information about the interaction between VOCs and absorbents (Table 18-20). The variation of K with temperature can be interpreted in light of a Van't Hoff type equation. The variation of the enthalpy is related to the interactions between the VOC and the absorbent in the liquid phase whereas the variation of entropy reveals the changes in the

absorbent structure linked with the VOC dissolution, both determining the partition of the VOC between the vapor phase and the liquid phase.

$$\Delta G = -RT \ln \left(\frac{1}{K} \right) = \Delta H - T\Delta S \quad (\text{Eq.9})$$

where ΔG (kJ mol^{-1}) is the Gibbs energy involved in the transfer of the VOC from the gas phase to the solution, T (in K) is the temperature, R is the universal gas constant ($8.314 \text{ J mol}^{-1} \cdot \text{K}^{-1}$) and ΔH (in kJ mol^{-1}) and ΔS (in $\text{J mol}^{-1} \cdot \text{K}^{-1}$) are the molar enthalpy and entropy changes, respectively, during VOCs absorption.

Table 18. Comparison of enthalpies ($\text{kJ} \cdot \text{mol}^{-1}$), entropies ($\text{J} \cdot \text{mol}^{-1} \cdot \text{K}^{-1}$), and Gibbs free energies ($\text{kJ} \cdot \text{mol}^{-1}$) of toluene absorption in different absorbents.

Absorbents °C	ΔG (kJ mol^{-1})			ΔH	ΔS
	30	45	60	$\text{kJ} \cdot \text{mol}^{-1}$	$\text{J} \cdot \text{mol}^{-1} \cdot \text{K}^{-1}$
C ₈ :C ₁₂ ^a	-19.29	-17.63	-16.48	-47.67	-93.90
C ₉ :C ₁₂ ^a	-19.39	-17.65	-16.26	-51.17	-97.65
C ₁₀ :C ₁₂ ^a	-19.09	-17.42	-16.25	-47.83	-95.05
C ₁₀ :C ₁₂ ^b	-19.07	-18.03	-	-39	-67
ChCl:Lev ^c	-	-	-	-43	-31
TBAb:Dec ^c	-	-	-	-29	-12
PC ^a	-16.95	-16.14	-16.02	-21.78	-17.03

Table 19. Enthalpies ($\text{kJ} \cdot \text{mol}^{-1}$), entropies ($\text{J} \cdot \text{mol}^{-1} \cdot \text{K}^{-1}$), and Gibbs free energies ($\text{kJ} \cdot \text{mol}^{-1}$) of limonene absorption in different absorbents.

Absorbent °C	ΔG ($\text{kJ} \cdot \text{mol}^{-1}$)					ΔH	ΔS
	-20	0	30	45	60	($\text{kJ} \cdot \text{mol}^{-1}$)	($\text{J} \cdot \text{mol}^{-1} \cdot \text{K}^{-1}$)
C ₈ :C ₁₂	-	-	-22.78	-21.93	-21.43	-36.51	-45.44
C ₉ :C ₁₂	-	-	-22.72	-21.99	-21.52	-34.86	-40.18
C ₁₀ :C ₁₂	-	-	-22.89	-22.05	-21.60	-36.08	-43.69

Propylene carbonate	-18.72	-18.34	-18.25	-17.80	-17.39	-22.42	-14.59
Propylene glycol	-16.68	-16.50	-16.44	-15.10	-14.78	-21.50	-22.61
Propylene glycol 16	-11.94	-11.76	-11.21	-9.65	-9.45	-20.35	-29.35

Table 20. Enthalpies ($\text{kJ}\cdot\text{mol}^{-1}$), entropies ($\text{J}\cdot\text{mol}^{-1}\cdot\text{K}^{-1}$), and Gibbs free energies ($\text{kJ}\cdot\text{mol}^{-1}$) of siloxane D4 absorption in different absorbents.

Absorbent	ΔG ($\text{kJ}\cdot\text{mol}^{-1}$)					ΔH ($\text{kJ}\cdot\text{mol}^{-1}$)	ΔS ($\text{J}\cdot\text{mol}^{-1}\cdot\text{K}^{-1}$)
	$^{\circ}\text{C}$	-20	0	30	45		
$\text{C}_8:\text{C}_{12}$	-	-	-20.47	-19.64	-18.48	-40.59	-66.19
$\text{C}_9:\text{C}_{12}$	-	-	-20.51	-19.63	-18.64	-39.38	-62.21
$\text{C}_{10}:\text{C}_{12}$	-	-	-20.33	-19.57	-18.36	-40.16	-65.21
Propylene carbonate	-14.20	-14.15	-13.10	-12.05	-11.57	-23.13	-34.15
Propylene glycol	-12.05	-11.33	-11.09	-9.98	-9.44	-19.74	-30.26
Propylene glycol 16	-10.25	-9.52	-9.00	-8.22	-6.95	-19.42	-35.87

In particular, it is clear from the negative value of ΔG that all VOCs are favorably solubilized in absorbents under our experimental conditions. The negative ΔH values indicate that the dissolution of VOCs is an exothermic process. Notably, the $|\Delta H|$ values in the case of toluene and DESs (51.1 to 47.6 kJ mol^{-1}) are higher than those of conventional solvents (23.2 to 20.2 kJ mol^{-1}) reflecting a stronger toluene dissolution tendency in the DESs. For all studied absorbents the $|\Delta H|$ of VOC absorption is always higher than $|T\Delta S|$, showing an enthalpically controlled process.

The ΔG values for toluene in propylene carbonate was -16.95 kJ mol^{-1} at 30 $^{\circ}\text{C}$, while it was -19.39 kJ mol^{-1} in $\text{C}_9:\text{C}_{12}$ at the same temperature, confirming the previous statement that the hydrophobic DESs in possess higher absorption capacities than conventional studied solvents. Similar results were observed for limonene and siloxane D4, again showing that lowering the temperature had a favorable effect on VOC uptake.

I.4.4. Effect of initial VOC concentration

The effect of initial VOC concentration on the absorbed amount of VOC was investigated for the different VOCs and solvents. As can be seen from Figure 24, in the case of C₉:C₁₂, the toluene absorption capacity increases with initial toluene concentration. The values ranged from 0.29 to 2.6 mg toluene/g DES for initial concentrations between 59 and 531 ppm. These results showed that the absorption of toluene in hydrophobic DESs is concentration sensitive. Similar observations were found in ILs and DESs [1,15,26]. It has to be noted that the DESs were able to absorb >99.8% of the initial VOC amount added in the vial and that the absorbents are not saturated. Results indicate also a high absorption for low VOC concentrations, underlining a great potential for impurities removal in biogas as VOCs are present at low concentrations (<300 ppm) [27].

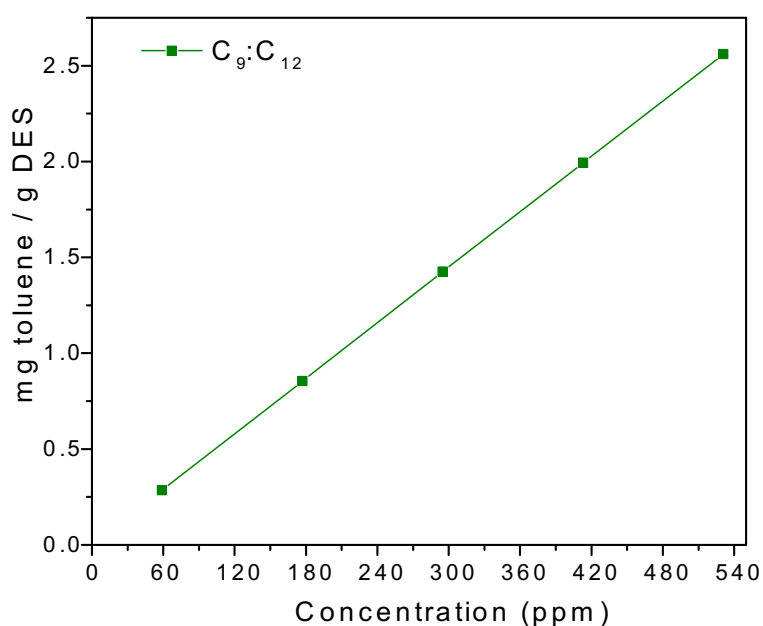


Figure 24. Effect of initial toluene concentration on the absorption capacities of C₉:C₁₂ at 30 °C.

I.4.5. Effect of water on VOC absorption

Another critical factor that could affect the absorption of VOCs is the water content of absorbent [12]. Therefore, the effect of water addition (10, 30 and 50 wt%) on the partition coefficient of toluene, limonene and siloxane D4 in propylene carbonate, propylene glycol and C₉:C₁₂ was evaluated at 30 °C (Figure 25). Additionally, also the effect of water addition (10, 20, 30, 40, 50, 60, 70, 80, 90, 95, and 99 wt%) were prepared for the three VOCs in ChCl:Lev and Rameb:Lev in order to evaluate the K-value (Figure 25). The increase of K values obtained for VOCs in the different solvents as a function of water content underline a lower absorption of VOC upon water addition as observed previously for organic solvents [12,16,18].

The K value of toluene in propylene carbonate increases from 1.20E-03, to 3.66E-03 in propylene carbonate with 50 wt% water. Similar observations could be done for propylene glycol where K value increases from 3.31E-03 to 8.75E-02 in propylene glycol with 50 wt% water. The same observation was done for C₉:C₁₂ with K increasing from 4.55E-04 to 1.33E-03 with 50 wt% water. This behavior is also observed for limonene and siloxane D4 (Figure 25).

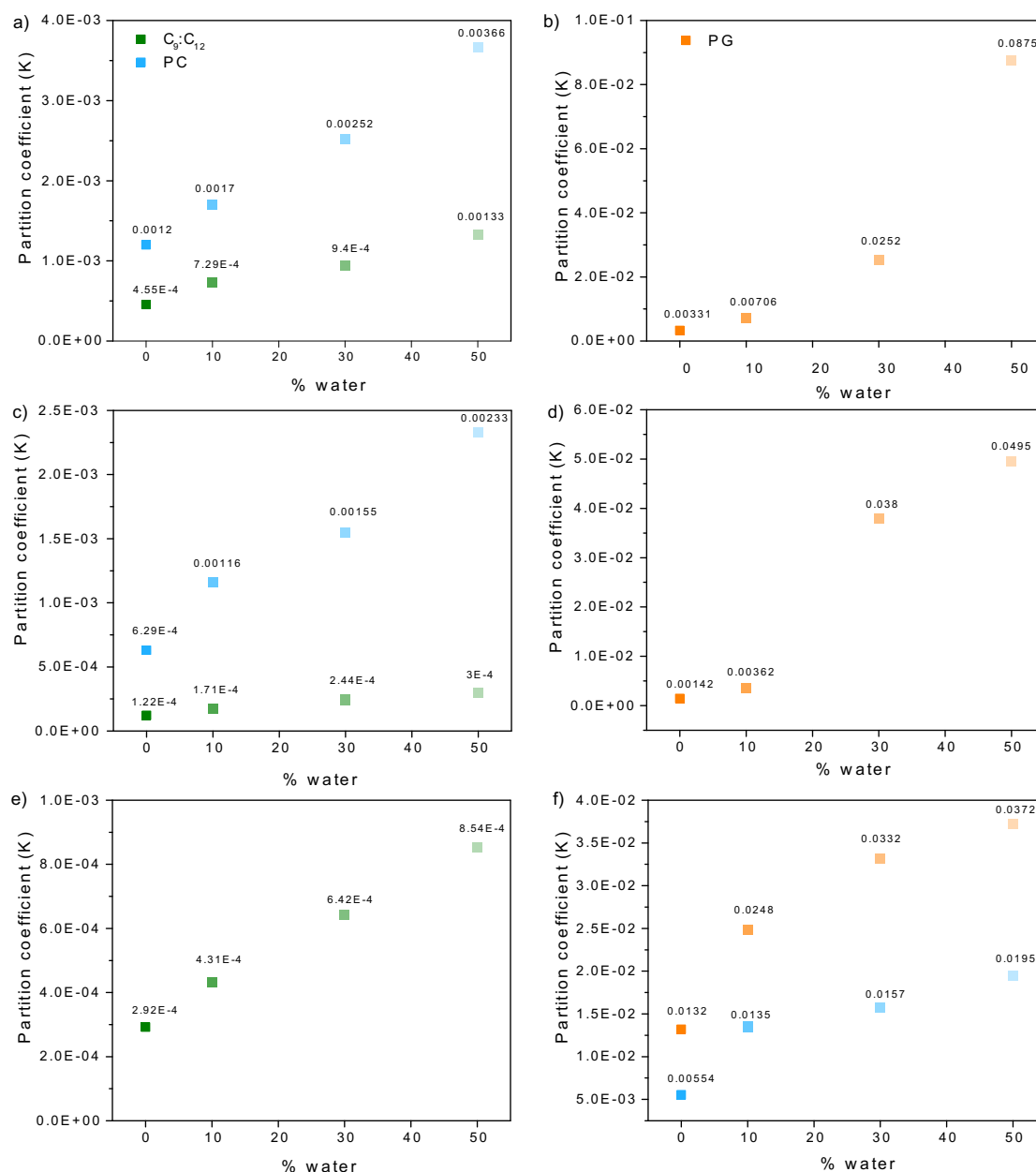


Figure 25. Partition coefficient (K) of a, b) toluene, c, d) limonene and e, f) siloxane D4 in propylene carbonate (blue), propylene glycol (orange) and C₉:C₁₂ DES (green) with different amount of water (10, 30 and 50 wt%) at 30 °C

In the case of toluene in ChCl:Lev the K value increases from 4.15E-03 (pure) to 0.270 with 90 wt% water (Figure 26). For toluene in Rameb:Lev the K value increased from 1.80E-03 (pure) to 0.126 with 90 wt% water. The obtained K value of 2.91E-02 in Rameb:Lev with 60% of water is similar to ChCl:Lev with 40% of water (2.63E-02) and PG with 30 wt% (2.52E-02), it shows in this case that by adding more water in Rameb:Lev the K value is similar between them.

Meanwhile, the K value of 3.66E-03 in PC with 50 wt% water showed similar values compared to Rameb:Lev with 10% water (3.71E-03), Therefore, once again showing great absorption capacity of PC even with 50 wt% water.

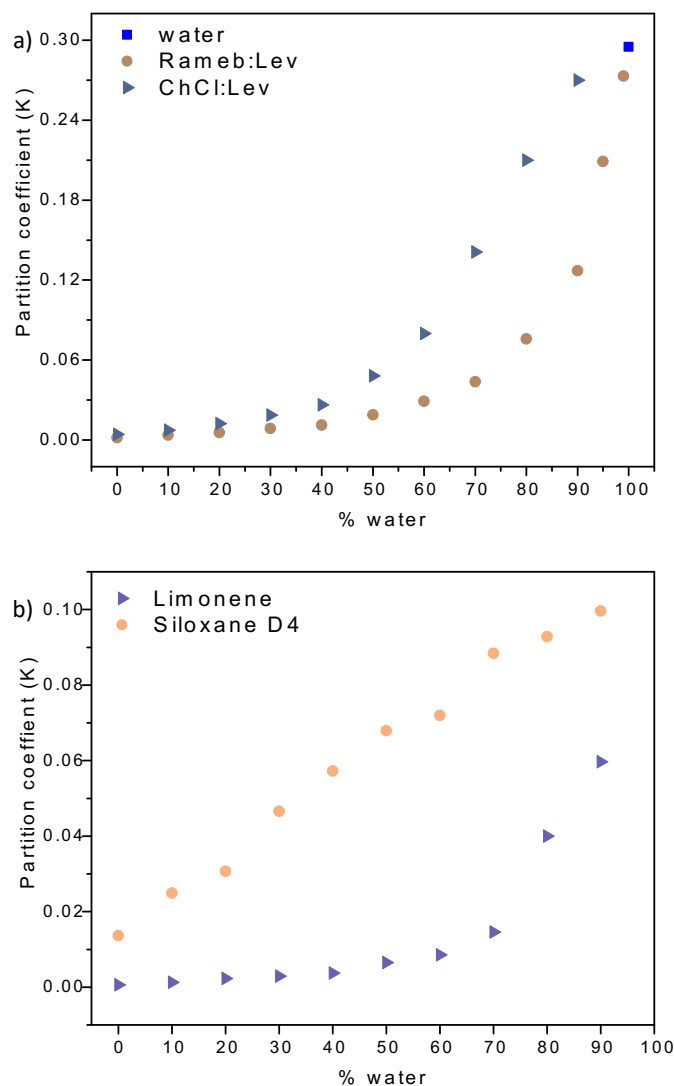


Figure 26. K values of a) toluene in water, Rameb:Lev and ChCl:Lev in function of water and b) limonene and siloxane D4 in Rameb:Lev at 30 °C.

I.4.6. Toluene absorption in industrial solvents and water/solvent mixtures

In this section, we wanted to evaluate the absorption capacity of various industrial solvents towards toluene. Indeed, toluene is often use as a representative of VOCs and is found in numerous gaseous effluents.

As industrial effluents often contain both hydrophobic and hydrophilic VOCs as well as moisture, a mixture of water and organic solvent may be sometimes more interesting than a pure solvent. Therefore, from a fundamental, practical and economic point of view, it is important to study the effect of water concentration on the absorption capacity of solvent [2,12,16,18].

The obtained partition coefficients (K) of toluene in water, solvents and water/solvent mixtures are presented in Table 21 along with the $K_{\text{water}}/K_{\text{absorbent}}$ ratio [3,18,19].

Table 21. Partition coefficients values (K) of toluene in water, solvents and water/solvent mixtures at 30 °C, and $K_{\text{water}}/K_{\text{absorbent}}$ ratio.

Absorbent	H ₂ O (%)	K	$K_{\text{water}}/K_{\text{absorbent}}$
Water	100	2.94E-01 ^{a,b}	-
		2.51E-01 ^c	
		2.68E-01 ^d	
Acetic acid	90	2.23E-01 ^a	1.3
	80	1.46E-01 ^a	2
	60	5.99E-02 ^a	4.9
	0	7.14E-04 ^a	412
	90	1.14E-02 ^a	26
	80	4.26E-03 ^a	69
Benzyl alcohol	60	2.15E-03 ^a	137
	20	8.67E-04 ^a	340
	0	6.04E-04 ^a	488
Propylene glycol	16	1.48E-02 ^{a,b}	20

^a This work [19] ^bRef. [18] ^cRef. [3] ^dRef. [8]

The K values obtained in the solvents and water/solvent mixtures ranged between 6.04E-04 and 3.26E-01 (up to 488-fold lower than in water). A lower K value corresponds to a higher solubility of the VOC in the solvent. Therefore, the decrease in K values observed for toluene in all solvents compared to water indicates a better absorption of toluene into the liquid phase. The lowest K value was obtained using benzyl alcohol (BA). A slightly higher K value was obtained for acetic acid (AA).

The K value obtained for the commercial solution of propylene glycol (PG16) could be explained by the amount of water (16%) that lower the absorption efficiency of the solvent [12].

Indeed, in a previous study, the K value of PG was found to be lower than that of PG16 [18]. The increases in K values obtained for toluene in water/solvent mixtures as a function of water content underline a lower absorption upon water addition as previously observed for other organic solvents. The K value of toluene in BA increases from 6.04E-04 to 1.14E-02 (from 0 to 90 wt% of water). Similar results were observed for AA, with K value increasing from 7.14E-04 to 2.23E-01 (from 0 to 90 wt% of water). However, the effect of water is different for AA and BA. Indeed, adding 60 wt% of water to BA still gives a K value 137 lower than that of water, whereas for AA this ratio is only 4.9, for the same amount of water.

Toluene is widely considered as a model for hydrophobic and aromatic VOCs and thus has often been studied. Table 22 summarizes the obtained K values found in the literature for DESs, ILs, silicone oil or other organic solvents [14–17].

Table 22. Comparison of partition coefficient (K) for toluene in various solvents.

Absorbents	HBA:HBD (molar ratio)	T °C	K (dimensionless)
Glycerol	-		4.06E-02 ^b
N ₄₄₄₄ Br:C ₁₀	1:2	30	1.00E-03 ^c
N ₄₄₄₄ Br:Lev	1:6		1.00E-03 ^c
ChCl:lev	1:2		4.00E-03 ^c
			4.50E-03 ^d
RAMEB:Lev	1:27		1.00E-03 ^e
C ₄ mim:PF ₆	-		9.60E-04 ^f
Silicone Oil	-		8.90E-04 ^g
DEHA	-	25	3.50E-04 ^h
n-Hexadecane	-		1.00E-03 ⁱ
PEG 400	-		6.00E-04 ^j

^a This work ^bRef. [18] ^cRef. [2] ^dRef. [1] ^eRef. [3] ^fRef. [25] ^gRef. [17] ^hRef. [28] ⁱRef. [26] ^jRef. [12].

The K values of toluene in pure BA and AA are lower or in the same order of magnitude than some previously studied solvents. The water/benzyl alcohol (60:40) mixture with a K value of 2.15E-03 exhibited interesting absorption capacities, close to the K value observed in DESs or silicone oil. Therefore, adding 40% of BA to water can significantly increase its absorption and thus have a positive impact from an economic point of view.

The absorption capacities at 30 °C for an initial amount of toluene of 295 ppm are presented in Figure 27. The absorption capacities of the studied solvents and water/solvent mixtures range from 1.424 to 0.728 (mg of toluene per gram of solvents) compared to 0.066 mg for water. They gradually decreased as the amount of added water increased. It should be noted that the absorption capacities will depend on the initial amount of toluene as previously described [18] and that at this toluene concentration between 99.8 and 95% of the toluene is trapped in the solvent for BA and water/BA mixtures and between 99.7 and 51% for AA and water/AA mixtures.

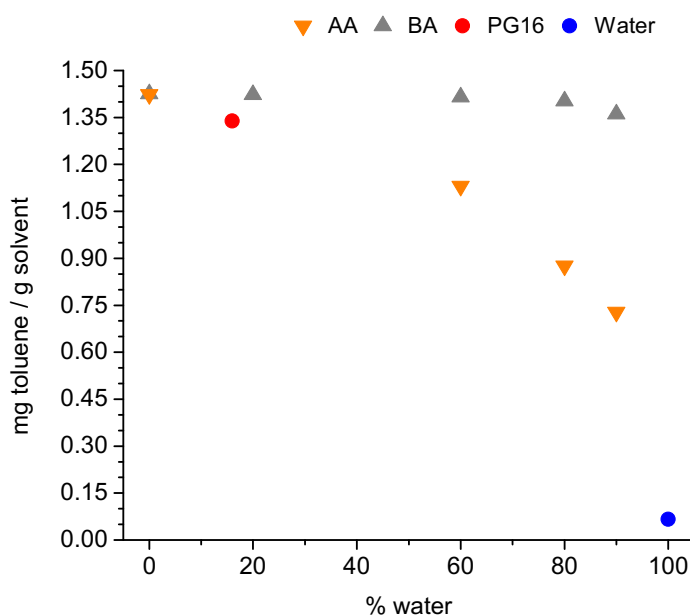


Figure 27. Absorption capacity of toluene (295 ppm) at 30 °C in the studied solvents and water/solvent mixtures.

I.4.7. Effect of VOC mixtures

Real gaseous effluents and raw biogas generally contain a wide variety of VOCs. Therefore, we evaluated the effect of VOC mixtures on the partition coefficient of individual VOCs. We

prepared a mixture of VOC based on toluene (aromatic hydrocarbon), limonene (terpenes), octamethylcyclotetra-siloxane D4 (siloxanes) and decane (alkanes) called TLSD₂ to represent the industrial reality. All these VOCs have also a significant concentration in raw biogas. The four VOCs are combined in equimolar amounts in a single stock solution. Various amounts of this stock solution were then added to the vials previously filled with the solvent.

The K values were determined for individual and mixed VOCs in water and eight absorbents under the same experimental conditions described before [18]. We only modified the GC parameter to obtain effective chromatographic peak separation (Table 23).

Table 23. Experimental conditions used in gas chromatography for measurements of VOCs mixture.

VOCs	VOC	GC Parameters		
		Column temperature °C	Analysis time / min	Retention time / min
TLSD ₂	Toluene	120	7	2.3
	Limonene			6.1
	Siloxane D4			4.2
	Decane			4.8

The K values of VOCs individually or in VOC mixtures in water are nearly the same, as shown in Table 24. These results show that no interactions appear between the VOC in the mixture.

Table 24. K values of VOCs individually or in VOC mixtures in water (30°C).

	Partition coefficient (K)			
	Toluene	Limonene	Siloxane D4	Decane
Individuals	0.29	2.32	4.00	18.00
Mixture	0.33	2.45	4.06	18.90

The K values for toluene, limonene, siloxane D4 and decane individually and in mixture at 30°C are shown in Figure 28. We note that the K value of a given VOC is not that affected by the

presence of other VOCs, like in water. This result may be due to the similar structure of the VOCs in the TLSD₂ mixture.

The hydrophobic fatty acid DESs, CO and BA led a high absorption capacity for VOCs separately as showed previously. The majority of the K values were in the same order of magnitude as those obtained for the individual VOCs. The K values of TLSD₂ mixture in the C₁₀:C₁₂ DES showed the same range, as can be seen in Figure 28a. The same trend is observed for CO and BA.

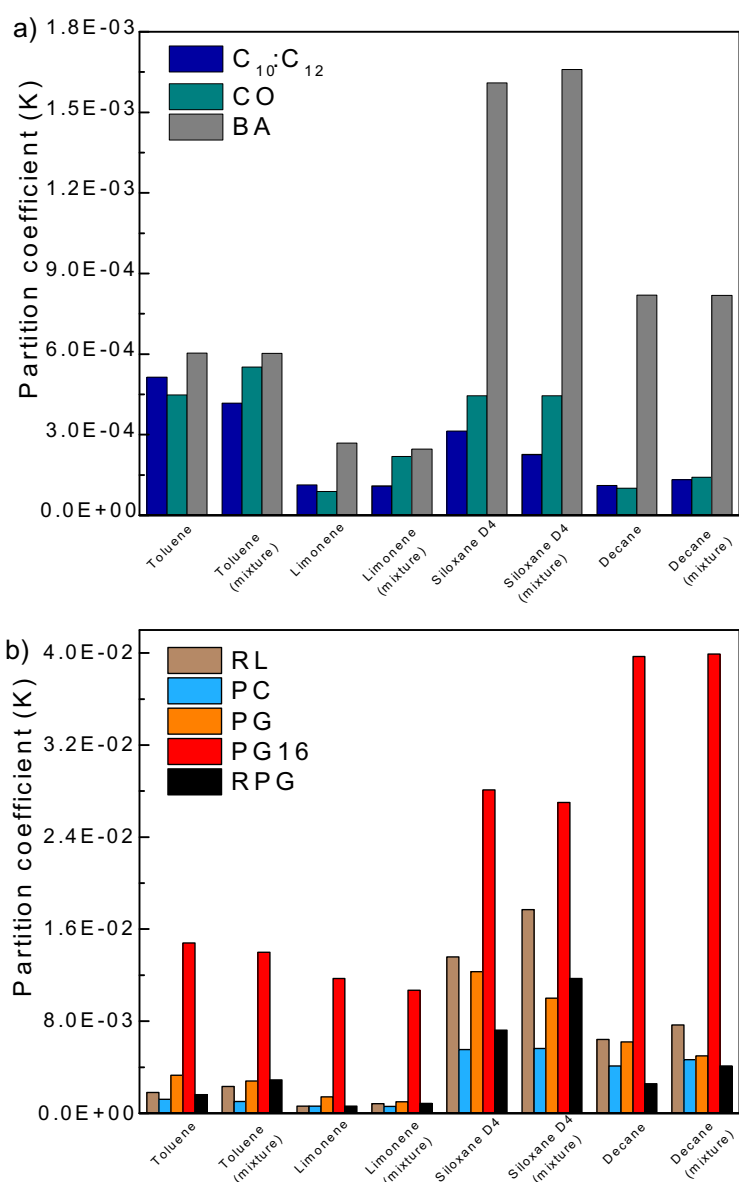


Figure 28. Partition coefficient (K) of a, b) TLSD₂ mixture in C₁₀:C₁₂, CO, BA, RL, PC, PG, PG16 and RPG at 30 °C.

In Figure 28b, the K values of the TLSD₂ mixture in RL, PC, PG, PG16 and RPG had similar values to the individual VOCs. However, in the case of RL and RPG, the K values showed a modest variation between the siloxane D4 alone and in the mixture with a slightly increased of K value. These results show that the affinities between the absorbents and the VOC mixture are maintained by the physical absorption of the VOCs in these absorbents.

I.4.8. Regeneration of the absorbent

The regeneration of absorbents is a critical issue for many industrial operations. After being used in processes such as absorption, these solvents must be returned to their original or desired state in order to be reused. As in an absorption column, solvent replacement is very costly and therefore regeneration process is crucial for sustainability, cost effectiveness and maintaining process efficiency. Solvent regeneration reduces resource consumption, waste generation and operating costs. In addition, minimizing the disposal of contaminated or used solvents supports environmental responsibility. The type of solvent and the application influence the choice of regeneration process. There are several ways to regenerate absorbents, including distillation, inert gas bubbling, thermal desorption, adsorption using common adsorbents, and others. In order to achieve high impurities removal efficiency, all absorbents regeneration process often require high temperatures. However, not all studied absorbents (DES or conventional solvents) can be used at such high temperatures. Some of them have properties that can cause degradation and be lost during the regeneration process, including limited thermal stability, low degradation temperature, and high vapor pressure.

I.4.8.1. DES regeneration

Conventional thermal desorption (heating + stirring) is one of the most widely used regeneration method. It was the first method that we evaluated for the regeneration of the absorbents after analysis. The lower K values obtained at higher temperatures have been utilized as a desorption condition. After analysis, the vials containing the solvents loaded with VOCs were uncapped and stirred at 60 °C for 48 h. As the absorbent is heated, the non-covalent bonds formed between the DES and VOCs lengthen and weaken. The VOCs then move to the gas phase after evaporating from the solvent. Therefore, vials were afterwards analyzed by HS-GC to determine if there was any trace of VOCs remaining in the solvents after

regeneration. Then, the absorption capacities of the solvents were evaluated once more by putting them in contact with the VOCs using the procedure described before. The absorption and desorption cycles were repeated five times. As can be seen from Figure 29, in the case of toluene and $C_9:C_{12}$, the DES retained its absorption capacities during the five cycles. All the studied solvents could be regenerated, however, in the case of $C_8:C_{12}$ a weight loss of 12% was observed. The hydrophobic DES and solvents used in this work maintains a high VOCs absorptivity between 99.6 and 99.9% after five consecutive reuse cycles, demonstrating that a facile and feasible recycling of the proposed absorbent can be achieved [18].

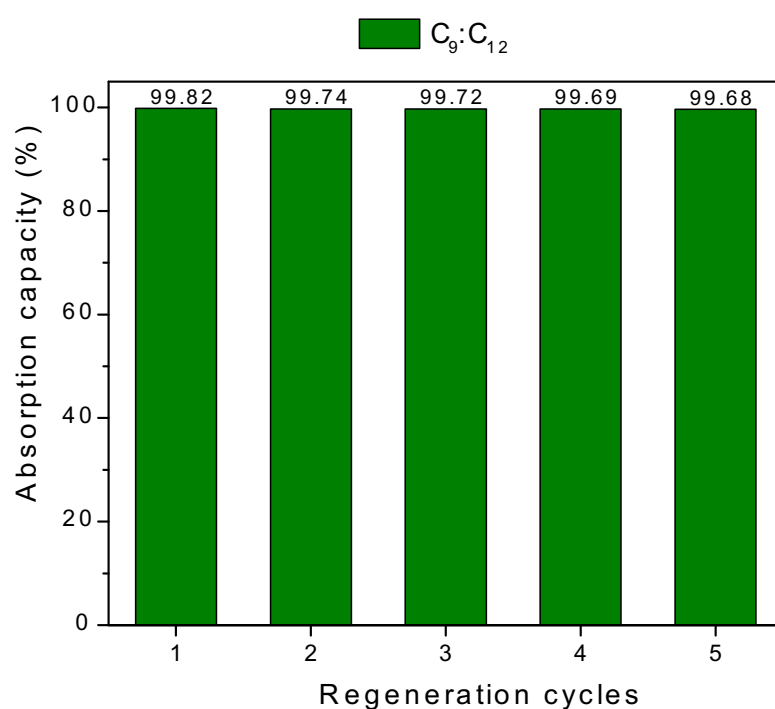


Figure 29. Absorption capacities of $C_9:C_{12}$ for toluene during five consecutive cycles.

However, five cycles are not enough from an industrial point of view to make the procedure cost-effective. In addition, in a typical industrial system consisting of an absorption column and a desorption column, the regeneration time of the absorbent is too long to allow process stability. A method used to boost efficiency and cut down absorbent regeneration time is by increasing the process temperature. However, setting it might cause the evaporation of the absorbent, thus, changing the efficiency of the absorbents and causing their loss. Consequently, regenerating temperature needs to be set according to the absorbent being used.

Therefore, two other methods were studied to ensure a shorter regeneration time for absorbents. We evaluated the effect of bubbling nitrogen (heating and non-heating) in order to compare this regeneration process to the thermal desorption (heating + stirring) as shown in Figure 30. This method is the opposite of how absorption typically happens. Once nitrogen is introduced to absorbent that has absorbed VOCs, the pollutants are desorbed and released from the liquid to the gas phase [1,2,22,23,26,29–34].

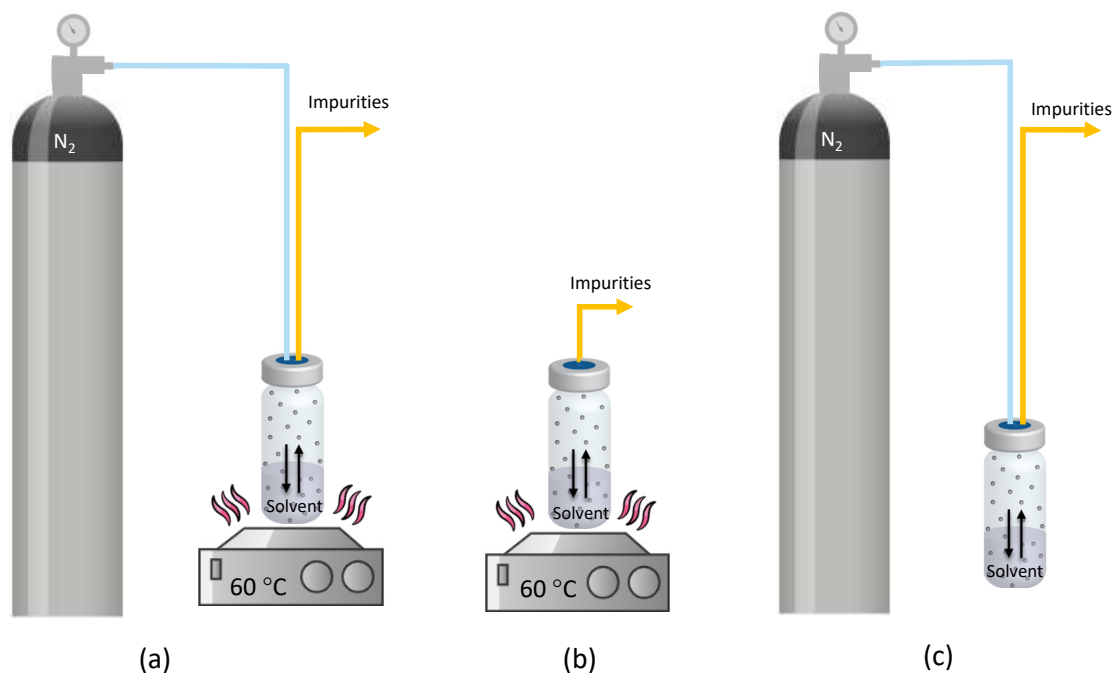


Figure 30. DES regeneration methods a) bubbling nitrogen + heating b) thermal desorption and c) bubbling nitrogen.

The three methods such as heating + stirring and bubbling nitrogen (heating and non-heating) with flow rate controlled (100 mL.min) can effectively remove toluene from DES. However, the regeneration time can change for an absorbent to another. In this study, we first evaluate the time needed to regenerate the C₁₀:C₁₂ absorbent and then perform several absorption/desorption cycles.

In the experiments after twelve cycles of absorption-desorption of the absorbent loaded with toluene (295 ppm). No significant changes in the absorption capacity were observed, as was the case for C₁₀:C₁₂, which maintained up to 99.5% of its absorption capacity. In the previous experiments, the regeneration of the C₉:C₁₂ charged with toluene concentration (295 ppm)

was evaluated five times by thermal desorption at 60 °C for 48 hours, for a total of 240 hours. However, the regeneration time of the C₁₀:C₁₂ can be reduced to 2.5 hours using bubbling nitrogen at 60 °C. The C₁₀:C₁₂ was evaluated twelve times totaling 30 hours. In the case of bubbling nitrogen non-heating and heating at 60 °C, the same time (six hours) was required for the full regeneration of the DES, for a total of 72 hours. The weight loss of C₁₀:C₁₂ was less than 1% for the three types of regeneration. However, compared to other method, bubbling nitrogen with heating showed to be more effective due to its faster regeneration. This method works better for an industrial system as it takes a brief time for the absorbent regeneration. As shown in Figure 31, the absorption capacity (%) of toluene concentration (295 ppm) in DES remained stable during twelve cycles.

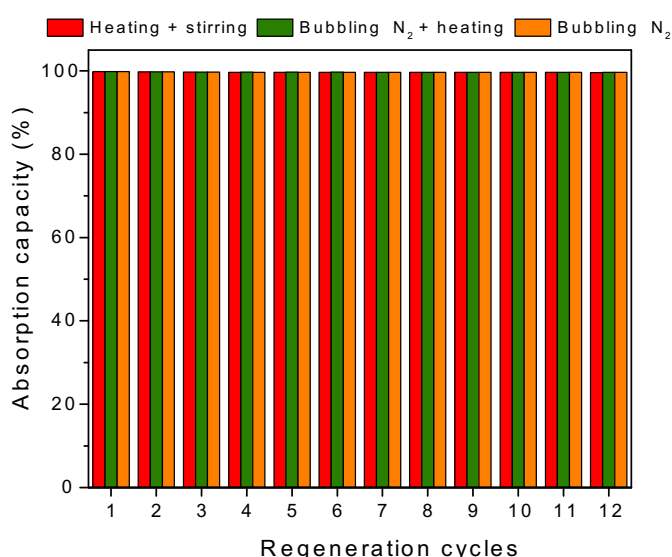


Figure 31. Three different types of regeneration capacity for absorption C₁₀:C₁₂ for toluene during a period of twelve consecutive cycles.

I.4.8.2. Regeneration of the industrial solvents and water/solvent mixtures

For this experiment in the section I.4.5, the conventional thermal desorption (heating + stirring) was used. After the determination of K, the samples were uncapped and stirred at 45 °C for 12 hours to reverse the absorption process. The samples were then analyzed by static headspace-gas chromatography to ensure that there was no detectable toluene. After 12 h, no more toluene could be detected. The weight loss of BA was only 2% whereas for water/BA mixtures we observed a weight loss of 30 %. The loss is therefore due to water, which could

be added after regeneration at no additional cost. For pure AA the weight loss was 13%, while for the water/AA mixtures, it was also 30%. For PG16, a weight loss of 10% was observed. We also further evaluated the regeneration and weight loss of water/BA and water/AA mixtures with 60 wt% of water and PG16 using the dynamic absorption set-up. After 3 hours, water/BA, water/AA mixtures and PG16 were completely regenerated. The observed weight loss was 14, 15 and 5% for water/BA, water/AA and PG16, respectively.

II. Determination of CO₂ sorption capacity

II.1. Overview of the method

This work was performed in collaboration with the School of Chemistry and Chemical Engineering at Queen's University, Belfast. Dr Leila Moura developed a new screening method combining quantitative GC analysis of equilibrated headspace with the pressure drop technique on materials placed in pressurized headspace GC vials at various mbar pressures. Gas analysis was carried out using a Perkin Elmer Clarus 500 gas chromatograph (GC) attached to a Turbomatrix 40 headspace (HS) autosampler using helium as a carrier and a flame ionization detector (FID) equipped with a methaniser using a nickel catalyst.

Compared to conventional solubility or gas uptake measurements, simple sample preparation and feeding, real-time equilibration of a large number of samples, and uncomplicated quantitative headspace gas analysis allow for rapid efficiency achievements. Using single or mixed permanent gases such as CO₂, CH₄, H₂ and NH₃, this technique enables the screening of solids, volatile and non-volatile liquids, physisorbents and chemisorbents for CO₂ absorption.

Three steps are used for preparing sample or calibration vials *i)* Pressurization: a needle is inserted into the gray septum of the vial to be connected to a gas/vacuum line, then all gases are removed from the vial by the vacuum, then the vial is pressurized with the desired gas and pressures, which are precisely measured, *ii)* Equilibration time: once pressurized, the vial is removed from the gas-line and allowed to equilibrate at the desired temperature and *iii)* HS-GC measurements: after reaching the equilibrium time, the vial is ready for measurement and can be carried out by the HS-GC. Using equation 10, the amount of gas sorbed is based on the correlation of the pressure-volume-temperature (pVT) measurement with the GC peak area measurement.

$$n_g^{tot} = \frac{p_{ini}(V_{ini})}{(p_{ini}, T_{ini})RT_{ini}} \quad (\text{eq.10})$$

where the quantity of gas introduced into the vial, n_{tot} , is determined by measuring the estimated room pressure and temperature (initial pressure and temperature, p_{ini} and t_{ini} , respectively) in the predetermined volume of the vial, V_{vial} . This volume is obtained by measuring the weight of distilled water filling a model vial, minus the volume of the sorbent (if it is liquid), the volume of the glass-encapsulated stirring bar or glass beads contained.

II.2. Results of gas sorption

The gas absorption of sorbents has been studied using the screening method developed by combining gas pressurization on absorbents in vials with HS-GC analysis for two hours equilibrium. Direct sampling and gas analysis were used to determine the partial pressures and compositions of the remaining unabsorbed gas at pressures varying from 300 to 4110 mbar and at 35 °C. The absorption of CO₂ (99%), CH₄ (99%) and a mixture of CO₂ (50%)/CH₄ (50%) absorption was evaluated using four DES, C₈:C₁₂, C₉:C₁₂, C₁₀:C₁₂, and RL with 5 ml of absorbents for five days equilibrium.

Figure 32a depicts the CO₂ (99%) absorption capacity of the four different DES at 35 °C. The three hydrophobic DES C₈:C₁₂, C₉:C₁₂, and C₁₀:C₁₂ demonstrated nearly identical CO₂ absorption, reaching 7.53 mg CO₂/g C₉:C₁₂ at 3189 mbar, while RL showed a slightly lower CO₂ absorption at nearly the same pressure, reaching 5.42 mg CO₂/g RL at 3250 mbar.

Except for RL, the same procedure was performed for CH₄ (99%). The absorption capacity of CH₄ in C₈:C₁₂, C₉:C₁₂ and C₁₀:C₁₂ showed the same absorption tendency due to the same properties, as shown in Figure 32b. The highest absorption of CH₄ was 3.08 mg CH₄/g C₉:C₁₂ at 3927 mbar. In the case of the CO₂/CH₄ mixture in C₈:C₁₂, the absorption of CH₄ was lower than that of CO₂. This was expected due to the fact that the individual CO₂ absorption was higher than the individual CH₄ absorption. In the Figure 32c, the highest CO₂/CH₄ mixture absorbed was 9.40 and 3.79 mg (CO₂/CH₄) /g C₈:C₁₂ at 4110 mbar. Their absorbency varies according to the initial pressure.

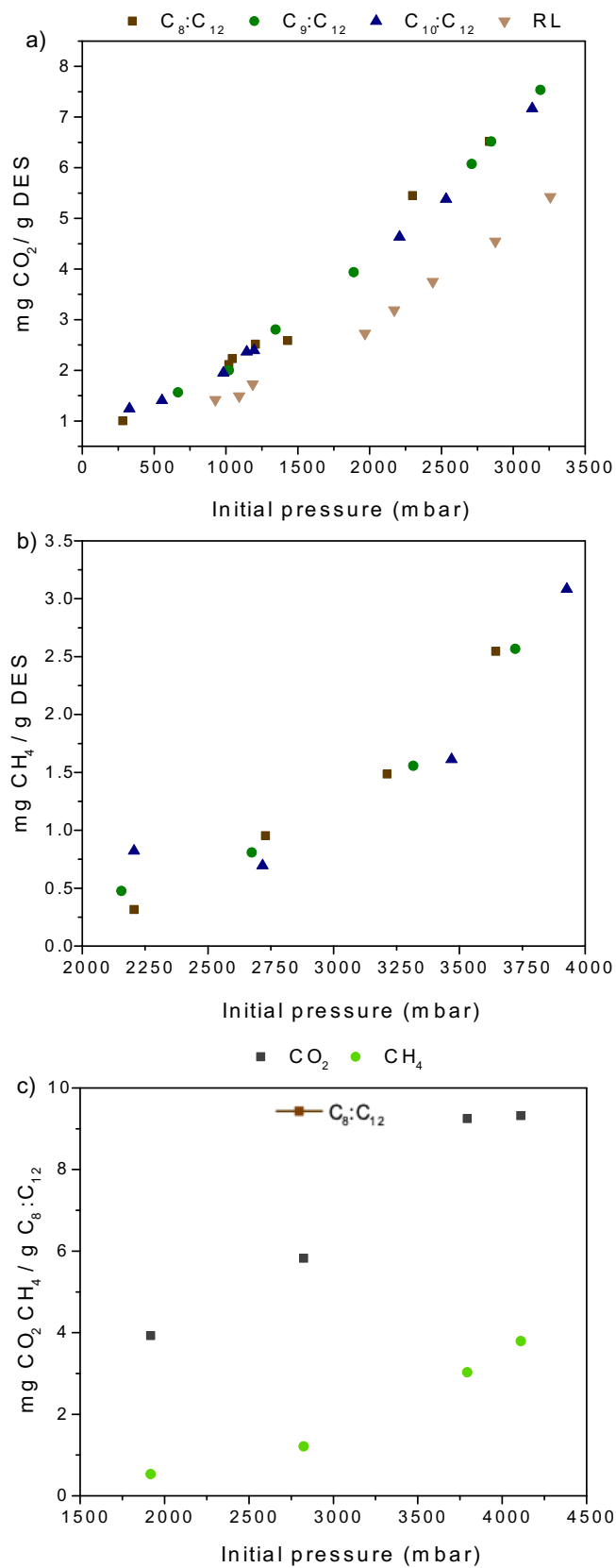


Figure 32. Absorption capacity of a) CO₂ (99%) in C₈:C₁₂, C₉:C₁₂, C₁₀:C₁₂ and RL, b) CH₄ (99%) in C₈:C₁₂, C₉:C₁₂, C₁₀:C₁₂, and c) CO₂ (50%) and CH₄ (50%) in C₈:C₁₂ at 35 °C.

The absorption capacity of CO₂ in the studied DES are lower in comparison to the ionic liquid [C₆C₁Im][NTf₂] which was 3.52 mg CO₂ / g IL, although it has similar values to ethylene glycol and octanol which 1.17 and 2.64 mg CO₂ / g solvent, respectively at 35 °C and 1000 mbar. Regarding the results obtained, it is important to compare the CO₂ and CH₄ absorption. CH₄ is less absorbed than CO₂ in the studied DES C₈:C₁₂. Considering that biogas is mainly composed of CH₄, the higher CO₂ absorption in terms of biogas upgrading can be relevant to increase the efficiency of the process.

III. Dynamic absorption from laboratory to industrial scale

III.1. Methodology and experimental set-up

In order to mimic industrial absorption processes, which are generally based on a scrubber, a dynamic bubbling set-up has been developed at laboratory scale developed in collaboration with the common center of analysis (CCM) (Figure 33) [8]. In case of VOC absorption, a model polluted gas was produced by injecting liquid VOC into nitrogen as carrier using a syringe-mounted dispenser at desire flow rate respectively. However, for CO₂ absorption, a bottle of CO₂ was used and mixed with nitrogen as carrier in order to have the desired CO₂ concentration. In addition, a cylinder with a storage system was used for raw biogas sampling. In order to control the flow rate of the biogas, a mass flow mixer / humidity generator (Fensor) was used. The biogas was sampled from a landfill site in north of France by the common center of analysis (CCM) and the catalytic team of UCEIV.

The flow rates of the stream were monitored by mass flow controllers. The desire gas concentration of the inlet and outlet gas was monitored with a Micro GC Fusion (Chemlys) or total hydrocarbon analyzer (Envea) (depending on the compound used). In each experiment, a desire precise mass of the absorbent was used, and the temperature was controlled using a thermostat cable-controlled thermostat heater coupled to a temperature sensor. The gas flows through the by-pass and is analyzed by the GC or total hydrocarbon analyzer. When the concentration stabilizes, both valves are switched, and the gas flows through the absorbent. The outlet gas concentration is monitored until the absorbent is fully saturated (outlet gas value equal to the initial inlet value). For the desorption process the feed (inlet) is removed, and nitrogen gas is used to strip the saturated solvent, thereby regenerating it. The amount of compound absorbed by the solvent can be determined by integrating the curves obtained.

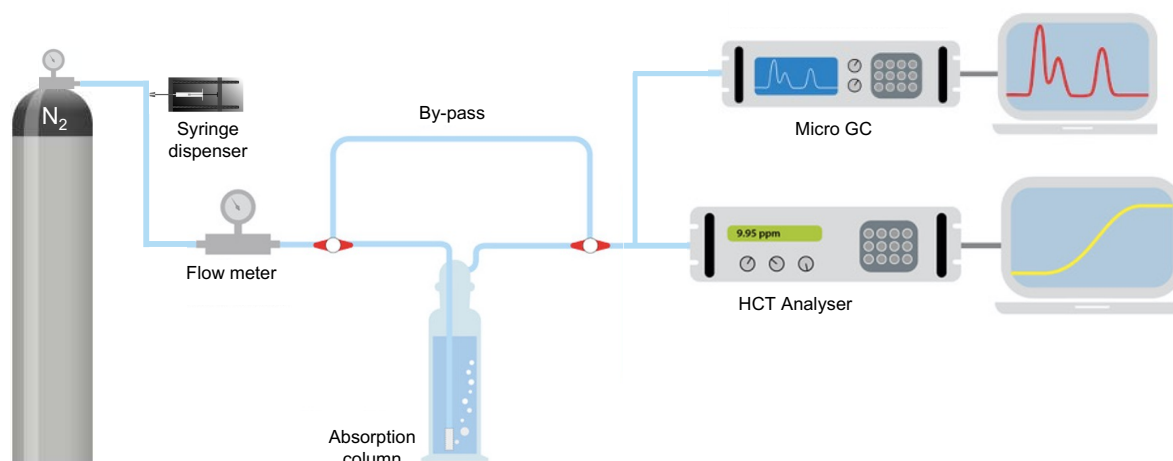


Figure 33. Dynamic absorption set-up used. For VOC absorption with syringe dispenser and N_2 . In case of CO_2 absorption, the syringe is replaced by a CO_2 cylinder. For biogas absorption the N_2 and syringe are replaced by a cylinder of biogas.

III.2. VOC absorption results

The partition coefficient of the VOC in the absorbent is related to the absorption capacity of the VOC in the absorbent by dynamic process. In order to evaluate the performance of DES under conditions that simulate an absorption column, we selected a solvent that showed high absorption capacity and utility for various VOCs using the lab-scale bubbling set-up [19]. In the first experiments three VOCs (toluene, limonene, and siloxane D4) were selected due to the fact that these VOCs are found in biogas. Five absorbents were selected: $C_{10}:C_{12}$, Rameb:Lev, water, PG16 and CO studied at various temperature and flow rate. The mixture of toluene, limonene, and siloxane D4 (TLS) was also evaluated. In each experiment, a specific mass of the absorbent (about 20 g) was used, and the temperature was set between 25 and 30 °C depending on the experiment. The absorption capacity of toluene in water, PG16, AA, BA, and water/solvents was also evaluated.

III.2.1. Individuals VOCs absorption

The absorption capacity of toluene, limonene and siloxane in six absorbents were evaluated at 30 °C, with a VOC flow rate of $20 \mu L \cdot h^{-1}$ and a N_2 flow rate of $10 L \cdot h^{-1}$ are shown in Figure

34. Under these conditions, the concentrations of toluene, limonene, and siloxane D4 were 100, 120, and 50 ppm, respectively.

Comparing the absorption capacities, we observed that water has the smallest one, as expected from previous partition coefficient studies. The C₁₀:C₁₂ fatty acid showed better affinity for toluene and an absorption capacity of 0.884 mg toluene / g C₁₀:C₁₂. The K values obtained in the static method are in good agreement with the absorption capacities found in the dynamic method. In dynamic adsorption, the viscosity can affect the results. Indeed, the viscosity of CO is 51.56 mPa.s, while the viscosity of C₁₀:C₁₂ is 9.096 mPa.s. Therefore, if K values are similar for both absorbents, the absorption capacity of CO of 0.57 mg toluene / g CO is smaller than the one obtained for C₁₀:C₁₂. Rameb:Lev has a slightly lower absorption efficiency than BA + 60 wt% water, with a capacity of 0.255 mg toluene per g RL compared to 0.335 mg toluene/g solvent for BA + 60 wt% water. Despite the high viscosity of RL (208 mPa.s), the absorption capacity was better than PG16 and AA + 60 wt% water, 0.155 and 0.038 mg toluene/g solvent, respectively. This confirms that the static method is in agreement with the dynamic method.

Regarding limonene, C₁₀:C₁₂ again showed the best absorption capacity compared to all solvents (0.326 mg limonene/g DES at 30 °C). In the static method, the highest absorption capacity is obtained for the CO, which has the lowest K. The absorption capacity for limonene in CO is 0.228 mg VOC / g solvent, at 30 °C. PG16 and RL have a better absorption capacity than water that showed to be the least effective with a capacity around of 0.03 mg VOC /g water at 30 °C. The conventional solvents and Rameb:Lev absorption capacities for limonene are 0.106 and 0.151 mg per g of PG16 and RL, respectively, at 30 °C.

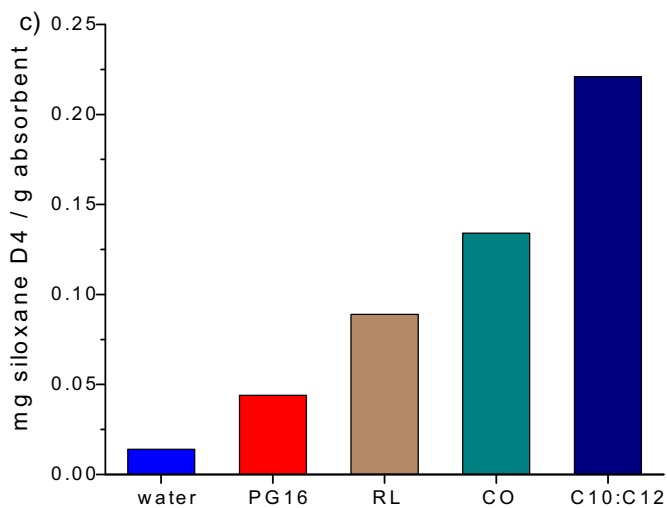
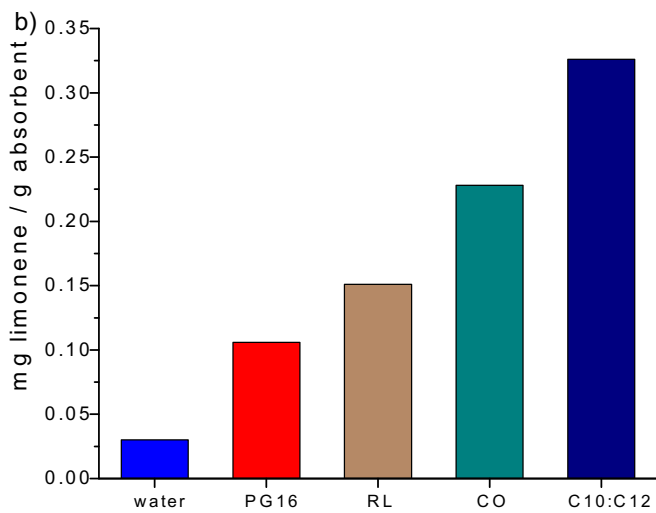
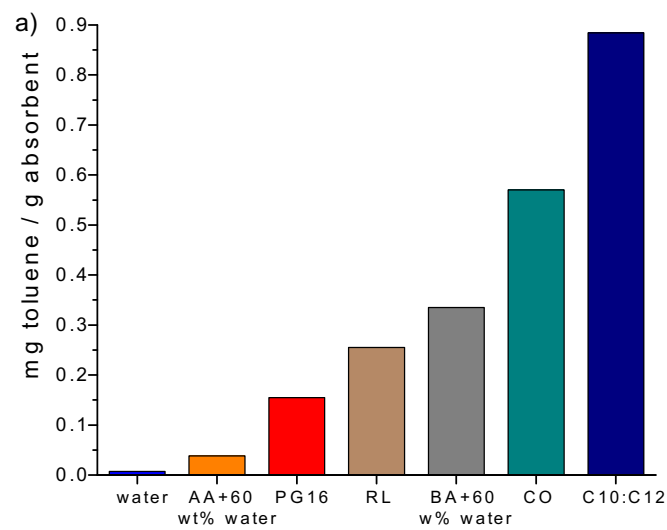


Figure 34. Absorption capacity (mg/g) of individuals VOCs, a) toluene, b) and c) siloxane D4 in water, PG16, RL, CO and C₁₀:C₁₂ at 30 °C.

As expected, there is good agreement between all of the measurements of the siloxane D4 absorption capacity in water, PG16, RL, CO, and C₁₀:C₁₂ and the K values from the static method. As a result, hydrophobic DES C₁₀:C₁₂ once more showed a higher absorption of 0.221 mg siloxane / g absorbent. However, siloxane absorption in CO did not exhibit the same trends as that shown in the absorption of toluene and limonene. Consequently, siloxane absorption in CO was 0.134 mg siloxane / g solvent. The highest absorption capacity between water, PG16, and RL was obtained for RL, with an absorption capacity of 0.089 mg siloxane / g absorbent, whereas water and PG16 had absorption capacities of (0.014 and 0.044 mg siloxane / g absorbent). All these results are consistent with the K values obtained in static method compared to the dynamic method, except for CO. Therefore, the K values are obtained at thermodynamic equilibrium where viscosity does not influence the absorption capacity.

III.2.2. Effect of toluene initial concentration

The effect of the initial toluene concentration was investigated using five different flow rates of 10, 20, 40, 80 and 100 $\mu\text{L}\cdot\text{hr}^{-1}$ with nitrogen flow rate at 15 $\text{L}\cdot\text{hr}^{-1}$ at 30 °C. As shown in Figure 35, the amount of captured toluene increased linearly with increasing the flow rate of toluene in C₁₀:C₁₂. The increase of flow rates leads to an increase in the initial toluene concentration. This shows that the increase in toluene concentration has a positive relationship with the toluene absorption in C₁₀:C₁₂. A similar tendency is found in the literature [2]. The results obtained from the different flow rates of toluene in C₁₀:C₁₂ were 0.422, 0.883, 1.768, 3.94 and 5.91 mg toluene per g of DES. The maximum absorption capacity of toluene in DES was 5.91 mg toluene/g DES for an inlet toluene concentration at 525 ppm. However, we still didn't reach the saturation of the absorbent.

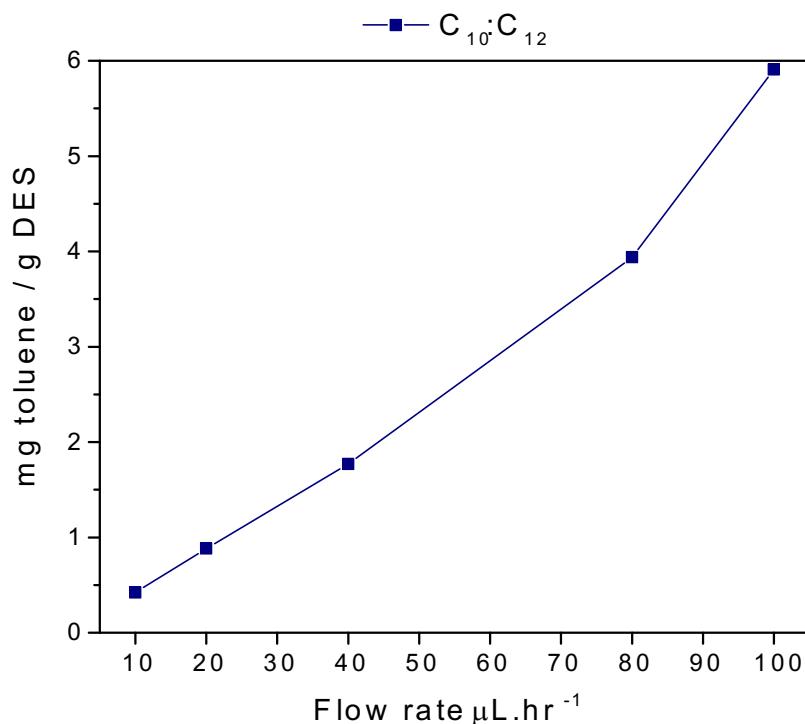


Figure 35. Absorption capacity for different initial concentrations of toluene in $C_{10}:C_{12}$ with different flow rates at 30 °C.

The values obtained in the literature for toluene in $\text{ChCl}:\text{Lev}$ and $\text{TBABr}:\text{Dec}$ were 0.55 mg per g DES and 2.37 mg per g DES with quite similar flow rate $73 \mu\text{L}\cdot\text{hr}^{-1}$ [10]. However, it showed lower absorption capacity for toluene compared to the $C_{10}:C_{12}$ DES which was 3.94 mg per g DES at $80 \mu\text{L}\cdot\text{hr}^{-1}$.

Altogether, our results indicate that the solubility of toluene in hydrophobic DES is sensitive to concentration conditions, also indicating that the toluene absorption process is reversible and can be subjected to regeneration by increasing the temperature and/or decreasing the concentration. Therefore, this demonstrates that hydrophobic DES are very efficient at absorbing low concentrations of toluene, which is a practical and industrial application that is well fulfilled. In addition, by increasing the initial concentration, the absorption capacity of toluene in DES could increase to more than 5.91 mg of toluene per g of DES, without reaching the saturation limit of toluene in DES.

III.2.3. Toluene absorption in available industrial solvents and water/solvent mixtures

In these experiments the aim was to find the best solvent in terms of absorption capacity, but also in terms of cost. We decided with our industrial partner to evaluate only the water/solvent mixtures. The performance is related to the K value of toluene in the solvent. In order to be close to industrial conditions, we used a dynamic bubbling set-up. The water/solvents used is shown in Table 21. The absorption capacities of toluene for the three solvents at 25 °C for a VOC flow rate of 20 $\mu\text{L}\cdot\text{hr}^{-1}$ are shown in Figure 36.

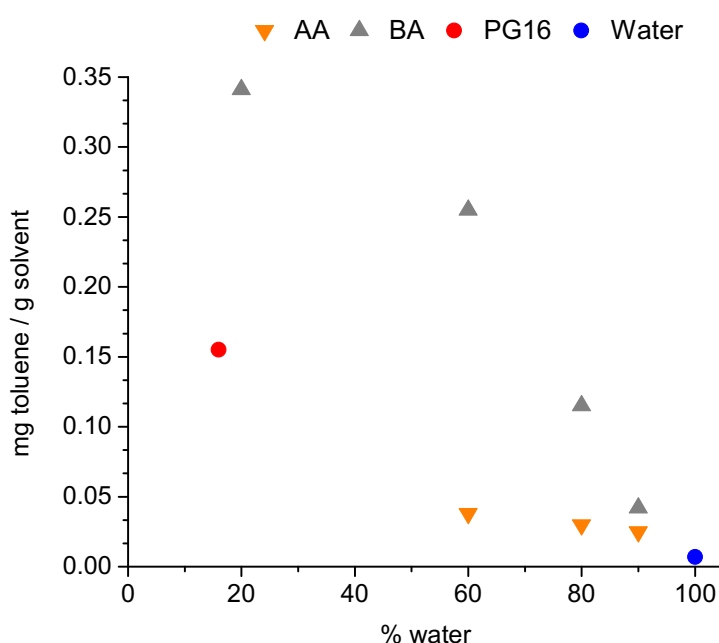


Figure 36. Absorption capacity of toluene in the water/solvent mixtures at 25 °C.

Water was the least effective solvent with a capacity of 0.007 mg toluene per g of water at 25 °C. In the case of BA and AA with 90 wt% of water, the absorption capacity reached 0.042 and 0.025 mg toluene per g of solvent, corresponding to a 6 and 3.6-fold increase compared to water, respectively. However, increasing the amount of solvent in the water improves the absorption capacity to a greater or lesser extent, depending on the solvent. Thus, for 80 and 60 wt% of water, we observed an increase from 0.115 to 0.255 mg of toluene per g of solvent for BA and from 0.030 to 0.038 mg per g of solvent for AA. Regarding PG16, the absorption capacity was 0.155 mg toluene per g of solvent. The mixture of BA with 80 wt% water has a similar absorption value, while PG16 contains only 16% water. Figure 37 shows absorption

curves obtained in the case of water/BA mixtures with an inlet toluene concentration of 1300 ppm. In these curves, we can follow the outlet gas concentration as a function of time. The curves are similar in shape, but the saturation of the solvent is reached later with a lower amount of water.

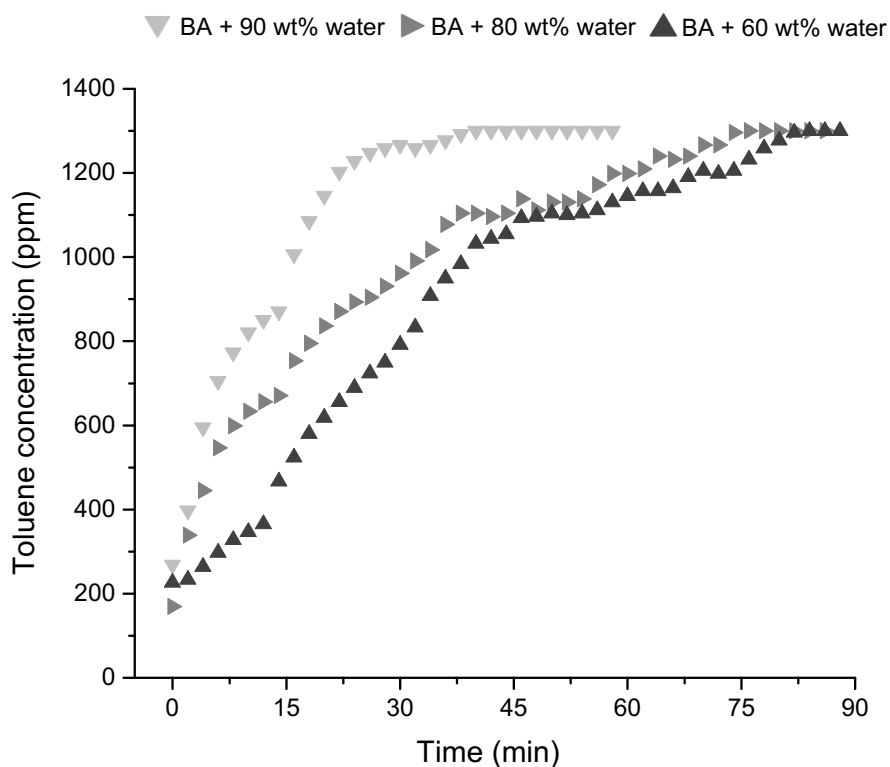


Figure 37. Toluene concentration in the outlet gas at 25 °C.

III.2.4. Effect of VOC mixtures

From an industrial point of view, it is interesting to study the absorption capacity of VOC mixtures in absorbents on a laboratory scale. Therefore, with the same conditions as for individual VOCs, the absorption of TLS mixture in five absorbents was evaluated in order to compare to individual VOCs (Figure 38). The absorption capacities of the absorbents show similar behavior with respect to the effect of the VOC mixture on the partition coefficient.

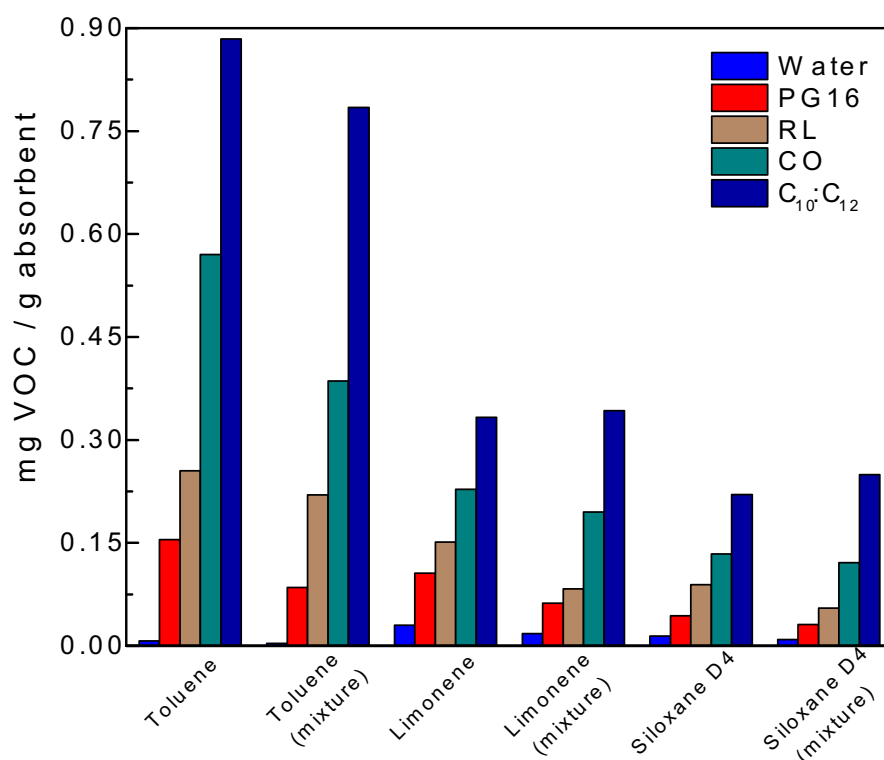


Figure 38. Absorption capacity of TLS mixture in water, PG16, RL, CO and C₁₀:C₁₂ at 30 °C.

As expected, C₁₀:C₁₂ was again the best absorber for TLS mixture absorption. A slight decrease from 0.88 to 0.77 mg toluene/ g C₁₀:C₁₂ was observed. For limonene and siloxane D4 in the mixture, they maintained approximately the same absorption capacity of the individual VOCs. For limonene individual and mixture for were 0.33 and 0.34 mg VOC / g C₁₀:C₁₂ and siloxane were 0.22 and 0.23 mg VOC / g C₁₀:C₁₂. Thus, maintaining the same behavior of VOC mixture on the partition coefficient.

In the case of CO, most of the characteristics are identical to those obtained for the VOC mixtures on the partition coefficient. In the case of toluene, the absorption capacity of VOC mixture in CO was 0.39 mg / g CO, while for individual toluene was 0.57 mg toluene / g CO. For limonene and siloxane D4 in the mixtures were 0.195 and 0.121 mg VOC / g CO, respectively. While for individual limonene and siloxane D4 were 0.228 and 0.134 mg VOC / g CO. The same tendency is observed for RL, PG16 and water with a slightly decrease in absorption of VOC in the mixture compared to the pure, as shown in the Figure 38. In the case of water, it is the least effective absorbent, reducing its absorption capacity by almost half.

Their absorption capacity of TLS mixture was 0.0036, 0.0018 and 0.0090 mg VOC / g water, respectively. Although industrial streams contain mixtures of VOCs of the same or different types, DES retains its high VOC retention capacity. Consequently, the partition coefficient of the VOC mixture in the absorbents showed comparable trend results, highlighting that using a static method can provide a good understanding of the absorption of individual VOCs and the VOC mixture in the absorbents.

III.3. Carbon dioxide and raw biogas absorption

The crucial process of absorbing carbon dioxide (CO₂) from biogas has numerous impacts on both environmental sustainability and industrial applications. Raw biogas is composed primarily of methane (CH₄). However, the presence of CO₂ in biogas reduces its energy content and makes it difficult to use. In that context, CO₂ absorption from biogas is critical step to improving biogas quality, energy content, and environmental advantages. This method of removing CO₂ from biogas involves chemical or physical absorption processes, resulting in biomethane a high-quality, purified biogas [35]. In the first experiments we evaluated the absorption capacity of CO₂ (50%) mixed with N₂ (50%) in absorbents such as water, PG, C₈:C₁₂, C₁₀:C₁₂, Rameb:Lev, tetraethylenepentamine (TEPA):C₈:C₁₂:water_{20%} (8:3:1) and TEPA+water_{20%}. Then we evaluated the absorption capacity of raw biogas in C₈:C₁₂, RL and water. In a typical test, 200 ml min⁻¹ of simulated flue gas (50% CO₂, 50% N₂) was introduced into 180 g of the solution and allowed to react to saturation at 30 °C and 1 bar.

III.3.1. Experimental methods and devices

For rapid screening, an experimental setup was developed at atmospheric pressure. It was designed to determine the CO₂ absorption capacity of the absorbents and to observe the phenomena in the absorption process. The simulated flue gas (concentration) of the inlet and outlet gas was measured by gas chromatograph. For the first experiments, before the absorption, CO₂ and N₂ were mixed in a constant flow rate (flow meter) and then introduced into the gas chromatography to detect the initial and stabilized concentration. Then, for the following studies, the same procedure was used for biogas absorption.

The concentration is obtained by calibrating and measuring the standard curve of the gas chromatograph using the external standard method. In the experiments, Micro GC (Fusion)

gas chromatograph (carrier gas helium), was used with two independently programmed module, A for CO₂/CH₄ and B for VOCs. The GC is consisting of an injector, a temperature programmable column and a detector. For the module A, the temperature of the sample inlet was 70 °C, the temperature of the column chamber was 47 °C kept for 70 seconds, and the sample pump of 15 seconds. For the module B, the temperature of the sample inlet was 70 °C, the temperature of the column chamber was 140 °C for 15 seconds with a ramp time of 60 seconds, then increases to 200 °C for 45 seconds, and the sample pump of 15 seconds. In order to measure CO₂/CH₄ quantitatively, the standard gas calibration method is adopted. Therefore, define absorption rate γ_{CO_2/CH_4} as the mole number of CO₂/CH₄ absorbed by absorbers per unit mass at a certain time, mol kg⁻¹s⁻¹ can be determined by equation (11).

$$\gamma_{CO_2} = \frac{(C_{CO_2CH_4, in} - C_{CO_2CH_4, out})}{22.4 * m_A (1 - C_{CO_2CH_4, in})(1 - C_{CO_2CH_4, out})} \quad (\text{eq.11})$$

In a typical test, 200 (mL/min) of simulated flue gas (50% CO₂, 50% N₂) for the first experiment and (27% CO₂, 27% CH₄ + VOCs mixture) for the second experiment were added into 200 g of absorbent at 30 °C and 1 bar. Total CO₂ loading (α_t , mol CO₂ mol⁻¹ absorbent) was measured as follow the equation (12):

$$\alpha_t = \frac{V_{CO_2CH_4, in} * \int_0^t \frac{C_{CO_2CH_4, in} - C_{CO_2CH_4, out}}{C_{CO_2CH_4, in}}}{22.4 * 10^3 * n_A} \quad (\text{eq.12})$$

Where: α_t represents the total absorption loading of CO₂/CH₄ per unit molar mass of absorbent, mol mol⁻¹; n_A represents the amount of absorbent mol; m_A represents the mass of absorbent, kg. The CO₂/CH₄ absorption capacity R (unit: mol kg⁻¹) is as follows in equation (13):

$$R = \frac{\alpha_t * n_A}{m_A} \quad (\text{eq.13})$$

III.3.2. CO₂ absorption results

The absorption capacity of the absorbents used to capture CO₂ is related to the screening method of CO₂ sorption in absorbents, except for TEPA. Therefore, in order to evaluate the capacity of the absorbents in conditions that mimic an absorption column, we selected solvents that have high and moderate absorption capacity and versatility. Figure 39 shows the absorption of CO₂ (50%) (200 ml min⁻¹) in water, PG, C₈:C₁₂, C₁₀:C₁₂ and Rameb:Lev, tetraethylenepentamine (TEPA):C₈:C₁₂:water_{20%} (8:3:1) at 30 °C. After 100 min, the TEPA:C₈:C₁₂:water_{20%} is basically saturated by CO₂, which shows that the contribution of TEPA in C₈:C₁₂ provides a longer absorption compared to other absorbents but still not as good as for TEPA+water_{20%}. A similar saturation time (10 min) were observed for the other absorbents.

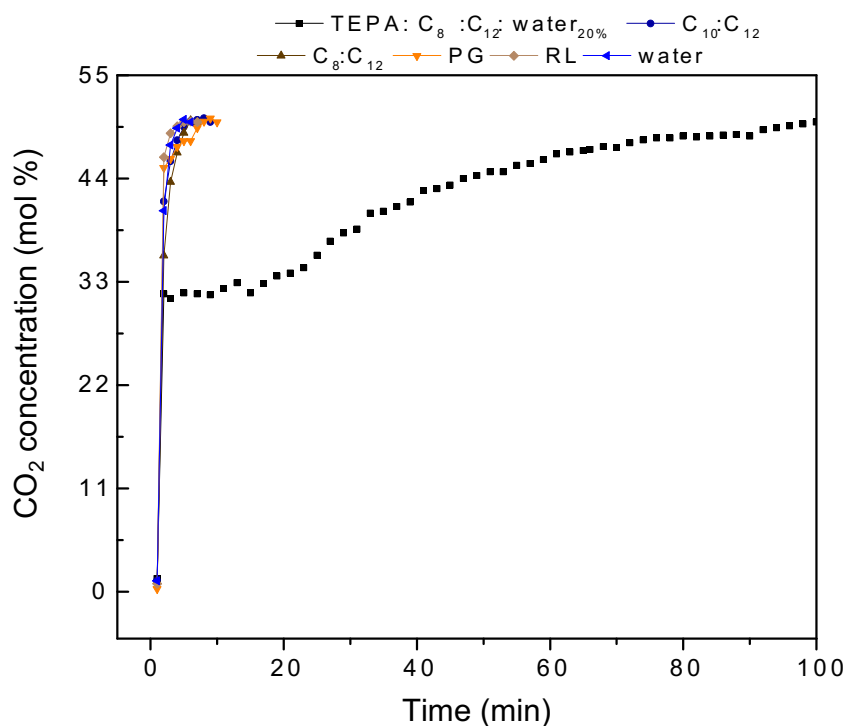


Figure 39. Absorption rate of an initial CO₂ (50%) in TEPA:C₈:C₁₂:water_{20%}, C₁₀:C₁₂, C₈:C₁₂, PG, RL and water at 30 °C.

The absorption capacity of CO₂ in the absorbents are listed in Table 25. As expected, TEPA + water_{20%} has the highest absorption capacity with 2.87 mol CO₂ / kg TEPA+water_{20%}. These measurements are in good agreement with the literature, which reported TEPA-ethanol-

water (2.48 mol CO₂ / kg absorbent) [36]. Among them, DES-based TEPA showed a significant absorption with 0.9 mol CO₂ / kg TEPA:C₈:C₁₂:water_{20%}, which is mainly due to the influence of the amine. Based on DES, C₈:C₁₂ had a slightly higher absorption, with 0.05 mol CO₂ / kg C₈:C₁₀. The absorption capacities of C₈:C₁₀, C₁₀:C₁₂ and RL, on the other hand, are in good agreement with previously reported CO₂ sorption values by screening method. All tested absorbent shows similar absorption values, close to water.

Table 25. Absorption capacity of CO₂ (50%) in different absorbents at 30 °C.

Absorbents	TEPA:C ₈ :C ₁₂ : water _{20%}	C ₈ :C ₁₂	C ₁₀ :C ₁₂	RL	PG	water	TEPA+ wate _{20%}	TEPA+ ethanol+ water
Absorption capacity mol CO ₂ kg ⁻¹	0.9 ^a	0.050 ^a	0.045 ^a	0.030 ^a	0.043 ^a	0.038 ^a	2.870 ^a	2.48 ^b

^aThis work. ^b Ref. [36] at 40 °C.

Regarding the composition of biogas, in addition to CO₂, biogas also contains various contaminants such as VOCs and H₂S. These contaminants can have a strong affinity for some absorbents and can contribute to a better absorption capacity of the absorbents, thus upgrading the biogas to biomethane.

III.3.3. Biogas absorption

In order to evaluate the absorption of the biogas in the absorbents, it was necessary to know the concentration of the biogas. The characteristics of the biogas can vary depending on the feedstock. Therefore, raw biogas was stored in a pressurized cylinder. The concentrations of the biogas were CO₂ (26%) and CH₄ (28%), H₂S (4%), VOCs varied between 50 and 100 ppm. Table 26 shows the absorption capacity of raw biogas CO₂ (26%) and CH₄ (28%) at 38 ml min⁻¹ in C₈:C₁₂ and RL at 30 °C.

Table 26. Absorption capacity of CO₂ (26%) CH₄ (28%) in different absorbents at 30 °C.

Absorbents	CO ₂ C ₈ :C ₁₂	CO ₂ RL	CH ₄ C ₈ :C ₁₂	CH ₄ RL
Absorption capacity mol kg ⁻¹	0.047	0.044	0.030	0.031

The results show that as the flow rate and CO₂/CH₄ concentration decreased, the absorption capacity is not quickly saturated, which extends the absorption equilibrium time, and remains stable. As a result, the absorption capacity of the absorbent for CO₂/CH₄ showed a mass transfer comparable to the previous results. A time-dependent CO₂/CH₄ absorption capacity can be observed depending on several factors such as pressure, temperature, concentration, flow rate, etc. This behavior can be seen in the Figure 40, where RL has a slightly longest absorption time compared to C₁₀:C₁₂, therefore maintained similar absorption capacities as can be seen in Table 25 and 26.

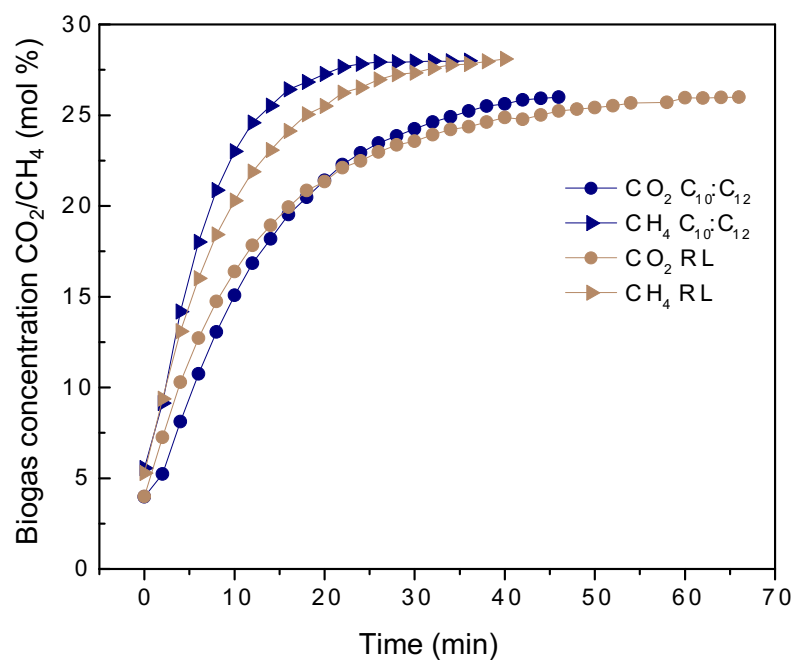


Figure 40. Absorption rate of biogas with initial concentration of CO₂ (26%) and CH₄ (28%) in C₁₀:C₁₂ and RL at 30 °C.

During the absorption process, the time in which an absorbent absorbs CO₂ and CH₄, plays a fundamental role in the enhancement process. Typically, CO₂ and CH₄ have different absorption kinetics when interacting with a liquid absorbent. The cause of this variation is based on factors such as solubility, molecular dimensions, and chemical composition of the absorbent. Longer CO₂ absorption rates contribute significantly to the overall efficiency of the biogas upgrading to biomethane.

III.4. Dynamic method regeneration

Absorbent regeneration is a critical step in several industrial processes, including gas absorption, where absorbent materials can capture specific contaminants such as CO₂ or impurities. Therefore, the absorption performances of the regenerated absorbents were determined. The regeneration experiments were conducted using the dynamic absorption set-up by following the desorption of absorbents at 60 °C. During the desorption process, N₂ is put into contact with the absorbents loaded with VOCs/CO₂/CH₄ or biogas, at a flow rate of 100 ml min⁻¹. In all the desorption studies, the temperature was increased to accelerate the regeneration, confirming the benefit of preheating the desorption column to reduce the duration and cost of the entire process.

III.5. Industrial scale dynamic absorption

The transition from laboratory-scale studies to industrial-scale operations is an important and often difficult step in many fields, including chemistry and engineering. The majority of laboratory experiments are carried out in a controlled environment on small scales. Scaling up to an industrial scale confirms if the concepts and procedures developed in the lab are practical and effective in real-world applications. Companies must determine the economic viability of a method before investing in large-scale production. Scaling up enables cost analysis, including material and energy expenses, which can help in evaluating the prospective return on investment. Industrial operations can have a significant impact on the environment. Assessing and minimizing these impacts is critical to ensuring regulatory compliance and minimizing environmental impact.

Based on these conditions, the purpose of this study was to evaluate and compare the efficiency of industrially available solvents such PG16, AA, BA and their water mixtures in removing toluene from exhaust gas from laboratory to industrial scale. In collaboration with our partner, Terraotherm. The experiments were carried out at Coudekerque-Branche, France. The Terraao absorber (Terraao[®]) is a direct heat and mass exchanger with the advantage of small geometric dimensions (1m² on the ground for 5 000 Nm³/h and 2 m high whatever the flow rate) [37]. The gas flow passes through the liquid of the exchanger in order to exchange the solvent-soluble compounds. This exchange then induces a movement of turbulence in the liquid phase to increase the probability of encounter between the solvent

and the gas, and thus improve the exchange of materials. The Terra^o® exchanger is equipped with a hydraulic pumping system to replace the saturated solvent with the backup solvent in case of solvent saturation and increasing also the turbulence of the liquid. In our experiments, a toluene concentration of 2 000 mg/m³ was used. The feed gas flow rate was 2 000 m³/h and the Terra^o® was fed with 300 liters of solvent. The toluene concentration in the inlet and outlet gas was monitored with a total hydrocarbon analyzer (Envea). The experimental set-up is shown in Figure 41.

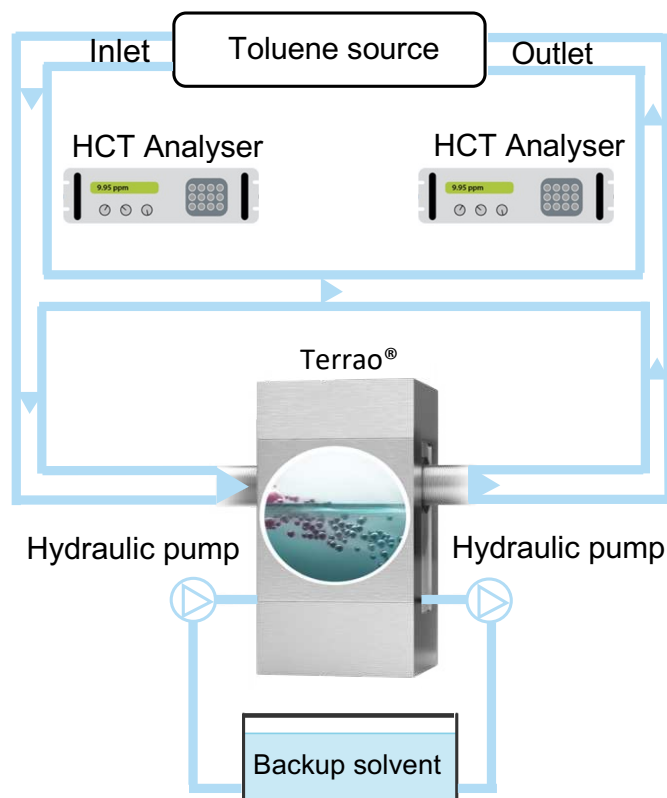


Figure 41. Industrial-scale experiments with Terra^o® exchanger.

The absorption capacities obtained at 20 °C are shown in Figure 42. The results are in good agreement with laboratory scale measurements [19]. Whatever the wt% of water, the water/BA mixtures exhibit higher absorption capacities than AA and PG16. The 20 wt% water shows the highest absorption capacity for toluene (22.70 g of toluene per L of solvent), while water scrubbing is the least effective solvent with 0.56 g of toluene per L of solvent.

As previously observed, the absorption capacity of the solvent decreases as the wt% of water increases. Regarding PG16, the absorption capacity is still lower than BA at the same wt% of water with an average absorption of 6.51 g of toluene per L of solvent.

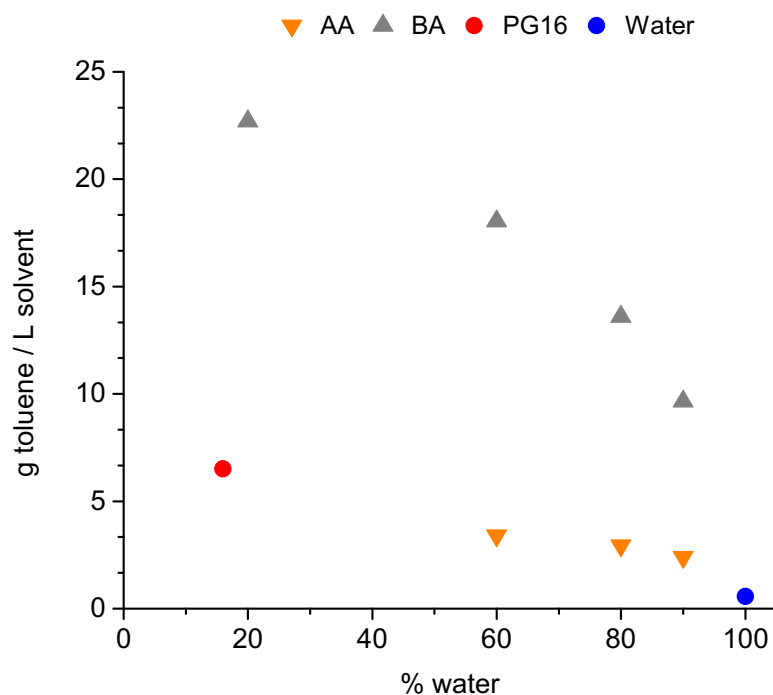


Figure 42. Absorption capacity of toluene in the solvents and water/solvent mixtures at 20 °C.

Figure 43 shows the concentration of toluene in the exhaust (outlet) gas for water/BA mixtures. The absorption curves are similar in shape and, similarly to the lab scale experiment, the best performance is obtained with the smaller amount of water. Although the industrial setup is closed-loop, no regeneration experiments were carried out.

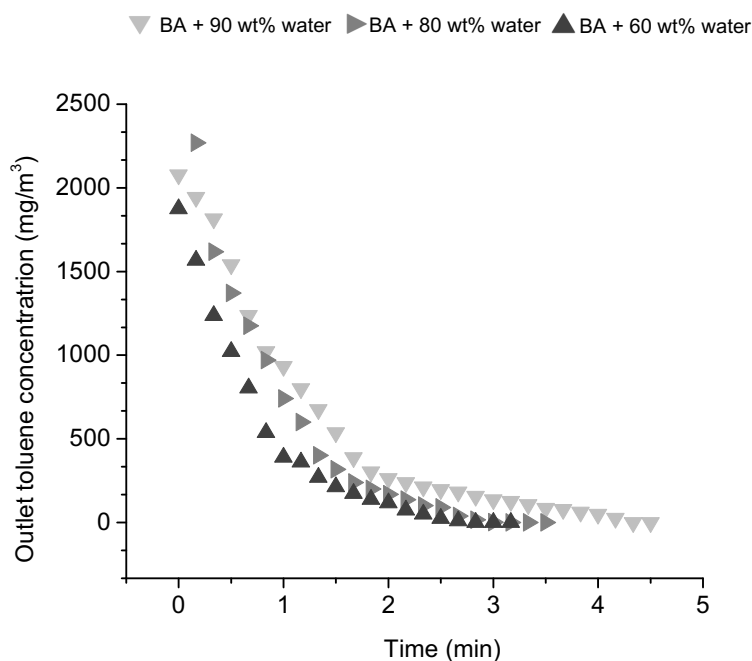


Figure 43. Concentration of toluene in the outlet gas in water/BA mixtures at 20 °C.

IV. Absorption mechanism revealed by Conductor-like Screening Model for Real Solvents (COSMO-RS)

This work was performed in collaboration with Pr Zhigang Lei and Chengmin Gui at Beijing University of Chemical Technology. The aim of the study was to uncover the absorption mechanism and analyze the uptake thermodynamic. The σ profiles of the studied molecules and the Gibbs free energy of solvation for toluene in different absorbents such water, AA, BA, PG16 and their mixtures in water were calculated by COSMO-RS model.

The COSMO-RS is a popular molecular thermodynamic method used to calculate important physicochemical properties, phase behavior and molecular characteristics, especially in the field of absorption and extraction with DES and ILs [38–41]. In this study, COSMOthermX (version 2021) was used to predict the Gibbs free energy of solvation for toluene in different absorbents. The σ -profiles, regarded as the fingerprint of molecules in the COSMO-RS model, were obtained from the built-in “COSMOTZVP” database [42]. [18]

IV.1. Analysis of σ -profiles

The COSMO-RS σ -profiles for toluene and different absorbents are depicted in Figure 44. The molecule segments with positive polarization charge densities are located in the hydrogen bond donor (HBD) region, while the negative surface pieces are in the hydrogen bond acceptor (HBA) region. Besides, the interval of $-0.0082 \text{ e}/\text{\AA}^2 < \sigma < 0.0082 \text{ e}/\text{\AA}^2$ are nonpolar region. It is noticeable that the σ -profile of toluene are almost entirely in nonpolar region, indicating its weak ability to form HB with other molecules, such as water. The solubility of toluene in water is the lowest among several solvents studied, as water has strong peaks in both the HBD and HBA regions, leaving only a small part in non-polar region. BA has a similar shape of σ -profile with toluene in nonpolar region due to the benzene ring in their structures, which facilitates the formation of van der Waals (vdW) interaction between them. Besides, there are small peaks in HBD region and HBA region resulting from its hydrogen atom and oxygen on the hydroxyl group. Compared with BA, AA and PG express higher peaks in the HBA region, demonstrating that AA and PG are more likely to form HB as hydrogen bond acceptors with other molecules. However, as mentioned before, being a strong HBA cannot effectively enhance the interaction with toluene. Therefore, BA may be the optimal absorbent from the point of view of molecular interaction.

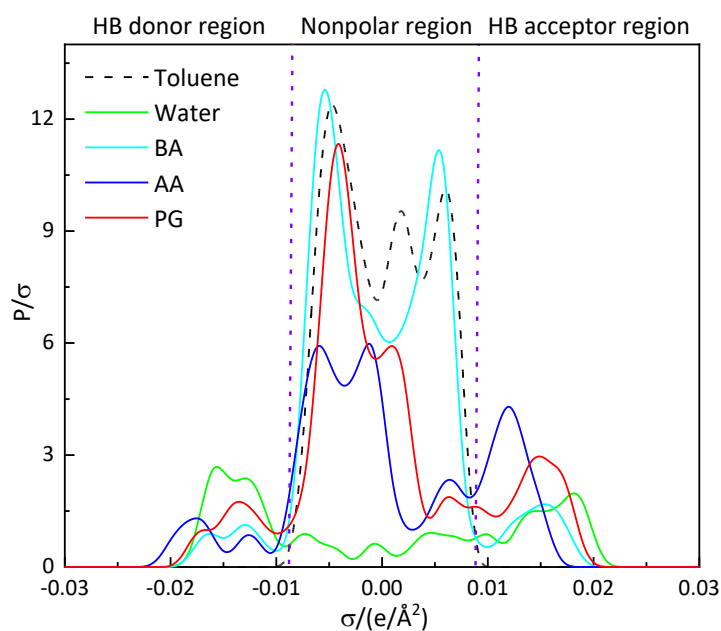


Figure 44. σ -Profiles of toluene, water, BA, AA and PG.

IV.2. Gibbs free energy of solvation

To investigate the influence of absorbent type and temperature on the absorption thermodynamic, the Gibbs free energy of solvation (ΔG_{sol}) of toluene in different absorbents at various temperatures was calculated by COSMO-RS model. Defined as the free energy in the process of solute from gas phase diverted into liquid absorbent, ΔG_{sol} reflects the affinity capacity between solute and solvent [43]. As shown in Figure 45a, the magnitude of ΔG_{sol} for different kinds of absorbents at the same wt% of water follows the sequence BA > AA > PG. For all three absorbents, the $-\Delta G_{\text{sol}}$ decreases with increasing amount of water, which is in good agreement with the partition coefficients results in section I.4.5. It is observed from Figure 45b that the higher the temperature, the lower the value of $-\Delta G_{\text{sol}}$ in pure absorbents, illustrating that low temperature is favorable for the toluene absorption process. Obviously, the ΔG_{sol} magnitude for water is much lower than the other three organic absorbents. Overall, the analysis of absorption thermodynamics confirms the σ -profiles result and is consistent with the partition coefficients result, that is, BA is a more promising toluene absorbent than AA and PG.

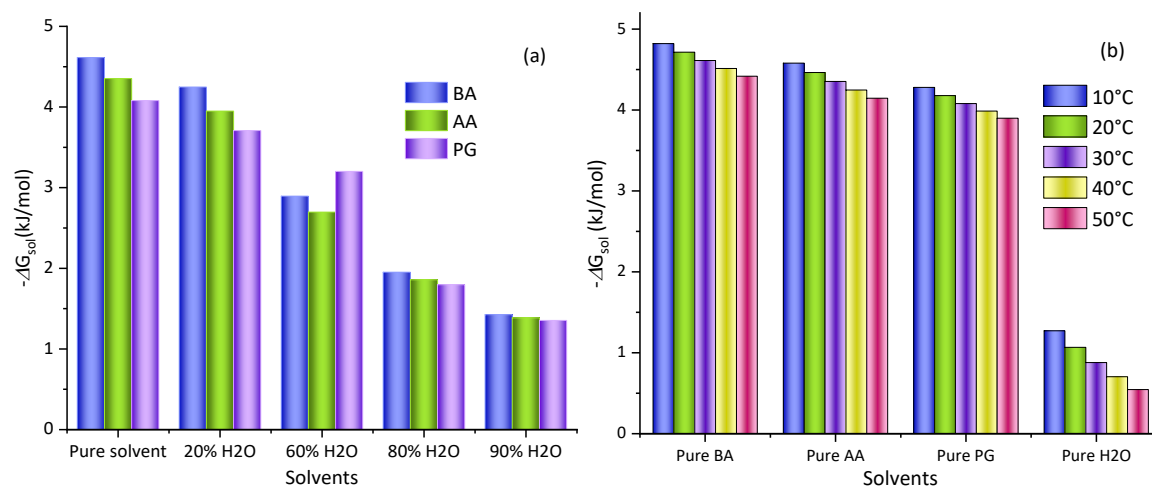


Figure 45. The free energy of solvation (ΔG_{sol}) of toluene in different solvents at 30°C (a); the influence of temperature on the ΔG_{sol} of toluene in different pure solvents (b).

In addition, analysis of the σ -profile indicates that the formation of vdW interactions between the absorbent and toluene, rather than the formation of HB, was the key to improving the absorption performance. Additionally, BA has the most negative Gibbs free energy of solvation value for toluene compared to other absorbents under study.

V. References

- [1] F. Fahri, K. Bacha, F.F. Chiki, J.P. Mbakidi, S. Panda, S. Bouquillon, S. Fourmentin, Air pollution: new bio-based ionic liquids absorb both hydrophobic and hydrophilic volatile organic compounds with high efficiency, *Environ Chem Lett.* 18 (2020) 1403–1411. <https://doi.org/10.1007/s10311-020-01007-8>.
- [2] L. Moura, T. Moufawad, M. Ferreira, H. Bricout, S. Tilloy, E. Monflier, M.F. Costa Gomes, D. Landy, S. Fourmentin, Deep eutectic solvents as green absorbents of volatile organic pollutants, *Environ Chem Lett.* 15 (2017) 747–753. <https://doi.org/10.1007/s10311-017-0654-y>.
- [3] S. Panda, S. Fourmentin, Cyclodextrin-based supramolecular low melting mixtures: efficient absorbents for volatile organic compounds abatement, *Environmental Science and Pollution Research.* 29 (2022) 264–270. <https://doi.org/10.1007/s11356-021-16279-y>.
- [4] B. Kolb, L.S. Ettre, *Static Headspace–Gas Chromatography*, in: Wiley, 2006. <https://doi.org/10.1002/0471914584>.
- [5] T. Moufawad, *Développement de nouveaux solvants de lavage pour l'absorption des Composés Organiques Volatils*. PhD of Université du Littoral Côte d'Opale., 2019.
- [6] J.M. Gossett, Measurement of Henry's Law Constants for C1 and C2 Chlorinated Hydrocarbons, *Environ. Sci. Technol.* 21 (1987) 202–208. <https://doi.org/https://doi.org/10.1021/es00156a012>.
- [7] J.L. Hamelink, P.B. Simon, E.M. Silberhorn, Henry's Law Constant, Volatilization Rate, and Aquatic Half-Life of Octamethylcyclotetrasiloxane, *Environ Sci Technol.* 30 (1996) 1946–1952. <https://doi.org/10.1021/es950634j>.
- [8] P. Blach, S. Fourmentin, D. Landy, F. Cazier, G. Surpateanu, Cyclodextrins: A new efficient absorbent to treat waste gas streams, *Chemosphere.* 70 (2008) 374–380. <https://doi.org/10.1016/j.chemosphere.2007.07.018>.
- [9] A.P. Karman, S.E. Ebeler, N. Nitin, S.R. Dungan, Partitioning, solubility and solubilization of limonene into water or short-chain phosphatidylcholine solutions, *J Am Oil Chem Soc.* 98 (2021) 979–992. <https://doi.org/10.1002/aocs.12535>.
- [10] T. Moufawad, M. Costa Gomes, S. Fourmentin, Deep eutectic solvents as absorbents for VOC and VOC mixtures in static and dynamic processes, *Chemical Engineering Journal.* 448 (2022) 137619. <https://doi.org/10.1016/j.cej.2022.137619>.
- [11] A.S. Rodriguez Castillo, P.F. Biard, S. Guihéneuf, L. Paquin, A. Amrane, A. Couvert, Assessment of VOC absorption in hydrophobic ionic liquids: Measurement of partition and diffusion coefficients and simulation of a packed column, *Chemical Engineering Journal.* 360 (2019) 1416–1426. <https://doi.org/10.1016/j.cej.2018.10.146>.
- [12] M.-D. Vuong, A. Couvert, C. Couriol, A. Amrane, P. Le Cloirec, C. Renner, Determination of the Henry's constant and the mass transfer rate of VOCs in solvents, *Chemical Engineering Journal.* 150 (2009) 426–430. <https://doi.org/10.1016/j.cej.2009.01.027>.
- [13] A. Kochetkov, J.S. Smith, R. Ravikrishna, K.T. Valsaraj, L.J. Thibodeaux, Air-water partition constants for volatile methyl siloxanes, *Environ Toxicol Chem.* 20 (2001) 2184–2188. <https://doi.org/10.1002/etc.5620201008>.
- [14] P. Makoś-Chełstowska, E. Słupek, J. Gębicki, Deep eutectic solvent-based green absorbents for the effective removal of volatile organochlorine compounds from

- biogas, *Green Chemistry*. 23 (2021) 4814–4827. <https://doi.org/10.1039/D1GC01735G>.
- [15] C.C. Chen, Y.H. Huang, S.M. Hung, C. Chen, C.W. Lin, H.H. Yang, Hydrophobic deep eutectic solvents as attractive media for low-concentration hydrophobic VOC capture, *Chemical Engineering Journal*. 424 (2021) 130420. <https://doi.org/10.1016/j.cej.2021.130420>.
- [16] E. Dumont, G. Darracq, A. Couvert, C. Couriol, A. Amrane, D. Thomas, Y. Andrès, P. Le Cloirec, Determination of partition coefficients of three volatile organic compounds (dimethylsulphide, dimethyldisulphide and toluene) in water/silicone oil mixtures, *Chemical Engineering Journal*. 162 (2010) 927–934. <https://doi.org/10.1016/j.cej.2010.06.045>.
- [17] M.J. Patel, S.C. Papat, M.A. Deshusses, Determination and correlation of the partition coefficients of 48 volatile organic and environmentally relevant compounds between air and silicone oil, *Chemical Engineering Journal*. 310 (2017) 72–78. <https://doi.org/10.1016/j.cej.2016.10.086>.
- [18] P. Villarim, E. Genty, J. Zemmouri, S. Fourmentin, Deep eutectic solvents and conventional solvents as VOC absorbents for biogas upgrading: A comparative study, *Chemical Engineering Journal*. 446 (2022) 136875. <https://doi.org/10.1016/j.cej.2022.136875>.
- [19] P. Villarim, C. Gui, E. Genty, Z. Lei, J. Zemmouri, S. Fourmentin, Toluene absorption from laboratory to industrial scale: An experimental and theoretical study, *Sep Purif Technol*. 328 (2024) 125070. <https://doi.org/10.1016/j.seppur.2023.125070>.
- [20] D. Bir, Partition coefficient calculation of selected terpenes and low molecular weight solvents between tall oil fatty acid and air and polydimethyl siloxane oil and air, *J Am Oil Chem Soc*. 77 (2000) 163–169. <https://doi.org/10.1007/s11746-000-0026-4>.
- [21] R. Santiago, C. Moya, J. Palomar, Siloxanes capture by ionic liquids: Solvent selection and process evaluation, *Chemical Engineering Journal*. 401 (2020) 126078. <https://doi.org/10.1016/j.cej.2020.126078>.
- [22] P. Makoś-Chełstowska, E. Słupek, A. Kramarz, J. Gębicki, New Carvone-Based Deep Eutectic Solvents for Siloxanes Capture from Biogas, *Int J Mol Sci*. 22 (2021) 9551. <https://doi.org/10.3390/ijms22179551>.
- [23] E. Słupek, P. Makoś-Chełstowska, J. Gębicki, Removal of siloxanes from model biogas by means of deep eutectic solvents in absorption process, *Materials*. 14 (2021) 1–20. <https://doi.org/10.3390/ma14020241>.
- [24] E. Słupek, P. Makoś, J. Gębicki, Deodorization of model biogas by means of novel non-ionic deep eutectic solvent, *Archives of Environmental Protection*. 46 (2020) 41–46. <https://doi.org/10.24425/aep.2020.132524>.
- [25] G. Quijano, A. Couvert, A. Amrane, G. Darracq, C. Couriol, P. Le Cloirec, L. Paquin, D. Carrié, Potential of ionic liquids for VOC absorption and biodegradation in multiphase systems, *Chem Eng Sci*. 66 (2011) 2707–2712. <https://doi.org/10.1016/j.ces.2011.01.047>.
- [26] C.-C. Chen, Y.-H. Huang, J.-Y. Fang, Hydrophobic deep eutectic solvents as green absorbents for hydrophilic VOC elimination, *J Hazard Mater*. 424 (2022) 127366. <https://doi.org/10.1016/j.jhazmat.2021.127366>.
- [27] C. Tanios, C. Gennequin, H.L. Tidahy, A. Aboukais, E. Abi-Aad, F. Cazier, C. Tanios, M. Labaki, C. Tanios, B. Nsouli, H₂ production by dry reforming of biogas over Ni-Co-Mg-Al mixed oxides prepared via hydrotalcite route, in: 2016 7th International Renewable

- Energy Congress (IREC), IEEE, 2016: pp. 1–6. <https://doi.org/10.1109/IREC.2016.7478866>.
- [28] F. Heymes, P. Manno-Demoustier, F. Charbit, J.L. Fanlo, P. Moulin, A new efficient absorption liquid to treat exhaust air loaded with toluene, *Chemical Engineering Journal*. 115 (2006) 225–231. <https://doi.org/10.1016/j.cej.2005.10.011>.
- [29] J. González-Rivera, C. Pelosi, E. Pulidori, C. Duce, M.R. Tiné, G. Ciancaleoni, L. Bernazzani, Guidelines for a correct evaluation of Deep Eutectic Solvents thermal stability, *Current Research in Green and Sustainable Chemistry*. 5 (2022). <https://doi.org/10.1016/j.crgsc.2022.100333>.
- [30] F. Abu Hatab, O.A.Z. Ibrahim, S.E.E. Warrag, A.S. Darwish, T. Lemaoui, M.M. Alam, T. Alsufyani, V. Jevtovic, B.H. Jeon, F. Banat, S. W. Hasan, I.M. Alnashef, Y. Benguerba, Solvent Regeneration Methods for Combined Dearomatization, Desulfurization, and Denitrogenation of Fuels Using Deep Eutectic Solvents, *ACS Omega*. 8 (2022) 626–635. <https://doi.org/10.1021/acsomega.2c05776>.
- [31] E. Słupek, P. Makoś, J. Gębicki, Theoretical and economic evaluation of low-cost deep eutectic solvents for effective biogas upgrading to bio-methane, *Energies (Basel)*. 13 (2020) 3390. <https://doi.org/10.3390/en13133379>.
- [32] M. Mu, X. Zhang, G. Yu, R. Xu, N. Liu, N. Wang, B. Chen, C. Dai, Effective absorption of dichloromethane using deep eutectic solvents, *J Hazard Mater*. 439 (2022) 129666. <https://doi.org/10.1016/j.jhazmat.2022.129666>.
- [33] P. Makoś-Chełstowska, E. Słupek, A. Kramarz, D. Dobrzyniewski, B. Szulczyński, J. Gębicki, Green monoterpenes based deep eutectic solvents for effective BTEX absorption from biogas, *Chemical Engineering Research and Design*. 188 (2022) 179–196. <https://doi.org/10.1016/j.cherd.2022.09.047>.
- [34] P. Makoś-Chełstowska, VOCs absorption from gas streams using deep eutectic solvents – A review, *J Hazard Mater*. 448 (2023) 130957. <https://doi.org/10.1016/j.jhazmat.2023.130957>.
- [35] M. Ellacuriaga, J. García-Cascallana, X. Gómez, Biogas Production from Organic Wastes: Integrating Concepts of Circular Economy, *Fuels*. 2 (2021) 144–167. <https://doi.org/10.3390/fuels2020009>.
- [36] J. Liu, J. Qian, H. Hu, Effect of H₂O on absorption performance of tetraethylenepentamine-ethanol-CO₂ two-phase absorbent and its mechanism, *International Journal of Greenhouse Gas Control*. 110 (2021) 103406. <https://doi.org/10.1016/j.ijggc.2021.103406>.
- [37] Zemmouri J., Device for producing and treating a gas stream through a volume of liquid, and facility and method implementing said device., WO2016071648A2, 2016.
- [38] T. Quaid, T. Reza, COSMO-RS predictive screening of type 5 hydrophobic deep eutectic solvents for selective platform chemicals absorption, *J Mol Liq*. 382 (2023) 121918. <https://doi.org/10.1016/j.molliq.2023.121918>.
- [39] A.S. Darwish, T. Lemaoui, J. AlYammahi, H. Taher, Y. Benguerba, F. Banat, I.M. AlNashef, Molecular insights into potential hydrophobic deep eutectic solvents for furfural extraction guided by COSMO-RS and machine learning, *J Mol Liq*. 379 (2023) 121631. <https://doi.org/10.1016/j.molliq.2023.121631>.
- [40] C. Gui, G. Li, Z. Lei, Z. Wei, Y. Dong, Experiment and Molecular Mechanism of Two Chlorinated Volatile Organic Compounds in Ionic Liquids, *Ind Eng Chem Res*. 62 (2023) 1160–1171. <https://doi.org/10.1021/acs.iecr.2c04163>.

- [41] M. Nala, E. Auger, I. Gedik, N. Ferrando, M. Dicko, P. Paricaud, F. Volle, J.P. Passarello, J.C. de Hemptinne, P. Tobaly, P. Stringari, C. Coquelet, D. Ramjugernath, P. Naidoo, R. Lugo, Vapour-liquid equilibrium (VLE) for the systems furan+n-hexane and furan+toluene. Measurements, data treatment and modeling using molecular models, *Fluid Phase Equilib.* 337 (2013) 234–245. <https://doi.org/10.1016/j.fluid.2012.08.005>.
- [42] R. Calvo-Serrano, M. González-Miquel, G. Guillén-Gosálbez, Integrating COSMO-Based σ -Profiles with Molecular and Thermodynamic Attributes to Predict the Life Cycle Environmental Impact of Chemicals, *ACS Sustain Chem Eng.* 7 (2019) 3575–3583. <https://doi.org/10.1021/acssuschemeng.8b06032>.
- [43] C. Dai, M. Chen, W. Mu, B. Peng, G. Yu, N. Liu, R. Xu, N. Wang, B. Chen, Highly efficient toluene absorption with π -electron donor-based deep eutectic solvents, *Sep Purif Technol.* 298 (2022) 121618. <https://doi.org/10.1016/j.seppur.2022.121618>.

Conclusion and perspectives

The aim of this study was to evaluate DESs and conventional solvents as new absorbents for biogas impurities such as VOCs and CO₂ by physical absorption. This study was carried out in collaboration with an industrial partner (Terrao®) that developed new mass and heat exchangers. In this aim, we studied different types of DES and conventional solvents and characterized them, such as water content, viscosity, density and IR. Moreover, to get as close as possible to real conditions, we evaluated the absorption capacity of individual VOCs their mixture and CO₂/CH₄ in different absorbents. The VOCs selected for our study were based on the impurities in biogas and their structural diversity used in industry.

The partition coefficient values obtained at 30 °C were used to plot the efficiency of the absorbents with respect to all VOCs in the form of a color-coded pie as can be seen in Figure 46.

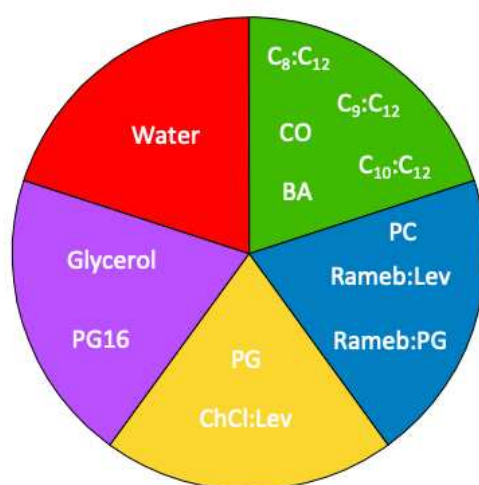


Figure 46. Absorption efficiency of VOCs in DESs and conventional solvents.

The least effective absorbent is shown in red and the most effective in green. We can see that the hydrophobic fatty acid-based DES and two solvents cooking oil and benzyl alcohol have the greatest versatility for the studied VOCs, with a high absorption capacity for most of the VOCs. However, the higher viscosity of CO and higher volatility of BA in comparison to the

hydrophobic DESs could be less effective in terms of high energy and regeneration, respectively.

In addition, there is a linear trend in absorption capacity as the initial VOC concentration increases. The absorption capacity of VOCs by absorbents was monitored at different temperatures. The volatility of VOCs increases with temperature and, consequently, the capacity of the absorbent to trap VOCs decreases. These behaviors indicate that the absorption of VOCs by DESs and solvents is a physical absorption, and an easily reversible process, leading to less costly regeneration of the sorbent.

We observed that the absorption capacities of DESs did not vary between pure VOCs and VOCs in a mixture. Then, the absorption of CO_2 , CH_4 and their mixture in absorbents has been studied using the screening method developed by combining gas pressurization on absorbents in vials with HS-GC analysis. This study was carried out in collaboration with Dr Leila Moura from the School of Chemistry and Chemical Engineering at Queen's University, Belfast. The absorption capacity of the hydrophobic DESs was moderate and not promising for this application.

To get closer to the real conditions of an absorption column, we then evaluated the efficiency of DES and conventional solvents to absorb VOCs/ CO_2 and raw biogas in a dynamic process. In addition, the transition from laboratory to industrial scale shows consistent results.

The static method measurements using static (SH-GC) for the determination of K values and the screening method for CO_2 can evaluate with accuracy which solvent is suitable for VOCs or CO_2 absorption. The results are fast and cost-effective using only a few quantities of solvent for the experiments.

Lastly, the absorption mechanism and analysis of the uptake thermodynamic were uncovered by COSMO-RS model in collaboration with Pr Zhigang Lei and Chengmin Gui at Beijing University of Chemical Technology. The good agreement between the experimental and theoretical results shows that COSMO-RS could also be used to predict affinity between VOC and absorbent. However, it is better to use this method in close combination with experimental results.

The aim as researchers is to close the gap between what is known now and what is possible in the future. This section focuses on how future work can fill existing gaps in the previous studies, improve current knowledge, and clarify some of the key findings of this research.

- Evaluate different types of DESs or new solvents that may be suitable and appropriate for absorption of other impurities from biogas such as CO₂, H₂S, O₂ and etc.
- Explore the absorption mechanism, speculate on chemical reaction paths, and obtain chemical reaction equilibrium constants.
- Evaluate the oxidation and degradation of the absorbents upon heating
- Carry out process simulation and operating parameter optimization for industrial-scale VOCs and CO₂ capture by Aspen Plus, and further improve the absorption and regeneration process, such as using interstage cooling process and rich liquid split process.
- Conduct an economic feasibility and environmental assessment of new VOCs and CO₂ absorption processes.
- GROMACS software can be used to simulate the CO₂ absorption process, display the microscopic separation phenomena and characteristics of the studied system, and reveal the separation mechanism. Gaussian 09, which is based on density functional theory, will be used to calculate the free energy barrier of the CO₂ absorption/desorption process.

List of publications and communication

Publications

- **P. Villarim**, E. Genty, J. Zemmouri, S. Fourmentin, Deep eutectic solvents and conventional solvents as VOC absorbents for biogas upgrading: A comparative study, Chemical Engineering Journal 446 (2022), 136875.
<https://doi.org/10.1016/j.cej.2022.136875>
- **P. Villarim**, C. Gui, E. Genty, Z. Lei, J. Zemmouri, S. Fourmentin, Toluene absorption from laboratory to industrial scale: An experimental and theoretical study, Separation and Purification Technology 328 (2024) 125070.
<https://doi.org/10.1016/j.seppur.2023.125070>
- Chengmin Gui, Pedro Villarim, Zhigang Lei, Sophie Fourmentin, "VOC absorption in supramolecular deep eutectic solvents: Experiment and molecular dynamic studies". Separation and Purification Technology journal (2024).
<https://doi.org/10.1016/j.cej.2024.148708>

Poster communication

- **P. Villarim**, E. Genty, J. Zemmouri, S. Fourmentin., Effective VOC Capture by Hydrophobic Deep Eutectic Solvents Using Static and Dynamic Processes. 3rd International Meeting on Deep Eutectic Solvents, Lisbon, Portugal, 19-22 June 2023.

Oral communication

- **P. Villarim**, E. Genty, J. Zemmouri, S. Fourmentin., New compact systems for biogas upgrading, My thesis in 180s, Journée du Pôle MTE, Dunkerque, 12 juillet 2022.

Abstract

Biogas is a renewable energy source produced naturally by the anaerobic digestion of organic matter. It consists mainly of methane (CH_4) and carbon dioxide (CO_2). It also contains traces of water vapour, volatile organic compounds (VOCs) and hydrogen sulphide. Biogas upgrading to biomethane requires the removal of contaminants in the raw biogas, reducing the level of impurities to achieve high CH_4 content of about 90 to 99%. The uses of biomethane are the same as natural gas while being a 100% renewable and non-fossil energy source. Many technologies have been tested and applied to remove impurities from biogas, such as water scrubbing, physical and chemical scrubbing, membrane separation, pressure swing adsorption, biological methods, etc. Absorbents play an important role in removing impurities from biogas. Therefore, the development of novel absorbents with high absorption capacity and high recyclability is mandatory. The suitable absorbent should also have low viscosity, relatively low toxicity, low vapor pressure, high boiling point, high absorption capacity, and low cost. Deep eutectic solvents (DESs) are a mixture of two or three chemical compounds (usually a hydrogen acceptor compound, HBA and a compound hydrogen donor, HBD), which combine via hydrogen bonds that have a lower melting point than each of their pure components. These solvents have physico-chemical properties that can be tuned depending on the nature of the individual compounds and their ratio. The purpose of the thesis was to evaluate DESs and conventional green solvents as VOCs/ CO_2 absorbers for biogas upgrading. We evaluated and compared the efficiency of different DESs and conventional absorbents for the absorption of nine VOCs and CO_2 . The vapor–liquid partition coefficient (K) of the VOCs in the studied solvents and the absorption capacity of CO_2 in DES were determined using static headspace-gas chromatography. The effect of VOC mixture, temperature water content was evaluated. The absorption capacities of individuals VOCs, their mixture and CO_2/CH_4 in DESs and conventional solvents were also evaluated using a dynamic set-up which simulated an industrial absorption column. Both static and dynamic results are in good agreement. Also, the absorption capacities of industrial absorbents were evaluated on an industrial scale using an exchanger developed by our industrial partner (Terrao®).



Thèse de Doctorat

Mention : Chimie

Spécialité : Chimie théorique, physique, analytique

présentée à l'*Ecole Doctorale en Sciences Technologie et Santé (ED 585)*

de l'**Université du Littoral Côte d'Opale**

par

Pedro Villarim

pour obtenir le grade de Docteur de l'Université du Littoral Côte d'Opale

Nouveaux systèmes compacts pour la purification du biogaz

Soutenue le 15 Décembre 2023, après avis des rapporteurs, devant le jury d'examen :

Pr Alessandro Triolo, ISM-CNR Italien
Pr Christophe Coquelet, IMT Mines Albi
Dr Leila Moura, Queen's University Belfast
Dr Patrycia Makos Chelstowska, École polytechnique de Gdańsk
Pr Abdenacer Idrissi, Université de Lille
Pr Annabelle Couvert, ENSCR de Rennes
Pr Sophie Fourmentin, ULCO
Pr Jaouad Zemmouri, TerraO

Rapporteur
Rapporteur
Examinateur
Examinateur
Examinateur
Président
Directeur
Co-directeur



1. Introduction

Le biogaz est une source d'énergie verte et rentable qui peut être produite à partir de divers déchets, notamment par la méthanisation de la biomasse et des déchets organiques, la digestion anaérobie des boues d'épuration, le compostage commercial, les décharges et la co-digestion anaérobie du fumier animal. Le biogaz peut contenir diverses impuretés, notamment du CH₄ (35 à 75 %) et du CO₂ (25 à 60 %), qui peuvent avoir des effets secondaires sur l'environnement, la santé et la technologie. La valorisation du biogaz en biométhane nécessite l'élimination des contaminants pour atteindre une teneur en CH₄ de 90 à 99 %. Les applications du biogaz sont similaires à celles du gaz naturel, mais il s'agit d'une source d'énergie 100 % renouvelable et non fossile. Des technologies telles que l'épuration à l'eau, l'épuration physique et chimique, la séparation par membrane, l'adsorption modulée en pression et les méthodes biologiques ont été testées pour éliminer les impuretés du biogaz [1–3].

L'absorption physique est considérée comme une méthode appropriée qui répond aux normes de technologie et d'ingénierie vertes. Les absorbants jouent un rôle important dans l'élimination des impuretés du biogaz. Par conséquent, le développement de nouveaux absorbants dotés d'une capacité d'absorption élevée et d'une recyclabilité élevée est d'actualité. L'absorbant approprié doit également avoir une faible viscosité, une toxicité relativement faible, une faible pression de vapeur, un point d'ébullition élevé, une capacité d'absorption élevée et un faible coût. L'eau, qui combine toutes ces propriétés, est généralement utilisée dans les procédés de purification du biogaz, principalement pour le captage du CO₂. Cependant, la majorité des COV étant hydrophobes, l'eau n'est pas le solvant le plus adapté pour ces composés. Par conséquent, des solvants verts alternatifs sont recherchés pour remplacer les solvants organiques actuellement utilisés. Les premiers solvants alternatifs bien étudiés sont les liquides ioniques (ILs), qui sont des sels à l'état liquide [2–4].

Récemment, une nouvelle génération de solvants verts, à savoir les solvants eutectiques profonds (DESs), a également été utilisée avec succès comme absorbants pour les COV. Les DESs sont un mélange de deux ou trois composés chimiques qui présente un point de fusion inférieur à celui de chacun de leurs composants purs. Les composants typiques du DES sont des accepteurs de liaisons hydrogène (HBA), tels que les sels d'ammonium quaternaire, combinés à des donneurs de liaisons hydrogène (HBD), tels que des amides, des amines, des alcools et des acides carboxyliques, dans divers rapports molaires. Les DESs ont des propriétés physiques et chimiques similaires aux ILs et présentent certains avantages tels qu'une préparation plus facile, un coût inférieur, une non-toxicité, une non-réactivité, une recyclabilité, une non-corrosivité, etc. Les propriétés des DESs sont des facteurs importants dans leurs applications. Les solvants physiques tels que le glycérol, le propylène glycol et le carbonate de propylène, qui sont considérés comme des solvants respectueux de l'environnement et verts, ont également été étudiés pour l'absorption des COV ou des gaz [5–8].

Dans ce contexte, l'objectif de la thèse était d'évaluer des DESs et des solvants verts conventionnels comme absorbeurs de COV/CO₂ pour la valorisation du biogaz. La caractérisation des DESs étudiés et des solvants conventionnels a été réalisée. Nous avons mesuré la teneur en eau, les viscosités, les densités en fonction de la température. La capacité d'absorption des DESs pour différents COV purs et leurs mélanges, en déterminant leur coefficient de partage entre la phase gazeuse et l'absorbant, à différentes températures, concentrations et effets de l'eau a été déterminée. La capacité d'absorption de CO₂/CH₄ dans le DES a également été évaluée. Pour simuler une colonne d'absorption industrielle, la capacité d'absorption a été étudiée en méthode de barbotage dynamique. Cette configuration nous a permis de tester différentes conditions : COV individuels et leur mélange, concentration de COV et absorption de CO₂/CH₄. Cela nous a rapproché de la réalité d'un effluent industriel. Enfin, nous avons déterminé les capacités d'absorption des absorbants à l'aide d'un échangeur développé par notre partenaire industriel (Terrao[®]).

2. Matériels et méthodes

2.1. Préparation des DESs étudiés

Au cours de cette étude, divers DESs ont été préparés en utilisant de l'acide octanoïque (C₈), de l'acide nonanoïque (C₉), de l'acide décanoïque (C₁₀), du chlorure de choline (ChCl) et de la β-CD méthylée de manière aléatoire (RAMEB) comme HBA, et l'acide dodécanoïque (C₁₂), l'acide lévulinique (Lev) et le propylène glycol (PG) comme HBD. La composition des DESs évalués ainsi que leur teneur en eau sont données dans le tableau 1. Les DESs ont été préparés en agitant les deux composants (HBA et HBD) au rapport molaire souhaité à 60 °C jusqu'à formation d'un liquide clair et homogène. Tous les composés ont été utilisés sans prétraitement pour préparer le DES, à l'exception du chlorure de choline (ChCl), qui est séché dans une étuve à 60 °C pendant au moins deux semaines afin de le sécher. De plus, neuf COVs, CO₂ et CH₄ ont été choisis pour représenter les composants du biogaz brut.

Tableau 1. Composition des DES étudiés et leur teneur en eau (%).

Solvants		Rapport	Abréviation	Teneur en eau (%)
HBA	HBD			
Acide octanoïque	Acide dodécanoïque	3:1	C ₈ :C ₁₂	0,11
Acide nonanoïque		3:1	C ₉ :C ₁₂	0,07

Acide décanoïque	2 :1	C ₁₀ :C ₁₂	0,05
ChCl	1:2	CL	0,06
Acide lévulinique		RL	2h00
Rameb	1h30	RPG	14h30
Propylène glycol			
Carbonate de propylène	-	PC	0,07
	-	PG	0,52
Propylène glycol	-	PG16	16h00
Glycérol	-	G	0,36
Acide lactique	-	LA	9h00
Acide acétique	-	AA	0,05
Alcool benzylique	-	BA	0,06
Huile de cuisson	-	CO	0,04

2.2. Caractérisation des solvants étudiés

Les propriétés physicochimiques telles que la densité et la viscosité sont des paramètres importants qui peuvent affecter les processus de transport de masse, influençant ainsi leurs performances. Nous avons étudié les propriétés physicochimiques des DESs et des solvants traditionnels utilisés pour évaluer leur capacité à absorber les impuretés du biogaz. Afin de caractériser le DES et les solvants conventionnels, nous présentons les méthodologies et méthodes utilisées pour mesurer la viscosité, la densité, la spectroscopie infrarouge et la teneur en eau. La viscosité et la densité des solvants étudiés ont été mesurées à l'aide du SVM 3001 (Anton Paar) et la teneur en eau a été déterminée par titrage Karl Fischer (Titrateur Mettler Toledo C20S KF).

2.3. Méthode statique

2.3.1. Détermination du coefficient de partage vapeur-liquide (K)

Le coefficient de partage vapeur-liquide (K) est un paramètre fondamental qui exprime la répartition massique entre deux phases (gaz et liquide) en équilibre, la phase liquide étant soit de l'eau, soit des solvants. Cela dépend de la solubilité de l'analyte dans la phase liquide et est défini comme le rapport des concentrations du composant dans chaque phase. Les valeurs de K ont été mesurées par chromatographie gazeuse statique dans l'espace de tête (SH-GC), en suivant une combinaison de deux méthodes : la variation du rapport de phase et l'étalonnage de la phase vapeur. Le K est défini par l'équation suivante (Eq.1)

$$K = \frac{C_G}{C_L} \text{ (Éq.1)}$$

où C_G et C_L sont les concentrations respectives du soluté en phase gazeuse et liquide à l'équilibre.

Les valeurs K des trois COV dans les trois DES et quatre solvants ont été mesurées par espace de tête statique couplé à la chromatographie statique en phase gazeuse (SH-GC) en suivant une combinaison de deux méthodes décrites précédemment (Figure 1).

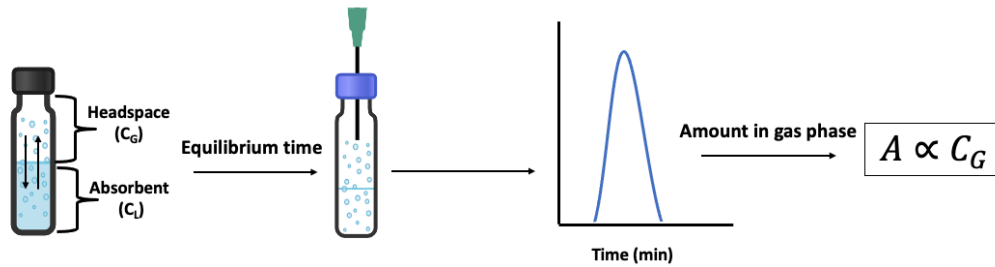


Figure 1 : Représentation schématique de la mesure des coefficients de partage vapeur-liquide (K) par chromatographie statique-espace de tête-gaz (SH-GC).

La méthode de variation du rapport de phase a été utilisée pour déterminer la valeur K dans l'eau comme décrit par Kolb et Ettre. A cet effet, la même quantité de COV a été ajoutée dans plusieurs flacons contenant différentes quantités d'eau. Les valeurs K ont été déterminées par le rapport entre les zones de pics chromatographiques respectives et le rapport volumétrique vapeur-liquide (Eq2).

$$\frac{1}{AV_L} = \frac{1}{\alpha V_L} + \frac{1}{\alpha K} \quad \text{(Éq.2)}$$

où A est l'aire du pic, α est une constante intégrant plusieurs paramètres, V_G est le volume de la phase gazeuse et V_L est le volume de liquide. La méthode d'étalonnage en phase gazeuse a été utilisée pour déterminer le coefficient de partage des COV dans l'absorbant (équation 3).

$$C_G = \frac{n_{VOCK}}{V_L + KV_G} \quad \text{(Éq.3)}$$

où n_{COV} est la quantité totale de COV ajoutée à chaque flacon. Comme C_G est proportionnel à l'aire sous le pic chromatographique (A), nous pouvons tracer la courbe d'étalonnage entre l'aire et la concentration du gaz [9].

Toutes les mesures ont été effectuées avec un échantillonneur automatique d'espace de tête Thermo Scientific TriPlus™ 500 couplé à une chromatographie en phase gazeuse Trace 1300 équipé d'un détecteur à ionisation de flamme et d'une colonne DB 624 en utilisant de l'azote comme gaz porteur. La température de la colonne GC a été fixée à 80 °C pour le toluène, l'heptane et la méthyléthylcétone, à 120 °C pour le limonène, le siloxane D4, le décane, le décène, le pinène et à 40 °C pour le dichlorométhane. Les COVs étudiés ont été ajoutés à une concentration connue dans une masse précise de DES ou de solvant conventionnel (environ 3,5 g) placée dans des flacons de 20 mL. Les échantillons ont été équilibrés pendant 24 heures sous agitation magnétique pour atteindre l'équilibre avant l'analyse SH-GC. Les COVs se répartiront entre les deux phases selon la constante d'équilibre contrôlée thermodynamiquement. L'effet de la température (-20, 0, 30, 45 et 60°C) et de la teneur en eau (10, 30 et 50 % masse) sur le coefficient de partage a été étudié. Enfin, l'effet du mélange de COV et de la concentration initiale de COV sur les capacités d'absorption des solvants a été étudié de 59 à 531 ppm.

2.3.2. Détermination de la capacité de sorption du CO₂

Ce travail a été réalisé en collaboration avec l'École de chimie et de génie chimique de l'Université Queen's de Belfast. Le Dr Leila Moura a développé une nouvelle méthode de criblage combinant l'analyse quantitative par GC d'un espace de tête équilibré avec la technique de chute de pression sur des matériaux placés dans des flacons GC sous pression à différentes pressions (en mbar). L'analyse des gaz a été réalisée à l'aide d'une chromatographie en phase gazeuse Perkin Elmer Clarus 500 fixé à un échantillonneur automatique d'espace de tête Turbomatrix 40 utilisant de l'hélium comme support et un détecteur à ionisation de flamme. Après avoir atteint le temps d'équilibre, le flacon est prêt pour la mesure et peut être réalisée par HS-GC. En utilisant l'équation 4, la quantité de gaz absorbée est basée sur la corrélation de la mesure pression-volume-température avec la mesure de la surface du pic GC.

$$n_g^{tot} = \frac{p_{ini}(V_{ini})}{(p_{ini}T_{ini})RT_{ini}} \quad (\text{éq.4})$$

L'absorption gazeuse des absorbants a été étudiée à l'aide de la méthode de criblage développée en combinant la pressurisation du gaz sur les absorbants dans des flacons avec l'analyse HS-GC pendant deux heures à l'équilibre. L'échantillonnage direct et l'analyse des gaz ont été utilisés pour déterminer les pressions partielles et les compositions du gaz non absorbé restant à des pressions variant de 300 à 4 110 mbar et à 35 °C. L'absorption du CO₂ (99 %), du CH₄ (99 %) et d'un mélange d'absorption de

CO₂ (50 %)/CH₄ (50 %) a été évaluée à l'aide de quatre DES, C₈:C₁₂, C₉:C₁₂, C₁₀:C₁₂ et RL avec 5 ml d'absorbants après cinq jours d'équilibre

2.4. Absorption dynamique

2.4.1. Échelle de laboratoire

Afin d'imiter les processus d'absorption industriels, qui sont généralement basés sur un épurateur, un système de barbotage dynamique a été développé à l'échelle du laboratoire, comme le montre la figure 2. Pour l'absorption de COVs, un gaz pollué modèle a été produit en injectant le COV liquide dans l'azote comme support à l'aide d'un distributeur monté sur seringue ayant un débit réglable. Pour l'absorption du CO₂, une bouteille de CO₂ a été utilisée et mélangée à de l'azote comme support afin d'avoir la concentration de CO₂ souhaitée. De plus, un cylindre doté d'un système de stockage a été utilisé pour l'échantillonnage du biogaz brut. Afin de contrôler le débit du biogaz, un mélangeur à débit massique/générateur d'humidité a été utilisé. Le biogaz a été échantillonné dans une décharge du nord de la France par le Centre Commun de Mesures et l'équipe TCEP de l'UCEIV. La concentration souhaitée du gaz d'entrée et de sortie a été mesurée avec une Micro GC Fusion ou un analyseur d'hydrocarbures totaux. Lorsque la concentration se stabilise, les deux vannes sont commutées et le gaz traverse l'absorbant. La concentration du gaz de sortie est mesurée jusqu'à ce que l'absorbant soit complètement saturé.

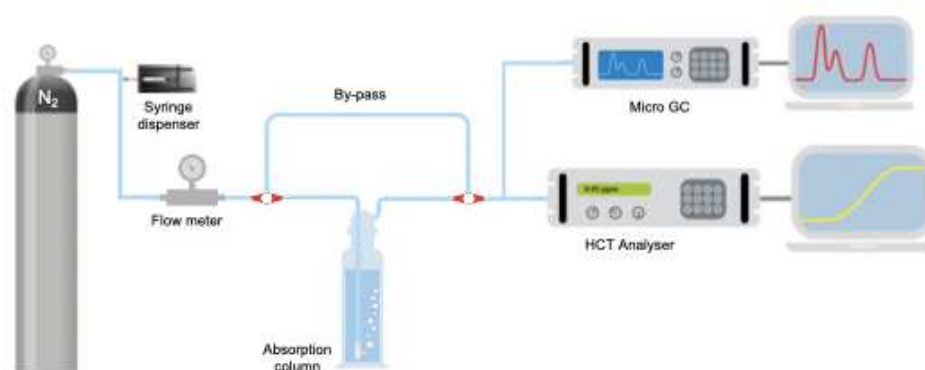


Figure 2. Configuration d'absorption dynamique utilisée. Pour les COV, CO₂ et l'absorption du biogaz brut.

Afin d'évaluer les performances des DESs dans des conditions simulant une colonne d'absorption, nous avons sélectionné un solvant présentant une capacité d'absorption et une utilité élevées pour divers COV en utilisant l'installation de barbotage à l'échelle du laboratoire. Lors des premières expériences, trois COV (toluène, limonène et siloxane D4) ont été sélectionnés car ces COV se trouvent dans le biogaz. Cinq absorbants ont été sélectionnés : C₁₀:C₁₂, Rameb:Lev, eau, PG16 et CO et étudiés à différentes températures et débits. Le mélange de toluène, limonène et siloxane D4 (TLS) a

également été évalué. Dans chaque expérience, une masse spécifique d'absorbant (environ 20 g) a été utilisée et la température a été réglée entre 25 et 30 °C selon l'expérience. La capacité d'absorption du toluène dans l'eau, le PG16, l'AA, le BA et l'eau/solvants a également été évaluée.

Dans le cas de l'absorption du dioxyde de carbone et de biogaz brut, dans les premières expériences nous avons évalué la capacité d'absorption du CO₂ (50%) mélangé au N₂ (50%) dans des absorbants tels que l'eau, PG, C₈:C₁₂, C₁₀:C₁₂, Rameb:Lev, tétraéthylènepentamine (TEPA) : C₈:C₁₂ : eau à 20 % (8:3:1) et TEPA + eau à 20 %. Nous avons ensuite évalué la capacité d'absorption du biogaz brut avec C₈:C₁₂, RL et l'eau. Enfin, 200 mL.min⁻¹ de gaz de combustion simulés (50 % CO₂, 50 % N₂) ont été introduits dans 180 g de la solution et laissés réagir jusqu'à saturation à 30 °C et 1 bar.

2.4.2. Échelle industrielle

La transposition des études à l'échelle du laboratoire aux opérations à l'échelle industrielle est une étape importante et souvent difficile dans de nombreux domaines, notamment la chimie et l'ingénierie. Sur la base de ces conditions, le but de cette étude était d'évaluer et de comparer l'efficacité des solvants disponibles industriellement tels que PG16, AA, BA et leurs mélanges avec l'eau pour éliminer le toluène des gaz d'échappement du laboratoire à l'échelle industrielle. En collaboration avec notre partenaire Terraotherm. Les expériences ont été réalisées à Coudekerque - Branche, France. L'absorbeur Terraos[®] est un échangeur direct de chaleur et de masse présentant l'avantage de petites dimensions géométriques (1 m² au sol pour 5 000 Nm³/h et 2 m de hauteur quel que soit le débit). Le flux gazeux traverse le liquide de l'échangeur afin d'échanger les composés solubles dans le solvant. Cet échange induit alors un mouvement de turbulence dans la phase liquide pour augmenter la probabilité de rencontre entre le solvant et le gaz, et ainsi améliorer l'échange de matières. L'échangeur Terraos[®] est équipé d'un système de pompage hydraulique permettant de remplacer le solvant saturé par le solvant de secours en cas de saturation du solvant et augmentant les turbulences du liquide. Dans nos expériences, une concentration de toluène de 2 000 mg/m³ a été utilisée. Le débit de gaz d'alimentation était de 2 000 m³/h et le Terraos[®] était alimenté avec 300 litres de solvant. La concentration de toluène dans les gaz d'entrée et de sortie a été surveillée avec un analyseur d'hydrocarbures totaux (Envea). Le dispositif expérimental est illustré à la figure 3 [10].

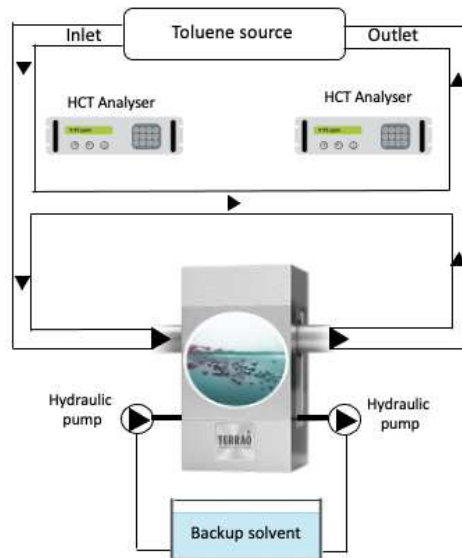


Figure 3. Expériences à l'échelle industrielle avec l'échangeur Terao[®].

2.5. Régénération des absorbants

Pour la méthode statique, trois méthodes telles que chauffage + agitation et barbotage d'azote (chauffage et non chauffage) avec un débit contrôlé ($100 \text{ mL}\cdot\text{min}^{-1}$) ont été évaluées pour éliminer le toluène du DES. Cependant, le temps de régénération peut varier d'un absorbant à l'autre. Dans cette étude, nous avons évalué d'abord le temps nécessaire pour régénérer l'absorbant $\text{C}_{10}:\text{C}_{12}$ puis nous avons effectué douze cycles d'absorption/désorption. Dans le cas de la méthode dynamique, des études de régénération ont été réalisées en utilisant la configuration d'absorption dynamique en suivant la désorption des absorbants à $60 \text{ }^\circ\text{C}$. Durant le processus de désorption, l'azote entre en contact avec des absorbants chargés de $\text{COV}/\text{CO}_2/\text{CH}_4$ ou de biogaz à un débit de $100 \text{ mL}\cdot\text{min}^{-1}$

3. Résultats et discussion

3.1. Viscosité et densité

L'étude expérimentale s'est concentrée sur la détermination de la viscosité des solvants eutectiques profonds (DESs) et des solvants conventionnels en fonction de la température. Le modèle Vogel-Fulcher-Tammann (VFT) a été utilisé pour ajuster les valeurs expérimentales de viscosité en fonction de la température, et les résultats sont présentés sur la figure 4. Une diminution constante de la viscosité avec l'augmentation de la température a été observée pour les DESs et les solvants conventionnels. Ce comportement correspond aux modèles couramment décrits pour les DESs et les solvants conventionnels. Les DESs à base d'acides gras présentent une faible viscosité à température ambiante, et une diminution progressive à des températures élevées par rapport aux solvants très visqueux.

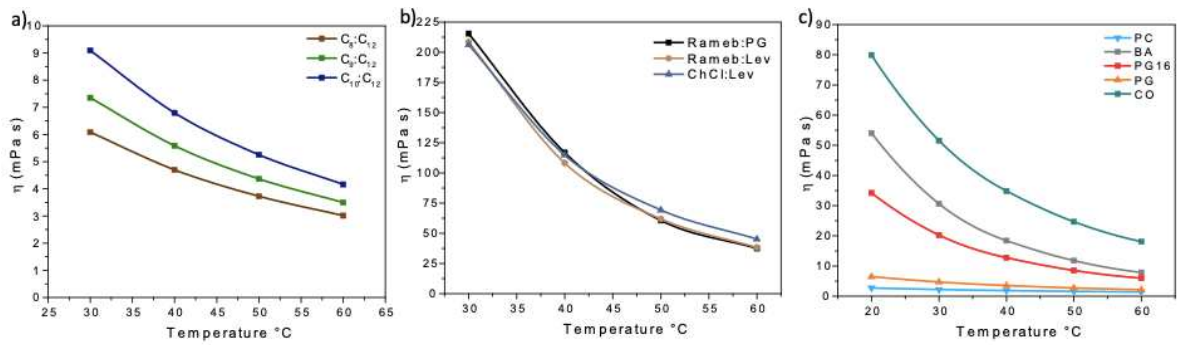


Figure 4. Viscosité expérimentale des DES étudiés (a et b) et des solvants conventionnels (c) en fonction de la température.

Les valeurs de viscosité des acides gras hydrophobes varient entre 6 et 9 mPa.s à 30 °C. La viscosité est influencée par la longueur de la chaîne alkyle, dans l'ordre : $C_8:C_{12} < C_9:C_{12} < C_{10}:C_{12}$. Les valeurs de viscosité obtenues pour les DES d'acides gras hydrophobes sont nettement inférieures à celles des DESs hydrophiles et à base de cyclodextrine, ainsi que des absorbants conventionnels comme le glycérol. Des valeurs de viscosité plus faibles indiquent des processus d'absorption et de désorption plus rapides, qui nécessitent moins d'énergie dans les opérations impliquant des colonnes d'absorption. L'étude souligne l'intérêt industriel de liquides moins visqueux pour des opérations d'absorption-désorption efficaces. Les travaux de recherche donne un aperçu des caractéristiques de viscosité des DES et des solvants conventionnels, en mettant l'accent sur l'impact de la température et de la longueur de la chaîne alkyle sur leur comportement rhéologique [5,11].

3.2. Coefficients de partage (K)

Les valeurs dans l'eau sont proches de celles de la littérature. Concernant le siloxane D4, on peut observer de grandes variations dans la littérature selon la méthode utilisée ou le temps d'équilibre. La diminution des valeurs de K observée pour tous les COVs dans tous les solvants par rapport à l'eau indique qu'une plus grande quantité de COV a été absorbée dans ces solvants. De plus, les valeurs K des COVs dans les DESs hydrophobes sont inférieures à celles des autres DESs étudiés. Parmi les solvants physiques étudiés, le glycérol a montré la plus faible capacité d'absorption des COV. Le carbonate de propylène, l'huile de cuisson, l'alcool benzylique, l'acide acétique et l'acide lactique présentent des capacités d'absorption des COVs bonnes à modérées. Cependant, en raison de leur viscosité élevée, nous avons décidé d'abandonner l'acide lactique et le glycérol.

L'un des COV les plus étudiés dans la littérature est le toluène. Il sert de COVs modèle des COVs hydrophobes. Les valeurs K obtenues pour le toluène dans les six DESs étudiés et huit solvants conventionnels se situent entre $4,55E-05$ et $4,06E-02$. Concernant le limonène, les valeurs de K dans les DES hydrophobes varient entre $1,13E-04$ à $1,19E-04$, ce qui correspond à une diminution jusqu'à

20 531 fois par rapport à l'eau. Les DESs ont montré une fois de plus la plus grande capacité à absorber le limonène par rapport aux autres solvants, à l'exception de l'huile de cuisson qui était de $9,73E-05$. De plus, la valeur K de l'alcool benzylique était l'une des plus faibles parmi les solvants conventionnels. Le pinène appartenant à la même classe que le limonène, les mêmes profils d'affinité sont observés. Les valeurs K du siloxane D4 varient entre $2,92E-04$ et $3,14E-04$ dans les DESs et entre $8,42E-02$ et $4,45E-04$ dans les solvants conventionnels. Cela fait encore une fois des DESs hydrophobes, de l'huile de cuisson et du carbonate de propylène les absorbants les plus efficaces. Peu d'études ont été consacrées à l'évaluation des solvants pour l'absorption des siloxanes, qui ont été évalués par plusieurs DESs à base de bromure de tétrapropylammonium et de glycols et à base de carvone comme absorbants pour l'élimination des siloxanes du flux de biogaz modèle. Leurs résultats ont souligné que les DES composés de carvone et d'acides carboxyliques présentaient une forte affinité pour les siloxanes. Cette observation est en bon accord avec la forte affinité observée dans notre cas entre les DESs à base d'acides carboxyliques et le siloxane D4 par rapport aux solvants conventionnels. En raison des valeurs de K plus élevées des COVs dans le glycérol, ainsi que de sa viscosité élevée, aucune autre évaluation de ce solvant n'a été réalisée. Les valeurs K de BA et PC montrent une meilleure absorption, correspondant à une valeur 17 fois supérieure. Cependant, ils sont du même ordre de grandeur que les DES hydrophobes.

Dans le cas du dichlorométhane, on note une capture similaire dans le PC par rapport aux DESs composé d'acides gras et d'autres solvants classiques.

3.2.1. Effet de la température

La température est un facteur critique qui pourrait affecter l'absorption des COVs. L'influence de la température sur l'absorption des COVs a été étudiée à -20 , 0 , 30 , 45 et 60 °C. Comme le montre la figure 5, les valeurs K de tous les COV étudiés ont augmenté avec la température, quel que soit le solvant étudié. La valeur K du toluène dans $C_8:C_{12}$ est de $4,75E-04$ à 30 °C, alors qu'elle augmente jusqu'à $2,60E-03$ à 60 °C. Concernant les solvants classiques, l'abaissement de température leur permet d'atteindre des valeurs proches de celle obtenue à 30 °C pour les DESs hydrophobes. Ces observations sont similaires pour le limonène et le siloxane D4. Il ressort très clairement des résultats que l'abaissement de la température a eu un effet bénéfique sur l'absorption des COVs étudiés et pourrait être utilisé comme paramètre pour ajuster l'efficacité des solvants. En effet, pour le PC la valeur K diminue de $3,08E$ pour 03 à 60 °C à $2,65E-04$ à -20 °C, cette dernière valeur est dans la même fourchette que celle obtenue avec les DESs. Ces observations sont similaires pour le limonène et le siloxane D4 [11].

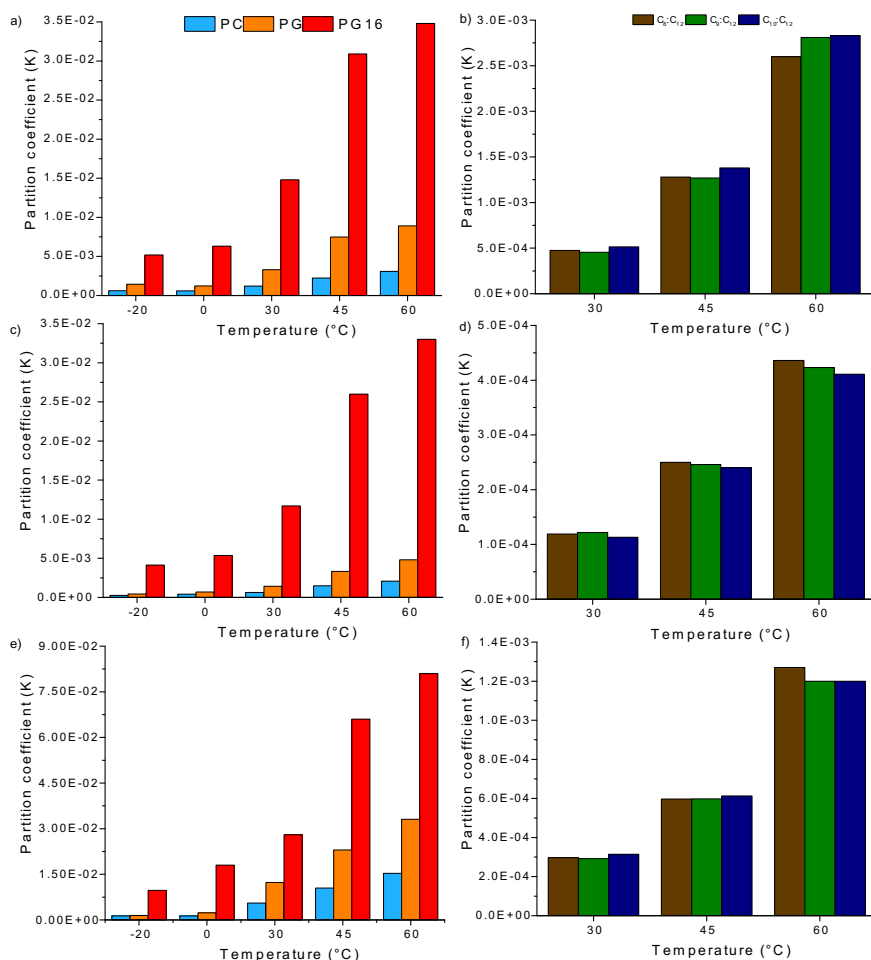


Figure 5. Valeurs de K pour a, b) toluène, c, d) limonène et e, f) siloxane D4 dans les solvants étudiés à différentes températures.

3.2.2. Effet de la concentration initiale de COV

L'effet de la concentration initiale de COV sur la quantité absorbée de COV a été étudié pour les différents COVs et solvants, comme le montre la figure 6. Dans le cas du toluène, la capacité d'absorption varie de 0,29 à 2,6 mg de toluène/g de DES pour des concentrations initiales comprises entre 59 et 531 ppm. Ces résultats montrent que l'absorption du toluène dans les DESs hydrophobes est sensible à la concentration et qu'aucune saturation n'a été observée. Les résultats indiquent également une absorption élevée pour de faibles concentrations de COV, soulignant un grand potentiel d'élimination des impuretés dans le biogaz, car les COV y sont présents à de faibles concentrations (<300 ppm).

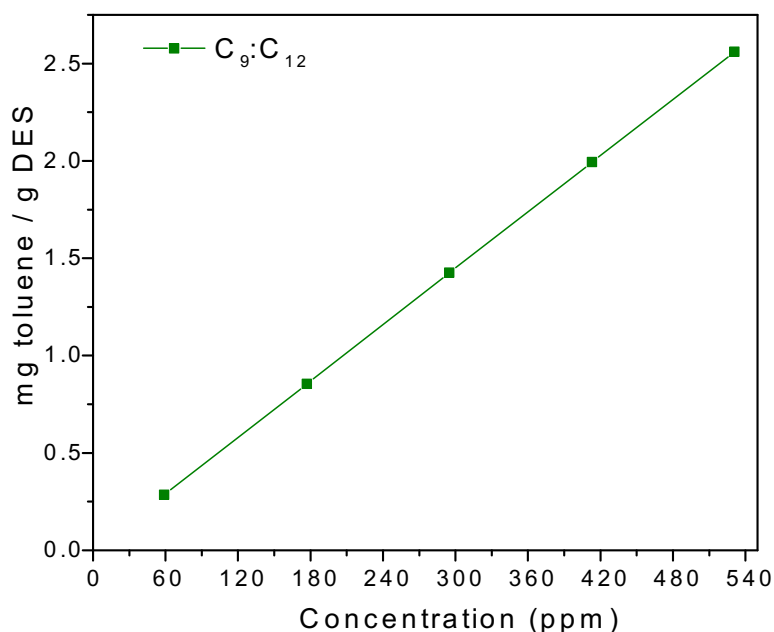


Figure 6. Effet de la concentration initiale de toluène sur les capacités d'absorption de $C_9:C_{12}$ à 30 °C.

3.2.3. Effet de l'eau sur l'absorption des COV

Un autre facteur critique pouvant affecter l'absorption des COV est la teneur en eau de l'absorbant. Par conséquent, l'effet de l'ajout d'eau sur le coefficient de partage du toluène, du limonène et du siloxane D4 dans le carbonate de propylène, le propylène glycol et $C_9:C_{12}$ a été évalué à 30 °C comme le montre la figure 7. La valeur de K du toluène dans le carbonate de propylène augmente de $1,20E-03$ à $3,66E-03$ dans le carbonate de propylène avec 50 % en masse d'eau. Des observations similaires peuvent être faites pour le propylène glycol où la valeur K augmente de $3,31E-03$ à $8,75E-02$ dans du propylène glycol avec 50 % en masse d'eau. Ce comportement est également observé pour le toluène dans Rameb:Lev et ChCl:Lev. La valeur de K augmente de $4,15E-03$ à 0,270 avec 90 % en masse d'eau. Pour le toluène dans Rameb:Lev, la valeur K est passée de $1,80E-03$ à 0,126 avec 90 % en masse d'eau. L'augmentation des valeurs K obtenues pour les COV dans les différents solvants en fonction de la teneur en eau souligne une plus faible absorption des COV lors de l'ajout d'eau comme observé précédemment pour les solvants organiques. [11].

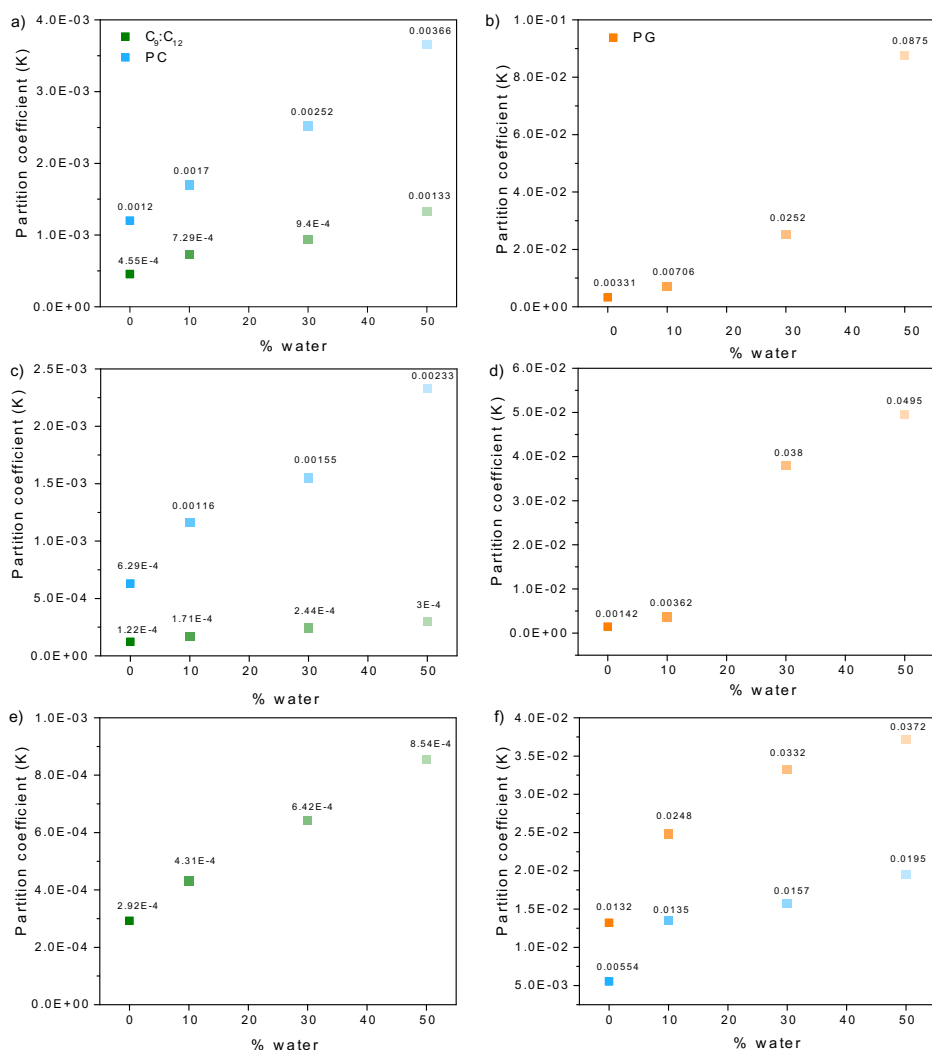


Figure 7. Valeurs de K pour a, b) toluène, c, d) limonène et e, f) siloxane D4 dans PC (bleu), PG (orange) et C₉:C₁₂ DES (vert) avec différentes quantités d'eau (10, 30 et 50 % en masse à 30 °C).

3.2.4. Effet des mélanges de COV

Les valeurs de K du toluène, du limonène, du siloxane D4 et du décane individuellement et en mélange à 30 °C sont présentées dans la figure 8. Nous notons que la valeur de K d'un COV donné n'est pas affectée par la présence d'autres COV. Ce résultat peut être dû à la structure similaire des COV dans le mélange TLSD₂.

Les DESs hydrophobes, CO et BA ont présenté une capacité d'absorption élevée pour les COV individuels, comme indiqué précédemment. La majorité des valeurs de K sont du même ordre de grandeur que celles obtenues pour les COV individuels.

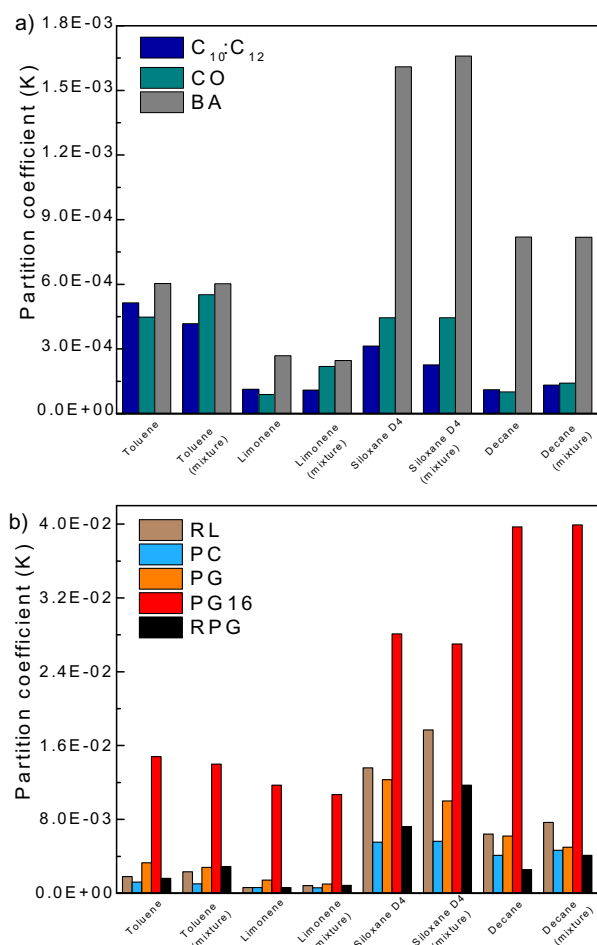


Figure 8. Valeurs de K pour a, b) mélange TLSD₂ dans C₁₀:C₁₂, CO, BA, RL, PC, PG, PG16 et RPG à 30 °C.

Sur la figure 8b, les valeurs de K du mélange TLSD₂ dans RL, PC, PG, PG16 et RPG présentent des valeurs similaires à celles des COV individuels. Cependant, dans le cas du RL et du RPG, les valeurs K ont montré une légère variation entre le siloxane D4 seul et dans le mélange avec une légère augmentation de la valeur de K. Ces résultats montrent que les affinités entre les adsorbants et le mélange de COV sont maintenues par l'absorption physique des COV dans ces adsorbants.

3.3.5. Adsorption du dioxyde de carbone

La figure 9 représente la capacité d'absorption de CO₂ dans quatre DESs à 35 °C. Les trois DES hydrophobes C₈:C₁₂, C₉:C₁₂ et C₁₀:C₁₂ ont démontré une absorption de CO₂ presque identique, atteignant 7,53 mg de CO₂/g C₉:C₁₂ à 3 189 mbar, tandis que RL a montré une absorption de CO₂ légèrement inférieure à presque la même pression, atteignant 5,42 mg CO₂/g RL à 3250 mbar.

L'absorption la plus élevée pour le CH₄ est de 3,08 mg CH₄/g C₉:C₁₂ à 3 927 mbar. Dans le cas du mélange CO₂/CH₄ dans C₈:C₁₂, l'absorption du CH₄ est inférieure à celle du CO₂. Ceci était attendu du

fait que l'absorption individuelle de CO₂ était supérieure à l'absorption individuelle de CH₄. Leur absorption varie en fonction de la pression initiale.

La capacité d'absorption du CO₂ dans le DES étudié est inférieure à celle de liquide ionique qui était de 3,52 mg CO₂/g d'IL, bien qu'elle ait des valeurs similaires à celles de l'éthylène glycol et de l'octanol qui étaient respectivement de 1,17 et 2,64 mg CO₂/g de solvant. à 35 °C et 1000 mbar. Concernant les résultats obtenus, il est important de comparer l'absorption du CO₂ et du CH₄.

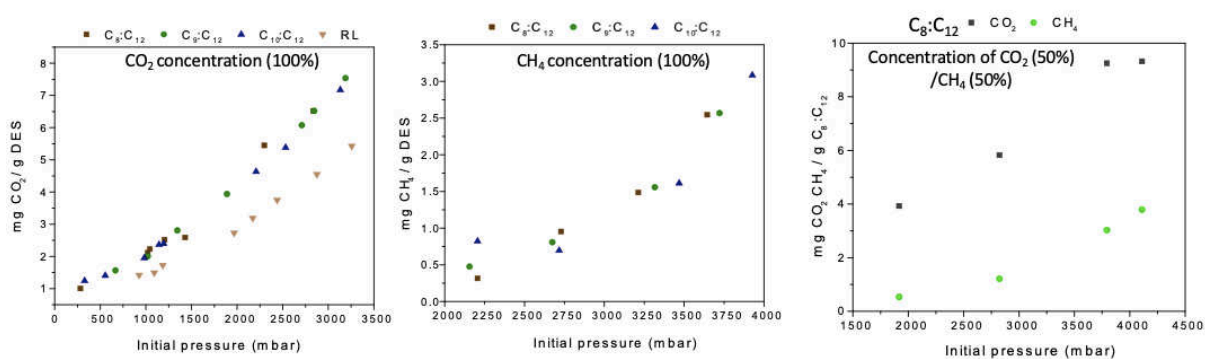


Figure 9. Capacité d'absorption de a) CO₂ (99%) dans C₈:C₁₂, C₉:C₁₂, C₁₀:C₁₂ et RL, b) CH₄ (99%) dans C₈:C₁₂, C₉:C₁₂, C₁₀:C₁₂, et c) CO₂ (50%) et CH₄ (50%) dans C₈:C₁₂ à 35 °C.

3.4. Absorption dynamique

La capacité d'absorption du toluène, du limonène et du siloxane dans l'eau et dans les six absorbants a été évaluée à 30 °C, avec un débit de COV de 20 µL.h⁻¹ et un débit de N₂ de 10 Lh⁻¹. Dans ces conditions, les concentrations de toluène, de limonène et de siloxane D4 étaient respectivement de 100, 120 et 50 ppm. En comparant les capacités d'absorption, nous avons observé que l'eau possède la capacité la plus petite, comme prévu par les études précédentes sur les coefficients de partage. Ainsi, si les valeurs de K sont similaires pour les deux absorbants, la capacité d'absorption pour CO de 0,57 mg de toluène /g de CO est inférieure à celle obtenue pour C₁₀:C₁₂. Rameb:Lev a une efficacité d'absorption légèrement inférieure à celle de BA + 60 % en poids d'eau, avec une capacité de 0,255 mg de toluène par g RL par rapport à 0,335 mg de toluène/g de solvant pour BA + 2,0 % en poids d'eau. Malgré la viscosité élevée du RL, la capacité d'absorption est meilleure que celle du PG16 et de l'AA + 60 % en masse d'eau, 0,155 et 0,038 mg de toluène/g de solvant, respectivement. Ce comportement est également observé pour le limonène et le siloxane D4. Cela confirme que la méthode statique est en accord avec la méthode dynamique. Par conséquent, les valeurs K sont obtenues à l'équilibre thermodynamique où la viscosité n'influence pas la capacité d'absorption.

3.4.1. Effet de la concentration initiale de toluène

L'effet de la concentration initiale de toluène a été étudié en utilisant cinq débits différents de 10, 20, 40, 80 et 100 $\mu\text{L}\cdot\text{h}^{-1}$ avec un débit d'azote de 15 $\text{L}\cdot\text{h}^{-1}$ à 30 °C. La quantité de toluène capturé augmente linéairement avec l'augmentation du débit de toluène en $\text{C}_{10}:\text{C}_{12}$. Une tendance similaire se retrouve dans la littérature. Les résultats obtenus à partir des différents débits de toluène dans $\text{C}_{10}:\text{C}_{12}$ sont de 0,422, 0,883, 1,768, 3,94 et 5,91 mg de toluène par g de DES. Les valeurs obtenues dans la littérature pour le toluène en $\text{ChCl}:\text{Lev}$ et $\text{TBABr}:\text{Dec}$ étaient de 0,55 mg par g de DES et de 2,37 mg par g de DES avec un débit assez similaire de 73 $\mu\text{L}\cdot\text{h}^{-1}$. Cependant, il a montré une capacité d'absorption inférieure pour le toluène par rapport au DES $\text{C}_{10}:\text{C}_{12}$ qui était de 3,94 mg par g de DES à 80 $\mu\text{L}\cdot\text{h}^{-1}$. Globalement, nos résultats indiquent que la solubilité du toluène dans le DES hydrophobe est sensible aux conditions de concentration, ce qui indique également que le processus d'absorption du toluène est réversible et peut être soumis à une régénération en augmentant la température et/ou en diminuant la concentration [12,13].

3.4.2. Effet du mélange de COV

D'un point de vue industriel, il est intéressant d'étudier la capacité d'absorption des mélanges de COVs dans des absorbants à l'échelle du laboratoire. Par conséquent, l'absorption du mélange TLS dans cinq absorbants a été évaluée afin de la comparer aux mélanges individuels. Les capacités d'absorption des absorbants sont similaires pour le mélange de COV.

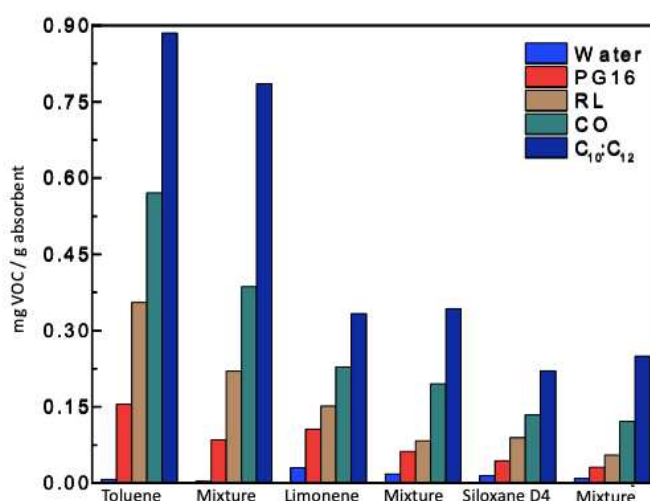


Figure 10. Capacité d'absorption du mélange TLS dans l'eau, PG16, RL, CO et $\text{C}_{10}:\text{C}_{12}$ à 30 °C

Pour le limonène, seul et en mélange les valeurs de K sont de 0,33 et 0,34 mg de COV/g de $\text{C}_{10}:\text{C}_{12}$ et pour le siloxane de 0,22 et 0,23 mg de COV/g de $\text{C}_{10}:\text{C}_{12}$. Ainsi, on conserve le même comportement

pour le mélange de COV. Dans le cas du toluène, la capacité d'absorption du mélange de COV dans le CO était de 0,39 mg/g de CO, tandis que pour le toluène individuel il était de 0,57 mg de toluène/g de CO. La même tendance est observée pour le RL, le PG16 et l'eau avec une légère diminution de l'absorption. De COV dans le mélange par rapport au pur, comme le montre la figure 10. Dans le cas de l'eau, c'est l'absorbant le moins efficace, réduisant sa capacité d'absorption de près de moitié. La capacité d'absorption du mélange TLS est respectivement de 0,0036, 0,0018 et 0,0090 mg de COV/g d'eau. Par conséquent, le coefficient de partage du mélange de COV dans les absorbants a montré des résultats de tendance comparables, soulignant que l'utilisation d'une méthode statique peut fournir une bonne compréhension de l'absorption des COVs individuels et du mélange de COV dans les absorbants.

3.5. Absorption du dioxyde de carbone et du biogaz brut

La capacité d'absorption du CO₂ et de biogaz brut dans les absorbants sont répertoriés dans le tableau 2. Comme prévu, le mélange TEPA + eau 20 % a la capacité d'absorption la plus élevée avec 2,87 mol CO₂/ kg TEPA + eau 20 %. Parmi eux, le TEPA à base de DES a montré une absorption significative avec 0,9 mole CO₂ / kg TEPA:C₈:C₁₂ :eau 20 %, ce qui est principalement due à l'influence de l'amine. Concernant les DESs, C₈:C₁₂ présente une absorption légèrement supérieure, avec 0,05 mole de CO₂ / kg de C₈:C₁₀. Tous les absorbants testés présentent des valeurs d'absorption similaires, proches de celles de l'eau. Concernant la composition du biogaz, outre le CO₂, le biogaz contient également divers contaminants tels que des COV et du H₂S.

Tableau 2. Capacité d'absorption du CO₂ (50%) dans différents absorbants à 30 °C.

Absorbants	TEPA:C ₈ :C ₁₂ : eau 20%	C ₈ :C ₁₂	C ₁₀ :C ₁₂	R.L.	PG	eau	TEPA+ eau 20%	TEPA+ éthanol+ eau
Capacité d'absorption mol CO ₂ kg	0,9	0,050	0,045	0,030	0,043	0,038	2,870	2,48

Afin d'évaluer l'absorption du biogaz dans les absorbants, il était nécessaire de connaître la concentration du biogaz. Le biogaz brut était donc stocké dans une bouteille sous pression. Les concentrations du biogaz étaient de CO₂ (26%) et CH₄ (28%), H₂S (4%), les COV variaient entre 50 et 100 ppm. Le tableau 3 montre la capacité d'absorption du biogaz brut CO₂ (26%) et CH₄ (28 %) à 38

ml min⁻¹ dans le DES C₈ : C₁₂ et RL à 30 °C. En conséquence, la capacité d'absorption de l'absorbant pour le CO₂/CH₄ a montré un transfert de masse comparable aux résultats précédents.

Tableau 3. Capacité d'absorption du CO₂ (26%) CH₄ (28%) dans différents absorbants à 30 °C.

Absorbants	CO ₂ _ C ₈ :C ₁₂ _	CO ₂ _ R.L.	CH ₄ _ C ₈ :C ₁₂ _	CH ₄ _ R.L.
Capacité d'absorption mol kg ⁻¹	0,047	0,044	0,030	0,031

3.6. Absorption dynamique à l'échelle industrielle

Les capacités d'absorption obtenues à 20 °C sont présentées sur la figure 11. Les résultats sont en bon accord avec les mesures à l'échelle du laboratoire. Quelque soit le % en masse d'eau, les mélanges eau/BA présentent des capacités d'absorption supérieures à celles de l'AA et de PG16. Le mélange BA/eau à 20 % en masse présente la capacité d'absorption la plus élevée pour le toluène (22,70 g de toluène par L de solvant), tandis que l'épuration à l'eau est le solvant le moins efficace avec 0,56 g de toluène par L de solvant. Comme observé précédemment, la capacité d'absorption du solvant diminue à mesure que le % en masse d'eau augmente. Concernant le PG16, la capacité d'absorption est toujours inférieure à celle du BA à même % en masse d'eau. Comme le dispositif industriel soit en boucle fermée, aucune expérience de régénération n'a été réalisée.

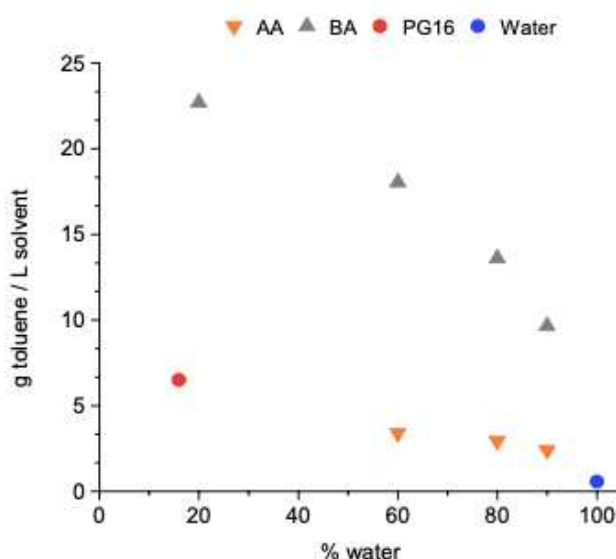


Figure 11. Capacité d'absorption du toluène dans les solvants et les mélanges eau/solvant à 20 °C.

3.7. Régénération de solvants pour méthodes statiques et dynamiques

Pour la méthode statique, la capacité d'absorption d'un absorbant chargé en toluène, $C_{10} : C_{12}$, est restée stable après douze cycles d'absorption-désorption. Le temps de régénération de $C_{10} : C_{12}$ a été réduit à 2,5 heures en utilisant de l'azote barbotant à 60°C, par rapport au procédé précédent de désorption thermique à 60°C pendant 48 heures. Cette méthode est plus efficace en raison de sa régénération plus rapide, ce qui la rend plus adaptée aux systèmes industriels. La perte de masse de $C_{10} : C_{12}$ était inférieure à 1 % pour toutes les méthodes de régénération. La capacité d'absorption de toluène dans le DES est restée stable pendant douze cycles. Dans le cas de l'absorption dynamique, les expériences de régénération ont été réalisées en utilisant le stripping. Dans toutes les études de désorption, la température a été augmentée pour accélérer la régénération, confirmant l'avantage du préchauffage de la colonne de désorption pour réduire la durée et le coût de l'ensemble du processus [14].

4. Conclusion

Le but de cette étude était d'évaluer des DESs et des solvants conventionnels comme nouveaux absorbants des impuretés du biogaz telles que les COVs et le CO_2 par absorption physique. Cette étude a été réalisée en collaboration avec un partenaire industriel qui a développé de nouveaux échangeurs de masse et de chaleur. Dans ce but, nous avons étudié différents types de DESs et de solvants conventionnels et les avons caractérisés, tels que la teneur en eau, la viscosité, la densité et l'IR. Nous avons évalué la capacité d'absorption de COVs individuels, de leur mélange et du CO_2 / CH_4 dans différents absorbants. Les COVs sélectionnés pour notre étude étaient basés sur les impuretés du biogaz et leur diversité structurale utilisée dans l'industrie. Les valeurs K obtenues à 30 °C ont été utilisées pour représenter l'efficacité des absorbants par rapport à tous les COV sous la forme d'un diagramme à code couleur, comme le montre la figure 12.

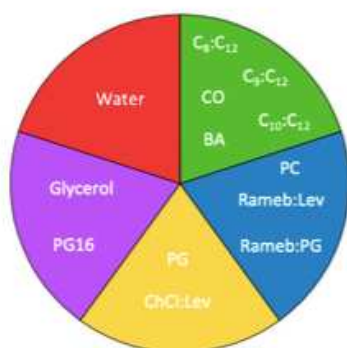


Figure 12. Efficacité d'absorption des COV dans les DES et les solvants conventionnels

L'absorbant le moins efficace est indiqué en rouge et le plus efficace en vert. Cependant, la viscosité plus élevée du CO et la volatilité plus élevée du BA, par rapport aux DESs hydrophobes, pourraient être moins efficaces en termes d'énergie élevée et de régénération, respectivement. De plus, il existe une tendance linéaire de la capacité d'absorption à mesure que la concentration initiale de COV augmente. La capacité d'absorption des COV par les absorbants a été contrôlée à différentes températures. La volatilité des COV augmente avec la température et, par conséquent, la capacité de l'absorbant à piéger les COV diminue. Ces comportements indiquent que l'absorption des COV par les DESs et les solvants est une absorption physique et un processus facilement réversible, conduisant à une régénération moins coûteuse de l'absorbant. La capacité d'absorption du CO₂ et CH₄ des DESs hydrophobes est faible et peu prometteuse pour ces composés comparativement aux COVs. Pour se rapprocher des conditions réelles d'une colonne d'absorption, nous avons ensuite évalué l'efficacité du DES et des solvants conventionnels pour absorber les COV/CO₂ et le biogaz brut dans un processus dynamique. De plus, le passage de l'échelle laboratoire à l'échelle industrielle montre des résultats cohérents.

5. Références

- [1] M.E. López, E.R. Rene, M.C. Veiga, C. Kennes, *Biogas Technologies and Cleaning Techniques*, in: *Environmental Chemistry for a Sustainable World*, Springer Netherlands, 2012: pp. 347–377. https://doi.org/10.1007/978-94-007-2439-6_9.
- [2] C. Ma, C. Liu, X. Lu, X. Ji, *Techno-economic analysis and performance comparison of aqueous deep eutectic solvent and other physical absorbents for biogas upgrading*, *Appl Energy*. 225 (2018) 437–447. <https://doi.org/10.1016/j.apenergy.2018.04.112>.
- [3] J. Niesner, D. Jecha, P. Stehlík, *Biogas upgrading technologies: State of art review in european region*, in: *Chem Eng Trans*, Italian Association of Chemical Engineering - AIDIC, 2013: pp. 517–522. <https://doi.org/10.3303/CET1335086>.
- [4] E. Ryckebosch, M. Drouillon, H. Vervaeren, *Techniques for transformation of biogas to biomethane*, *Biomass Bioenergy*. 35 (2011) 1633–1645. <https://doi.org/10.1016/j.biombioe.2011.02.033>.
- [5] C.-C. Chen, Y.-H. Huang, J.-Y. Fang, *Hydrophobic deep eutectic solvents as green absorbents for hydrophilic VOC elimination*, *J Hazard Mater*. 424 (2022) 127366. <https://doi.org/10.1016/j.jhazmat.2021.127366>.
- [6] P. Makoś-Chełstowska, E. Słupek, J. Gębicki, *Deep eutectic solvent-based green absorbents for the effective removal of volatile organochlorine compounds from biogas*, *Green Chemistry*. 23 (2021) 4814–4827. <https://doi.org/10.1039/D1GC01735G>.
- [7] S. Fourmentin, D. Landy, L. Moura, S. Tilloy, H. Bricout, Ferreira M., *Process for Purifying a Gaseous Effluent*, WO 2018/091379 A1, 2018.
- [8] C. Florindo, L. Romero, I. Rintoul, L.C. Branco, I.M. Marrucho, *From Phase Change Materials to Green Solvents: Hydrophobic Low Viscous Fatty Acid-Based Deep Eutectic Solvents*, *ACS Sustain Chem Eng*. 6 (2018) 3888–3895. <https://doi.org/10.1021/acssuschemeng.7b04235>.

- [9] B. Kolb, L.S. Ettre, *Static Headspace–Gas Chromatography*, in: Wiley, 2006. <https://doi.org/10.1002/0471914584.fmatter>.
- [10] Zemmouri J., Device for producing and treating a gas stream through a volume of liquid, and facility and method implementing said device., WO2016071648A2, 2016.
- [11] P. Villarim, E. Genty, J. Zemmouri, S. Fourmentin, Deep eutectic solvents and conventional solvents as VOC absorbents for biogas upgrading: A comparative study, *Chemical Engineering Journal*. 446 (2022). <https://doi.org/10.1016/j.cej.2022.136875>.
- [12] L. Moura, T. Moufawad, M. Ferreira, H. Bricout, S. Tilloy, E. Monflier, M.F. Costa Gomes, D. Landy, S. Fourmentin, Deep eutectic solvents as green absorbents of volatile organic pollutants, *Environ Chem Lett*. 15 (2017) 747–753. <https://doi.org/10.1007/s10311-017-0654-y>.
- [13] T. Moufawad, M. Costa Gomes, S. Fourmentin, Deep eutectic solvents as absorbents for VOC and VOC mixtures in static and dynamic processes, *Chemical Engineering Journal*. 448 (2022) 137619. <https://doi.org/10.1016/j.cej.2022.137619>.
- [14] P. Villarim, C. Gui, E. Genty, Z. Lei, J. Zemmouri, S. Fourmentin, Toluene absorption from laboratory to industrial scale: An experimental and theoretical study, *Sep Purif Technol*. 328 (2024) 125070. <https://doi.org/10.1016/j.seppur.2023.125070>.

Résumé

Le biogaz est une source d'énergie renouvelable produite naturellement par la digestion anaérobie de matières organiques. Il se compose principalement de méthane (CH_4) et de dioxyde de carbone (CO_2). Il contient également des traces de vapeur d'eau, de composés organiques volatils (COV) et de sulfure d'hydrogène. La valorisation du biogaz en biométhane nécessite l'élimination des contaminants présents dans le biogaz brut, en réduisant le niveau d'impuretés afin d'obtenir une teneur élevée en CH_4 , de l'ordre de 90 à 99 %. Les utilisations du biométhane sont les mêmes que celles du gaz naturel, mais il s'agit d'une source d'énergie non fossile et renouvelable à 100 %. De nombreuses technologies ont été testées et appliquées pour éliminer les impuretés du biogaz, telles que le lavage à l'eau, le lavage physique et chimique, la séparation par membrane, l'adsorption par variation de pression, les méthodes biologiques, etc. Les absorbants jouent un rôle important dans l'élimination des impuretés du biogaz. Il est donc impératif de mettre au point de nouveaux absorbants dotés d'une capacité d'absorption et d'une recyclabilité élevées. L'absorbant approprié doit également avoir une faible viscosité, une toxicité relativement faible, une faible pression de vapeur, un point d'ébullition élevé, une grande capacité d'absorption et un faible coût. Les solvants eutectiques profonds (DESs) sont un mélange de deux ou trois composés chimiques (généralement un composé accepteur d'hydrogène, HBA, et un composé donneur d'hydrogène, HBD), qui se combinent par le biais de liaisons hydrogène et dont le point de fusion est inférieur à celui de chacun de leurs composants purs. Ces solvants ont des propriétés physico-chimiques qui peuvent être ajustées en fonction de la nature des composés individuels et de leur ratio. L'objectif de cette thèse était d'évaluer des DES et des solvants verts conventionnels en tant qu'absorbants pour les COV/ CO_2 . Nous avons évalué et comparé l'efficacité de différents DESs et absorbants conventionnels pour l'absorption de neuf COV et du CO_2 . Le coefficient de partage vapeur-liquide (K) des COV dans les solvants étudiés et la capacité d'absorption du CO_2 dans les DES ont été déterminés à l'aide de la chromatographie en phase gazeuse couplée à l'espace de tête statique. L'effet du mélange de COV, de la température et de la teneur en eau a été évalué. Les capacités d'absorption des COV individuels, de leur mélange et du CO_2/CH_4 dans les DES et les solvants conventionnels ont également été évaluées à l'aide d'un dispositif dynamique simulant une colonne d'absorption industrielle. Les résultats statiques et dynamiques obtenus sont en bon accord. Les capacités d'absorption d'absorbants industriels ont également été évaluées à l'échelle industrielle en utilisant un échangeur développé par notre partenaire industriel (Terra[®]).